AD-A174 577

SAFETY CHARACTERISTICS OF NON-LITHIUM BATTERY SYSTEMS

BY   RICHARD F. BIS   ROBERT M. MURPHY (ADVANCED BATTERY GROUP)

RESEARCH AND TECHNOLOGY DEPARTMENT

JULY 1986

DTIC
ELECTE
S
NOV 2 6 1986
D
D

NAVAL SURFACE WEAPONS CENTER

Dahlgren, Virginia 22448   •   Silver Spring, Maryland 20910

OTIC FILE COPY

86 11 25 078

REPORT DOCUMENTATION PAGE

1a. REPORT SECURITY CLASSIFICATION UNCLASSIFIED	1b. RESTRICTIVE MARKINGS

2a. SECURITY CLASSIFICATION AUTHORITY	3. DISTRIBUTION/AVAILABILITY OF REPORT Approved for public release; distribution is unlimited.
2b. DECLASSIFICATION/DOWNGRADING SCHEDULE	

4. PERFORMING ORGANIZATION REPORT NUMBER(S)	5. MONITORING ORGANIZATION REPORT NUMBER(S) NSWC TR 84-302, Revision 1

6a. NAME OF PERFORMING ORGANIZATION Advanced Battery Group	6b. OFFICE SYMBOL (If applicable)	7a. NAME OF MONITORING ORGANIZATION Naval Surface Weapons Center

6c. ADDRESS (City, State, and ZIP Code) 269 Westwood Road Lancaster, NY 14086	7b. ADDRESS (City, State, and ZIP Code) White Oak Laboratory 10901 New Hampshire Avenue Silver Spring, MD 20903-5000

8a. NAME OF FUNDING/SPONSORING ORGANIZATION Naval Surface Weapons Center	8b. OFFICE SYMBOL (If applicable) R33	9. PROCUREMENT INSTRUMENT IDENTIFICATION NUMBER N60921-84-C-0027

8c. ADDRESS (City, State, and ZIP Code) White Oak Laboratory 10901 New Hampshire Avenue Silver Spring, MD 20903-5000	10 SOURCE OF FUNDING NUMBERS			
	PROGRAM ELEMENT NO.	PROJECT NO.	TASK NO.	WORK UNIT ACCESSION NO.

11. TITLE (Include Security Classification)

SAFETY CHARACTERISTICS OF NON-LITHIUM BATTERY SYSTEMS

12. PERSONAL AUTHOR(S)
Robert M. Murphy, Richard F. Bis

13a. TYPE OF REPORT Final	13b. TIME COVERED FROM 10/83 TO 9/84	14. DATE OF REPORT (Year, Month, Day) July 1986	15. PAGE COUNT 298

16. SUPPLEMENTARY NOTATION

17. COSATI CODES			18. SUBJECT TERMS (Continue on reverse if necessary and identify by block number)
FIELD	GROUP	SUB-GROUP	Primary Batteries NAVSEAINST 930.1A Performance
10	03		Secondary Batteries Short Circuit Self-discharge
			Safety Hazards Overdischarge Charging

19. ABSTRACT (Continue on reverse if necessary and identify by block number)

A study was conducted to determine the safety characteristics for both primary and secondary non-lithium battery systems. Of particular interest was the behavior of these battery systems when subjected to the electrical and thermal abuse testing procedures of NAVSEAINST 9310.1A (i.e., short circuit, forced overdischarge, and incineration). Also included are the safety/hazard characteristics associated with charging primary batteries and overdischarging secondary batteries. This report also summarizes the manufacture, electrical performance, failure mechanisms, self-discharge, and applications for twenty-two primary and nineteen secondary battery systems.

This revision (Revision 1) superseies the July 1984 edition of this technical report.

20. DISTRIBUTION/AVAILABILITY OF ABSTRACT ☐ UNCLASSIFIED/UNLIMITED ☐ SAME AS RPT. ☐ DTIC USERS	21. ABSTRACT SECURITY CLASSIFICATION
22a. NAME OF RESPONSIBLE INDIVIDUAL	22b. TELEPHONE (Include Area Code)	22c. OFFICE SYMBOL

DD FORM 1473, 84 MAR	83 APR edition may be used until exhausted. All other editions are obsolete.	SECURITY CLASSIFICATION OF THIS PAGE UNCLASSIFIED

19.   Key Words (cont.)

Failure Mechanisms
Applications

FOREWORD

A study was conducted to determine the safety characteristics for both primary and secondary non-lithium battery systems. Of particular interest was the behavior of these battery systems when subjected to the electrical and thermal abuse testing procedures of NAVSEAINST 9310.1A (i.e., short circuit, forced overdischarge, and incineration). Also included are the safety/hazard characteristics associated with charging primary batteries and overcharging secondary batteries. This report also summarizes the manufacture, electrical performance, failure mechanisms, self-discharge, and applications for twenty-two primary and nineteen secondary battery systems.

This revision (Revision 1) supersedes the July 1984 edition of this technical report.

Approved by:

JACK R. DIXON, Head
Materials Division

Accesion For		
NTIS CRA&I	☑	
DTIC TAB	☐	
Unannounced	☐	
Justification		
By		
Distribution /		
Availability Codes		
Dist	Avail a·d / or Special	
A-1		

CONTENTS

CONTENTS (Cont.)

TABLES

CHAPTER 1

INTRODUCTION

Lithium battery systems have been developed within the past fifteen years which exhibit high energy densities, wide ranges of operating temperatures, and long shelf life characteristics when compared to more conventional battery systems. In addition, lithium systems containing such positive electrode materials as sulfur dioxide (SO_2), thionyl chloride $(SOCl_2)$, sulfuryl chloride (SO_2Cl_2), carbon monofluoride $(CF)_n$, manganese dioxide (MnO_2), and vanadium pentoxide (V_2O_5), exhibit both high operating voltages and flat discharge curves. Because of the highly energetic and reactive nature of lithium batteries, safety related incidents have been reported which involve ventings, fires, and explosions. Such incidents have resulted in both property damage and injuries to personnel. As a consequence, many studies have been conducted to determine the hazard characteristics associated with a variety of lithium primary systems. The most intensive investigations have been concerned with the spiral-wound design for the lithium-sulfur dioxide, Li/SO_2, organic battery system[1-45] and for the lithium-thionyl chloride, $Li/SOCl_2$, inorganic battery system.[46-91] Because the development of the lithium-sulfuryl chloride, Li/SO_2Cl_2, inorganic battery was not as advanced as either the Li/SO_2 or $Li/SOCl_2$ systems, safety evaluation data have been reported only within the past four years.[92-96]

Recently, several lithium-solid cathode systems have also been studied to determine the hazard characteristics for cells subjected to a variety of electrical, mechanical, and thermal abuse testing. These investigations have resulted in safety data for such systems as lithium-carbon monofluoride, $Li/(CF)_n$,[97-99] lithium-copper (II) oxide, Li/CuO,[100-103] lithium-copper (II) sulfide, Li/CuS,[104,105] lithium-manganese dioxide, Li/MnO_2,[106-108] and lithium-vanadium pentoxide, Li/V_2O_5.[109]

The responsibilities and procedures for lithium battery safety within the U.S. Navy are set forth in NAVSEAINST 9310.1A.[110] In accordance with the above, lithium batteries and corresponding end items must be tested and approved prior to the introduction of the devices for general Fleet use. The technical authority relative to the lithium battery safety program for the U.S. Navy is the Naval Sea Systems Command, SEA 06H. The lead laboratory for the program is the Naval Surface Weapons Center (NSWC) under the direction of Dr. R.F. Bis.

Currently, the three abusive tests used to evaluate the safety characteristics of the lithium batteries and lithium powered end items are summarized as follows:

1. Constant current discharge and voltage reversal test.

   Three properly instrumented end units are discharged under constant current conditions using a DC power supply. The internal fusing of each test unit must be bypassed and the discharge be carried out at a current level equal to the fuse value of the battery pack. After the battery voltage reaches zero volts, the discharge is to be continued into battery voltage reversal at the fuse current value until 1.5 times the advertised capacity of the battery pack has been attained. Voltage, pressure, and temperature are continuously monitored and recorded.

2. Short circuit test.

   Three properly instrumented end units are short circuited through a resistive load of 0.01 ohm or less for a minimum period of 24 hours. All internal electrical protective devices must be bypassed. Voltage, pressure, current, and temperature are monitored continuously and recorded.

3. High temperature exposure test.

   Three properly instrumented end units are subjected to a heating rate of 20°C per minute until a limiting temperature of 500°C is achieved. Voltage, temperature, and pressure are monitored continuously and recorded.

Many Navy applications require higher current levels or longer operational lifetimes than could be provided by a battery comprised of a single series string of cells at a specified operational voltage. As a result, some end units could contain two or more parallel strings of cells in order to meet the required levels of performance. There exists the possibility, therefore, that one or more of the parallel strings could induce a charging mode with a weaker (depleted or partially depleted) string of cells. Such an occurrence could lead to a hazardous condition, particularly in the case of lithium batteries. In view of the above, a fourth safety test may be incorporated in NAVSEAINST 9310.1A to evaluate the hazardous characteristics associated with electrically charging a series string of cells.* At the present time, details relative to the charging test have not yet been approved.

Lithium batteries presently fulfill the requirements of many U.S. Navy specialized applications which require high energy densities, high operating voltages, low temperature operation, and extended shelf life. It is important to note, however, that the majority of Fleet battery applications require operational characteristics which are achieved by a variety of non-lithium primary and secondary battery systems. The safety characterization of many such non-lithium battery systems, however, has neither been widely published in the technical literature nor systematically correlated and tested in accordance with procedures such as those given in NAVSEAINST 9310.1A.

---

*Bis, R. F., Code R33, Naval Surface Weapons Center, Silver Spring, White Oak, Maryland, Private Communication, 1983.

Safety related incidents involving conventional battery systems in the United States are reported to the U.S. Consumer Product Safety Commission.[111] From data obtained through the emergency rooms from a sample of hospitals, the National Electronic Injury Surveillance System (NEISS) then calculates a projected estimate to the total U.S. population based upon the number of injuries in the sample. For the calendar year 1982, an estimated $21,972 \pm 6470$ (95 percent confidential interval) injuries occurred in the U.S. and its territories which were the direct result of incidents involving batteries. NEISS classifies the batteries only as "wet cells," "dry cells," or "battery, not specified" so that individual battery systems are not given in the data.

Additional data obtained from the National Injury Information Clearinghouse (NIIC) does indicate both the extent of injuries and sufficient information to determine the battery systems involved in the incidents.[111] For example, from the data representing the accident reports to NIIC for the period 1 January 1982 to 31 January 1984, it is apparent that 50 percent of the incidents involved lead-lead dioxide Starting, Lighting, and Ignition (SLI) batteries after being subjected to short circuit, charge, or forced discharge through various means. Further, nearly 40 percent of the incidents were related to those battery systems commonly used in flashlights, small, portable, electronic devices, toys, and cameras (i.e., Leclanche and "alkaline" systems). Eight percent of the injuries were the result of children swallowing small batteries used as power sources for wrist watches, hearing aids, and small hand held calculators. It is interesting to note that only one incident was reported which involved a lithium battery.

The specific intention of the present work is the correlation of data relative to the safety characteristics of non-lithium primary and secondary battery systems of interest to the U.S. Navy. In particular, prime importance is placed upon the safety issues of these systems as they directly relate to the four specific test procedures of NAVSEAINST 9310.1A. However, the scope of the work is not limited to NAVSEAINST 9310.1A procedures and extends to further include specific safety related issues unique to each non-lithium primary and secondary system. Tables 1 and 2 list those non-lithium primary and secondary battery systems, respectively, which are included in the present study. It should be noted, however, that some of the battery systems listed in Tables 1 and 2 are not well represented in the technical literature or are presently of little interest to the U.S. Navy. As a consequence, discussion of these systems may be limited. Examples include the zinc-potassium iodate, zinc-sodium dichromate, zinc-silver chloride, magnesium-bismuth oxide, magnesium-sulfur primary batteries as well as the iron (III)chromium (II) "REDOX," cadmium-silver chloride, and cadmium-oxygen secondary batteries. On the other hand, some battery systems given in the tables are, at present, in the research and development or advanced development phases and are not yet commercially available. There exists the very definite possibility that many such systems will be of importance to the U.S. Navy in a variety of applications. These systems include the calcium-thionyl chloride and calcium-sulfuryl chloride primary systems as well as aluminum-oxygen, sodium-sulfur, zinc-bromine, and zinc-chlorine secondary systems. Consequently, relevant data for these systems are included in this study with the intention that the data be revised once the systems are available for U.S. Navy applications.

TABLE 1.   PRIMARY BATTERY SYSTEMS INCLUDED IN STUDY
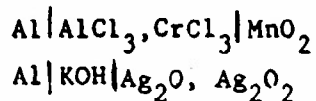
A.   ALUMINUM SYSTEMS

$Al \mid AlCl_3, CrCl_3 \mid MnO_2$
$Al \mid KOH \mid Ag_2O, Ag_2O_2$

B.   CADMIUM SYSTEMS

$Cd \mid KOH \mid HgO$

C.   CALCIUM SYSTEMS

$Ca \mid Ca(AlCl_4)_2 \mid SOCl_2$
$Ca \mid Ca(AlCl_4)_2 \mid SO_2Cl_2$

D.   LAD SYSTEMS

$Pb \mid HBF_4 \mid PbO_2$
$Pb \mid HClO_4 \mid PbO_2$

E.   MAGNESIUM SYSTEMS

$Mg \mid MgBr_2 \mid Bi_2O_3$
$Mg \mid Sea\ Water \mid PbCl_2$
$Mg \mid MgBr_2 \mid MnO_2$
$Mg \mid Mg(NO_3)_2, NaNO_2 \mid O_2$
$Mg \mid Sea\ Water \mid AgCl$
$Mg \mid MgBr_2 \mid S$

F.   THERMAL SYSTEMS

$Ca \mid KCl, LiCl \mid CaCrO_4$

G.   ZINC SYSTEMS

$Zn \mid NH_4Cl \mid MnO_2$
$Zn \mid NH_4Cl, ZnCl_2 \mid MnO_2$
$Zn \mid KOH \mid MnO_2$
$Zn \mid KOH \mid HgO$
$Zn \mid KOH \mid HgSO_4 \cdot 2HgO$
$Zn \mid KOH \mid O_2$
$Zn \mid H_2SO_4 \mid KIO_3$
$Zn \mid Mg(ClO_4)_2 \mid AgCl$
$Zn \mid KOH \mid Ag_2O, Ag_2O_2$
$Zn \mid H_2SO_4 \mid Na_2Cr_2O_7$

4

TABLE 2. SECONDARY BATTERY SYSTEMS INCLUDED IN STUDY

A. ALUMINUM SYSTEMS

$Al|Sea Water|O_2$

B. CADMIUM SYSTEMS

$Cd|KOH|NiOOH$
$Cd|KOH|O_2$
$Cd|CdCl_2,ZnCl_2|AgCl$
$Cd|KOH|Ag_2O,Ag_2O_2$

C. HYDROGEN SYSTEMS

$H_2|KOH|NiOOH$
$LaNi_5H_6|KOH|O_2$
$H_2|KOH|Ag_2O,Ag_2O_2$

D. IRON SYSTEMS

$Fe^{3+}|HCl|Cr^{2+}$
$Fe|KOH|NiOOH$
$Fe|KOH|O_2$
$Fe|KOH|Ag_2O,Ag_2O_2$

E. LEAD SYSTEMS

$Pb|H_2SO_4|PbO_2$

F. SODIUM SYSTEMS

$Na|\beta''-Al_2O_3|S$
$Na|Na^{1+} glass|S$

G. ZINC SYSTEMS

$Zn|ZnBr_2|Br_2$
$Zn|ZnCl_2|Cl_2$
$Zn|H_2SO_4|PbO_2$
$Zn|KOH|NiOOH$
$Zn|KOH|Ag_2O, Ag_2O_2$
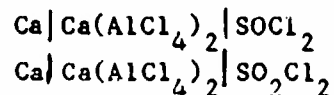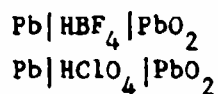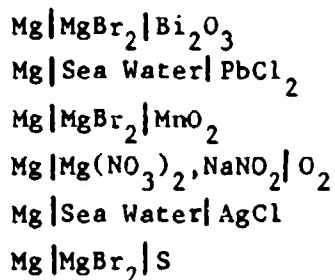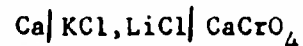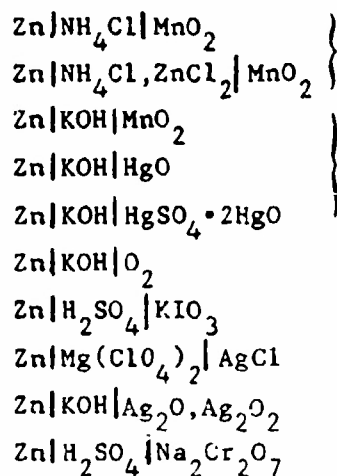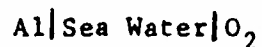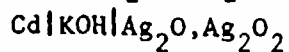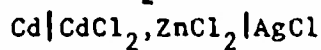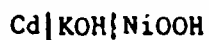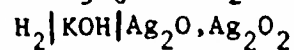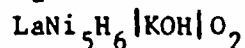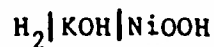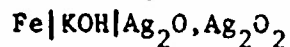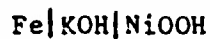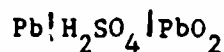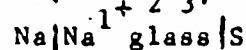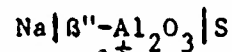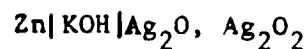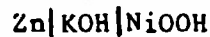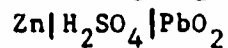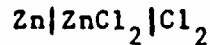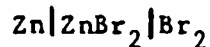
Many electrochemical systems exist which are of no interest to the U.S. Navy or are beyond the scope of this work. Table 3 gives some examples of the systems which are excluded from the present study. Since standard cells[112,113] are not power sources and are never utilized in applications which require the delivery of current, the employment of such devices as reference voltage standards represents virtually no hazard to the user relative to NAVSEAINST 9310.1A testing. A number of battery systems also exist which were formerly of importance to many U.S. Navy applications. These systems have been superseded in recent years by either more advanced conventional systems or lithium primary systems. Though the performance and safety characteristics of these outdated systems are not discussed herein, sufficient data has been published for some of the systems to be included in a similar study should the need arise. Further, solid state systems, fuel cell systems, and lithium systems are not considered in the present study and are beyond the scope of this work. It should be noted, however, that a parallel study for lithium battery systems is presently being conducted.*

STUDY APPROACH

A significant number of non-lithium battery systems have been developed and are currently used in a wide variety of applications by the U.S. Navy. It is reasonable to assume, however, that there are deficiencies associated with such systems. Most notable are the safety aspects associated with specialized applications requiring high rates of discharge leading to possible voltage reversal of some cells within the battery, the inadvertent short circuiting of the battery, and the exposure of the battery to a high temperature environment. In addition, some primary batteries may be charged electrically through use of an external power supply or by one or more parallel strings of the same battery or secondary batteries may be overcharged at high rates beyond the cutoff voltage level. The above conditions may lead to situations in which personnel and equipment are exposed to hazardous conditions. Though non-lithium battery systems possess less specific energy and less reactive characteristics than lithium battery systems, safety incidents have nonetheless occurred, as noted previously.

While detailed investigations have been conducted on the performance and shelf life characteristics for many of the conventional battery systems, relevant data concerning the safety features have not been correlated. The specific intent of this study is the determination of the safety characteristics for a number of primary and secondary systems of interest to the U.S. Navy and to correlate the known safety data in relation to the testing specified in NAVSEAINST 9310.1A. It should be further noted that the data are not restricted to the specific electrical and thermal abuse testing of NAVSEAINST 9310.1A and extend beyond the scope of NAVSEAINST 9310.1A to include those safety related characteristics intrinsic to each battery system.

---

*Bis, R. F., Code R33, Naval Surface Weapons Center, Silver Spring, White Oak, Maryland, Private Communication, 1983.

TABLE 3.   ELECTROCHEMICAL SYSTEMS EXCLUDED IN STUDY

I.   Standard Cells

    A.   Daniell $Zn|ZnSO_4-CuSO_4|Cu$

    B.   Clark $Zn|ZnSO_4-Hg_2SO_4|Hg$

    C.   Weston $Cd|CdSO_4-Hg_2SO_4|Hg$

    D.   Gouy $Zn|ZnSO_4-HgO|Hg$

    E.   Carhart-Clark $Zn|ZnSO_4-Hg_2SO_4|Hg$

    F.   Weston-Clark $Zn|ZnSO_4-Hg_2SO_4|Hg$

    G.   Helmholtz $Zn|ZnCl_2-HgCl|Hg$

    H.   De La Rue $Zn|ZnCl_2-AgCl|Ag$

II.   Outdated Systems

    A.   Ammonia Reserve Batteries (Vapor and liquid)

    B.   Lalande/Chaperon: $Zn|NaOH|CuO$

    C. $Mg|Sea Water|PbO_2$

    D.   Al (alloy)$|AlCl_3-NaCl|Cl_2$

    E. $Cd|H_2SO_4|PbO_2$

    F. $Mg|MgCl_2|CuCl$

    G. $Zn|NH_4OH|V_2O_5$

    H. $In|KOH|HgO$

    I. $Mg|MgBr_2|m$-dinitrobenzene

III.   Solid State Systems

IV.   Fuel Cell Systems

V.   Lithium Systems

In order to accomplish the study goals as given above, a number of data sources were extensively reviewed to obtain as much pertinent information relative to the safety and operational characteristics for each electrochemical system. The nature and extent of each source is described below:

1. Information retrieval sources - A significant number of documents relating to the safety/hazards and performance characteristics for a variety of state-of-the-art primary and secondary batteries are listed in various governmental and private database systems. The databases employed for the present study and the search period covered are given as follows:

    o   CA SEARCH, Chemical Abstracts, American Chemical Society, (1967 to 1983).

    o   NTIS, National Technical Information Service, U.S. Dept. Commerce (1964 to 1984).

    o   DOE ENERGY, Department of Energy (1974 to 1984).

    o   ELECTRIC POWER DATABASE, Electric Power Research Institute (1972 to 1983).

    o   ENERGYLINE, Environmental Information Center, Inc. (1971 to 1983).

    o   Ei ENGINEERING MEETINGS, Engineering Information, Inc. (1980 to 1983).

    o   SCISEARCH, Institute for Scientific Information (1974 to 1983).

    o   CONFERENCE PAPERS INDEX, Cambridge Scientific Abstracts (1973 to 1983).

    o   SSIE CURRENT RESEARCH, National Technical Information Service, U.S. Dept. Commerce (1978 to mid-1982).

2. Open technical literature - Many primary and secondary battery systems were developed and achieved the state-of-the-art status prior to the successful use of information retrieval services. Some examples include the lead-lead dioxide, nickel-cadmium, and silver-zinc secondary systems as well as the familiar Leclanche (carbon-zinc), zinc-air, mercury-zinc, and mercury-cadmium primary systems. As a result, the search included examination of data from technical papers and books published prior to the onset of machine-readable data systems. The most recent data, published following the termination of the database searches, are included in this study. It should be noted that a literature search independent of the references obtained from the information retrieval systems was conducted to account for literature containing comparative safety studies between lithium batteries and conventional battery systems and to compliment the reference works cited by the database retrieval services. In addition, a number of reference volumes were consulted to determine the electrical, performance, storability, safety, and constructional characteristics for the systems in this study.[114-137]

3. User survey - Some battery systems are exclusively employed as power sources for very specialized applications. As a result, data relative to the performance characteristics may be present in the literature, but very little specific data detailing the safety characteristics was found. One such example found was the absence of relevant safety data for thermal batteries, particularly in reference to NAVSEAINST 9310.1A testing. As a consequence, personnel at the Naval Surface Weapons Center (NSWC) and Harry Diamond Laboratories, U.S. Army Electronics Research and Development Command (ERADCOM), were surveyed. Much of the safety information for thermal batteries included in this study was obtained from personal communication with J. T. Nelson, W. E. Kuper, and M. B. Templeman of Harry Diamond Laboratories and from the reports of B. Larrick of NSWC.

4. Independent test facilities - Extensive safety testing was conducted for the zinc-chlorine electric vehicle battery and the zinc-bromine load leveling battery by Dr. Robert G. Zalosh, at Factory Mutual Research Corporation, Norwood, MA.[138,139] The data from the reports generated by the studies contributed to the preparation of the safety sections for zinc-chlorine and zinc-bromine battery systems.

5. Manufacturer's survey - Many major U.S. battery manufacturers and suppliers were contacted in the effort to obtain relevant safety data generated by the research and development, reliability, or applications engineering departments of each organization. The responses to these inquiries were limited to less than ten percent of the companies contacted. Those organizations and personnel which did respond to the survey are listed below:

    o   Energy Development Associates (a Gulf and Western Company), C. J. Warde; zinc-chlorine battery.

    o   Burgess, Inc., V. Stern; Leclanche, mercury-zinc, and "alkaline" batteries.

    o   Union Carbide Inc., M. Berger; silver-zinc, mercury-zinc, Leclanche, "alkaline," and nickel-cadmium.

    o   Eagle-Picher Inc., R. L. Higgins, R. Parker, J. Degruson; silver-zinc, nickel-iron, thermal batteries.

    o   VARTA Batteries Inc., Leclanche, "alkaline," mercury-zinc.

    In addition, the Independent Battery Manufacturer's Association Inc. (IBMA) responded with safety information and statistics for the lead-lead dioxide battery.

6. Patent literature - Many battery systems possess chemical, mechanical, electrical or electrochemical internal protective safety mechanisms. In many instances, these mechanisms have been patented. In view of the above, a patent literature survey was conducted to define specific electrical devices or safety mechanisms for many of the state-of-the-art battery systems. This search has yielded much relevant information which has been incorporated into this study.

Collectively, the data from the above sources provide a comprehensive survey of all non-lithium, state-of-the-art battery systems included in this study. It should be noted, however, that safety data gaps do exist for some of these systems, particularly relative to NAVSEAINST 9310.1A testing procedures. Specific recommendations for testing such systems in accordance with NAVSEAINST 9310.1A or testing beyond the scope of NAVSEAINST 9310.1A will be discussed in Chapter 4.

DATA PRESENTATION FORMAT

In order to fully understand the safety characteristics for an electrochemical power source, it is important to include the cell reaction, performance/electrical characteristics, storability, and construction parameters for each system included in this study. The format used to present these data for primary systems (Chapter 2) is given below:

1. System name according to negative electrode material (common system names)

2. Electrochemical symbol for the cell

3. Generally accepted cell reaction

4. Cell components:

   o   Negative electrode
   o   Positive electrode
   o   Electrolyte
   o   Separator
   o   Structural considerations

5. Performance/electrical features:

   o   Open circuit voltage
   o   Practical/theoretical energy densities
   o   Operational temperature range
   o   Discharge characteristics

6. Effect of Additives

7. Storability, shelf life

8. Uses

9. Major U.S. manufacturers, suppliers, or developers

10. Safety characteristics

    o   Relative to short circuit, voltage reversal, thermal abuse and charging (NAVSEAINST 9310.1A)

    o   Safety considerations intrinsic to the subject battery system

o   Design considerations

o   Safety mechanisms/patented devices

11. References

Additional performance/electrical features must be included for secondary battery systems (Chapter 3). These include the examination of the discharge/charge characteristics and charging methods as well as the charge retention and acceptance parameters for each secondary system.

Chapter 4 contains a summary of the results for each system included in the study and details deficiencies in available safety related data. For those systems with little or no relevant safety/hazards data or specific data gaps with respect to U.S. Navy applications, four recommendations are proposed:

1.   Testing in strict accordance with NAVSEAINST 9310.1A testing regimes

2.   Testing in accordance with appropriately modified NAVSEAINST 9310.1A testing regimes

3.   Specific testing outside the scope of NAVSEAINST 9310.1A testing regimes

4.   No future testing in the event that the subject battery system is of little interest to the U.S. Navy or in the event that the subject battery module is too large (stationary, load leveling, and electric vehicle power systems) to be tested safely at the appropriate U.S. Navy facilities.

References for Chapters 1 and 4 appear at the end of each respective chapter. References for each battery system discussed in either Chapter 2 or Chapter 3 follow the text for that battery system.

REFERENCES

1. James, S. D., Smith, P. H., and Kilroy, W. P., _J. Electrochem. Soc._, 130, 1983, p. 2037.

2. Walk, C. R., _Lithium Batteries_, Gabano, J. P., ed. (London: Academic Press, 1983) p. 281.

3. Abraham, K. M., and Pitts, L., _J. Electrochem. Soc._, 130, 1983, p. 1618.

4. Crafts, C. C., and Levy, S. C., _Safety Investigation of Discharged Lithium Sulfur Dioxide Cells_, NTIS DE82015652, U.S. Dept. Commerce, Springfield, VA, 1983.

5. Attewell, A., _Power Sources 9, Proc. 13th Int. Symp. Power Sources_, Thompson, J., ed. (London: Academic Press, 1983), p. 473.

6. Abraham, K. M., Rupich, M. W. and Pitts, L., _Investigation of Lithium-Sulfur Dioxide Battery Safety Hazards-Chemical Studies_, NTIS AD-A118363, U.S. Dept. Commerce, Springfield, VA, 1982.

7. Ebner, W. B., Kim, K. Y., Venkatasetty, H. V., _Lithium-Sulfur Dioxide (Li/SO_2) Battery Safety Hazards-Thermal Studies_, NTIS AD-A119381, U.S. Dept. Commerce, Springfield, VA., 1982.

8. Halpert, G., and Anderson, A., _Lithium/Sulfur Dioxide Cell and Battery Safety_, NTIS N83-14684, U.S. Dept. Commerce, Springfield, VA, 1982.

9. Moroz, W. J., _Safety Design Considerations for Lithium Batteries in C.F. Applications_, NTIS AD-A107619, U.S. Dept. Commerce, Springfield, VA, 1981.

10. Rupich, M. W., and Abraham, K. M., _Investigation of Lithium-Sulfur Dioxide (Li/SO_2) Battery Safety Hazard_, NTIS AD-A104326, U.S. Dept. Commerce, Springfield, VA, 1981.

11. Dey, A., _The 1980 Goddard Space Flight Center Battery Workshop_, NASA Conference Publication 2177, 1981, p. 83.

12. Dallek, S., James, S. D., and Kilroy, W. P., _J. Electrochem. Soc._, 128, 1981, p. 508.

REFERENCES (Cont.)

13. Bis, R. F., Warburton, D. L., Freeman, C. A., Hoff, G. F. and Kowalchik, L. A.. *Safety Evaluation of Photo Finish*, NTIS AD-A130203, U.S. Dept. Commerce, Springfield, VA, 1981.

14. Kilroy, W. P., and James, S. D., *J. Electrochem. Soc.*, 128, 1981, p. 934.

15. Reiss, E. H., Jr., *Proc. Power Sources Symp. 29*, 1981, p. 116.

16. Bene, J., *The 1980 Goddard Space Flight Center Battery Workshop*, NASA Conference Publication 2177, 1981, p. 111.

17. DiMasi, G. J., and Christopulos, J. A., *The 1980 Goddard Space Flight Center Battery Workshop*, NASA Conference Publication 2177, 1981, p. 61.

18. Walk, R., *The 1980 Goddard Space Flight Center Battery Workshop*, NASA Conference Publication 2177, 1981, p. 39.

19. Dey, A. N., and Holmes, R. W., *J. Electrochem. Soc.*, 127, 1980, p. 1877.

20. Dey, A. N., *J. Electrochem. Soc.*, 127, 1980, p. 1886.

21. Dallek, S., Bis, R. F., and Bowers, F. M., *Proc. Power Sources Symp. 29*, 1980, p. 109.

22. Dey, A. N., and Holmes, R. W., *J. Electrochem. Soc.*, 127, 1980, p. 775.

23. Dey, A. N., *J. Electrochem. Soc.*, 127, 1980, p. 1000.

24. Dey, A. N., and Holmes, R. W., *Analysis of Pressure Producing Reactions in Lithium-Sulfur Dioxide Cells*, NTIS AD-A064977, U.S. Dept. Commerce, Springfield, VA, 1979.

25. Dey, A. N., and Witalis, P., *Safety Studies of Lithium-Sulfur Dioxide Cells*, NTIS AD-A077277, U.S. Dept. Commerce, Springfield, VA, 1979.

26. Dey, A. N., and Holmes, R. W., *Analysis of Pressure Producing Reactions in Lithium-Sulfur Dioxide Cells*, NTIS AD-A077379, U.S. Dept. Commerce, Springfield, VA, 1979.

27. Blagdon, L. J., and Randall, B., *Safety Studies of Lithium-Sulfur Dioxide Cells*, NTIS AD-A078961, U.S. Dept. Commerce, Springfield, VA, 1979.

28. Dey, A.N., and Holmes, R. W., *J. Electrochem. Soc.*, 126, 1979, p. 1637.

29. Blagdon, L. J., and Randall, B., *Safety Studies of Lithium-Sulfur Dioxide Cells*, NTIS AD-A066378, U.S. Dept. Commerce, Springfield, VA, 1979.

30. DiMasi, G. J., and Christopulos, J. A., *Proc. Power Sources Symp. 28*, 1978, p. 179.

REFERENCES (Cont.)

31. Dallek, S., Bis, R. F., and Bowers, F. M., Temperature Profile in Lithium/Sulfur Dioxide Cells During Discharge, NTIS AD-A070378, U.S. Dept. Commerce, Springfield, VA, 1978.

32. Taylor, H., Bowden, W., and Barella, J., Proc. Power Sources Symp. 28, 1978, p. 183.

33. Shah, P.M., Proc. Power Sources Symp. 28, 1978, p. 188.

34. Dey, A. N., Safety Studies of Lithium-Sulfur Dioxide Cells, NTIS ADA062708, U.S. Dept. Commerce, Springfield, VA, 1978.

35. Kilroy, W. P., and Dallek, S., Thermal Analysis of Some Components of the Lithium-Sulfur Dioxide Cell, NTIS AD-A062983, U.S. Dept. Commerce, Springfield, VA, 1978.

36. Kilroy, W. P., and Dallek, S., J. Power Sources, 3, 1978, p. 291.

37. Bene, J., The 1977 Goddard Space Flight Center Battery Workshop, NASA Conference Publication 2041, 1977, p. 565.

38. Bowers, F. M., Safe, Useful Lithium Batteries for the Navy, NTIS ADA080166, U.S. Dept Commerce, Springfield, VA, 1977.

39. DiMasi, G., Proc. Power Sources Symp. 27, 1976, p. 75.

40. Taylor, H., and McDonald, B., Proc. Power Sources Symp. 27, 1976, p. 66.

41. Hunger, H. F., and Christopulos, J. A., Preliminary Safety Analysis of Lithium Batteries, NTIS AD-A006149, U.S. Dept. Commerce, Springfield, VA, 1975.

42. Giltner, J., Nonhazardous Primary Lithium-Organic Electrolyte Batteries, NTIS AD-A014066, U.S. Dept. Commerce, Springfield, VA, 1975.

43. Watson, T., Nonhazardous Primary Lithium-Organic Electrolyte Battery BA-5590/U, NTIS AD-A003312, U.S. Dept. Commerce, Springfield, VA, 1974.

44. Abens, S., Nonhazardous Lithium Organic Electrolyte Batteries, NTIS AD-A020144, U.S. Dept. Commerce, Springfield, VA, 1974.

45. Warburton, D. L., Proc. Power Sources Symp. 26, 1974, p. 34.

46. Attia, A. I., Gabriel, K. A., and Burns, R. P., Investigation of Lithium Thionyl Chloride Battery Safety Hazards, NTIS AD-A128382, U.S. Dept. Commerce, Springfield, VA, 1983.

47. Peled, E., Lombardi, A., and Schlaikjer, C. R., J. Electrochem, Soc., 130, 1983, p. 1365.

REFERENCES (Cont.)

48. Doddapaneni, N., Safety Studies on Li/SOC$_2$ Reserve Battery, NTIS ADA132279, U.S. Dept. Commerce, Springfield, VA, 1983.

49. Boyle, G. H., and Goebel, F., Proc. Power Sources Symp. 30, 1983, p. 215.

50. Attia, A. I., Goebel, K. A., and Burns, R. P., Investigation of Lithium-Thionyl Chloride Battery Safety Hazards, NTIS AD-A128382, U.S. Dept. Commerce, Springfield, VA, 1983.

51. James, S. D., Smith, P. H., and Kilroy, W. P., J. Electrochem. Soc., 130, 1983, p. 2037.

52. Attewell, A., "Power Sources 9," Proc. 13th Symp. Power Sources, Thompson, J., ed. (London: Academic Press, 1983), p. 473.

53. Carter, B., Williams, R., Tsay, F., Rodriguez, A., and Frank, H., Proc. 17th IECEC, American Society of Mechanical Engineers, 2, 1982, p. 638.

54. Salmon, D. J., Peterson, M. E., Henricks, L. L., Abels, L. L., and Hall, J. C., J. Electrochem. Soc., 129, 1982, p. 2496.

55. Kim, K. Y, and Chua, D. L., Prog. Batteries Sol. Cells, 4, 1982, p. 58.

56. N. Marincic and J. Epstein, Prog. Batteries Sol. Cells, 4, 1982, p. 37.

57. Dey, A. N., and Hamilton, N., J. Appl. Electrochem., 12, 1982, p. 33.

58. McDonald, R. C., Dampier, F. W., Wang, P., and Bennett, J. M., Investigation of Lithium-Thionyl Chloride Battery Safety Hazards, NTIS AD-A129302/6, U.S. Dept. Commerce, Springfield, VA, 1982.

59. McDonald, R. C., Investigation of Lithium-Thionyl Chloride Battery Safety Hazards, NTIS AD-A129301, AD-A129300, AD-A129299, U.S. Dept. Commerce, Springfield, VA, 1982, 1982, 1981.

60. Murphy, R. M., Krehl, P. W., and Liang, C. C., Proc. 16th IECEC, American Society of Mechanical Engineers, 1, 1981, p. 97.

61. Kilroy, W. P., and James, S. D., J. Electrochem. Soc., 128, 1981, p. 934.

62. Kim, K. Y., and Chua, D. L., Proc. Power Sources Symp., 29, 1981, p. 125.

63. Johnson, L. J., and Willis, A. H., Proc. Power Sources Symp., 29, 1981, p. 138.

64. Murphy, R. M., The 1980 Goddard Space Flight Center Battery Workshop, NASA Conference Publication 2177, 1981, p. 23.

65. Wong, D., Bowden, W., Hamilton, N., Cubbison, D., and Dey, A. N., Lithium Thionyl Chloride Battery, NTIS AD-A098727, U.S. Dept. Commerce, Springfield, VA, 1981.

REFERENCES (Cont.)

66. Liang, C. C., Krehl, P. W., and Danner, D. A., J. Appl. Electrochem., 11, 1981, p. 563.

67. Zolla, A. E., Waterhouse, R., DeBiccari, D., and Griffin, C. L., Primary Lithium-Thionyl Chloride Cell Evaluation, NTIS AD-A094660, U.S. Dept. Commerce, Springfield, VA, 1981.

68. Dallek, S., James, S. D., and Kilroy, W. P., J. Electrochem. Soc., 128, 1981, p. 508.

69. Zolla, A. E., High Energy Density Battery Lithium Thionyl Chloride Improved Reverse Voltage Design, NTIS AD-A113498, U.S. Dept. Commerce, Springfield, VA, 1981.

70. Goebel, F., McDonald, R., and Younger, G., Lithium Inorganic Electrolyte Battery Development, NTIS AD-A098711, U.S. Dept. Commerce, Springfield, VA, 1981.

71. Dey, A. N., and Hamilton, N., "Power Sources 8," Proc. 12th Int. Symp. Power Sources, Thompson, J., ed. (London: Academic Press, 1981), p. 41.

72. Babai, M., Prog. Batteries Sol. Cells, 3, 1980, p. 110.

73. Marincic, N., and Goebel, F., J. Power Sources, 5, 1980, p. 73.

74. Dey, A. N., J. Power Sources, 5, 1980, p. 57.

75. Zupancic, R. L., Urry, L. F., and Alberto, V. S., Proc. Power Sources Symp. 29, 1980, p. 157.

76. Garoutte, K. F., and Chua, D. L., Proc. Power Sources Symp. 29, 1980, p. 153.

77. Johnson L. J., and Willis, A. H., Proc. Power Sources Symp. 29, 1980, p. 138.

78. Babai, M., and Zak, V., Proc. Power Sources Symp. 29, 1980, p. 150.

79. Abraham, K. M., and Mank, R. M., Proc. Power Sources Symp. 29, 1980, p. 150.

80. Abraham, K. M., Mank, R. M., and Holleck, G. L., Investigations of the Safety of Li/SOC_2 Batteries, NTIS AD-A081998, U.S. Dept. Commerce, Springfield, VA, 1980.

81. Abraham, K. M., Mank, R. M., and Holleck, G. L., Investigations of the Safety of Li/SOC_2 Batteries, NTIS AD-A077894, U.S. Dept. Commerce, Springfield, VA, 1979.

82. Abraham, K. M., Mank, R. M., and Holleck, G. L., Investigations of the Safety of Li/SOC_2 Batteries, NTIS AD 7 P 2, U.S. Dept. Commerce, Springfield, VA, 1979.

REFERENCES (Cont.)

83. Abraham, K. M., Mank, R. M., and Holleck, G. L., <u>Investigations of the Safety of Li/SOC$_2$ Batteries</u>, NTIS AD-A069797, U.S. Dept. Commerce, Springfield, VA, 1979.

84. Abraham, K. M., Gudrais, P. G., Holleck, G. L., and Brummer, S. B., <u>Proc. Power Sources Symp. 28</u>, 1978, p. 255.

85. Dey, A. N., <u>Proc. Power Sources Symp. 28</u>, 1978, p. 251.

86. Chua, D. I., Crabb, J. O., and Deshpande, S. L., <u>Proc. Power Sources Symp. 28</u>, 1978, p. 247.

87. Morley D., and Solar, R. J., <u>Proc. Power Sources Symp. 28</u>, 1978, p. 232.

88. McCartney, J. F., Shipman, W. H., Gunderson, C. R., and Koehler, C. W., <u>Development of Lithium Inorganic Electrolyte Batteries for Navy Applications</u>, NTIS AD-A047658, U.S. Dept. Commerce, Springfield, VA, 1977.

89. Chua D. L., and Walk, C. R., <u>Lithium Inorganic Electrolyte Battery Investigation</u>, NTIS AD-A043364, U.S. Dept. Commerce, Springfield, VA, 1977.

90. Dey, A. N., <u>Proc. Power Sources Symp. 27</u>, 1976, p. 42.

91. McCartney, J. F., Shipman, W. H., and Gunderson, C. R., <u>Development of Lithium Electrolyte Batteries for Navy Applications</u>, NTIS AD-A020844, U.S. Dept. Commerce, Springfield, VA, 1975.

92. Murphy, R. M., and Liang, C. C., <u>J. Electrochem. Soc.</u>, <u>130</u>, 1983, p. 1231.

93. Murphy, R. M., and Liang, C. C., <u>J. Appl., Electrochem.</u>, <u>13</u>, 1983, p. 439.

94. Liang, C. C., Bolster, M. E., and Murphy, R. M., <u>J. Electrochem. Soc.</u>, <u>128</u>, 1981, p. 1631.

95. Murphy, R. M., Krehl, P. W., and Liang, C. C., <u>Proc. 16th IECEC</u>, American Society of Mechanical Engineers, 1, 1981, p. 97.

96. Murphy, R. M., <u>The 1980 Goddard Space Flight Center Battery Workshop</u>, NASA Conference Publication 2177, 1981, p. 23.

97. Potts, T. M., <u>Proc. Power Sources Symp. 30</u>, 1983, p. 183.

98. Attewell, A., "Power Sources 9," <u>Proc. 13th Int. Symp. Power Sources</u>, Thompson, J., ed. (London: Academic Press, 1983), p. 473.

99. Kawauchi, S., Kawakubo, E., Aoki, K., and Eza, M., <u>Prog. Batteries Sol. Cells</u>, 4, 1982, p. 87.

100. Attewell, A., "Power Sources 9," <u>Proc. 13th Int. Symp. Power Sources</u>, Thompson, J., ed. (London: Academic Press, 1983), p. 473.

REFERENCES (Cont.)

101. Bates, R. E., Murphy, B. P., White, G. D., and Attewell, A., _Proc. Power Sources Symp. 30_, 1983, p. 175.

102. Bates R., and Jumel, Y., _Lithium Batteries_, Gabano, J. P., ed. (London: Academic Press, 1983), p. 73.

103. Arzur, J. P., _Prog. Batteries Sol. Cells_, 4, 1982, p. 49.

104. Bredland, A. M., Messing, T. G., and Paulson, J. W., _Proc. Power Sources Symp. 29_, 1980, p 82.

105. Cuesta, A. J., and Bump, D. D., _Proc. Electrochem. Soc. Mtg._, 80-4, 1980, p. 95.

106. Hampartzumian, K., and Iltchev, N., "Power Sources 8," _Proc. 12th Int. Symp. Power Sources_, Thompson, J., ed. (London: Academic Press, 1982), p. 35.

107. Ikeda, H., Hara, M., Narukawa, S., and Nakaido, S., _Proc. Manganese Dioxide Symp._, 1981, p. 395.

108. Ikeda, H., Nakaido, S., and Satoshi, S., _Proc. Power Sources Symp. 29_, 1980, p. 91.

109. Walk, C. R., _Lithium Batteries_, Gabano, J. P., ed. (London: Academic Press, 1983), p. 265.

110. Johnson, D. M., NAVSEAINST 9310.1A, Dept. of the Navy, Naval Sea Systems Command, Washington, D.C. (1982). Availability: Commanding Officer, Naval Publications and Forms Center, 5801 Tabor Ave., Philadelphia, PA. 19120.

111. Johnston, N. S., Director, National Injury Information Clearinghouse, U.S. Consumer Product Safety Commission, Washington, D.C., 1984.

112. Mantell, C. L., _Batteries and Energy Systems_, Second Edition (New York: McGraw Hill, 1983), p. 8.

113. Vinal, G. W., _Primary Batteries_, (New York: John Wiley and Sons, 1950), p. 165.

114. Falk, S. U., and Salkind, S. A., _Alkaline Storage Batteries_ (New York: John Wiley and Sons, 1969).

115. Smith, G., _Storage Batteries_ (London: Sir Isaac Pitman and Sons, 1964).

116. Friedman, E. J., Mouchahoir, G. E., Farah, O. G., Ouellette, R. P., and Cheremisinoff, P. N., _Electrotechnology, Volume 3_, Ann Arbor, MI, 1980.

117. Vinal, G. W., _Primary Batteries_ (New York: John Wiley and Sons, 1950).

REFERENCES (Cont.)

118. Vinal, G. W., Storage Batteries, (New York: John Wiley and Sons, 1940).

119. Mantell, C. L., Batteries and Energy Systems, Second Edition (New York: McGraw Hill, 1983).

120. Tobias, C. W., ed., Advances in Electrochemistry and Electrochemical Engineering, Volume 8, Wiley Interscience, New York, 1971.

121. Crompton, T. R., "Small Batteries," Volume I, Secondary Cells (New York: John Wiley and Sons, 1982).

122. T. R. Crompton, "Small Batteries," Volume 2, Primary Cells (New York: John Wiley and Sons, 1983).

123 Bockris, J. O'M., Conway B. E., Yeager, E., and White R. E., eds., Comprehensive Treatise of Electrochemistry, Volume 3, Electrochemical Energy Conversion and Storage (New York: Plenum Press, 1981).

124. Thirsk H. R., ed., "Electrochemistry," Volume 4, The Chemical Society, London, 1974.

125. Heise G. W., and Cahoon N. C., eds., The Primary Battery, Volume 1 (New York: John Wiley and Sons, 1971).

126. Heise, G. W., and Cahoon, N. C., eds., The Primary Battery, Volume II (New York: John Wiley and Sons, 1974).

127. Barak, M., ed., Electrochemical Power Sources, Primary and Secondary Batteries, IEE Energy Series I (London: Peter Peregrinus Ltd., 1980).

128. Kordesch, K. V., ed., Batteries, Volume I, Manganese Dioxide (New York: Marcel Dekker, Inc., 1974).

129. Ouellette, R. P., Ellerbusch, F., and Cheremisinoff, P. N., eds., Electrotechnology, Volume 2, Applications in Manufacturing, Ann Arbor Science, Ann Arbor, MI, 1978.

130. Bode, H., Lead-Acid Batteries, translated by R. J. Brodd and K. V. Kordesch (New York: John Wiley and Sons, 1977).

131. McCallum, J., Thomas, R. F., and Waite, J. H., Accelerated Testing of Space Batteries, NASA SP-323, National Aeronautics and Space Administration, NTIS, Springfield, VA, 1973.

132. Scott, W. R., and Rusta, D. W., "Sealed-Cell Nickel Cadmium Battery," Applications Manual, NASA Reference Publication 1062, National Aeronautics and Space Administration, Greenbelt, MD, 1979.

133. Gregory, D. P., Metal-Air Batteries (London: Mills and Boon Limited, 1972).

REFERENCES (Cont.)

134. Hamilton, W., "Electric Automobiles," Energy, Environmental, and Economic Prospects for the Future (New York: McGraw-Hill Book Company, 1980.)

135. Colie, M. J., ed., "Electric and Hybrid Vehicles," Energy Technology Review, No. 44, Noyes Data Corp., Park Ridge, NJ, 1979.

136. Kordesch, K. V., ed., "Batteries," Volume 2, Lead-Acid Batteries and Electric Vehicles, Marcel Dekker, New York, 1977.

137. Fleischer, A., and Lander, J. J., eds., Zinc-Silver Oxide Batteries (New York: John Wiley and Sons, 1971).

138. Zalosh, R. G., Bajpai, S. N., Short T. P., and Tsui, R. K., Chlorine Hazard Evaluation for the Zinc-Chlorine Electric Vehicle Battery, Final Technical Report COO-5088-1, Factory Mutual Research Corporation, Norwood, MA, 1980.

139. Zalosh, R. G., and Bajpai, S. N., Comparative Hazard Investigation for a Zinc-Bromine Load-Levelling Battery, Final Technical Report RC80-T-53, Factory Mutual Research Corporation, Norwood, MA., 1980.

CHAPTER 2

PRIMARY BATTERY SYSTEMS

A. ALUMINUM-MANGANESE DIOXIDE
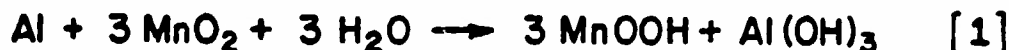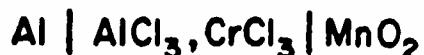
$$AI \mid AICl_3, CrCl_3 \mid MnO_2$$

$$AI + 3\,MnO_2 + 3\,H_2O \longrightarrow 3\,MnOOH + AI(OH)_3 \quad [1]$$

Aluminum has been studied extensively as a candidate material for negative electrodes in a number of electrochemical systems.[1] Its advantages include low cost, availability, low equivalent weight (9.0 grams per equivalent), and safety in handling. Several problems, however, have inhibited the use of the metal in many commercial power source devices. Bare aluminum will undergo excessive corrosion and liberate hydrogen:

$$2Al + 6H_2O \longrightarrow 2Al(OH)_3 + 3H_2 \qquad (2)$$

In addition, aluminum may be less anodic than zinc in NH_4Cl electrolyte due to its oxide protective layer. Practical aluminum cells also exhibit voltage delay characteristics following load application. Pure aluminum corrodes unevenly, leading to premature cell failure due to can perforation.

A number of attempts have been made to alleviate the above problems. One method employed the use of a two layer electrode comprised of aluminum alloys of different electrode potentials.[2] The innermost alloy would necessarily be more anodic and protect the outermost alloy from corrosion. Much work was also carried out to develop more anodic alloys having increased corrosion resistance.[3] All developmental efforts of the aluminum-manganese dioxide system have made use of the two layer electrode method.[4,5] The inner electrode layer was fabricated from aluminum (99.8% purity) and one to five percent zinc while the outer layer was an alloy of aluminum (99.8% purity and 1.2% manganese).

Various compositions of either Gold Coast or electrolytic manganese dioxide with Shawinigan acetylene black were mixed with electrolyte and compacted at 200 psi into the aluminum cans. The electrolyte salts of $AlCl_3 \cdot 6H_2O$ and $CrCl_3 \cdot 6H_2O$ were found to be less corrosive than either the NH_4Cl or the mixture of NH_4Cl and $ZnCl_2$ electrolyte salts used in Leclanche cells. A corrosion inhibitor of $(NH_4)_2CrO_4$ was also added to the positive electrode mixture. One further advantage found for the addition of $(NH_4)_2CrO_4$ was that no further increase in voltage delay upon load application was observed. A centrally located carbon rod inserted into the above mixture served as the current collector.

Most separator materials normally used in Leclanche cells were found to be unstable in the acidic solutions described above. As a result, some tests were performed using uncoated paper. However, it was found that, for commercial applications, such papers exhibited poor wet strength,excessive porosity, and nonuniformity which would lead to internal short circuiting of the cell. In view of the above, a separator was developed[6] which consisted of the colloids of locust bean and karaya gum coated onto a high wet-strength paper. These colloids swell in the electrolyte solution and fill the voids between the paper and aluminum electrode surface. The use of the separator improved the storability and reduced the voltage delay. Only D size cells were fabricated and tested in all cited investigations.

The open circuit voltages for the cells as described above were observed to be between 1.58 and 1.62 V. The performance characteristics were determined for D cells discharged under resistive loads using continuous and intermittent test regimes. Leclanche cells were similarly tested for comparison purposes. Results showed that the aluminum-manganese dioxide cells were far superior to Leclanche cells when discharged continuously (e.g., 6.25 h versus 3.3 h to a 0.90 V cutoff for $Al-MnO_2$ and $Zn-MnO_2$ D cells respectively, discharged under 4.0 ohm loads). When cells were discharged on intermittent or long-term test regimes, however, the $Zn-MnO_2$ cells were clearly superior (e.g., 11.7 h versus 8.7 h to a 0.90 V cutoff for $Zn-MnO_2$, and $Al-MnO_2$, D cells, respectively, intermittently discharged under 4.0 ohm loads).

Two factors were found to limit the capacity of aluminum-manganese dioxide cells.[4] First, the anode corrosion reaction (equation 2) consumed hydrogen ions, exceeding the buffer capabilities of the electrolyte and the pH of the electrolyte rose. As a result, the voltage of the MnO_2 half cell reaction was reduced and the cell voltage level reached a given cutoff voltage more quickly. Secondly, the internal resistances of the cells increased considerably after only short periods of discharge. The cause for the increase in resistance was believed to be the accumulation of voluminous amounts of $Al(OH)_3$ from both the cell and the corrosion reactions (equations 1 and 2).

Storability tests have yielded mixed results. Discharge test results for the best cells indicated that the capacity retention was 95 to 100 percent for cells stored three years and 60 to 75 percent for cells stored seven years. Other cell lots yielded much poorer results.[1]

Gas evolution during continuous discharge invariably caused seal rupture and leakage of cells.[4] Cells which were fabricated with dimethyl silicone vent structures however, did not leak during continuous discharge test regimes. It should be noted that no hydrogen-air (oxygen) gas explosions were reported in the literature for the aluminum-manganese dioxide system,[3-9] even though excessive gassing was reported.

No safety/hazards data were reported for the aluminum-manganese dioxide system. In view of the fact that the system is not presently available commercially (the technological problems cited herein must first be overcome), testing in accordance with NAVSEAINST 9310.1A could not be initiated at this time.

22

REFERENCES

1. Stokes, J. J., Jr., and Belitskus, D., _The Primary Battery_, Volume II, Heise, G. W., and Cahoon, N. C., eds. (New York: John Wiley and Sons, Chapter 3, 1976).

2. Stokes, J. J., Jr., U.S. Patent 2,796,456, 1957.

3. Glicksman, R., _J. Electrochem. Soc._, 106, 1959, p. 457.

4. Belitskus, D., _J. Electrochem. Soc._, 119, 1972, p. 295.

5. Stokes, J. J., Jr., _Electrochem. Technol._, 6, 1968, p. 36.

6. Cahoon N. C., and Korver, M. P., _J. Electrochem. Soc._, 106, 1959, p. 469.

7. Brodd, R. J., Kozawa, A., and Kordesch, K. V., _J. Electrochem. Soc._, 125, 1978, p. 271 C.

8. _Kirk-Othmer Encyclopedia of Chemical Technology_, Second Edition, Vol. 3, 1964, p. 99.

9. _Kirk-Othmer Enclyclopedia of Chemical Technology_, Third Edition, Vol. 3, 1978, p. 503.

B. ALUMINUM-SILVER OXIDE

$$Al \mid KOH \mid Ag_2O_2$$

$$4\,Al + 3\,Ag_2O_2 + 4\,KOH \longrightarrow 4\,KAlO_2 + 6\,Ag + 2\,H_2O \qquad [1]$$
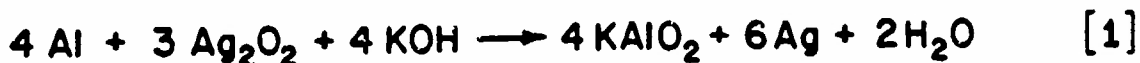
The aluminum-silver oxide battery is currently under development by Yardney Electric Corporation as a power source for the U.S. Navy's Advanced Lightweight Torpedo (ALWT) program. The unit consists of proprietary aluminum alloy negative electrodes and Ag_2O_2 positive electrodes in a pile construction with devices for electrolyte circulation and heat exchange.

Aluminum will undergo reaction with water in basic media and produce hydrogen in accordance with either:

$$2Al + 2H_2O + 2KOH \longrightarrow 2KAlO_2 + 3H_2 \tag{2}$$

or

$$2Al + 6H_2O \longrightarrow 2Al(OH)_3 + 3H_2 \tag{3}$$

The corrosion rate (equations 2 or 3) under open circuit conditions was found to be much greater than that observed for the battery under practical loading conditions (i.e., at current densities as great as 1.2 A/cm^2). Initial efforts concerned the development of an aluminum alloy electrode (RX808Al) capable of high current densities within high rate discharge regimes and minimal corrosion under operating conditions. It was further found that the addition of approximately 20 grams per liter of $NaSn(OH)_6$ to the electrolyte mixture significantly reduced the corrosion reaction.

The positive plates consisted of sintered silver oxide (Ag_2O_2) electrodes containing 0.89 mm diameter glass beads used for interelectrode separation. The total interelectrode separation for the battery was determined to be between 0.50 mm and 0.64 mm based upon optimum reaction product removal requirements as well as stack resistance considerations.

A heat exchanger is necessary to reject both the excess heat due to the potential drop under load conditions (I^2R heating) and the heat from the aluminum corrosion reaction. It was found that, when the battery approaches open circuit voltage, the heat generation rate also increases due to the predominance of the aluminum corrosion reaction.

The successful operation of the battery is dependent upon a pump to circulate the electrolyte throughout the cell stack. The function of electrolyte circulation is threefold: (1) removal of H_2 from the interelectrode and intercell spacings, (2) removal of the voluminous reaction products from both the intercell spacings and the pores of the silver oxide electrodes, and (3) provision for heat rejection capability. Should electrolyte circulation not be provided, the operation of the battery would be severely limited, particularly in view of the intended application requirements.

The optimum KOH concentration levels for the proper maintenance of cell load voltages and gas evolution rates was found to be between 15 and 35 weight percent in sea water. In order to maintain a balance between the dissolution and consumption rates of KOH, KOH in the form of flakes, pellets, and cast blocks were included. When the torpedo is launched, sea water dissolves the KOH flakes rapidly, bringing both the concentration and temperature to the desired operational levels. As battery discharge continues, the KOH concentration is maintained by the slower dissolution rates of the pellets and blocks.

The open circuit voltage for the aluminum silver oxide system is approximately 2.4 V. Discharge tests were performed at electrolyte temperatures of 60°C and 100°C. The results showed that the load voltage levels are significantly higher at the higher temperature for cells discharged at identical current densities. For example, for cells discharged at current densities of $0.78 \ A/cm^2$ and $1.24 \ A/cm^2$, the load voltages at 60°C were 1.53 V and 1.38 V, respectively, while at 100°C the corresponding load voltages were 1.60 V and 1.53 V, respectively. The hydrogen evolution rates, however, were significantly lower for cells discharged at the lower temperature ($0.078 \ cm^3/cm^2/minute$, average) than for cells discharged at the higher temperature ($0.46 \ cm^3/cm^2/minute$, average).

Comparison of the discharge characteristics for the aluminum-silver oxide cell to similar characteristics for either the zinc-silver oxide or magnesium-silver chloride cells showed that the load voltage levels average approximately 0.7 volt higher for the $Al-Ag_2O_2$ cell at current densities up to $0.5 A/cm^2$. The load voltages for both the zinc-silver oxide and magnesium-silver chloride cells dropped precipitously at current densities greater than $0.5 \ A/cm^2$ while a cell load voltage of 1.57 V was maintained for the $Al-Ag_2O_2$ cell at current densities up to $1.09 \ A/cm^2$.

Since the $Al-Ag_2O_2$ system remains, at the present time, in the developmental stages, no pertinent safety data was given. Should the system be selected as a power source for the ALWT, however, some testing in accordance with appropriately modified NAVSEAINST 9310.1A procedures may be necessary, particularly in view of both the high energy density (180 to 220 Wh/kg) and high power capability per unit electrode area ($1.5 \ W/cm^2$). Of special interest would be the short circuit, forced overdischarge and charge tests performed upon the activated battery under static and circulating electrolyte conditions.

26

REFERENCES

1.   Smith, D., and Kennedy, J., Proc. Power Sources Symp. 29, 1981, p. 51.

C. CADMIUM-MERCURIC OXIDE (MERCAD)

Cd | KOH | HgO

$$Cd + HgO + H_2O \longrightarrow Cd(OH)_2 + Hg \qquad [1]$$
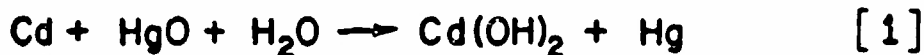
The cadmium-mercuric oxide battery system is characterized by long shelf life over a wide range of environmental conditions, discharge capability over a wide temperature range, and tolerance to extreme shock and vibration conditions. In addition, cells may be hermetically sealed due to the absence of appreciable gas evolution under storage or cell discharge conditions. In view of the above features, cadmium-mercuric oxide batteries may be utilized for many oceanographic applications[1] (e.g., Naval mines, underwater telemetry devices, air launched ground attack weapons,[16] and sealed metering devices.)[3]

Cadmium electrode material may be prepared by the reduction of cadmium oxide with zinc powder in a solution of potassium hydroxide.[2] The cadmium powder is then washed free of zinc, zinc oxide, water and potassium hydroxide and dried thoroughly under a vacuum. A second method used to prepare the cadmium electrode involved the electrodeposition of cadmium powder from a 0.2 M solution of a cadmium salt in either an acid or alkaline media at temperatures of 30°C or below.[4] The cadmium electrodes for button cell designs are formed by pressing this powder into the can. Electrical contact with the cell case is maintained through use of a cellulosic absorber which swells in contact with electrolyte solution. Centrally located cadmium electrodes in bobbin cells possess current collectors within the cadmium matrix, while electrodes for prismatic cell designs are fabricated by pressing cadmium powder onto expanded nickel screens. Typical cadmium electrode porosities vary from about 40 to 60 percent, with some reported porosities of 80 percent for specific cell operational requirements.[4]

The discharge mechanism and film formation for the cadmium electrode in alkaline electrolyte solutions have been reported by Weininger and Breiter,[5] Barnard, et al.,[6] Vijayavalli, et al.,[7] and Armstrong, et al.[8,9] A summary survey of the electrochemical behavior of sintered plate and planar cadmium negative electrode in KOH solution has been given by Armstrong, et al.[10]

The reaction for the cadmium electrode in alkaline media is given by:

$$Cd + 2OH^- \longrightarrow Cd(OH)_2 + 2e^- \tag{2}$$

The standard potential for reaction 2 is +0.809 V. One possible side reaction which could occur at the cadmium electrode to produce hydrogen gas is given by:

$$2H_2O + 2e^- \longrightarrow 2OH^- + H_2 \tag{3}$$

The standard potential for reaction 3 is -0.828 V. Therefore, the cadmium electrode is approximately 0.02 V more positive than the reversible hydrogen evolution potential. As a result, the possibility for cadmium to reduce water does exist. However, it has been shown[2] that the equilibrium pressure of H_2 in an electrolyte solution of 30 percent KOH (7M) is 7,500 Pa. Consequently, in a hermetically sealed cadmium-mercuric oxide cell, evolution of a very small amount of hydrogen would produce the equilibrium pressure and the production of H_2 would cease. In addition, the high overvoltage for hydrogen evolution on the cadmium electrode further inhibits hydrogen production in the cell, thus eliminating the possibility of reaction 3 in the cell as not energetically feasible.[11]

Gas evolution measurements from cadmium-mercuric oxide cells stored at 71°C for six months showed that approximately 0.04 cm^3 of hydrogen per gram of Cd was evolved during the initial few days of storage.[4] This hydrogen was found to be dissolved in the cadmium during the electrodeposition process. Further, the solubility of cadmium in 31 percent (7M) KOH solution was found to be only 8.5×10^{-5} M at 25°C.[1]

The mercury oxide electrode for prismatic cells is comprised of a mixture of about 75 weight percent red HgO blended with 25 weight percent of silver powder.[2] This composition produces a silver amalgam on cell discharge. The positive electrode mixture is then pressed at about 2800 kg/cm^2 onto silverplated nickel mesh or silver mesh.[2] The mercuric oxide electrodes for the button and bobbin cells are pressed directly into the container to a porosity of about 18 percent.[4] Porosities of approximately 40 percent or more are required for cell operation at temperatures less than -20°C.

The reaction for the mercuric oxide electrode in alkaline media is given by:

$$HgO + H_2O + 2e^- \longrightarrow Hg + 2OH^- \tag{4}$$

The standard potential for reaction 4 is +0.098 V. A possible side reaction which could produce gas at the mercuric oxide electrode is:

$$2H_2O + O_2 + 4e \longrightarrow 4OH^- \tag{5}$$

The standard potential for equation 5 is 0.401 V. Therefore, it can be seen that the mercuric oxide electrode is more stable by about 0.3 V negative to the reversible oxygen evolution potential. The tendency of the mercuric oxide to decompose water with the subsequent formation of mercury and oxygen gas is thus minimal. Further, the high overvoltage for oxygen evolution on the mercuric oxide electrode further precludes oxygen production in the cadmium-mercuric oxide cell.

The solubility of mercuric oxide in 31 percent (7M) KOH solution was found to be 5×10^{-4}M at 25°C.[1] This low concentration of mercury species coupled with the low solubility of cadmium in the electrolyte results in very low capacity losses due to side reactions in solution. Indeed, studies have been conducted which show that the mercury/mercuric oxide electrode is stable at temperatures up to 250°C in 5M NaOH solutions.[12] Measurements of the half cell potentials of mercuric oxide-mercury (versus the hydrogen electrode) do show a decrease from approximately 0.926 V at 25°C to 0.87 V at 200°C, however. The mercuric oxide, although exhibiting no evidence of decomposition in 0.1 M NaOH solution to 280°C was sufficiently soluble in 1 M NaOH solution at 210°C to cause contamination problems.

Two additional factors contribute to minor capacity losses in the cadmium-mercuric oxide cell during storage: crystal growth of the cadmium electrode into the cellulosic electrolyte absorber and the reduction of dissolved mercury species at the cadmium electrode.[1,2,4] Crystal growth results in the loss of capacity for cells discharged at high rates due to a reduction in the effective surface area of the cadmium electrode. This effect can be minimized through use of a chemically grafted polyethylene membrane (e.g., Permion 2291). The reduction of mercury at the cadmium electrode is caused by diffusion of a mercury species through the separator, resulting in the formation of an amalgam with cadmium. The resultant internal short circuit from the positive to the negative electrode reduces the cell capacity. Multiple layers of Permion 2291, or a similar polyethylene membrane surrounding the mercuric oxide electrode have proven to reduce the mercury species transfer markedly in button and bobbin cells[4] and prismatic cells.[2]

In view of the stability of the cadmium and mercuric oxide electrodes in the 7M KOH solution, cells are typically hermetically sealed. However, in the event of incomplete or faulty closure, oxygen may enter the cell. As a result, a cathodic reaction between the cadmium electrode and a dissimilar metal in contact with the cadmium (e.g., cell case or current collector) and electrolyte film may occur. The result would be the corrosion of the cadmium/dissimilar metal interface and the production of hydroxide ions in accordance with equation 5.[11,13] As the corrosion reaction proceeds, the cell will exhibit leakage of the alkaline electrolyte and a deterioration in performance.

The observed open circuit voltage for the cadmium-mercuric oxide cell is 0.903 V. The performance characteristics for prismatic cadmium-mercuric oxide cells of 6.2 Ah (1.3 cm x 3.75 cm x 3.7 cm) and 12.4 Ah (1.3 m x 5.2 cm x 5.1 cm) nominal capacities were obtained for the temperature range of -25°C to + 60°C.[2] The results obtained for 6.2 Ah cells showed little variation from the nominal capacity when discharged at 3-8 mA at temperatures of 0°C to +60°C to a voltage cutoff level of 0.67 V. There was, however, a loss of about 1.0 Ah (16%) for cells discharged at -25°C. This trend was also observed for the larger cells discharged at 3 and 10 mA.

The ability of the cadmium-mercuric oxide button cell to operate at low temperatures was demonstrated by Barnhart and Boden.[1] Cells of nominal capacities of 600 mAh were discharged at rates of 1 mA and 10 mA in the temperature range of -40°C to +27°C. Capacities of 600 mAh or higher were obtained for cells discharged at the 1 mA rate over the entire temperature range. However, for cells discharged at the 10 mA rate, the realized capacities

31

were 400 mAh at -40°C, 550 mAh at 0°C and 600 mAh at 27°C. Cells discharged at higher rates of 100 mA yielded realized capacities of 200 mAh at 0°C and 570 mAh at 27°C.

Button cells of 600 mAh nominal capacity were discharged at rates of 0.03 mA to 300 mA at 21°C.[1] Realized capacities of 600 mAh or higher were obtained for cells discharged at currents of 0.03 mA to 16 mA. The corresponding load voltages were 0.90 V to 0.85 V. However, marked decreases in both capacity and load voltage levels were noted for cells discharged at 40 to 300 mA. For example, cells discharged at the 71 mA rate yielded capacities of 450 mAh at an average load voltage of 0.68 V. The theoretical energy density for the cadmium-mercuric oxide system is about 150 Wh/kg.[14] The practical energy densities for the system vary from about 10 to 30 Wh/kg in the temperature range of -40°C to +50°C for cells discharged at low rates.

The cadmium-mercuric oxide cell system possesses exceptional capacity retention after storage at temperatures of 27°C to 100°C.[15] Capacity retention of 97 to 100 percent was observed for cells stored at 24°C for 3.5 years. Cells were stored at the higher temperatures of 74°C for three months, 93°C for four weeks, and 149°C for 36 hours. The observed realized capacities for these cells were 95-97 percent, 70 percent, and 88 percent, respectively, of the initial capacities. The average loss in capacity for stored cells was only 1.1 percent per day at 100°C, 0.2 percent per day at 72°C, and 0.02 percent per day at 45°C. Further, after one year storage at 21°C, no measurable capacity losses were observed. Therefore, a conservative estimate of the shelf life for the system is at least 10 years.[15,16]

The major manufacturers or developers of the cadmium-mercuric oxide system are ELCA (Electrochimica Corporation), General Electric Company, Mallory (Duracell International), and the Ray-O-Vac Division of ESB.

No safety data has been reported which detail the results of short circuit, incineration, forced overdischarge, or charging tests. In view of the facts that cells are hermetically sealed and can withstand severe shock, vibration, and spin testing,[1] the design of the cell must exhibit great structural strengths. Therefore, testing in accordance with NAVSEAINST 9310.1A would undoubtedly result in an eventual case rupture due to internal pressure considerations.* Such pressure would be the result of the electrolysis of water in cells subjected to forced overdischarge (H_2 on the mercuric oxide electrode and O_2 on the cadmium electrode) and to charging (H_2 on the cadmium electrode and O_2 on the mercuric oxide electrode). The pressure increase will also be the result of higher water vapor pressure due to increased internal cell heating during testing. Similar case ruptures would be expected for cells subjected to incineration testing.

---

*Mahy, T. X., Private Communication, 1984.

REFERENCES

1. Barnhart, R. G., and Boden, D. P., Proc. of the 1971 IECEC, American Society of Mechanical Engineers, 1, 1971, p. 529.

2. Thornton, R. F., Proc. Power Sources Symp. 26, 1975, p. 169.

3. Crompton, T. R., "Small Batteries," Volume 2, Primary Cells (New York: John Wiley and Sons, 1983), p. 3.

4. Przybla, F. J., Ramsey, G. R., and Scandariato, J., Proc. Power Sources Symp. 26., 1975, p. 166.

5. Weininger, J. L., and Breiter, M. W., "Power Sources 1966," Proc. Fifth Int. Symp., Joint Services Electrical Power Sources Committee, Collins, D. H., ed. (London: Pergamon Press, 1967), p. 269.

6. Barnard, R., Edmondson, K., Lee, J. A., and Tye, F. L., J. Applied Electrochem, 6, 1976, p. 107.

7. Vijayavalli, R., Vasudeva Rao, P. V., and Vdupa, H. V. K., Electrochim Acta, 16, 1971, p. 1197.

8. Armstrong, R. D., and West, G. D., J. Electroanal Chem., 30, 1971, p. 385.

9. Armstrong, R. D., Sperrin, A. D., Tye, F. L., and West, G. D., J. Applied Electrochem, 2, 1972, p. 265.

10. Armstrong, R. D., Edmondson, K., and West, G. D., Electrochemistry, Volume 4, Thirsk, H. R., senior reporter (London: The Chemical Society, 1974), p. 18.

11. Baugh, L. M., Cook, J. A., and Tye, F. L., "Power Sources 7," Proc 11th Int. Symp. Power Sources, Joint Services Electrical Power Sources Committee, Collins, D. H., ed. (London: Academic Press, 1979), p. 519.

12. Case, B., and Bignold, J., J. Applied Electrochem., 1, 1971, p. 141.

13. Hull, M. N., and James, H. I., J. Electrochem. Soc., 124, 1977, p. 332.

14. Klein, M. G., and Eisenberg, M., Electrochem. Technol., 3, 1965, p. 58.

15. Falk, S. U., and Salkind, A. J., Alkaline Storage Batteries (New York: John Wiley and Sons, 1969), pp. 555 and 372.

16. Attewell, A., and Tattershall, P., Proc. Power Sources Symp. 29, 1981, p. 53.

D. CALCIUM- CALCIUM CHROMATE (THERMAL)

$$Ca \mid KCl-LiCl \mid CaCrO_4$$

$$3Ca + 2\ CaCrO_4 + 6\ LiCl \longrightarrow 3\ CaCl_2 + Cr_2O_3 \cdot 2CaO \qquad [1]$$
$$+ 3\ Li_2O$$
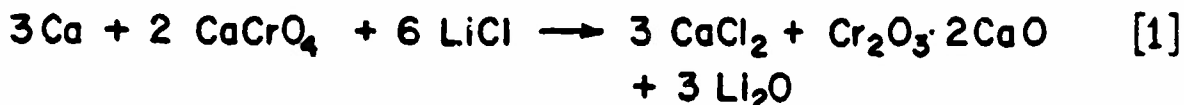
Thermal batteries have been used extensively in ordnance fuzing and missile applications. Of all the possible thermal systems, the calcium-calcium chromate battery has found the broadest practical use and has been the most widely studied and characterized. The cell consists of a calcium negative electrode, the fused salt eutectic of LiCl and KCl as the electrolyte, and a positive electrode of calcium chromate. This system possesses several highly desirable characteristics required to comply with military ordnance specifications: (1) operation over a wide range of temperatures, (2) long shelf life, (3) high cell voltage, (4) chemically stable electrolyte, (5) high reliability, (6) operational lifetimes of a few seconds to almost one hour, and (7) the ability to endure the extreme environmental conditions of shock, vibration, and spin.

Thermal batteries are hermetically sealed reserve power supplies which are activated by a pyrotechnic device. Historically, several cell designs have been employed in the manufacture of the thermal batteries. These include the cup cell design,[1-3] the open cell/tape electrolyte design,[2,4] the glazed depolarizer design,[2,4] multilayer pellets/heat paper design,[5,6] and the heat pellet/DEB pellet design.[2,4,7] Of the five cell designs, the heat pellet/DEB pellet design is presently in general use for nearly all applications. The cup cell and open cell possessed short activated stand characteristics as well as intricate design considerations (i.e., difficulty in manufacture). The heat source tended to induce thermal shocks which resulted in limited battery operation. In addition, tests have shown that the cup design thermal batteries exhibited poor shelf life characteristics due to progressive hydrolysis of the calcium from moisture in cell components and leaks in the hermetic seal. In addition, a coating of polyvinylalcohol was found on the calcium surface.[8]

The heat pellet/DEB cell design utilizes a bipolar construction with three layers or pellets. The heat pellet (Thermite) is comprised of powdered iron and potassium perchlorate (typically 86-88% iron, 14-12% $KClO_4$). The burn rate for the 14 percent $KClO4$ heat pellet is approximately 17 cm/sec with a caloric output of 255 cal/g (1.07 kJ/g). After supplying the required amount of heat, the residual iron serves as the intercell connector. The DEB (Depolarizer,

Electrolyte, and Binder) pellet consists of about 35-40 percent $CaCrO_4$, 50-55 percent LiCl-KCl eutectic mixture, and 15-5 percent binder (either Kaolin or a fumed silica such as Cab-O-Sil). The third layer consists of the calcium electrode fabricated by either vacuum deposition or mechanical attachment onto stainless steel,[9] iron,[10] or nickel substrates.[11] The resultant cell configuration requires that the pellets be stacked in the sequence: heat pad, DEB pellet, calcium electrode, heat pad, etc. Further advantages of the heat pellet/DEB cell design compared to the heat paper design include the shape retention of the heat source and the capability of the resultant iron mass to retain heat for longer periods of time.

Cells constructed as above can be stacked and connected to obtain the desired end voltage level. Since the case must be isolated, electrical as well as thermal insulation is required within the stainless steel battery case. Formerly, the choice for insulation materials included asbestos mixed with silica or glass but modern insulation such as Min K, Fiberfrax, and BeO are now in common use. The thermal conductivities of these insulation materials are approximately 5×10^{-3} W/cm^{-2}°C/cm at 500°C.[12] The stack assembly is then inserted into a stainless steel case lined with insulation material. The header/lid, containing glass to metal electrode seals and match leads, is attached to the cell stack and hermetically sealed using a heliarc or TIG weld while pressure is exerted on the header/lid and cell stack assembly. Optimum closing pressures of approximately 0.1 kg/cm^2 are used to ensure proper wetting of the calcium. Low pressures result in poor wetting and battery performance deterioration. It has also been found that increased closing pressure on the battery stack results in electrolytic leakage and the formation of a calcium and lithium alloy during battery operation.[13] In addition, high closing pressures have resulted in high peak temperatures in production batteries.

The ignition system consists of an electrical match (Atlas M-100/M-200 or Hercules) and a pyrotechnic ignition strip (fuse train) in contact with the heat pellets of each cell. The fuse train paper strip of 28 percent Zn powder and 72 percent $BaCrO_4$ has a caloric output of 465 cal/g (1.95 kJ/g). Typically, the initiation sequence is begun by an external signal of at least 160 K ergs to ignite the electric match having a resistance of about 1.0 to 1.5 ohms.* The match then ignites the fuse train and, finally, the heat pellets in the cells. Activation times of 0.05 to several seconds are observed for the calcium-calcium chromate thermal batteries dependent upon both battery size and construction. A typical activation time of 0.5 second is observed for most calcium-calcium chromate thermal batteries.

The calcium electrode displaces lithium from the molten LiCl-KCl eutectic electrolyte at 352°C and higher and eventually forms the alloy, $CaLi_2$, with a melting point of 231°C:[4,6,12,15]

$$Ca_{(s)} + 2\ Li^+ \longrightarrow Ca^{2+} + 2\ Li_{(l)} \tag{2}$$

---

*Kuper, W. E., Harry Diamond Laboratories (U.S. Army Electronics Research and Development Command), Private Communication, 1984.

The molten lithium then reacts with calcium metal to form the alloy:

$$Ca_{(s)} + 2 \ Li_{(l)} \longrightarrow CaLi_{2(l)} \tag{3}$$

The liquid alloy can flow down the cell stack and cause catastrophic short circuiting in adjacent cells unless the current density is high. Several remedies to the formation or containment of the $CaLi_2$ alloy have been proposed. These have included an increase in the concentration of calcium ions at the calcium-electrolyte interface by either directly adding $CaCl_2$,[9] or by heating the calcium electrodes in acetic acid.[15] The latter method produces a double salt, $3Ca(CH_3COO)_2 \cdot 2CH_3COOH$, which decomposes to $CaCO_3$, in the battery operating temerature range of 400-600°C. The Ca^{2+} retards the displacement of lithium in the electrolyte. An alternate method of alloy control is the grooving of the DEB pellet to accumulate the alloy and restrict the reaction of the alloy with adjacent cells.[9] A second effect of the alloy formation results in serious voltage fluctuations (noise) during battery discharge accompanied by the dropout of some cells.

At high current densities, the increase in calcium ion concentration at the calcium-electrolyte interface leads to the formation of a double salt, $KCaCl_3$ on the surface of the calcium electrode:[16,17]

$$CaCl_2 + KCl \longrightarrow KCaCl_3 \tag{4}$$

The double salt has a melting point of about 485°C. Since the optimum operating temperature range of the calcium-calcium chromate thermal battery has been found to be 470°C-530°C, the formation of the double salt, whether in the liquid or solid state, increases the internal resistance of the cells and masks reaction sites at the calcium electrode. In addition to an overall decrease in battery efficiency, the formation of the $KCaCl_3$ also limits the pulsing capabilities of the system.

The formation of a second film on the calcium electrode has been found to be the complex salt, Ca_2CrO_4Cl[16,17] which is more diffuse than the $KCaCl_3$. It is believed that both films prevent the direct chemical reaction of the $CaCrO_4$ with the calcium electrode at the battery operating temperatures of 400°C-600°C. However, breakdown of the films occur at temperatures greater than 600°C, resulting in a direct chemical reaction between calcium and calcium chromate and a thermal runaway condition.[11,12] The formation of both films continues as the battery discharges. As a result, the capacity of the calcium electrode is, for all practical purposes, limited to only 30 percent of the total calcium available.

The electrolyte is the eutectic mixture of LiCl (58.5 mol %) and KCl.[18] The specific conductance of the pure eutectic mixture in the battery operating temperature range of 400°C to 600°C varies from 1.23 to 2.28 $ohm^{-1}cm^{-1}$, respectively. The specific conductance for a saturated aqueous solution of NaCl at 15°C is 0.2 $ohm^{-1}cm^{-1}$. Therefore, significantly higher current levels can be maintained in the fused salt calcium-calcium chromate batteries compared with aqueous systems. In addition to the above, the eutectic of LiCl and KCl is stable towards both oxidation and reduction in the voltage range of the calcium-calcium chromate cell (i.e., approximately 3 V).

The observed open circuit voltage for the calcium-calcium chromate thermal
battery is approximately 2.7 to 3.0 V per cell at 500°C.[*,14] Proper design of
the thermal characteristics relative to the amount of thermite contained in the
heat pellets allows battery operation between 400°C and 600°C for batteries
equilibrated at initial temperatures of -54 to +74°C. Long life batteries (10.3
cm high, 12.2 cm diameter, 2.96 kg) were discharged at initial temperatures of
1°C, 25°C, and 40°C at a current density of 55 mA/cm^2 at 28 V.[9] The
performance characteristics for the batteries discharged at the initial
temperatures of 25°C to 40°C varied little (i.e., realized capacities of
approximately 1.1 Ah for the 15 minute discharge). The energy densities were
approximately 10.5 Wh/kg. However, lower capacities and energy densities were
obtained for batteries discharged at 0°C. The active life for this battery was
found to be only 12 minutes compared to those batteries discharged at the higher
temperatures.

Performance characteristics were also obtained for 12 cell calcium-calcium
chromate batteries subjected to a 300 rps spin environment.[10]. The dimensions
of the hermetically sealed battery were 4.4 cm diameter and 4.4 cm high and the
weight was 0.15 kg. Batteries were discharged at various current densities to a
24 V cutoff level. The results show energy densities of approximately 14.4,
15.4, 11.6 and 7.7 Wh/kg for batteries discharged at current densities of 100.
70, 40, and 20 mA/cm^2, respectively. It was found that the high spin
environment caused two failure modes: leakage of the electrolyte from the DEB
pellets resulting in short circuits of adjacent cells[10,19] and the loss of
contact of the fuse train with the heat pellets of each cell.[19] By increasing
the binder (SiO$_2$) concentration from 7 percent to 15-20 percent of the DEB
pellet and wrapping the cell with glass ribbon, these detrimental effects were
reduced.

Recent optimization studies[20] relative to the active components and
binder content of the calcium-calcium chromate battery have shown that the
CaCrO$_4$ content has little influence on the performance characteristics for
batteries discharged under light loads. Increased binder content was found to
reduce the rate of the chemical reaction between the calcium and calcium
chromate at the calcium-electrolyte interface. As a result, the peak battery
temperatures were also reduced. Optimum performance was obtained for a binder
content of 12 percent, especially for batteries activated at 74°C. In addition,
it was found that calcium electrodes with the highest nitrogen content were the
least reactive toward the calcium chromate/LiCl-KCl eutectic mixture. These
electrodes also yielded the best performance characteristics.

Studies have been conducted which compare the performance characteristics
of the calcium-calcium chromate battery to other thermal battery
systems.[4-6,11,12,21-23] In general, it was found that the calcium-calcium
chromate system was superior to almost all other non-lithium systems. Recently,
however, much work has involved the replacement of the calcium electrode by a
lithium aluminum alloy and the use of alternate positive electrode materials
such as FeS$_2$,[24-27] MoCl$_5$,[28-30] or CuCl$_2$.[29,31,32] These systems
offer higher energy densities at lower operating temperatures in comparison to
the calcium-calcium chromate system.

---

*Kuper, W. E., Harry Diamond Laboratories (U.S. Army Electronics Research and
Development Command), Private Communication, 1984.

The major research, development, and production of the calcium-calcium chromate thermal battery was carried out by Catalyst Research Corp., General Electric Company, KDI Score, Inc., Eagle Picher Industries, Inc., the Air Force Wright Aeronautical Laboratory, Harry Diamond Laboratories, Naval Ordnance Laboratory, and Sandia National Laboratory.

The safety characteristics of the calcium-calcium chromate battery may be discussed with respect to the operational status of the battery: nonactivated, activated, and discharged. Obviously, electrical abusive testing for batteries in the nonactivated state (i.e., short circuit, forced overdischarge and charge) will have no effect relative to the creation of hazardous conditions. However, incineration of the battery could result in the autoignition of the pyrotechnic material (the fuse train of Zn and $BaCrO_4$ as well as the thermite, Fe and $KClO_4$). The battery may then rupture or overheat to the extent of causing case distortion and discoloration.*/** It should be noted that most temperatures of incineration approximate the operating temperature of the battery. In addition, though the pyrotechnic matches are particularly sensitive, no battery has ever been activated spontaneously.* Penetration of the battery case by a conductive object will not result in a hazardous condition provided that the contents of the battery not be simultaneously exposed to copious amounts of water. Such an occurrence would cause a violent reaction with the production of H_2 gas and an explosion or fire hazard.*/**

No charging tests have been conducted with activated batteries. It is believed that, since the internal impedance of the battery is much less than one ohm and the leads are sized to match the load requirements, an external short circuit condition would incinerate the internal leads of the battery.* If the leads are capable of sustaining high currents for long periods of time, a thermal runaway condition would develop. The battery temperature would rapidly rise to approximately 800°C whereupon the cell would burn itself out. Case deformation, discoloration, or rupture would be evident. Similar results would be obtained should batteries be activated at temperatures above 65°C. The operating temperatures for these batteries would exceed 600°C and a thermal runaway would occur due to the breakdown of the $CaLi_2$ and $KCaCl_3$ films resulting in the direct chemical reaction between calcium and calcium chromate.[11,12,33],* Penetration of the battery case by a conductive object at the operating temperature would lead to massive internal short circuit and may cause a fire hazard due to the escape of flammable gases.[34]

Though no forced overdischarge tests have been conducted using activated batteries, it is reasonable**/*** to assume that some cells in a series string do experience cell voltage reversal conditions during battery operations. No instances of any hazardous conditions have been reported for these occurrences. Of particular note is activation of a battery containing excessive amounts of water.** A battery which had developed leaks in either the TIG weld or the

*Kuper, W. E., Harry Diamond Laboratories (U.S. Army Electronics Research and Development Command), Private Communication, 1984.

**Nelson, J. T., Harry Diamond Laboratories (U.S. Army Electronics Research and Development Command), Private Communication, 1984.

***Templeman, M. B., Harry Diamond Laboratories (U.S. Army Electronics Research and Development Command), Private Communication, 1984.

glass to metal seals was tested. Because the battery had been exposed to normal environmental conditions, there was a steady influx of atmospheric moisture during the storage period prior to activation. The result was a steam explosion and case rupture.

Electrical abuse testing after battery activation and operation would not result in any hazardous conditions. The pyrotechnic material, at this time would be totally consumed and the active materials would be either reduced or oxidized to various salts or oxides. Incineration of the spent batteries, however, does result in seal rupture due to the gases produced during discharge.*,[34] Following discharge at optimum cell operating conditions (560°C), the gas composition was found to be 35.6 percent H_2, 28.0 percent CO_2, 22.5 percent CO, 6.2 percent O_2, 5.8 percent N_2, 1.1 percent ethane, and 0.9 percent methane.[34] In view of the above, the battery must be carefully vented prior to any post-mortem examination.*

.

*Kuper, W. E., Harry Diamond Laboratories (U.S. Army Electronics Research and Development Command), Private Communication, 1984.

REFERENCES

1. Van Domelen, B. H., Proc. of the 9th IECEC, American Society of Mechanical Engineers, 1974, p. 686.

2. Crompton, T. R., "Small Batteries," Volume 2, Primary Cells, John Wiley and Sons, New York, 1983, p. 202.

3. Brodd, R. J., Kozawa, A., and Kordesch, K. V., J. Electrochem. Soc., 125, 1976, p. 275C.

4. Tepper, F., Proc. of the 9th IECEC, American Society of Mechanical Engineers, 1974, p. 671.

5. Jennings, C. W., The Primary Battery, Volume II, Heise G. W., and Cahoon, N. C., eds. (New York: John Wiley and Sons, Chapter 6, 1976).

6. Dand, P. V., Press, K. K., and Wisniewski, G. R., "Power Sources 7," Proc. 11th Int. Symp. Power Sources, Collins, D. H., ed. (London: Academic Press, 1979), p. 501.

7. Bush, D. M., Proc. Power Sources Symp., 26, 1975, p. 144.

8. Wong, P., and McCauley, J. W., Proc. Power Sources Symp., 28, 1979, p. 69.

9. Baldwin, A. R., Proc. Power Sources Symp., 26, 1975, p. 137.

10. Grothaus, K. R., Proc. Power Sources Symp., 26, 1975, p. 141.

11. Krieger, F. C., Thermal Battery Systems for Ordnance Fuzing, DTIC No. AD-A119155, Defense Logistics Agency, Alexandria, VA, 1982.

12. Attewell, A., and Clark, A. J., "Power Sources 8," Proc. 12th Int. Symp. Power Sources, Thompson, J., ed. (London: Academic Press, 1981), p. 285.

13. Levy, S. C., Proc. Power Sources Symp., 28, 1979, p. 72.

14. Clark, R. P., and Forsman, E. V., Proc. of the 9th IECEC, American Society of Mechanical Engineers, 1974, p. 678.

15. Clark R. P., and Grothaus, K. R., J. Electrochem. Soc., 118, 1971, p. 1680.

REFERENCES (Cont.)

16. Hlava, P. F., and Headley, T. J., Report SAND77-1317, Sandia National Laboratory, Albuquerque, N.M., 1977.

17. Nissen, D., J. Electrochem. Soc., 126, 1979, p. 176.

18. Janz, G. J., Allen, C. B., Bansal, N. P., Murphy, R. M., and Tomkins, R. P. T., "Physical Properties Data Compilations Relevant to Energy Storage," II Molten Salts: Data on Single and Multi-Component Systems, NSRDSNBS61, Part II, U.S. Dept. Commerce, Superintendent of Documents, U.S. Govt. Printing Office, Washington, D.C., 1979, p. 244.

19. Wilder, G. L., Battery WOX93E (Eagle-Picher Cap 6243), DTIC No. ADA026696, Defense Logistics Agency, Alexandria, VA, 1976.

20. Guidotti, R. A., Reinhardt, F. W., and Poole, R. L., Proc. Power Sources Symp. 30, 1983, p. 33.

21. Dand, P. V., Press, K. K., and Wisniewski, G. R., Proc. Power Sources Symp. 28, 1979, p. 75.

22. Thaller, L. H., J. Electrochem. Soc., 115, 1968, p. 116.

23. McManis, G. E., Miles, M. H., and Fletcher, A. N., Proc. Power Sources Symp. 30, 1983, p. 39.

24. Bush, D. M., and Nissen, D. A., Proc. Power Sources Symp. 28, 1979, p. 81.

25. DeGruson, J. A., Proc. Power Sources Symp. 28, 1979, p. 79.

26. Dand, P. V., and Press, K. K., Improved Thermal Battery, DTIC No. AD-AO75835, Defense Logistics Agency, Alexandria, VA, 1979.

27. Winchester, C. S., The LAN/FeS, Thermal Battery System, Catalyst Research Corp., Baltimore, MD, 1982.

28. Nardi, J. C., Erbacher, J. K., Hussey, C. L., and King, L. A., J. Power Sources, 3, 1978, p. 81.

29. Ryan, D. M., Advanced Thermal Batteries, DTIC No. AD-A085193, Defense Logistics Agency, Alexandria, VA, 1980.

30. Ryan, D. M., Marsh, R. A., and Bunting, R. K., Proc. Power Sources Symp. 28, 1979, p. 90.

31. Erbacher, J. K., Hussey, C. L., and King, L. A., Proc. Power Sources Symp. 28, 1979, p. 84.

32. Ryan, D. M., Advanced Thermal Batteries, DTIC No. AD-A125581, Defense Logistics Agency, Alexandria, VA, 1981.

REFERENCES (Cont.)

33. Clarke, R. P., _Thermochim. Acta_, 26, 1978, p. 49.

34. Burns, F. B., Guidotti, R. A., Reinhardt, F. W., and Rodacy, P. J., _Proc. Power Sources Symp._ 30, 1983, p. 37.

E. CALCIUM-SULFURYL CHLORIDE

$$Ca \mid Ca(AlCl_4)_2, LiAlCl_4 \mid SO_2Cl_2$$

$$2\,Ca + SO_2Cl_2 + 2\,LiAlCl_4 \longrightarrow Ca(AlCl_4)_2 + SO_2 + 2\,LiCl \qquad [1]$$

$$\text{and} \quad Ca + SO_2Cl_2 \longrightarrow CaCl_2 + SO_2 \quad \text{(proposed)} \qquad [2]$$
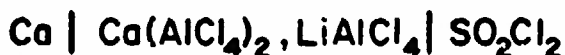
The substitution of calcium for lithium negative electrodes in cells containing either thionyl chloride or sulfuryl chloride may lead to future battery systems which exhibit high tolerances to thermal, electrical, and mechanical abuse. Though the majority of the research and development work to date has concerned the calcium-thionyl chloride system (refer: calcium-thionyl chloride primary battery, this work), recent work has been reported relative to the calcium-sulfuryl chloride system.[1-3] Though no practical cells have been fabricated and characterized for performance, storability or safety, several studies for the successful development of the system have, nonetheless, been completed.

Experimental cells were fabricated in the laboratory[1,2] which contain either 1.5M LiAlCl$_4$ or 0.4M Ca(AlCl$_4$)$_2$. The proposed reaction for cells containing LiAlCl$_4$ is represented by equation 1 for the beginning of cell discharge. As the discharge process proceeds, dissolved Ca(AlCl$_4$)$_2$ will result in the precipitation of both CaCl$_2$ and LiCl at the carbon electrode. No thermodynamic data was found for the calculation of the potential corresponding to equation 1 or to the situation where both LiCl and CaCl$_2$ are coprecipitated onto the carbon matrix. The thermodynamic potential of 3.82 V was calculated for the reaction given in equation 2, the probable reaction for cells using Ca(AlCl$_4$)$_2$ electrolyte. The difference between the observed OCV (3.2V) and the thermodynamic potential was attributed to the impedance of the solid electrolyte interface, CaCl$_2$.[4,5]

Conductivity studies of the electrolyte solutions showed that the specific conductivities are approximately ten times greater for the 1.5M LiAlCl$_4$ electrolyte than for the 0.4M Ca(AlCl$_4$)$_2$ electrolyte in sulfuryl chloride.

Polarization studies[1,2] showed that the calcium electrode is polarized by 0.6 V at low current densities in solutions containing either LiAlCl$_4$ or Ca(AlCl$_4$)$_2$. As the current densities increased, however, little or no further polarization occurred. The carbon electrode, on the other hand, exhibited little effect when at low current densities, but was significantly

affected at high current densities. Carbon electrode polarization was greater for electrodes immersed in the $Ca(AlCl_4)_2$ solution. This effect was attributed to the poorer electrolyte conduction in the carbon electrode pores.

Cells containing electrolyte solutions of $LiAlCl_4$ and $Ca(AlCl_4)_2$ were discharged at current densities of 5 mA/cm^2. It was shown that the realized capacities were only 10 percent and 30 percent for cells containing $Ca(AlCl_4)_2$ and $LiAlCl_4$, respectively, compared to a similar cell containing a lithium electrode and $LiAlCl_4$ electrolyte. It was also found that the cell capacity in these cells was limited by the carbon electrode. Microscopic examination of the carbon electrodes from lithium cells showed discrete aggregates of cubic LiCl. A similar examination of the carbon electrodes from calcium cells, however, showed an amorphous continuous layer of LiCl in a mixed calcium-lithium salt deposit. It was proposed that the transport of reactant, product, and ions between the cubic LiCl crystals was easier compared to transport within the amorphous layer. Results obtained through cyclic voltammetry experiments[3] further substantiated the fact that coprecipitation of LiCl and $CaCl_2$ in the carbon matrix resulted in poisoning of the electrodes and reduced capacities in calcium-sulfuryl chloride cells.

No safety data for the calcium-sulfuryl chloride system containing either $LiAlCl_4$ or $Ca(AlCl_4)_2$ electrolyte salts exist at the present time.

REFERENCES

1. Binder, M., Gilman, S., and Wade, W., Jr., J. Electrochem. Soc., 129, 1982, p. 897.

2. Binder, M., Wade, W., Jr., and Gilman, S., Proc. Power Sources Symp. 30, 1983, p. 154.

3. Behl, W. K., J. Electrochem. Soc., 130, 1983, p. 1712.

4. Meitav, A., and Peled, E., J. Electrochem. Soc., 128, 1981, p. 825.

5. Peled, E., Meitav, A., and Brand, M., J. Electrochem. Soc., 128, 1981, p. 1936.

F. CALCIUM-THIONYL CHLORIDE

Ca | LiAlCl$_4$ | SOCl$_2$

2 Ca + 2 SOCl$_2$ ⟶ 2 CaCl$_2$ + SO$_2$ + S   (proposed)   [1]
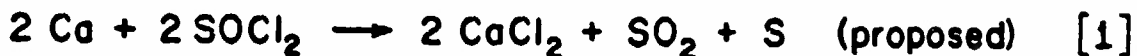
The substitution of calcium for lithium negative electrodes in cells containing such liquid cathode materials as thionyl chloride and sulfuryl chloride is especially attractive in view of the tendency of lithium cells to exhibit safety problems when subjecced to electrical, mechanical, and thermal abuse. Cells containing lithium (melting point: 180°C) may reach the thermal runaway state by internally driven cell conditions. However, replacement of lithium with calcium (melting point: 838°C) could result in cells which would not reach thermal runaway under similar conditions.

Recently, calcium-thionyl chloride cells have been fabricated and tested by Eagle Picher Industries under contract to Wright Aeronautical Laboratory to determine the performance, safety, and storability characteristics.[1-5] Five hermetically sealed cell sizes were used in the evaluation program: spirally wound half D-cells of 3.5 Ah nominal capacity and prismatic cell designs of 200, 600, 2000, and 7500 Ah nominal capacity. The calcium electrode material was sintered at 450°C for one hour under a pressure of 0.01 mm. Current collection was effected through use of expanded nickel screen and nickel tabs.

The carbon current collectors were fabricated using 50 percent compressed Shawinigan acetylene black bonded by Teflon compressed onto expanded nickel screens. The separator used in all test cells was a non-woven glass mat having an average thickness of 0.4 mm. The concentrations of the LiAlCl$_4$ electrolyte was 1.4 M for the half D cells and 1.5 M for the prismatic cells.

The half D cell package consisted of a 304 stainless steel can with a nickel 52 alloy terminal pin in a glass to metal seal. The cell was filled through a fill tube at the cell lid which was subsequently close welded. A 0.05 mm thick nickel diaphragm with an opening pressure of 100 psi was welded into the case bottom. All cells were of the case negative design.

Prismatic cells of 200, 600, 2000, and 7500 Ah nominal capacities were fabricated in stainless steel containers having 2.5 cm burst discs designed to open at 150 psi welded into the respective cell covers. Glass to metal seals

were used for cells of the 200 and 600 Ah designs while swedged Teflon seals were employed for the 2000 and 7500 Ah cells. Cells were filled through 1 cm diameter stainless steel valves.

The observed open circuit voltages for the calcium-thionyl chloride cells were approximately 3.25 V. If the reaction given in equation 1 were the true overall reaction for the system, an open circuit voltage of nearly 3.65 V should be expected. The disparity observed in the open circuit voltages could be the result of a resistive effect at the solid-electrolyte interface or the effect caused by surface corrosion of calcium.[6] The disparity may also indicate that the reaction scheme of equation 1 may not be correct. However, Higgins has found near stoichiometric amounts of $CaCl_2$ in the carbon electrodes of discharged cells.[3]

Half D cells were discharged at rates of 50 mA to 1.0 A at temperatures between -40°C and 74°C. The average load voltages at 20°C was approximately 2.5 for all cells tested. The realized capacities were more than 3.5 Ah at the 50mA rate, 3.2 Ah at the 250 mA rate, and 2.2 Ah at the 1.0 A rate. Similar results were found for cells tested at 48°C under low rates but decreased to 2.5 Ah at the 0.5 A rate. When a cell was discharged at the 1.0 A rate at 48°C, venting occurred when the cell skin temperature reached 80°C, though no electrolyte was expelled from the cell. The above cell continued to discharge and produced an additional capacity of 0.3 Ah. The realized capacities obtained for cells discharged at -18°C decreased from 3.3 Ah at the lowest rates to 2.1 Ah at the 1.0A rate. A realized capacity of 2.8 Ah was obtained for cells discharged at -29°C at the 50 mA rate. No cells exhibited load voltages above 2.0 V at -40°C.

Cells were subjected to short circuit (0.002 ohm), voltage reversal at 0.25 A for 10 h using cells discharged at 20°C and -29°C, charging (at rates to 1.0 A) under constant potential and constant current conditions (i.e., for fresh cells, 50 percent discharged at 20°C, 100 percent discharged at 20°C, 50 percent discharged at -29°C and 100 percent discharged at -29°C), crushing by a hydraulic press, and puncture by a steel spike to 75 percent of the cell thickness (fresh and partially discharged cells at 20°C and 29°C). Fresh and partially discharged cells (20°C and -29°C) were also incinerated above a propane flame. All cells exposed to the short circuit, charging, incineration, puncture, and voltage reversal tests vented mildly, exhibiting cell wall temperatures of 80°C-85°C. Cells which were crushed did not vent. No violent venting, flame, or explosion was observed for any of the test cells.

Half D cells were stored at 20°C for various periods up to 6 months. Subsequent testing showed only slight increases in voltage delay to the 2.0 V level and little or no capacity loss over the six month period. The impedance at 1000 Hz increased from 0.9 ohm after one month storage to 2.3 ohms at the six month period.

Cells having a nominal capacity of 200 Ah were discharged under resistive loads at 10°C to 13°C after an open circuit stand of 400 h. The cells realized capacities of 235 Ah at an average rate and voltage of 0.5 A and 2.9 V, respectively. Two cells were discharged at 1.5A at 12°C and produced a realized capacity of 210 Ah at an average load voltage of 2.6 V. Further discharge of these cells at 0.5 A produced 20 Ah in addition to the 210 Ah obtained at the higher rate. A third set of cells was discharged at 160 mA for 40 days and

continued at 0.5 A to a 2.0 V cutoff level. These cells yielded a total capacity of 230 Ah. A fourth test included the same regime as described above but included the imposition of a pulse load of 0.5 A during the 40 day period. The realized capacities found were 234 Ah. These results showed that the calcium electrode did not exhibit significant corrosion during either low rate discharge or pulse loading regimes.

Larger cells of 600 Ah nominal capacity yielded realized capacities of 630 Ah at an average voltage of 3.0 V. A fresh cell was subjected to short circuiting (50 mV/3000 A shunt for 5 minutes). The initial short circuit current was 500 A which decreased to approximately 180-200 A until a terminal failure occurred at the five minute mark. The same cell vented after four minutes of incineration and burned internally after eight minutes of incineration. A second partially discharged cell was subjected to 22 caliber bullet penetration. The cell neither vented nor burned even after 20 instances of bullet penetration halfway though the cell stack occurred. Penetration tests using 10 cm long steel spikes resulted in no venting although the internal cell pressure caused the cells to emit noise audible from 50 m.

Voltage reversal tests were performed upon cells of a normal capacity of 2000 Ah. Test cells were discharged normally at 5 A and were force discharged at the 5 A rate. After 28 hours, one cell potential decreased to -40 V and the current level dropped to 2 A, whereupon the cell vented mildly due to the gas pressure presumably produced by the electrolysis of the electrolyte solution.

More extensive testing was performed for 7500 Ah cells. Discharge tests were carried out using a resistive load of 0.050 ohm. The average cell load voltage and discharge current were 3 V and 60 A, respectively. After the load voltage decreased to 2.0 V after 92 hours, the cell was connected to a power supply and further discharged at 60 A into voltage reversal. The cell potential decreased to -12 V after 11 hours in voltage reversal and vented, emitting a white cloud for a ten minute period.

One externally short circuited 7500 Ah cell exhibited short circuit currents up to 700 A under a load of 0.017 mohm until the occurrence of venting 54 minutes from the initial short circuit. The cell was allowed to stand on open circuit for 15 minutes. It was then punctured by driving a 1 cm diameter spike 13 cm into the side of the cell. The cell voltage remained at 3 V or higher for approximately 3.5 hours before decreasing to 0.5 V. This cell was then shot four times with a 30-06 rifle, resulting in an internal fire lasting approximately two minutes. Other 7500 Ah cells exhibited venting following a period of 60 to 70 minutes under short circuit conditions.

It is interesting to note that no data was presented which included similar performance and safety testing using identical cells containing lithium electrodes.

The majority of cell performance and safety testing was carried out at temperatures of 49°C or below. When half D cells were discharged at 74°C at rates of 50, 100, 500, and 1000 mA, all cells discharged at rates less than 1000 mA produced full capacity. Cells discharged at 1000 mA vented due to internal heating.[2] No safety testing was performed at 74°C. It is interesting to note that all reported cell ventings occurred at cell wall temperatures of

80°C-85°C (boiling point pure thionyl chloride: approximately 79°C). If the ventings were effected through the burst diaphragms (half D cell - 100 psi, other cells - 150 psi burst strengths), other factors relative to the internal reactions or thermal management must be further considered.

Though the development of the calcium-thionyl chloride cell is presently continuing at Eagle Picher, it should also be noted that batteries comprised of some of the larger cell sizes may exhibit some safety characteristics which may not be in strict agreement with results obtained in single cell testing.

Investigations of the calcium-thionyl chloride system using $Ca(AlCl_4)_2$ as the elec olyte salt have also been reported.[7,8] The conductivity of the electrolyte was found to be approximately one-third that for corresponding solutions of $LiAlCl_4$ in thionyl chloride. Glass test cells containing calcium metal electrodes on both sides of a Teflon bonded carbon electrode and flooded electrolyte were used throughout these preliminary tests. Since the performance and safety data were obtained on laboratory test cells, the results are summarized below:

1. The preferred electrolyte concentrations were found to be 0.7M $Ca(AlCl_4)_2$ for low temperature applications and 1.25 M $Ca(AlCl_4)_2$ for applications in the 10°C-60°C range.

2. Initial open circuit voltage values were 2.9 to 3.0 V which increased to 3.20 to 3.25 V after a period of 50 to 200 hours.

3. The maximum realized capacities of 37 mAh/cm^2 were obtained for 10 cm^2 carbon electrodes discharged under 120 ohm loads at 25°C and using either 1.3 M $Ca(AlCl_4)_2$ or 0.7 M $Ca(AlCl_4)_2$. The average current densities were 1.1 mA/cm^2.

4. Several glass test cells were charged and force overdischarged at current densities of 0.1 to 30 μA/cm^2. The voltage levels of charged cells rose to 35 to 45 V and was accompanied by massive gas evolution. When the charging current was removed, the OCV fell to 3.7 to 4.0 V and slowly returned to the 3.2 V level. Cells charged at a constant voltage of 30 V exhibited current densities of 10 to 20 microamps after 2 hours. No gassing was observed for calcium-thionyl chloride cells containing $LiAlCl_4$.

5. Glass cells containing both $Ca(AlCl_4)_2$ and $LiAlCl_4$ were also force overdischarged. Cell voltage levels decreased to ~15 V for cells containing $Ca(AlCl_4)_2$ when driven into voltage reversal at low current densities (co 5 mA/cm^2). The voltages then increased to -30 V after 30 minutes. When higher current densities were applied, the voltage fell to -40 V and massive gas evolution occurred. Calcium-thionyl chloride cells containing $LiAlCl_4$ exhibited no gas evolution and steady cell voltage levels at all current densities.

REFERENCES

1. Higgins, R. L., and Cloyd, J. S., Proc. Power Sources Symp. 29, 1981, p. 147.

2. Higgins, R. L., Calcium Inorganic Electrolyte Battery Development, NTIS AD-A106199, U.S. Dept. Commerce, Springfield, VA, 1981.

3. Higgins, R., "Power Sources 8,"Proc. 12th Int. Symp. Power Sources, Thompson, J., ed. (London: Academic Press, 1981), p. 369.

4. Carr, D., Heaton, E., and Higgins, R., Calcium Inorganic Electrolyte Battery Development, NTIS AD-A115956, U.S. Dept. Commerce, Springfield, VA, 1982.

5. Higgins, R. L., Proc. Power Sources Symp. 30, 1983, p. 151.

6. Staniewicz, R. J., J. Electrochem. Soc., 127, 1980, p. 782.

7. Peled, E., Meitav, A., and Brand, M., J. Electrochem. Soc., 128, 1981, p. 1936.

8. Meitov A., and Peled, E., J. Electrochem. Soc., 129, 1982, p. 451.

G. LEAD-LEAD DIOXIDE (HBF$_4$)

$$Pb \mid HBF_4 \mid PbO_2$$

$$Pb + PbO_2 + 4\,HBF_4 \longrightarrow 2\,Pb(BF_4)_2 + 2\,H_2O \qquad [1]$$

The lead-lead dioxide fluoroboric acid system serves as a power supply for many military applications including proximity fuze batteries for artillery shells, radio sonde devices, and to a much lesser extent, torpedo propulsion. This system belongs in a class of lead batteries which produce soluble reaction products, in contrast to the lead-lead dioxide sulfuric acid system. Included with the fluoroboric acid system are the perchloric acid (HClO$_4$) and fluorosilicic acid (H$_2$SiF$_6$) systems. Though each of these systems does possess some degree of reversibility and can be charged to some extent, the batteries are exclusively employed as primary power sources in the military. These systems are not available on the consumer market.

Both the lead-lead dioxide fluoroboric acid and the lead-lead dioxide fluorosilicic acid batteries exhibit similar performance, storability, safety, and operational temperature characteristics. For example, identical batteries containing fluoroboric acid and fluorosilicic acid discharged at current densities of 155 mA/cm^2 yielded 11.7 and 10.3 Wh, respectively.[1] The performance for the fluorosilicic acid system consistently is 85-90 percent that for the fluoroboric acid system. In view of the similarities of the two systems, discussion of these lead systems having soluble reaction products will be primarily concerned with the lead-lead dioxide fluoroboric acid system. The lead-lead dioxide perchloric acid system, in contrast to the above two battery systems, does exhibit significant improvements in performance characteristics but also possesses certain safety anomalies associated with the perchloric acid electrolyte which could lead to fires or explosions. Therefore, this lead-lead dioxide system is discussed separately from the lead-lead dioxide fluoroboric and fluorosilicic acid systems (refer: lead-lead dioxide perchloric acid system, Chapter 2).

The lead negative electrode may be fabricated by electrodepositing lead onto nickel or copper expanded metal screen[1] or by sizing a sheet of pure lead.[2] The use of expanded metal screen increases the roughness of the lead electrode surface. This increased surface area results in a beneficial decrease in current density for batteries discharged at high rates. Since the reaction products are soluble in the electrolyte, only a small excess of lead above the

amount necessary to provide the required capacity is provided. Thus, the lead-lead dioxide fluoroboric acid battery occupies less volume and weighs significantly less than a lead-lead dioxide sulfuric acid battery of similar operational characteristics.

The non-porous lead dioxide positive electrode can be electrodeposited onto nickel screen[1] or can be formed using a thermoplastic binder.[2,3] The deposition of lead dioxide onto nickel screen creates an electrochemical cell in strong fluoroboric acid solution. As a result, the discharge life and activated stand period of the battery are limited by the rate at which the acid attacks the nickel substrate. In addition, the lead dioxide material often exhibits poor adhesion to the metal surface, thereby limiting the realized capacity. However, a metal substrate must be used for applications requiring especially high current densities. For low and medium applications, lead dioxide electrodes may be fabricated using a thermoplastic binder material with a nickel current collector tab inserted into the matrix during the positive electrode hot pressing stage. The exposed nickel tab material may be coated with either solder or potted in resin material after electrical connections have been made.

The electrolyte for the lead-lead dioxide fluoroboric acid system consists of a 40 to 50 percent aqueous solution of fluoroboric acid with a 2 to 3 percent boric acid inhibitor. The above solution is a liquid in the temperature range of approximately $-75°C$ to $+130°C$ and possesses high conductivities of about 0.6 $ohm^{-1} cm^{-1}$ at 25°C and 0.06 $ohm^{-1} cm^{-1}$ at $-60°C$. In addition, fluoroboric acid is both chemically and thermally stable, in direct contrast to the perchloric acid electrolyte in the lead-lead dioxide perchloric acid system (Chapter 2). In view of these properties, the normal operational temperature range for the lead-lead dioxide fluoroboric acid system is $-40°C$ to $+72°C$,[2] though some useful discharge can be obtained at lower temperatures.[1] The operational temperature range for the lead-lead dioxide perchloric acid system, on the other hand, is restricted to $+10$ to $+40°C$ due to the poorer performance characteristics at temperatures below $+10°C$ and the electrolyte reactivity at temperatures above $40°C$.[4]

The means of separation of the electrodes in these lead-lead dioxide batteries is dependent upon the operational parameters of the application. For example, mechanical separation is effected through use of a plastic material wound around the electrodes at various intervals in those batteries to be discharged at high rates[4] or to be subjected to either low spin or no spin regimens (i.e., power supplies for torpedos or radio sonde devices). Applications such as the proximity fuze power supply for artillary shells require battery function during high spin regimen. Therefore, the electrolyte must be immobilized between the electrodes to prevent intercell short circuiting and ensure satisfactory operation while the battery is in both the spin state and following the cessation of spin. A typical separator material in batteries for these applications is Dynel felt.

The battery reservoir may be located externally to the cell stack assembly[1,4] or may be located in a centrally located cavity within the cell stack. In the former case, activation of the battery may be accomplished by rupturing a burst disc to the cell stack through use of a spring loaded plunger or firing device. In the latter case, the electrolyte reservoir (glass or copper ampules) may be ruptured mechanically by a setback shock during artillery shell launching.[2]

The observed open circuit voltage for the lead-lead dioxide fluoroboric acid battery varies from 1.79 to 1.92 V for the corresponding fluoroboric acid concentration range of 35 to 55 weight percent. High rate cells designed for torpedo applications were discharged at current densities of approximately 160 mA/cm^2. The average discharge voltage to a cutoff level of 1.0 V was 1.43 V and the time of discharge was about 6.5 minutes. The average realized capacities and energies were found to be 8.2 Ah and 11.7 Wh, respectively.[1] These values for the realized capacities were approximately 84 percent those obtained for similarly fabricated cells containing perchloric acid.

Small proximity fuze batteries of four lead-lead dioxide fluoroboric acid cells in series with a total weight of 50 g were discharged at -37°C and +57°C at about the 1.15 mA rate.[2] The realized capacities of 0.074 and 0.091 Ah corresponded to discharge durations of 62 and 80 hours at -37 and +57°C. The energy densities for this battery varied from 8.4 to 9.9 Wh/kg over the temperature range of -37°C to +57°C.

Tests conducted to determine the activation times to an operational voltage level of 1.25 V for the proximity fuze battery showed that activation was met within 0.16 second at 23°C.[2] Two methods of activation were employed in these tests: 1) injection of the electrolyte into the spinning battery, or 2) fracture of the ampule followed by spinning the battery. Either method produced the same activation times. No data was presented which detailed the activated stand duration for the lead-lead dioxide fluoroboric acid battery. The ideal positive electrode should be non-porous since the reaction products are soluble in the electrolyte. However, some porosity does exist. In view of this, absorption of electrolyte could result in loss of electrolyte volume and loss of electrical contact of the lead dioxide and the current collector tab. In the former case, electrolyte continuity between the lead and lead dioxide electrodes could occur. In the latter case, the loss of contact between the lead dioxide and tab would result in cell dropout.

The major research, development, and manufacture relative to the lead-lead dioxide fluoroboric acid is presently performed by Globe-Union, Inc. (Division of Johnson Controls, Inc.) and Eagle-Picher Industries, Inc.

No safety abuse testing has been reported for the lead-lead dioxide fluoroboric acid system which detail the specific electrical test procedures of NAVSEAINST 9310.1A (i.e., short circuit, forced overdischarge, and charge). In addition, no data relative to the thermal abuse or the onset of thermal runaway of the battery were detailed in the literature. The operational temperature range for the system is -40°C to +72°C. In contrast, the lead-lead dioxide perchloric acid system is limited to temperatures of no higher than 40°C due to the possibility of fire or explosions. Lead-lead dioxide batteries containing fluoroboric or fluorosilicic acid electrolytes do not exhibit corresponding hazards characteristics.[1]

It is believed[1] that current will continue to flow through a series of cells should one cell fail for any reason other than complete loss of the fluoroboric acid electrolyte. Should this hypothesis be correct, the possibility of cell voltage reversal does exist. However, no specific details relative to the possibility of hazardous conditions were presented.

It should be noted that the lead-lead dioxide fluoroboric, fluorosilicic, and perchloric acid batteries do exhibit some reversibility and can be charged to some extent. Since these systems are used exclusively as primary systems, no data exist which detail charging current densities, charging methods, or the possibility of extensive gassing which may lead to hydrogen-oxygen fires or explosions.

This system has been investigated as possible candidate power supplies for torpedo propulsion. The load requirements[4] for such applications specify very high current densities (e.g., up to 250 mA/cm^2). Practical cells, therefore, would be discharged under resistive loads less than those specified for the short circuit test procedure in NAVSEAINST 9310.1A. Therefore, it is reasonable to assume that hazardous conditions would not arise in such cells at normal temperatures. No data was found for smaller cells discharged under resistive loads corresponding to the short circuit load of NAVSEAINST 9310.1A.

REFERENCES

1. Vinal, G. W., <u>Primary Batteries</u> (New York: John Wiley and Sons, Chapter 10, 1950).

2. McDonald, G. D., Weissman, E. Y., and Dettwiler, E. R., <u>Proc. Power Sources Symp. 26</u>, 1975, p. 120.

3. McDonald, G. D., Weissman, E. Y., and Roerman, T. S., <u>J. Electrochem. Soc.</u>, <u>119</u>, 1972, p. 660.

4. Bagshaw, N. E., "Power Sources 7, <u>Proc. 11th Int. Symp. Power Sources</u>, Collins, D. H., ed. (London: Academic Press, 1979), p. 667.

H. LEAD - LEAD DIOXIDE $(HClO_4)$

$$Pb \mid HClO_4 \mid PbO_2$$

$$Pb + PbO_2 + 4\ HClO_4 \longrightarrow 2\ Pb(ClO_4)_2 + 2\ H_2O \qquad [1]$$

The lead-lead dioxide perchloric acid electrochemical system serves as a power supply for many military applications such as torpedos, radio sonde devices, and ordnance fuzing. This system is distinguished from the lead-lead dioxide (H_2SO_4) SLI battery in that the discharge reaction products are soluble in the perchloric acid electrolyte while the discharge reaction of the SLI battery forms insoluble $PbSO_4$. A second distinguishing feature of the lead-lead dioxide perchloric acid system involves the use of nonporous electrodes since no accumulation of product takes place. As a result, there is a highly efficient utilization of the active materials in the battery. Thus, the lead-lead dioxide perchloric acid battery occupies less volume and weighs much less than a SLI (Starting, Lighting, and Ignition) battery of similar operational characteristics. Though the battery system does possess some degree of reversibility, it is exclusively employed as a primary reserve power supply. Indeed, charging SLI batteries containing perchloric acid instead of sulfuric acid results in extensive dendritic growth and gassing.[1]

The lead negative electrode may be fabricated by electrodepositing lead onto nickel or copper expanded screen[1] or by sizing a sheet of rolled lead alloy containing 1.5 percent tin and 0.06 percent calcium.[2] The latter electrodes possess the high mechanical strength required for long periods of storage. In addition, a thin deposit of pure lead is applied to the alloy electrode to prevent voltage delay when cells or batteries are activated after storage for extended periods of time.

During cell discharge at high current densities and low temperatures, passivation of the lead electrode can occur if the solubilty product constant for lead perchlorate is exceeded.[2,3] This results in the formation of a passivating film on the lead electrode and is accompanied by low realized capacities.

The lead dioxide positive electrode can be electrodeposited onto nickel screen[1,2] in a solution of lead perchlorate at current densities of about 50 mA/cm^2. Deposition of the lead dioxide onto such metals as iron or aluminum results in a severe corrosion attack on the exposed metal surface at the end of

discharge.[1] Iron also lowers the temperature threshold at which the electrolyte becomes hazardous. The deposition of lead dioxide onto nickel screen itself creates an electrochemical cell in strong perchloric acid solution. As a result, violent self-discharge can occur if the nickel current collector is exposed to the electrolyte on open circuit or at the end of discharge.

In view of the above, efforts have been made to mitigate the possibility of a violent self-discharge reaction. The most important factor involves the fabrication of a lead dioxide matrix surrounding the nickel screen which is crackfree and of extremely low porosity as well as possessing low stress characteristics.[2] Since the α-lead dioxide electrode exhibits high stress characteristics which result in electrode cracking during manufacture and storage, the preferred positive electrode is β-PbO$_2$.[2,5,6] Though the problems associated with electrode stress can be alleviated to a large extent through use of β-PbO$_2$ as the active positive electrode material, there still exist some internal stresses in the deposit which lead to electrode cracking. The addition of small amounts of H$_2$SO$_4$ (typically 0.5% or less) as an inhibitor causes the deposition of insoluble PbSO$_4$ at the electrolyte – positive electrode – nickel current collector interface. The resultant accumulation of PbSO$_4$ then serves as an insulating medium and retards further corrosion.

Applications for the lead-lead dioxide perchloric acid battery require high rate discharge conditions. In view of the above, substitution of the nickel current collector by a thermoplastic binder in the positive electrode and a nickel tab current collector is not possible. Therefore, the exposed nickel may be coated with solder, connected electrically with other positive electrode tabs, and potted in a resin material. This procedure results in good protection of the exposed nickel members from the electrolyte.[2]

The electrolyte for the lead-lead dioxide perchloric acid battery system consists of 40-60 percent perchloric acid containing approximately 0.5 percent H$_2$SO$_4$ as an inhibitor. Batteries containing electrolyte of the above composition are nonhazardous at the normal operating temperatures of the battery. It should be noted, however, that the use of iron metal and certain plastic materials lowers the threshold temperature at which the perchloric acid may become hazardous. For example, lucite and other plastics in contact with perchloric acid will detonate at about 160°C or lower.[1] In this regard, the upper operational temperature limit is normally restricted to 40°C or less (military applications require operation to 71°C).

No separator material is employed in the lead-lead dioxide perchloric acid cell. Instead, mechanical separation of the electrodes is effected through use of a plastic material compatible with the electrolyte (e.g., PCV) wound around the electrodes at various intervals.[2] After the battery elements are assembled, the unit is inserted into a polypropylene cell container. The terminals protrude through the base of the container and are sealed closed through use of gaskets. The electrolyte chamber typically is fabricated from polystyrene and is fitted with a burst disc. Activation of the battery is accomplished by rupturing the burst disc through use of a spring loaded plunger.[2]

The observed open circuit voltage for the lead-lead dioxide perchloric acid battery varies from 1.85 V to 2.05 V for the corresponding perchloric acid concentrations of 40 and 60 percent, by weight. Bagshaw[2] has detailed the performance characteristics for cells of nominal capacity of 75 Ah. Each cell contained 23 positive electrodes having a surface area of 179.5 cm^2 each and 24 negative electrodes of the same area. The weight of each cell (including the electrolyte chamber) was 4.15 kg. Cells discharged at 21°C at currents of 100, 250, 500, 750 and 1000 A yielded realized capacities of 89, 75, 61, 54, and 7.5Ah, respectively, to a voltage cutoff level of 1.33 V. Cells discharged at the 100 A rate at initial temperatures of 10°C, 38°C, 49°C, and 60°C yielded lower capacities than that obtained at 21°C. For cells discharged at the moderate and high rates of 250 to 1000 A, however, the highest realized capacities were obtained at either 49°C or 60°C. These results show that, at low temperatures, the lead electrode is passivated quickly in cells discharged at the higher rates due to formation of an insoluble lead perchlorate film. Cells discharged at the higher temperatures under low discharge rates (i.e., 100 A) exhibit the effects of self discharge. Energy densities of 21 and 29 Wh/kg were obtained for cells discharged at 21°C under constant current conditions of 750 and 250 A, respectively.

The activated stand duration for this system[2] varies from 446 hours to 11 hours for storage temperatures of 19°C to 60°C, respectively. The hydrogen evolution rate at the negative electrode under open circuit conditions at 25°C is low, approximately 1.5×10^{-3} cm^3 per hour per cm^2 of electrode surface.[1] If the grid material of the positive electrode is attacked by perchloric acid under open circuit conditions, the lead dioxide may be loosened, resulting in loss of electrical contact. The positive electrode, therefore, limits the activated stand life of the battery.

Tests conducted to determine the activation times to various voltage levels for cells under constant resistive loads show that, as the ambient temperature increases in the normal operating temperature range of 10°C to 60°C, the activation times decrease considerably.[2] For example, the times for cell voltage levels to reach 1.4 V at temperatures of 10°C, 21°C, and 60°C were 5.0, 4.0, and 2.8 seconds, respectively, for cells discharged under 1.8×10^{-3} ohm loads.

The development of the lead-lead dioxide perchloric acid battery was initially carried out by J.P. Schrodt and D.N. Craig at the National Bureau of Standards. The major manufacture and development work for this battery system is presently performed by Chloride Industrial Batteries Ltd. and McMurdo Instrument Company in England. At the present time, there exists no known U.S. manufacturer of the system.

No safety abuse testing has been reported for this system which detail the specific electrical test procedures in NAVSEAINST 9310.1A (short circuit, forced overdischarge, and charge). It is apparent from the discussion of the battery system that hazardous conditions do arise should the battery system be subjected to high temperature or incineration conditions. Perchloric acid becomes a powerful oxidizer at elevated temperatures. Therefore, the operational temperature range of the battery is usually restricted to values no higher than 40°C. This restriction also takes into account self-heating due to discharge at high current densities as well as chemical side reactions taking place within

NSWC TR 84-302

the battery during discharge. Storage of the activated battery for long periods at 60°C would result in accelerated self-discharge of the lead oxide positive electrode. The internal temperature of the battery could then increase to the extent to give rise to a thermal runaway condition[7] with a resultant fire or explosion.

Practical cells designed for use in a torpedo battery[2] can be discharged under resistive loads of 1.8×10^{-3} ohms. This resistance value is appreciably less than the value of 1×10^{-2} ohms set forth for the short circuit conditions in NAVSEAINST 9310.1A. Though the cell is quite large (4.5 kg total weight), it is reasonable to assume that hazardous conditions would not arise in such cells short circuited at normal temperatures. No other performance data was found for smaller cells discharged under resistive loads corresponding to the short circuit load of NAVSEAINST 9310.1A.

It is believed[1] that current will continue to flow through a series string of cells should one cell fail for any reason other than the complete loss of the perchloric acid electrolyte. Should this be the case, then the possibility does exist for cell voltage reversal to occur. No further details relative to the possibility of a hazardous condition were presented, however.

It is apparent that a potential hazard does exist in this system if the temperature of the battery increases to the point of thermal runaway. The increase in temperature may be brought on by a number of factors which include discharge or storage at elevated temperatures, the reaction of the electrolyte with the nickel current collector or certain plastic or organic materials, or by self heating as the result of side reactions and possible electrical abuse testing.

REFERENCES

1. Vinal, G. W., <u>Primary Batteries</u> (New York: John Wiley and Sons, Chapter 10, 1950).

2. Bagshaw, N. E., "Power Sources 7," <u>Proc. 11th Int. Symp. Power Sources</u>, Collins, D. H., ed. (London: Academic Press, 1979), p. 677.

3. Bushrod, C. J., and Hampson, N. A., <u>Brit. Corr.</u> J., 6, 1971, p. 129.

4. Bushrod, C. J., and Hampson, N. A., <u>Brit. Corr.</u> J., 6, 1971, p. 87.

5. Hampson, N. A., Jones, P. C., and Phillips, R. F., <u>Can. J. Chem.</u>, <u>45</u>, 1967, p. 2045.

6. Hampson, N. A., Jones, P. C., and Phillips, R. F., <u>Can. J. Chem.</u>, <u>46</u>, 1968, p. 1325.

7. Barak, M., "Power Sources 7," <u>Proc. 11th Int. Symp. Power Sources</u>, Collins, D. H., ed. (London: Academic Press, 1979), p. 677.

I. MAGNESIUM-AIR (MAGNESIUM-OXYGEN)

$$Mg \mid NaCl \mid O_2$$

$$Mg \mid Mg(NO_3)_2, NaNO_2 \mid O_2$$

$$2\,Mg + O_2 + 2\,H_2O \longrightarrow 2\,Mg(OH)_2 \qquad [1]$$
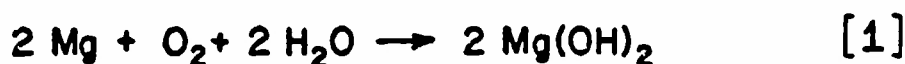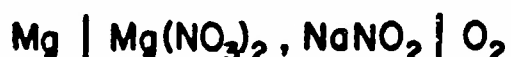
The magnesium-air electrochemical system was developed by the General Electric Company as an alternative power source to the zinc-air system.[1-3] The magnesium-air cell possesses a theoretical cell potential of 3.09 V and a theoretical energy density of approximately 6800 Wh/kg (based upon magnesium content only). It should be noted that the high cell potential is 2.26 V above the potential for hydrogen (0.83 V in alkaline media) so that the stability of magnesium electrode is decreased through self-discharge and hydrogen gas evolution in accordance with reaction 2:

$$Mg + 2H_2O \longrightarrow Mg(OH)_2 + H_2 \qquad (2)$$

The use of magnesium electrodes in neutral or slightly alkaline media results in increased hydrogen production as the current density is increased.[1,4,5] As cell discharge proceeds, an adherent protective film forms on part of the magnesium surface at low current densities. Since the film protects the magnesium electrode from reacting with water to produce hydrogen, only the bare magnesium surface is susceptible to attack. An increase in the current density would necessarily result in the further exposure of bare magnesium to corrosion attack. In addition, pulse loading of the magnesium cell results in severe voltage delays, dependent upon the film adherency and the time to create exposed magnesium electrode area. If the magnesium electrode – electrolyte interaction were to produce a non-adherent protective film on the magnesium surface, the corrosion rate would proceed unchecked. This would result in poor magnesium electrode efficiencies and low overall realized capacities.

In view of the above, a number of magnesium alloys have been investigated to find a composition which limits or reduces the corrosion reaction and yields high efficiencies in cells discharged at low rates. Pure magnesium electrodes exhibit particularly high corrosion rates and result in low cell potentials.

The magnesium alloy found to yield optimum results for the magnesium-air cell was AZ61 which represented a compromise between voltage and gassing behavior.[6] For example, at current densities of 10, 20, and 30 mA/cm^2 the cell voltage levels for magnesium-air cells containing AZ61 were 1.42, 1.31, and

1.20 V, respectively. The corresponding gassing rates at the above current densities were 0.030, 0.060, and 0.100 cm^3/minute/cm^2, respectively. Though other alloys gave higher cell potentials, none equalled the comparatively low gassing rate of AZ61. The approximate composition of AZ61 is 6.5 percent aluminum, 1.0 percent zinc, 0.45 percent manganese.

The air electrode used in the studies[1,2,6] consisted of a platinum black catalyst, a finely divided nickel powder (nickel carbonyl) and a Teflon binder. The thin film (0.05 cm thick) was pressed at 352 to 704 kg/cm^2 onto either a silver alloy or nickel expanded metal grid.

The electrolyte solutions contained NaCl in concentrations of seven to 18 percent by weight. The higher concentrations of the salt were found to yield lower resistive drops in the electrolyte and shorter voltage delay characteristics for cells subjected to increasing current densities. A number of electrolyte additives to the electrolyte were investigated.[6] The results are summarized below:

1. $MgBr_2$ or $MgCl_2$: Magnesium hydroxide precipitated in the air electrode when $MgBr_2$ or $MgCl_2$ was added to the electrolyte solution. Cell output decreased rapidly.

2. $CaCl_2$: The magnesium electrode passivated rapidly with the addition of $CaCl_2$.

3. Thickeners: With the addition of thickeners to increase the viscosity of the electrolyte, most of the electrolyte was expelled from cell due to the hydrogen evolution at the magnesium electrode.

4. Precipitation aids: The addition of precipitation aids caused the formation of dense sludge deposits which inhibited the efficient removal of spent magnesium electrodes.

The separator material for the magnesium-air cell was glycerinated cellophane. It was found that this material was superior in restraining the formation of $Mg(OH)_2$ on the air electrode. In addition, a 1 mm thick Vexar polyethylene film was placed between the separator and the magnesium electrode to keep the sludge product from dropping to the cell bottom. If sludge were allowed to accumulate in the bottom of the cell, discharge would be restricted due to increased resistance between the electrodes.

The observed open circuit voltage for the magnesium-air cell was 1.70 V, or about 1.39 V lower than the theoretical open circuit voltage for the cell. The loss is due to the polarization of the magnesium electrode by parasitic currents. When cells were discharged at current densities of less that 10 mA/cm^2 a steep drop in cell potential was realized. This was believed to be caused by the polarization of the air electrode. At current densities of ten to 70 mA/cm^2 the cell potentials decreased linearly from 1.30 to 1.12 V due to internal resistance drops. The magnesium electrode exhibited a constant potential over the current density range of 10 to 70 mA/cm^2. Because of the polarization of the cell electrodes and the corrosion reaction at the magnesium electrodes, a large amount of heat was evolved during cell discharge at current densities of 40 mA/cm^2 or higher. As a result, cooling must be provided to

keep the temperature of the electrolyte at 50°C or below. The air electrode life was dramatically shortened at temperatures of 50°C and higher. The observed energy density for this cell was 130 Wh/kg.

Recently, a magnesium-air cell was described which employed an electrolyte comprised of $Mg(NO_3)_2$ and $NaNO_2$.[7] The magnesium electrodes, AZ21 (2% Al, 1.2% Zn, 0.15% Mn, and 0.2% Ca), showed low open circuit corrosion and almost 90 percent utilization at current densities of 20 mA/cm. The cell possesses a shelf life of about one year due to the reported low open circuit corrosion rate. This result can be compared with the early findings by General Electric:[1,2] at room temperature with a 7 weight percent NaCl solution, 50 percent of the magnesium capacity was lost with the cell under open circuit conditions. It should be noted, however, that the magnesium-air system recently described is in the research and development phase and has not been produced as a practical power source (as in the case of General Electric).

No safety tests have been reported for the General Electric Mg-air system which detail results of short circuit, force overdischarge (cell reversal), charge, or incineration testing in accordance with NAVSEAINST 9310.1A procedures. However, because the magnesium electrode is highly irreversible, a large excess of heat is generated during normal operation. The thermal management of the cell has become a serious design problem. Should the cell be operated at high current densities, the boiling point of the NaCl electrolyte would be reached. The possibility does exist, therefore, of a thermal runaway condition.[3] The evolved hydrogen gas has not proven to be a hazard in either testing or use.[1,2] The NaCl electrolyte is not harmful to personnel in the event of either spilling or ingestion. The saline electrolyte is, however, corrosive to many metals. Should the magnesium-air system be a viable commercial product and of interest for use in U.S. Navy applications, further safety testing should be conducted in accordance with the NAVSEAINST 9310.1A in addition to the investigation into possible hydrogen-air fires or explosions created in unventilated areas.

REFERENCES

1. Carson, W. N., Jr. and Kent, C. E., "Power Sources 1966," _Proc. Fifth Int._ _Symp._, Joint Services Electrical Power Sources Committee, Collins, D. H., ed. (London: Pergamon Press, 1966), p. 119.

2. Kent. C. E., "Power Sources 1967," _Proc. Sixth Int. Symp._, Joint Services Electrical Power Sources Committee, Collins, D. H., ed. (London: Pergamon Press, 1967), p. 106.

3. Gregory, D. P., _Metal-Air Batteries_ (London: Mills and Boon Limited, 1972), p. 45.

4. Glicksman, R., _J. Electrochem. Soc._, 106, 1959, p. 457.

5. Robinson, H. A., _Trans. Electrochem. Soc._, 90, 1946, p. 485.

6. Hamlen, R. P., Jerabek, E. C., Ruzzo, J. C., and Swiek, E. G., _J._ _Electrochem. Soc., Elect   em. Technol._, 116, 1969, p. 1588.

7. Sathyanarayana, S., ar   ichandraiak, N., _J. Applied Electrochem._, 11, 1981, p. 33.

J. MAGNESIUM – BISMUTH OXIDE

$$\text{Mg} \mid \text{MgBr}_2 \mid \text{Bi}_2\text{O}_3$$

$$3\,\text{Mg} + \text{Bi}_2\text{O}_3 + 3\,\text{H}_2\text{O} \longrightarrow 2\,\text{Bi} + 3\,\text{Mg(OH)}_2 \qquad [1]$$
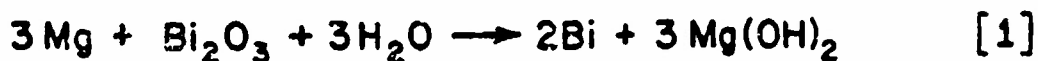
The magnesium-bismuth oxide electrochemical system was investigated as an alternative power source for the Leclanche and zinc-mercuric oxide battery sytems. All of the research efforts for this system has been carried out at RCA Laboratories by Morehouse and Glicksman.[1-3] The system, at present, has not progressed to either the advanced development or to the production stages. Nonetheless, it has been reported that the magnesium-bismuth oxide dry cells exhibit flatter discharge characteristics and higher realized capacities for cells cf comparable size than either the Leclanche or the magnesium-manganese dioxide systems.[1]

The reversible electrode potentials for pure magnesium electrodes are 2.37 and 2.69 V in acidic and basic media, respectively.[4] However, the true potential is not realized due to the protective oxide film on the metal surface. As a consequence, magnesium exhibits negative electrode potentials of only 0.3 to 0.6 V higher than zinc. In addition, magnesium will undergo a severe corrosion side reaction:

$$\text{Mg} + 2\,\text{H}_2\text{O} \longrightarrow \text{Mg(OH)}_2 + \text{H}_2 \qquad (2)$$

Reaction 2 is minimal under storage conditions since the oxide film affords the metal considerable corrosion protection. When the oxide film is removed during cell discharge, a rapid corrosion attack occurs with subsequent production of hydrogen[5] in accordance with equation 2.

The composition of the magnesium alloy, AZ10A (Dow), chosen as the optimum negative electrode for these studies included 1 percent aluminum, 0.4 percent zinc, 0.15 percent manganese, and 0.2 percent calcium. The inclusion of calcium is believed to minimize voltage delay characteristics.[6] The magnesium can for the AA size cells used as the test vehicle was impact extruded.

The positive electrode was comprised of 54.7 weight percent bismuth oxide, 6.8 weight percent Shawinigan acetylene black, and 1.9 weight percent barium chromate. The balance of the positive electrode mixture was an electrolyte solution of 1.7 M MgBr_2 and $6 \times 10^{-3}\text{M}$ Li_2CrO_4. The addition of both

Li_2CrO_4 and the slightly soluble $BaCrO_4$ was found to provide reduced corrosion under both open circuit and intermittent use conditions. The separator employed in these studies was Nibroc salt-free paper.

Cell construction was patterned after the Leclanche cell fabrication techniques. An extruded slug of the bismuth oxide was inserted into the magnesium can lined with the separator and a carbon rod served as the positive electrode current collector. Cell enclosure was effected using a rosin based wax.

The observed open circuit voltage for the above test cells was 1.60 to 1.65 V. It was postulated that the high open circuit voltage was the result of either a $Mg-O_2$ couple caused by adsorbed oxygen in the cathode mix or a $Mg-CrO_4^{2-}$ couple caused by interaction of magnesium with the chromate corrosion inhibitor system.

AA-size cells were discharged under constant resistive loads of 50, 150, and 300 ohms at 21°C. The corresponding realized capacities, obtained to a 0.90 V cutoff voltage level, were 1.60, 1.68, and 1.71 Ah, respectively. The average load voltage levels for the cells were approximately 1.05 V throughout the discharge period. There was a noted voltage delay observed for all cells tested. The delay characteristics were attributed to changes at the bismuth oxide electrode rather than at the magnesium electrode, as experienced with other magnesium dry cell systems.

Storability tests showed that approximately 80 percent of the initial capacity was retained for AA cells stored for two years at 21°C. However, it was also found that, in addition to the voltage delays as noted above, the cells exhibited high internal impedance values as well as low realized capacities when discharged under intermittent conditions.[1]

No safety data was reported for cells of the magnesium-bismuth oxide system. Three factors preclude the use of the system for any U.S. Navy applications: (1) bismuth oxide is intrinsically more expensive than manganese dioxide, (2) only little performance advantage is gained by the magnesium-bismuth oxide system, and (3) the system is not presently in the advanced developmental or production phases. In consideration of the above, no safety testing is recommended for cells of the system.

REFERENCES

1. Morehouse, C. K., and Glicksman, R., J. Electrochem. Soc., 106, 1959, p. 61.

2. Glicksman, R., and Morehouse, C. K., J. Electrochem. Soc., 104, 1957, p. 589.

3. Morehouse, C. K., and Glicksman, R., J. Electrochem. Soc., 103, 1956, p. 94.

4. Glicksman, R., J. Electrochem. Soc., 106, 1959, p. 457.

5. Robinson, J. L., The Primary Battery, Volume II, Heise, G. W., and Cahoon, N. C., eds. (New York: John Wiley and Sons, Chapter 2, 1976).

6. Kirk, R. C., George, P. F., and Fry, A. B., J. Electrochem. Soc., 99, 1952, p. 3?3.

K. MAGNESIUM - LEAD CHLORIDE

Mg | Sea Water | $PbCl_2$

$$Mg + PbCl_2 \longrightarrow MgCl_2 + Pb \qquad\qquad [1]$$

The magnesium-lead chloride system was developed as an alternative power source to the more expensive magnesium-silver chloride system by ESB Incorporated in the United States.[1] Both water activated systems have been employed as U.S. Navy power supplies for electric torpedos, emergency signalling devices, and passive sonobuoys. The magnesium-lead chloride system possesses a theoretical cell potential of approximately 2.1 V. However, the stability of the magnesium electrode is decr-ased through self-discharge and hydrogen gas evolution in accordance with the following reaction:

$$Mg + 2H_2O \longrightarrow Mg(OH)_2 + H_2 \qquad\qquad (2)$$

The above corrosion reaction in neutral or slightly basic media results in a magnesium potential over 1.0 V anodic to the theoretical reversible potential.[2] In addition, increased hydrogen production is observed in cells containing Mg electrodes as the current densities are increased.[3,4,5]

Early investigations[6] employed the same magnesium alloys AZ31 (3% Al, 1.0% Zn, 0.2% Mn, and 0.04% Ca) and AZ61 (6.5% Al, 0.7% Zn, and 0.2% Ca) which had been selected for exhibiting favorable performance characteristics for the older magnesium-silver chloride system. The lead chloride electrode was prepared by blending powdered $PbCl_2$ with graphite. Typical compositions consisted of at least 80 percent $PbCl_2$ and 20 percent or less of graphite. The most satisfactory binder for the $PbCl_2$ electrode was found to be an aqueous solution of urea and formaldehyde. The positive electrode mixture was then pasted onto an expanded copper grid, which was dried to reduce the water content of the binder, and finally pressed at 70.4 to 246 kg/cm^2 (1000 to 3500 $pounds/in^2$). The positive electrode plate was air dried for 24 hours and further cured at 110°C for 48 hours.

Construction of the cell followed the general procedures used for the magnesium-silver chloride system: each cathode was inserted between two magnesium alloy electrodes with physical separation maintained by spacers.[7] The cell was then encased and inserted into a container vessel fitted with electrolyte entry and exit ports positioned at diagonally opposite corners of

the container.[1] Efficient removal of hydrogen and the $Mg(OH)_2$ sludge was found to be essential for sustained cell performance. The electrolyte used in these preliminary studies was synthetic sea water for operating temperatures above 0°C and an aqueous solution of 21 weight percent LiCl for operating temperatures below 0°C.

The observed open circuit voltage for the magnesium-lead chloride system was 1.1 to 1.2 V (compared to that of 1.7 to 1.9 V for the Mg-AgCl system). Cells were discharged at -40°C, 0°C, and 21°C under constant current conditions corresponding to maximum current densities of 3.9 mA/cm^2. The average load voltages were approximately 1.05 V at 21°C, 0.9 to 1.0 V at 0°C, and 0.7 to 0.9 V at -40°C. It was found that increased concentration of binder as well as increased loading of the positive plate decreased utilization at the lower temperatures. It should be noted, however, that the discharged $PbCl_2$ electrodes were found to be structurally unaffected at the end of discharge at 21°C or below. At temperatures of 45°C, the electrodes softened due to increased $PbCl_2$ solubility. Prolonged exposure of the positive electrodes to electrolyte at temperatures of 45°C resulted in swelling and detachment from the copper grid.

Five cell batteries were constructed and intermittently discharged at -40°C, 0°C, and 21°C under constant currents of 171, 330, and 330 mA, respectively, for four hours per day. The corresponding current densities were 1.9 mA/cm^2 at -40°C and 3.7 mA/cm^2 at 0°C and 21°C. The results for the batteries discharged at -40°C showed that voltage reversal was reached at startup on the second and third days. In addition, the load voltage failed to meet the minimum requirement of 4.0 V on the third day. Batteries discharged continuously at 0°C and 21°C exhibited load voltage differences of only 0.2 V throughout the majority of discharge. These voltage differences increased at the end of the discharge period, however. The realized capacities were approximately 1.5 and 1.8 Ah, respectively, and the corresponding energy densities were 53 and 62 Wh/kg, based upon the dry weight of the batteries.

The successful operation of either the Mg-$PbCl_2$ or Mg-AgCl battery depends upon the circulation of sea water through the cells of the battery. The circulation is effected by the side reaction, equation 2, which produces hydrogen gas. Hydrogen evolution aids the flow of the sea water, resulting in the provision of fresh electrolyte, removal of sludge and $Mg(OH)_2$ from intercell spacings, and cooling of the battery. At a depth of 412 meters, the solubility of H_2 in the electrolyte is 99.8 percent.[8] At that depth, the circulation is no longer dependent on hydrogen evolution and is controlled by thermal gradients and natural convection within the battery. If $Mg(OH)_2$ builds up in the flow channels, however, the electrolyte circulation would decrease. Further, as the heat increases within the battery, gassing increases to the point of expelling all electrolyte from the cells. Optimization of the battery design[8] resulted in a magnesium-lead chloride battery system with the capability of operation which was independent of pressure, thus alleviating the problems.

Recent studies[2] have shown that the magnesium alloy, MN150 (1.5% Mn), operates at high efficiency for low power applications and delivers the maximum capacities at stable voltages over the operating temperature range of 0°C to +35°C. Performance test results for eleven cell batteries discharged under 26

ohm loads at the environmental extremes of 0°C with 1.6 percent NaCl solution and 35°C with 3.6 percent NaCl solution yielded realized capacities of 4.05 and 3.5 Ah, respectively.

No safety related studies were reported in the literature for the magnesium-lead chloride sea water activated battery. The battery was designed to allow free access to the cell stack by sea water. Under certain circumstances, however, it would appear that the activated battery could experience a clogging which would result in a thermal runaway condition and the expulsion of hot electrolyte containing $Mg(OH)_2$. In addition, the rate capability of the system is low compared to similarly designed sea water systems (e.g., magnesium-silver chloride). In view of the above conditions, it is unlikely that activated $Mg-PbCl_2$ cells or batteries would present serious hazardous conditions when subjected to short circuit, forced overdischarge, or charge testing. The possibility does exist for the occurrence of a fire or explosion caused by the accumulation of H_2 in sealed laboratory test vessels.

REFERENCES

1. Colbeck, D. B., and Purcell, T. H., U.S. Patent 3,508,971, 1970.

2. Bagshaw, N. E., Thompson, J., and Warrell, S., "Power Sources 8," _Proc. 12th Int. Symp. Power Sources_, Thompson, J., ed. (London: Academic Press, 1981), p. 117.

3. Carson, W. N., Jr. and Kent, C. E., "Power Sources 1966," _Proc. Fifth Int. Symp. Joint Services Electrical Power Sources Committee_, Collins, D. H., ed. (London: Pergamon Press, 1966), p. 119.

4. Glicksman, R., _J. Electrochem. Soc._, 106, 1959, p. 457.

5. Robinson, H. A., _Trans. Electrochem. Soc._, 90, 1946, p. 485.

6. Coleman, J. R., _J. Applied Electrochem. 1_, 65, 1971.

7. Doll, J. H., and Druesne, H. D., U.S. Patent 3,515,596, 1970.

8. Malaspina, F. P., _Proc. 10th IECEC_, American Society of Mechanical Engineers, 1, 1975, p. 817.

L. MAGNESIUM-MANGANESE DIOXIDE

$$Mg \mid MgBr_2 \mid MnO_2$$

$$Mg \mid Mg(ClO_4)_2 \mid MnO_2$$

$$Mg + 2\,MnO_2 + H_2O \longrightarrow Mg(OH)_2 + Mn_2O_3 \qquad [1]$$

Magnesium-manganese dioxide dry cell batteries have fulfilled the requirements for such military applications as portable transceivers, sonobuoys, and locator beacons.[1-3] Use of the Mg/MnO$_2$ reserve battery has been limited, however, to applications requiring operation at very low temperatures, e.g., meteorological radio transmitters. The major advantages of this system over the Leclanche system are higher energy and power densities as well as improved performance at both high and low temperatures.

The reversible electrode potentials for magnesium are 2.37 V and 2.69 V in acidic and basic media, respectively.[4] However, magnesium is protected by an oxide film which prevents realization of the true reversible potential. As a consequence, magnesium exhibits anode potentials of only 0.3 to 0.6 V higher than zinc. Magnesium will undergo the corrosion side reaction:

$$Mg + 2H_2O \longrightarrow Mg(OH)_2 + H_2 \qquad (2)$$

Under storage conditions, reaction 2 is slight since the oxide film affords the metal considerable corrosion protection. However, when the oxide film is removed during cell discharge, a rapid attack occurs and the magnesium decomposes water.[5] As reaction 2 proceeds, the water contained in the electrolyte decreases, thereby causing drying out of the cell.

Because of the inefficiency of the magnesium electrode caused by the IR difference between the theoretical voltage and operating voltage as well as the corrosion reaction, a significant amount of heat is evolved during the cell discharge.[6] It has been shown that the heat evolved during discharge of practical Mg/MnO$_2$ dry cells is approximately 1.6 kcal/Ah (6.7 kJ/Ah) of cell output.[7] The high heat output can be particularly advantageous at low operating temperatures if provision is made for thermal insulation.

In addition to the wasteful corrosion reaction, magnesium electrodes exhibit voltage delays immediately upon load application. The delay is believed to be caused by the resistance of the oxide protective film on the magnesium electrode. As the film is removed, the cell voltage increases to a value above

the original open circuit voltage and eventually decreases to the original OCV value. This is, therefore, an indication that the magnesium surface is more electrochemically active under open circuit conditions following load application. The corrosion rate also increases following partial discharge.[4]

A second hypothesis[6] to explain the voltage delay phenomenon suggests the intermediate formation of magnesium hydride to account for discrepancies between the theoretical (-1.9 V, versus SHE) and observed voltage (-1.3 V) for the reactions:

$$Mg \longrightarrow Mg^{2+} + 2e^{1-} \tag{3}$$

$$2H_2O + 2e^{1-} \longrightarrow 2OH^{1-} + H_2 \tag{4}$$

An alternative to the above, Kirk and Vermilyea[8] proposed the following intermediate reactions, also leading to the eventual formation of $Mg(OH)_2$ on the electrode surface:

$$Mg + 2H_2O + 2e^{1-} \longrightarrow MgH_2 + 2OH^{1-} \tag{5}$$

$$MgH_2 + 2OH^{1-} \longrightarrow Mg(OH)_2 + H_2 + 2e^{1-} \tag{6}$$
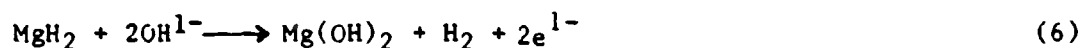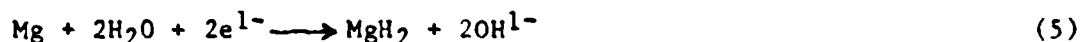
Thermodynamic considerations favor the latter hypothesis.

Much effort has been expended to develop suitable magnesium alloys which exhibit minimized corrosion and decreased voltage delays.[9,10] The three most widely studied alloys are AZ10A (1% Al, 0.4% Zn, 0.15% Mn, and 0.2% Ca), AZ21 (2% Al, 1.2% Zn, 0.15% Mn, and 0.2% Ca), and AZ31 (3% Al, 1% Zn, 0.2% Mn, and 0.04% Ca). The inclusion of calcium is believed to minimize voltage delay.[10] Of the three magnesium alloys, AZ10 corroded excessively during prolonged open circuit storage but exhibited decreased voltage delay characteristics. The AZ31 alloy, on the other hand, was characterized by improved anode efficiencies. The optimum alloy was found to be AZ21 which combined the improved anode efficiencies of AZ31 and the decreased voltage delay characteristics of AZ10. In addition, AZ21 exhibited less sensitivity to corrosion under open circuit conditions.

The manganese dioxide electrode mix is generally comprised of either chemically processed MnO_2 (African ore, type M) or electrolytic MnO_2 incorporated with acetylene black. Slightly soluble barium chromate, in concentration levels of approximately 3 percent, was found both to reduce the anode corrosion rate and to provide a beneficial catalytic influence on discharge performance. Capacity increases of seven to fifteen percent were found for cells containing $BaCrO_4$ compared to cells without the chromate inhibitor. The addition of a buffering agent of $Mg(OH)_2$ is believed to assist in the storability of the dry cell.[6]

The electrolyte salt of choice in the early developmental and production stages of the magnesium-manganese dioxide system was approximately 1.35 M $MgBr_2$.[4,10-12] However, 1.9 M $Mg(ClO_4)_2$ was found to reduce voltage delay and to be less corrosive than the $MgBr_2$ electrolyte.[13,14] In addition, small amounts of Li_2CrO_4 in the electrolyte further reduced corrosion during storage under open circuit conditions, due to the formation of a protective film

on the magnesium electrode. If the cell is discharged under intermittent regimes, the protective film is destroyed at each instance of circuit closing. As a result, the inhibitive effect of soluble Li_2CrO_4 would be limited. However, by incorporation of slightly soluble $BaCrO_4$ in the positive electrode mix, the supply of CrO_4^{2-} would remain constant throughout the discharge life, thereby renewing the protective film continuously.

The cell design may either conform to the construction characteristics for conventional Leclanche cells or employ a rolled magnesium can inside a steel jacket. Separation of the magnesium and manganese dioxide would be effected through use of uncoated Kraft paper.[5] The advantage of a rolled magnesium can over a conventional impact extruded can is the ability to withstand cell rupture caused by the large volume of discharge product, $Mg(OH)_2$ [5,6,10] and the uneven attack on the magnesium can when cells are discharged at low rates.[6] The volume of $Mg(OH)_2$ generated is approximately 1.5 times that for the magnesium electrode. As cell discharge progresses, the $Mg(OH)_2$ presses against the centrally located manganese dioxide mix which has been hardened through water loss in cell reactions 1 and 2. The resultant rupture does not usually cause the cell to leak electrolyte, but does have a dramatic effect on the performance characteristics (to be discussed in a later section).

Adequate sealing of the cell has been possible through use of self sealing vents[15-17] which allow hydrogen to escape, yet prevent moisture loss. In addition, the vents also prohibit the influx of oxygen, which would accelerate the corrosion reaction.

The open circuit voltage for the magnesium-manganese dioxide system is observed to be 1.8 to 2.0 V. The performance characteristics for D-cells of present manufacture[8] and containing $Mg(ClO_4)_2$ electrolyte were obtained for cells discharged at 21°C under constant resistive loads and continuous discharge regimes. The results show that realized capacities of 4.5, 4.8, 6.3, and 7.0 Ah were obtained for cells discharged under loads of 2,5,10, and 20 ohms, respectively, to a 0.90 V cutoff voltage level. The corresponding average load voltages were 1.50, 1.60, 1.72, and 1.80 V respectively. Similar data for C-cells show that capacities of 1.3, 2.1, 2.6, and 2.9 Ah were realized for cells discharged under 2,4,15, and 20 ohms, respectively. The corresponding average load voltages were 1.3, 1.5, 1.64, and 1.75 V, respectively. The nominal energy density for the ACR MAG cells is approximately 92 Wh/kg. Current manufacturers of the magnesium-manganese dioxide cell are ACR Electronics, Eagle Picher, and Marathon Battery Corporation.

As previously discussed, magnesium-manganese dioxide cells exhibit a tendency to rupture due to the large volume of $Mg(OH)_2$ reaction product formed in cells discharged at low rates. Since little or no electrolyte is lost during rupture, the cell is susceptible to further discharge caused by the leakage of oxygen into the cell.[10] In fact, increases of nearly 50 percent in the realized capacity have been observed for ruptured D cells. In the majority of instances of cell rupture, however, the added benefit of increased capacity is not desirable due to the unpredictability of cell performance and to the swelling of the ruptured cells strictly confined in battery packs.

The heat generated during the discharge of cells or batteries can be an advantage in high rate applications if it results in higher battery operating temperatures.[7] Small A size cells have been discharged under constant current conditions (20 mA) at 115°C. The load voltages were found to average 1.8 V and the utilization of the MnO_2 was approximately 73 percent. Further, the energy densities for these cells was 103 Wh/kg. Special provisions (e.g., thermal insulation) to minimize the heat loss have resulted in improved performance characteristics over uninsulated batteries.[6,7,19] In view of the above, magnesium-manganese dioxide batteries used for manpack communications equipment such as the AN/PRC-70 radio have successfully operated at -40°C with current densities of 20 mA/cm^2.[20] There is, however, a decrease in energy density of 25 percent at the low temperature (i.e., 88 Wh/kg for the battery discharged at 24°C versus 66 Wh/kg at -40°C).

A magnesium-manganese dioxide reserve battery may be used for applications requiring operation at very low temperatures (e.g., at altitudes of 31 km and temperatures of -52°C). Typically, the battery is activated at normal ambient temperatures, and, as the battery is introduced to the cold environment, the internal temperature of the battery will remain sufficiently high to maintain operation for the duration of the intended mission.

The storability characteristics for production run and special laboratory built Mg/MnO_2 cells containing $Mg(ClO_4)_2$ electrolyte have been studied by Wood.[6] The capacity retention data presented show that, for production cells stored at 72°C for periods of 5, 8, and 12 weeks, the median capacities retained were 95, 92, 83 percent, respectively, of the initial realized capacities for fresh production cells. This indicates a five percent per month decrease in capacity at 72°C. Special laboratory cells stored at 72°C for periods of 5, 12, and 20 weeks exhibited mean capacities of 100, 93, and 89 percent of the realized capacities for fresh cells. Thus, the observed decrease in realized capacity for carefully fabricated cells is only about two percent per month as compared to five percent per month for production cells.

The above data were obtained for cells which have not been discharged in any way prior to long-term, high temperature storage. It has been estimated[6] that the chromate inhibitor system deteriorates after approximately 25 percent of the capacity is withdrawn from cells. As a result, the corrosion reaction will proceed unchecked and the available capacity will be expended, dependent upon the length of storage time. Indeed, it has been reported* that if as little as one-half percent of the capacity is withdrawn from a cell, and the cell is subsequently stored at ambient conditions for one to two years, no capacity would be realized, even when the cell is discharged under light loads. Therefore, once cells have begun discharge, the optimum performance would be achieved if the cells are discharged continuously or if the intermittent periods are short.

The AC impedance characteristics for small (AA size) Mg/MnO_2 cells which had been discharged to 50 percent of nominal capacity under various resistive loads showed that the impedance was higher at low frequency for cells discharged

*Barnes, J. A., Naval Surface Weapons Center, White Oak, Silver Spring, MD, Private Communication, 1984.

under the lighter loads (e.g., 10 ohms impedance at frequencies of 10 Hz or less for cells discharged under 150 ohm loads). As the load increased, the impedence values remained constant throughout the frequency range (e.g., 0.5 ohm impedance for cells discharged under 4.0 ohm loads for the frequency range of 1 to 10 kHz). Recent studies[21] have shown that the impedance as diffusion controlled for undischarged cells but becomes charge transfer controlled as soon as the discharge process is begun.

Prior to the advent of high energy density lithium batteries, very little systematic safety testing was performed upon cells or batteries of conventional systems. Some safety data, however, does exist for the magnesium-manganese dioxide system. Long C cells (8.4 cm long, 2.39 cm diameter) were short circuited in open air at 23°C and in a constant temperature water bath at 21°C.[7] The results for cells short circuited in air showed an initial current of 4.5A which decreased to 3.7A after about 10 minutes. An abrupt increase in current to a maximum of 4.8 A was observed at the 16 minute mark. The current then gradually decreased to the 1 A level after 60 minutes on test. The cell wall temperature increased to a maximum of 107°C after 28 minutes on test and gradually decreased to 78°C at the end of the test. The efficiency, based upon utilization of manganese dioxide, was 45 percent of the theoretical capacity of MnO_2 available. No cell rupture or venting was reported.

Cells which had been short circuited in a 21°C constant temperature bath exhibited initial short circuit currents of 3.2 A immediately. The current then decreased to 1.5 A after five minutes and slowly dropped to the 1 A level after 22 minutes on test. The temperature of the cell increased only slightly from 21°C to a maximum of 27°C after five minutes and gradually decreased to 26°C after 52 minutes on test. The utilization to a 1 A cutoff level was only 21 percent that for the cell short circuited in air. No cell rupture or venting was reported.

No reports exist in the technical literature which detail the experimental results for cells which have been subjected to forced overdischarge (cell voltage reversal), charging, or incineration. However, one manufacturer[18] does state that "Experience has shown that Lithium (sic) can explode with some violence when short circuited or punctured. On the other hand, Magnesium (sic) has proven to be perfectly safe, even when thrown into open flames." No experimental details accompanied the above statements.

Hydrogen gas is evolved in magnesium-manganese dioxde cells during storage and operating conditions. There is, therefore, the possibility for hydrogen-oxygen fires and/or explosions[6] if proper means are not taken to avoid the accumulation of hydrogen in enclosed battery and electronic packages. Indeed, instances have been reported* which describe the occurrence of explosions for stored magnesium-manganese dioxide battery packs used as the power sources for military communications equipment. In view of the above, a study[22] was carried out to determine the hydrogen concentration levels in radio sets which would lead to either a fire or explosion. The data from reference 22 was summarized by Wood:[6] hydrogen-air mixtures of 4.1 percent or higher are flammable while explosive mixtures are obtained for hydrogen concentrations of 18 percent or higher.

---

*Mahy, T. X., Private Communication, 1984.

REFFRENCES

1. Brodd, R. J., Kozawa, A., and Kordesch, K. V., J. Electrochem. Soc., 125, 1978, 275C.

2. Crompton, T. R., Small Batteries, Volume 2, Primary Cells (New York: John Wiley and Sons, 1983), p. 127.

3. Hazkany, H., Peled, E., and Raz, B., Proc. Power Sources Symp. 29, 1931, p. 56.

4. Glickman, R., J. Electrochem. Soc., 106, 1959, p. 457.

5. Robinson, J. L., The Primary Battery, Volume II, Heise, G. W., and Cahoon, N. C., eds. (New York: John Wiley and Sons, Chapter 2, 1976).

6. Wood, D. B., "Batteries," Volume 1, Manganese Dioxide, Kordesch, K. V., ed. (New York: Marcel Dekker, Inc., Chapter 4, 1974).

7. Urry, L. F., J. Electrochem. Soc., 122, 1975, p. 715.

8. Kirk, C. F., and Vermilyea, D. A., J. Electrochem. Soc., 116, 1948, p. 1487.

9. Kirk, R. C., and Fry, A. B., Trans. Electrochem. Soc., 94, 1948, p. 277.

10. Kirk, R. C., George, P. F., and Fry, A. B., J. Electrochem. Soc., 99, 1952, p. 323.

11. Naylor, D. Contemporary Physics, 1, 1960, p. 287.

12. Morehouse, C. K., J. Electrochem. Soc., 99, 1952, p. 187C.

13. Lozier, G. S., Proc. Power Sources Symp., 16, 1962, p. 134.

14 Murphy, J. J., and Wood, D. B., Proc. Power Sources Symp., 21, 1967, p. 100.

15. Urry, L. F., U.S. Patent 3,494.801, 1970.

16. Beatty, T. R., U.S. Patent 4,251.602, 1981.

17. Beatty, T. R., U.S. Patent 4,255,499, 1981.

REFERENCES (Cont.)

18. Dhanji, S., *Magnesium, The Safe Power Solution*, paper presented at the Safe Symposium (Safety and Flight Equipment), Las Vegas, Nevada, 6-8 Dec 1982, Available: ACR Electronics Inc., 3901 North 29th Ave., Hollywood, FL. 33020.

19. Wood, D. B., *Proc. Power Sources Symp.*, 26, 1975, p. 154.

20. Wilburn, N. T., and Almerini, A. L., *Proc. 4th IECEC*, American Society of Mechanical Engineers, 1, 1969, p. 522.

21. Gopikanth, M. L., and Sathyanarayana, S., *J. Applied Electrochem.*, 9, 1979, p. 581.

22. Brooks, E. S., *Study of the Effect of Hydrogen-Air Atmospheres in Radio Sets AN/PRC-25 and AN/PRC-77*, availability: U.S. Army Electronics Command (presently, U.S. Army Electronics Research and Development Command), number AD 877707 (1970). Document not presently available.

M. MAGNESIUM - SILVER CHLORIDE

Mg | Sea Water | AgCl

$$Mg + 2\,AgCl \longrightarrow MgCl_2 + 2\,Ag \qquad [1]$$
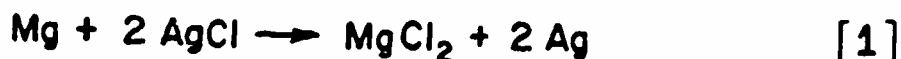
The magnesium-silver chloride water activated electrochemical system was developed during World War II under sponsorship of the U.S. Navy and U.S. Army. The system fulfilled the requirements for high current densities, low temperature performance, and the storability characteristics of ten years shelf life in the unactivated state. Indeed, the magnesium-silver chloride system has historically been the power source for electric torpedos, sonobuoys, air-sea rescue beacons, and emergency signalling devices.[1] Spirally wound cells and batteries are now commercially available as power sources for underwater searchlights, distress beacons, and life jackets.[2,3]

Magnesium possesses theoretical reversible electrode potentials of 2.37 and 2.69 V in acidic and alkaline media, respectively.[4] These high potentials are not achieved due to an adherent protective film of either magnesium oxide or magnesium hydroxide. In addition, corrosion of the magnesium electrode occurs during both open circuit stand in the activated state and during discharge:

$$Mg + 2H_2O \longrightarrow Mg(OH)_2 + H_2 \qquad (2)$$

The use of magnesium electrodes in neutral or slightly alkaline media results in increased hydrogen production (equation 2) as the current density is increased.[4-6]

The electrode and resultant film formation effects on the polarization characteristics have been investigated extensively. A summary of the findings are given below:

1. A large, local action, self-discharge current is established between anodic and cathodic sections of the same magnesium electrode. The cathodic areas exist where concentrations of impurity metals such as nickel and iron are present. These sites promote the evolution of hydrogen and the formation of $Mg(OH)_2$ in accordance with equation 2, above.

2. The film on the magnesium electrode during cell operation is primarily $Mg(OH)_2$. The permeability of this film is dependent upon both the electrolyte composition and pH. At low pH values, the permeability of the protective film is enhanced. It has been shown that chlorides and sulfates enter the $Mg(OH)_2$ film and form soluble magnesium salts. As a consequence, the permeability of the film is increased.[6-10]

3. The anodic areas which contribute to the cell reaction (equation 1) are free of film due to the generation of magnesium ions at a faster rate than hydroxyl ions can diffuse into the bare electrode region. Those magnesium electrode areas which do not generate a high concentration of magnesium ions are covered by the $Mg(OH)_2$ film. The overall result of film formation, therefore, is to force the operation of the magnesium electrode at high current densities, even though the cell is discharged at low currents.[11-13]

4. The magnesium electrode which operates at high current densities exhibits extensive polarization characteristics. At open circuit, the magnesium electrode also shows appreciable localized currents due to the self-discharge/corrosion reaction. It should be expected, therefore, that the electrode will be severely polarized even if the total currents are in the milli- or microampere range.

5. As cell discharge proceeds, the anodic region (i.e., that portion of the magnesium electrode in support of equation 1) does readjust as the magnesium is consumed. At any given time however, only a small area of the magnesium electrode is active in the useful discharge of the cell if the cell is operating at a current density level less than that required for film formation.

Historically, the magnesium electrode for the magnesium-silver chloride cell system was unalloyed and of very high purity.[14] These electrodes exhibited particularly high corrosion rates. In addition, discharge performance tests for cells containing these magnesium electrodes showed severe voltage delays and particularly low rate capabilities even for cells tested under light loads.

In view of the above, much effort has been expended to develop and test suitable magnesium alloys as candidate electrodes for many magnesium electrochemical systems. The primary objectives in this work were the development of specific alloys which exhibit minimal corrosion and voltage delay characteristics[9,12] as well as high efficiencies at low rates.[11,15,16] The three most widely studied alloys[15] for the Mg-AgCl system were Dow Chemical's AZ21 (2% Al, 1.2% Zn, 0.15% Mn, and 0.2% Ca), AZ31 (3% Al, 1% Zn, 0.2% Mn, and 0.04% Ca), and AZ61 (6.5% Al, 0.7% Zn, and 0.2% Mn). Other candidate electrode materials were pure magnesium, an amalgamated magnesium, and several alloys which contained little or no aluminum or zinc.

The magnesium alloy which was found to yield optimum results for a number of electrochemical systems including the Mg-AgCl couple was AZ61. This alloy exhibited high cell load voltages and comparatively low gassing rates. As a result, AZ61 magnesium alloy was used as the magnesium electrode in many applications requiring high discharge rates. One such application was the power source for the Mk 67 which required current densities of more than 230 mA/cm^2. To maintain the operating voltage of 1.07 V/cell, the reaction

products must be flushed from interelectrode spacings. The choice of AZ61 as the negative electrode material was partially based upon the ease in ridding the cell of reaction products. However, it was found that a few cells clogged during discharge and caused large voltage losses. These large voltage losses were, for the most part, the result of very adherent reaction products or "black clogging".[16] The "black clogging" was caused by the reduction of aluminum in solid solution, due to the precipitation heat treatment of the alloy. Proper heat treatment (e.g., solution heat treatment) of the AZ61 does not result in the formation of a secondary alloy phase, $Mg_{17}Al_{12}$. The presence of $Mg_{17}Al_{12}$ was correlated to the formation of the adherent film in cells containing AZ61 alloys which had undergone "black clogging."

In accordance with the above, later investigations relative to the optimization of the magnesium electrode confirmed the above findings.[11,17] In fact, properly treated AZ61 was found to be the only magnesium electrode material which did not produce the densely packed sludge and adherent coating in batteries designed for high rate applications.

The silver chloride electrode is prepared by electrochemically anodizing pure silver expanded metal screen in a sodium chloride electrolyte. A short high current discharge is applied to the plates before removing from the anodizing bath. The resultant electrode is porous and is capable of high current operation.[1,18,19] A similar process may be used to produce low capacity plates by treating silver foil with a sodium hypochlorite solution. Low rate, long-term silver chloride electrodes may be prepared by casting fused silver chloride. The resultant sheets are cut to size and small holes may be punched in the electrode sheet to improve electrolyte flow. The electronic conductor is prepared by treating the exposed silver chloride surface with photographic developing solution. Glass beads which have been pressed into the surface of the silver chloride electrode provide the separation means, particularly for high rate magnesium-silver chloride batteries.[20] The main objective of the glass bead separators is to provide for the rapid flow of electrolyte, to evacuate $Mg(OH)_2$ product, and to cool the cell during high rate discharge. An alternate method employs a nylon monofilament wrapped around the silver chloride electrode as the separator.[1]

The electrolyte for the magnesium-silver chloride battery may be either sea or fresh water. When the battery is activated by fresh water, there is a certain period of time needed to reach the normal working voltage of the cell. However, as the discharge proceeds, the $MgCl_2$, produced in accordance with reaction 1, dissolves and produces an effective electrolyte solution. With sea water employed as the electrolyte, the working voltage is attained sooner, but the formation of $MgCl_2$, is still relied upon to produce an electrolyte of high conductivity for high rate applications. The conductivities of $MgCl_2$ solution and solutions of NaCl and $MgCl_2$, in the cell have been measured.[21,22] The results show that the specific conductivities increase by a factor of ten for $MgCl_2$ concentrations of approximately 2 to 30 g/l at temperatures of 5°C to 45°C. Also, the addition of $MgCl_2$ to a NaCl solution increases the conductivity at temperatures of 5°C to 75°C. For example, the specific conductivity of a 3 percent NaCl solution at 25°C is approximately 5×10^{-2} ohm^{-1} cm^{-1}. The addition of 30 g $MgCl_2$ per liter doubles the conductivity to 1×10^{-1} ohm^{-1} cm^{-1}.

The effect of additives to the sea water electrolyte were studied in an effort to enhance the power output of the magnesium-silver chloride battery by increasing the load voltage of the magnesium electrode at high current densities.[11] The additives included strong and weak acids, buffers, hydrogen evolution inhibitors, and compounds which form films on the magnesium surface. Most of the additives (i.e., weak acids, hydrogen evolution inhibitors, and buffers) had little or no effect on the observed potential at current densities of 310 mA/cm^2. Mercuric chloride at concentrations of 0.01 to 0.10 M was found to increase the potential by 0.12 V at the current density of 310 mA/cm^2. In addition, most of the strong acids proved to be beneficial, the most promising being 0.1 to 0.2 M H_2SO_4. Gas evolution rates were, however, substantially higher for solutions containing strong acid additives. Magnesium electrodes amalgamated with up to 3.2 weight percent mercury exhibited high potentials compared to the AZ61 alloy, but produced either a black dense sludge or large amounts of black needles/flakes which could cause clogging and severe voltage losses in batteries.

The battery itself is comprised of many plate type cells connected in series to produce the desired voltage levels. Provision is made for activation of the battery by the inclusion of inlet and outlet ports at diagonally opposite corners of the battery container.[23] When the battery is activated, however, the incoming electrolyte contacts several of the series-connected cells. As a result, leakage currents develop between the positive and negative plates of adjacent cells as well as between plates separated in the series string at voltages higher than required for decomposition of electrolyte. Leakage currents result in decreased output voltage levels at the beginning of discharge and increased battery temperatures. As the electrolyte fills the porous silver chloride electrode and the interelectrode spacings, leakage currents diminish. The leakage currents result in the formation of a yellow-brown sludge on the perimeters of the electrodes in a few of the cells.[16] It is not considered a contributing factor in large voltage losses in the magnesium-silver chloride system, however. Furthermore, it has been found that the effect of such leakage currents at the beginning of discharge may be minimized by insulating the edges of the silver chloride electrode to increase the resistance of the leakage path.[1]

The observed open circuit voltage for the magnesium-silver chloride cell varies between 1.70 and 1.90 V. The discharge characteristics were determined for single cells containing AZ61 magnesium alloy electrodes and using solutions containing 3.6 percent NaCl and 3.6 percent NaCl with 0.2 M H_2SO_4.[11] The average load voltages for cells discharged at current densities of 310 mA/cm^2 were 0.98 V and 1.10 V for cells containing NaCl and NaCl with H_2SO_4 solutions, respectively. The corresponding durations for the above cells were six and seven minutes.

The performance characteristics for several pile type torpedo batteries have been discussed by Faletti.[24] The Mk 61 Mod 0 battery comprised of two parallel strings of 118 cells each was discharged using inlet electrolyte solutions of 31 to 38 percent salinity at temperatures of 1°C, 13°C, and 31°C. The average load voltages were 110, 130, and 140 V for the batteries discharged under constant loads of 0.58, 0.72 and 0.58 ohm, respectively. The corresponding current densities, based upon cathode areas of 396 cm^2 per cell (792 cm^2 for two parallel strings) were found to be 240, 230, and 305 mA/cm^2

at temperatures of 1°C, 13°C, and 31°C, respectively. It should be noted that the average discharge times were of short duration: 8, 10, and 7 minutes, respectively. Energy densities as high as 165 Wh/kg have been reported for the magnesium-silver chloride system.[1,25]

The major manufacturers, developers, or suppliers of the magnesium-silver chloride battery include the Burgess Battery Company, Eagle Picher Company, General Electric, McMurdo Instruments Ltd., SAFT, and Yardney Electric Corporation.

No specific safety testing has been performed with the magnesium-silver chloride battery system. However, Faletti,[26] in the effort to determine the cause for "gray clogging" in cells, did construct experimental magnesium cells with artificially induced massive internal short circuits. For example, short circuits were induced by elimination of the glass bead separators, placing silver foil between the silver chloride electrode in one cell to the silver chloride electrode in the adjacent cell of the series, or by placing silver chloride beads in contact with both electrodes in a cell. No report of any hazardous occurrence was given. The "gray clogging" was found to be the result of premature depletion of the silver chloride electrode resulting from internal short circuits.

It should be noted that the battery is designed to allow free access and exit to the cell stack by sea water. Under certain circumstances, however, it would appear that the battery could experience a severe clogging[11,16,17,26] of the interelectrode spacings. Complete clogging leading to the blockage of the electrolyte flow may subsequently lead to a thermal runaway condition. Expulsion of hot electrolyte containing reaction products may then occur. The magnesium-silver chloride system possesses a high rate capability for a particularly short duration following activation. In practical applications such as a torpedo battery, a few cells would undoubtedly be depleted faster (i.e., due to "gray clogging") than the majority of the other cells in series. This situation would cause voltage reversal in the depleted cells. This effect has not appeared to be a safety factor in large batteries. A similar argument may be made for the possibility of charging of one string of cells by a second string in parallel (e.g., the Mk 61 and Mk 67 torpedo batteries).

The possibility does exist, however, for the occurrence of a fire or explosion caused by the accumulation of hydrogen gas should cells or batteries be tested under laboratory conditions using sealed vessels.

REFERENCES

1. Doan, D. J., _The Primary Battery_, Volume II, Heise, G. W., and Cahoon, N. C., eds. (New York: John Wiley and Sons, Chapter 7, 1976).

2. Crompton, T. R., _Small Batteries_, Volume 2, Primary Cells (New York: John Wiley and Sons, 1983), p. 213.

3. Mantell, C. L., _Batteries and Energy Sys'ems_, Second Edition (New York: McGraw Hill, Chapter 12, 1983).

4. Glicksman, R., _J. Electrochem. Soc._, 106, 1959, p. 457.

5. Carson, W. N., Jr., and Kent, C. E., "Power Sources 1966," _Proc. Fifth Int. Symp._, Joint Services Electrical Power Sources Committee, Collins, D. H., ed. (London: Pergamon Press, 1966), p. 119.

6. Robinson, H. A., _Trans. Electrochem. Soc._, 90, 1946, p. 485.

7. Glicksman, R., and Morehouse, C. L., _J. Electrochem. Soc._, 102, 1965, p. 273.

8. Glicksman, R., _J. Electrochem. Soc._, 106, 1959, p. 853.

9. Kirk, R. C., George P. F., and Fry, A. B., _J. Electrochem. Soc._, 99, 1952, p. 323.

10. Robinson, H. A., and King, P. F., _J. Electrochem. Soc._, 108, 1961, p. 36.

11. Carson, W. N., Fischer, W. H., and Siwek, E. G., _Electrochem. Technol._, 5, 1967, p. 423.

12. Kirk, R. C., and Fry, A. B., _Trans. Electrochem. Soc._, 94, 1948, p. 277.

13. Morehouse, C. L., _J. Electrochem. Soc._, 99, 1952, p. 187C.

14. Blake, I. C., _J. Electrochem. Soc._ 99, 1952, p. 202C.

15. Wood, D. B., "Batteries," Volume I, _Manganese Dioxide_, Kordesch, K. V., ed. (New York: Marcel Dekker, Inc., Chapter 4, 1974).

16. Faletti, D. W., and Nelson, L. F., _Electrochem. Technol._, 3, 1965, p. 98.

REFERENCES (Cont.)

17. Hiroi, M., J. Applied Electrochem., 10, 1980, p. 203.

18. Burant, L. J., and Jones, K. R., U.S. Patent 3,352,717, 1967.

19. Abe, H., Shibata, J., and Ito, T., U.S. Patent 3,445,296, 1969.

20. Doll, J. H., and Druesne, H. D., U.S. Patent 3,515,596, 1970.

21. Faletti, D. W., J. Electrochem. Soc., 117, 1970, p. 1524.

22. Faletti D. W., and Gackstetter, M. A., J. Electrochem. Soc., 114, 1967, p. 299.

23. Colbeck, D. B., and Purcell, T. H., Jr., U.S. Patent 3,508,971, 1970.

24. Faletti, D. W., J. Electrochem. Soc., 120, 1973, p. 1145.

25. Yeager, E. B., and Yeager, J. F., Kirk-Othmer, Encyclopedia Chem. Tech., Second Edition, Volume 3 (New York: Wiley Interscience, 1964), p. 106.

26. Faletti, D. W., Electrochem. Technol., 4, 1966, p. 456.

N. MAGNESIUM-SULFUR

$$Mg \mid MgBr_2, Mg(OH)_2 \mid S$$

$$Mg + S + 2H_2O \longrightarrow Mg(OH)_2 + H_2S \quad \text{(proposed)} \qquad [1]$$
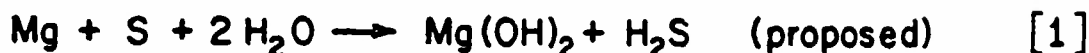
The magnesium-sulfur dry cell battery system was investigated as a candidate primary power source by Morehouse and Glicksman.[1] The system has not progressed to either the advanced developmental or production phases. Nonetheless, sulfur does possess several electrochemical advantages over other positive electrode materials for use as a potential cathode material in conventional cells. The most important advantages are the potential for high realized capacities of 1.68 Ah/g sulfur (3.46 Ah/cm^3). In addition, the sulfur electrode was shown to possess an efficiency of approximately 80 percent, based upon a two electron change per sulfur atom. Sulfur also is only slightly soluble in aqueous media and is inexpensive compared to other positive electrode materials.

The expected reversible potential for the magnesium-sulfur system is approximately 2.2 V. However, the true potential is not realized due to an oxide protective film on the magnesium surface. As a result, magnesium exhibits electrode potentials of only 0.3 to 0.6 V higher than zinc. In addition, magnesium experiences a severe corrosion side reaction:

$$Mg + 2H_2O \longrightarrow Mg(OH)_2 + H_2 \qquad (2)$$

Reaction 2 is minimal under storage conditions due to the protective oxide film on the magnesium. As the cell discharge proceeds, however, the film is removed whereupon a rapid corrosion attack occurs with subsequent hydrogen evolution.

The composition of the magnesium alloy selected for these studies was AZ10A (Dow) containing 1 percent aluminum, 0.4 percent zinc, 0.15 percent manganese, and 0.2 percent calcium. Calcium is believed to minimize the voltage delay characteristics intrinsic to magnesium electrochemical systems.[2]

AA-size cells containing an impact extruded magnesium can lined with uncoated Kraft paper were used as the test vehicle for the investigations. The positive electrode mixture contained equal weights of sulfur and Shawinigan acetylene black mixed with three weight percent of barium chromate. The electrolyte solution consisted of 8×10^{-4} $Na_2Cr_2O_7$ in 1.7 M $MgBr_2$.

The solution was mixed in equal weights with the sulfur-acetylene black mix and inserted into the lined can. A carbon rod with a brass cell cap was used as the positive electrode current collector. The cell was sealed using a rosin based wax. The inclusion of both the $BaCrO_4$ and $Na_2Cr_2O_7$ was found to provide corrosion resistance under storage as well as intermittent discharge conditions.

The observed open circuit voltage for the test cells was 1.60 to 1.65 V. The unexpected high voltage level was attributed to either adsorbed oxygen in the positive electrode-electrolyte mixture or to the interaction of magnesium with the chromate/dichromate corrosion inhibitor system. Cells were discharged under constant resistive loads of 50, 150, and 300 ohms to a voltage cutoff of 0.80 V at 21°C. The corresponding realized capacities were 0.70, 1.08, and 1.11 Ah, respectively. Except for cells discharged under the heaviest load, the average cell load voltages were 0.92 V. The load voltages for AA cells discharged under 50 ohm loads were 0.85 V.

Though the magnesium-sulfur system features good utilization of the sulfur electrode, a flat discharge curve, and comparatively inexpensive electrode materials; cells also show voltage delay characteristics, high internal impedance values, and a dramatic loss in capacity when discharged under intermittent discharge regimes. In addition, hydrogen sulfide gas is liberated during cell discharge.

No safety studies were reported for the magnesium-sulfur system. In view of the significant disadvantages of this system compared to the more conventional systems in present use for U.S. Navy applications, it is believed that the likelihood of future production of this system is minimal. As a result, no future testing is recommended.

REFERENCES

1. Morehouse, C. K., and Glicksman, R., J. Electrochem. Soc., 107, 1960, p. 651.

2. Kirk, R. C., George, P. F., and Fry, A. B., J. Electrochem. Soc., 99, 1952, p. 323.

O. ZINC-AIR (ZINC-OXYGEN)

Zn | KOH | O$_2$

$$2\,Zn + O_2 + 4\,KOH + 2\,H_2O \longrightarrow 2\,K_2Zn(OH)_4 \quad \text{(excess KOH)} \qquad [1]$$

$$Zn + O_2 \longrightarrow 2\,ZnO \quad \text{(neutral)} \qquad [2]$$
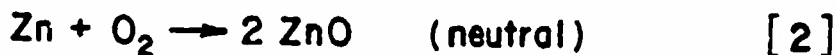
The first demonstration of a practical zinc-air cell was given by L. Maiche in the late 1870's.[1,2] Later, in 1932, Heise and Schumacher used a paraffin-impregnated porous carbon electrode with two amalgamated zinc electrodes and NaOH electrolyte to form the unit cell of a two cell battery[3] manufactured by Union Carbide for railway signalling and radio applications. Zinc-air button cells manufactured for hearing aid applications were the first of these cells commercially available to the public. A result of fuel cell developmental efforts led to the adaptation of the high current density carbon electrodes to the zinc-air system.

Both primary and secondary zinc-air or zinc-oxygen cells are in production at this time. Though this discussion specifically relates to the primary zinc-air cell system, a brief description of the secondary zinc-air or zinc-oxygen systems is warranted:

1. Mechanically rechargeable zinc-air cells allow the removal of the depleted zinc negative electrode and its replacement by a new zinc electrode. The electrolyte may also be replenished during this "charging" process. The mechanically rechargeable battery is the most mature of the available zinc-air systems. Indeed, these batteries have been produced by Leesona-Moos for use in military radio transceivers.[4] General Motors Corporation fabricated a 20 kW zinc-air battery for use in an experimental electric vehicle.[5] Though the electrical performance far exceeded that for the lead-acid battery similarly tested, the time required for mechanical recharging was excessive (many hours), electrolyte leakage caused short circuits, and the high temperatures caused large volume changes in the electrolyte. The development of a zinc-air battery with a recirculating zinc slurry coupled with tubular air electrodes has been carried out at the Laboratoires de Marcoussis (France) by the Compagnie Generale d'Electricite under sponsorship from SAFT.[6,7] This system could provide up to 110 Wh/kg and 80 Wh/kg in a 1000 kg electric vehicle. In addition, the problems of zincate solubility, zinc electrode shape change, zinc dendrite formation, and carbon dioxide contamination are at least partially alleviated by using colloid stabilizers, a high electrolyte flow rate, and regeneration outside the battery.

2. Electrically rechargeable zinc-air cells have several problems associated with both the zinc and air electrodes.[8] The deposition of zinc from a zincate solution results in the formation of dendrites which cause short circuits within the cell. In addition, zinc electrodes will severely passivate under peak power loads.[9] Two types of air electrodes have been used in zinc-air secondary cells: unifunctional and bifunctional. Since unifunctional electrodes only possess the capability of oxygen reduction:

$$O_2 + 2 H_2O + 4e^{1-} \longrightarrow 4 OH^{1-} \tag{3}$$

such third electrodes as nickel are required during the charging process. The use of the third electrode results in a reduction of cell voltages and increases in both cell weights and volumes.[10] This electrode will deteriorate under open circuit conditions during charging. This charging scheme also requires a switching mechanism. Bifunctional air electrodes not only permit the reduction of oxygen (reaction 3) but will also oxidize hydroxyl ion in accordance with:

$$O_2 + 2 H_2O + 4e^{1-} \underset{\text{charge}}{\overset{\text{discharge}}{\rightleftarrows}} 4 OH^{1-} \tag{4}$$
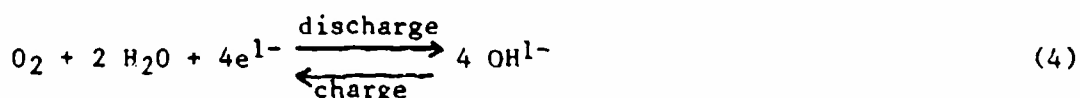
The bifunctional air electrodes (carbon) in zinc-air cells experience loss in physical integrity and oxidation at high charging potentials. Recently, Westinghouse has developed a carbon air electrode, catalyzed by tungsten carbide, which is utilized in iron-air cells.[10,11] However, in view of the severe problems associated with both electrodes, the requirement for oxygen removal during charge, and the low efficiencies of about 30 percent,[12] the outlook for the zinc-air electrically rechargeable system is not encouraging for such applications as load levelling, electric vehicle propulsion, or similar uses.[9]

Primary zinc-air batteries are classified as either reserve (i.e., water-activated prior to use) or non-reserve types. Water activated zinc-oxygen batteries have also been developed which utilize a self-contained, pressurized oxygen supply.[13] Primary zinc-air cells and batteries are used in several military (radio transceivers, buoys, navigational aids), space (NASA's space shuttle), oceanographic (oil platform lights, life support equipment, deep submergence vehicles), and consumer applications (hearing aids, calculators, watches).

The reaction of the zinc electrode in alkaline media is given by either:

$$Zn + 2 OH^{1-} \longrightarrow Zn(OH)_2 + 2e^{1-} \tag{5}$$

$$(Zn + 2 OH^{1-} \longrightarrow ZnO + H_2O + 2e^{1-})$$

or

$$Zn + 4 OH^{1-} \longrightarrow ZnO_2^{2-} + 2 H_2O + 2e^{1-} \tag{6}$$

$$(Zn(OH)_2 + 2 OH^{1-} \longrightarrow Zn(OH)_4^{2-})$$
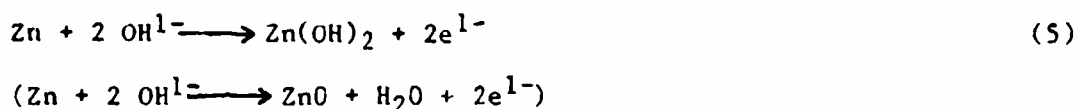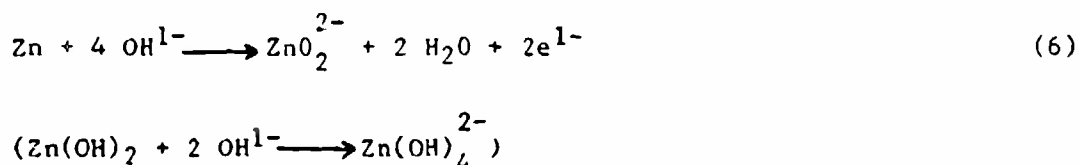
The standard potentials for equations 5 and 6 are 1.245 and 1.215 V, respectively. One possible side reaction which could occur at the zinc electrode to produce hydrogen gas is given by:

$$2 H_2O + 2e^{1-} \longrightarrow H_2 + 2 OH^{1-} \tag{7}$$

The standard potential for reaction 5 is -0.828 V. It can be seen, therefore, that the zinc electrode is approximately 0.4 V more positive than the reversible hydrogen evolution potential. As a result, zinc is thermodynamically unstable in strong alkaline media and will corrode, producing hydrogen gas. The corrosion reaction, however, may be significantly reduced by increasing the hydrogen overpotential of zinc by amalgamation and by using pure zinc. Inclusion of metal impurities such as nickel or iron results in the creation of cathodic sites on the zinc electrode.[14] Hydrogen could then be evolved with little decrease in zinc electrode potential. The addition of mercury results in an electrochemical couple where zinc is the negative electrode and mercury the positive electrode. The activation overpotential of hydrogen on mercury is high and the corrosion reaction is inhibited significantly. A summary of zinc passivation characteristics in alkaline media for high rate zinc primary cells is given for the zinc-mercuric oxide system. The zinc electrode for zinc-air cells consists of either a zinc powder preamalgamated with about 3 percent mercury in gelled electrolyte (small cells) or two amalgamated zinc plates (large cells, McGraw Edison Carbonaire).

The air positive electrode is typically a composite structure which includes a nickel plated steel current collector and also serves as a support structure for the catalyst. The catalyst is an absorbent carbon with porosity characteristics which allow gas transport to reaction sites without allowing the electrolyte to enter into the gross pores or void volumes. The preferred pore size spectrum is 0.05×10^{-3} mm to 50×10^{-3} mm (15). The carbons may then be thermally treated at temperatures of about 1000°C after treatment with precious metal salts or oxides. Surface areas of about 200 to 350 m^2/g are obtained using the above processes. These carbons are resistant to alkaline electrolytes but do require impregnation with wetproofing agents such as Teflon, waxes, or oils. Carbon electrodes treated with platinum permit cell operation at current densities up to 400 mA/cm^2. The outer layer of the electrode is a gas permeable, hydrophobic Teflon sheet which prevents the escape of the electrolyte through the electrode. Perforations in the cell case allows the free passage of air into the cell and the escape of small amounts of hydrogen. The overall reaction at the air electrode is given by equation 3:

$$O_2 + 2 H_2O + 4e^{1-} \longrightarrow 4 OH^{1-} \tag{3}$$

The electrolyte for the zinc-air cell is gelled 6M KOH. The separator assembly can be fabricated using several layers of cellulosic materials or a synthetic semipermeable membrane.

The theoretical open circuit voltage and energy density for the zinc-air cell is 1.62 to 1.65 V and about 1100 Wh/kg.[16] It should be noted that the observed open circuit voltages for these cells are 1.35 to 1.45 V. It is believed that the reaction at the air electrode does not proceed directly as that given in reaction 3, but involves the intermediate production of a peroxide ion[3,15]

$$O_2 + H_2O + 2e^{1-} \longrightarrow O_2H^{1-} + OH^{1-} \tag{8}$$

The peroxide ion would then chemically decompose at the air electrode surface according to:

$$2\,O_2H^{1-} \longrightarrow 2\,OH^{1-} + O_2 \tag{9}$$

The oxygen formed in equation 9 would then be reduced in accordance with reaction 8. The reversible potential for equation 8 is -0.076 V and that for equation 3 is +0.401 V. It appears that a mixed reaction occurs with a resultant potential between those for reactions 3 and 8.

The performance characteristics for small, low rate disc cells (Gould) were obtained at 0°C, 21°C, and 40°C. The physical dimensions of the cell were 2.03 cm diameter and 0.48 cm thick. The weight and nominal capacity were 5g and 1.2 Ah, respectively. Discharge curves were obtained for constant resistive loads of 255 ohm (about 5 mA) to a load voltage cutoff level of 1.0 V. The average load voltages observed for cell discharge at 0°C, 21°C, and 40°C were 1.25, 1.30 and 1.33 V, respectively, with corresponding realized capacities of 1.25, 1.30, and 1.40 Ah. The energy densities varied from about 300 Wh/kg at 0°C to about 375 Wh/kg at 40°C.

Military testing of a zinc-air radio transceiver battery was performed at -7°C.[17,18] The battery consisted of two parallel strings of 22 cells in series and weighed 3.41 kg. Discharge was performed using a constant current of 3A. The average load voltage for the battery was 22.5 V and discharge was continued to a 20 V cutoff voltage level. The realized capacity and energy density values obtained for this test were 21 Ah and 139 Wh/kg.

Other features of the zinc-air primary cell system are summarized below:

1. The operational temperature range is -20°C to +60°C.

2. The loss of capacity for small cells during storage is about 2 percent per year if the air access holes are covered with adhesive tape[19] (The hydrogen evolved by the zinc electrode corrosion reaction would escape through the taped holes). Storage of cells with open air accesses would accelerate either self-discharge or cell degradation due to water loss between the electrolyte and the environment, direct oxidation of the zinc electrode, and absorption of carbon dioxide.

3. The major United States manufacturers/suppliers of the zinc-air primary system are Gould, ESB, McGraw Edison, and VARTA.

4. A closed zinc-oxygen, water activated system was developed for oceanographic applications.[6] The positive electrode oxygen supply was contained in a pressurized gas cylinder at 250 psi (1720 kPa). The performance characteristics for batteries supplied with pure oxygen showed capacity and load voltage increases of about 6 percent and 10 percent higher, respectively, than for batteries supplied with air.

No safety testing was reported for any of the numerous types of zinc-air or zinc-oxygen cells or batteries. It should be noted that all cells and batteries, with the exception of closed systems, must employ an access for the influx of the positive electrode material. The porosity characteristics of the air electrode also allows the diffusion of minute amounts of evolved hydrogen to the atmosphere. As a result, the likelihood of cell rupture due to excessive internal pressures is slight. These cells will undoubtedly experience some heating when subjected to the electrical abuse tests of short circuit, forced overdischarge, and charge. A consequence of such testing may be cell leakage. The results of the above testing would also depend upon the rate at which oxygen would transfer into and out of the cell. This transfer is regulated by the number and size of access ports and by the porosity of the Teflon diffusion membrane. Both factors relate to the rate capability of the cell. The current capability of the cell would increase as both the access port diameter and membrane porosity increase until the current density at the air electrode becomes the limiting factor.

Incineration of open cells and batteries would also lead to cell leakage and the rapid oxidation of the plastic contents of the cell. Toxic vapors may then be emitted. Incineration of closed zinc-air or zinc-oxygen cells or batteries could result in a violent rupture of the pressurized container vessel.

REFERENCES

1. Vinal, G. W., _Primary Batteries_, (New York: John Wiley and Sons, 1950), p. 214.

2. Mantell, C. L., _Batteries and Energy Systems_, Second Edition (New York: McGraw Hill, 1983), p. 82.

3. Gregory, D. P., _Metal-Air Batteries_, M and B Monograph CE/6, Cook, J. G., ed. (London: Mills and Boon Ltd., 1972), p. 12.

4. Palmer, N. I., Jagid, B. E., and Staudinger, F. J., _Proc. of the Fourth IECEC_, American Society of Mechanical Engineers, 1969, p. 911.

5. Witherspoon, R. R., Zeitner, E. J., and Schulte, H. A., _Proc. of the Sixth IECEC_, American Society of Mechanical Engineers, 1971, p. 96.

6. Appleby, A. J., Pompon, J. P., and Jacquier, M., _Proc. of the Tenth IECEC_, American Society of Mechanical Engineers, 1975, p. 811.

7. Appleby, A. J., and Jacquier, M., _J. Power Sources_, 1, 1976/77, p. 17.

8. Kordesch, K. V., "Batteries," Volume 2, _Lead-Acid Batteries and Electric Vehicles_, Kordesch, K. V., ed. (New York: Marcel Dekker, Inc., 1977), p. 278.

9. Gross, S., _Energy Conversion_, 15, 1976, p. 95.

10. Bryant, W. A., Liu, C. T., and Buzzelli, E. S., _Proc. Power Sources Symp._, 28, 1979, p. 152.

11. Roberts, R., _Electrotechnology, Volume 2_, Ouellette, R. P., Ellerbusch, F., and Cheremisinoff, P. N., eds. (Michigan: Ann Arbor Science, Ann Arbor, 1978), p. 366.

12. Plust, H. G., _Electric Vehicle Development_, Electric Vehicle Development Group (Int. Conf. on Electric Vehicle Development, 31 May to 1 June 1977), (London: Peter Peregrinus Ltd., 1978), p. 17.

13. McCormick, R. J., _Proc. of the Sixth IECEC_, American Society of Mechanical Engineers, 1971, p. 536.

14. Glicksman, R., _J. Electrochem. Soc._, 106, 1959, p. 457.

REFERENCES (Cont.)

15. Schumacher, E. A., *The Primary Battery*, Volume 1, Heise, G. W., and Cahoon, N. C, eds. (New York: John Wiley and Sons, Chapter 8, 1971).

16. McBreen, J., "Comprehensive Treatise of Electrochemistry," Volume 3, *Electrochemical Energy Conversion and Storage*, Bockris, J. O'M., Conway, B. E., Yeager, E., and White, R. E., eds. (New York: Plenum Press, 1981), p. 308.

17. Almerini, A. L., and Bartosh, S. J., *Proc. Power Sources Symp. 26*, 1975, p. 148.

18. Biddick, R. E., Cretzmeyer, J. W., Douglas, D. L., and Jaggard, A. M., *Proc. Power Sources Symp. 26*, 1975, p. 151.

19. Pytches, D., *Electronics and Power*, 29, 1983, p. 577.

P. ZINC-MANGANESE DIOXIDE (CARBON-ZINC, LECLANCHE', DRY CELL, ZINC CHLORIDE LECLANCHE')

LECLANCHE': $Zn \mid NH_4Cl \mid MnO_2$

$$Zn + 2MnO_2 + 2NH_4Cl \longrightarrow Zn(NH_3)_2Cl_2 + 2MnOOH \qquad [1]$$

$$Zn + 2MnO_2 + 2NH_4Cl \longrightarrow Zn(NH_3)_2Cl_2 + Mn_2O_3 + H_2O \qquad [2]$$
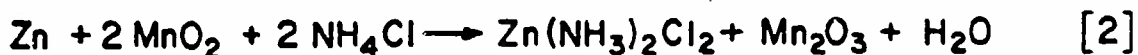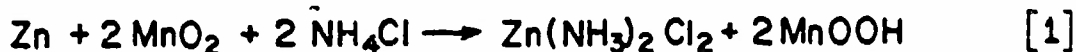
$ZnCl_2$ LECLANCHE': $Zn \mid NH_4Cl, ZnCl_2 \mid MnO_2$

$$4Zn + 8MnO_2 + 8H_2O + ZnCl_2 \longrightarrow ZnCl_2 \cdot 4Zn(OH)_2 + 8MnOOH \quad [3]$$
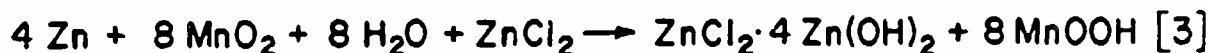
The zinc-manganese dioxide electrochemical system was developed by Georges Leclanche in the 1860's.[1,2] These earliest wet cells were comprised of a zinc rod anode, a mixture of manganese dioxide and carbon as the cathode material, a carbon rod current collector, and a saturated solution of ammonium chloride as the electrolyte. Unfortunately, such cells did not show efficient utilization of the MnO_2 when discharged even under light or intermittent discharge regimes. In 1887, Gassner first described a dry cell containing an electrolyte paste of NH_4Cl, ZnO, and plaster of Paris.[2] Other improvements in the system include the use of highly absorbent and conductive carbon black, amalgamation of the zinc electrode, the development of papers suitable for separators, the incorporation of zinc chloride as the major component of the electrolyte, the use of the zinc electrode as the cell container vessel, the production of electrolytic manganese dioxide (EMD), and the development of a gelled electrolyte.[2,6]

Detailed discussions relative to the various technical aspects for Leclanche cells are given by Heise,[1] Huber,[2] Kozawa,[3] Tye,[4] Franzese and Bharucha,[5] Brodd, Kozawa, and Kordesch,[6] Cahoon,[7] and Vinal.[8]

Three types of Leclanche type cells/batteries are currently available:[5,6,9]

1. The standard Leclanche cell is comprised of a zinc can anode, an electrolyte solution of NH_4Cl, natural MnO_2 ores and acetylene black as the cathode components, and a starch paste separator. Such cells are generally used in applications requiring low rate or intermittent discharge regimes.

2. The "heavy duty" Leclanche cell contains a zinc can anode, an electrolyte solution of NH_4Cl and some $ZnCl_2$, electrolytic manganese dioxide (EMD) or a mixture of EMD with natural MnO_2 ores with acetylene black as the cathode components, and a separator of starch paste or treated paper as the separator. These cells are employed in applications requiring heavy, intermittent, or medium rate continuous discharge regimes.

3. The "extra heavy duty" Leclanche cell is comprised of a zinc can anode, an electrolyte solution of $ZnCl_2$ with a small amount of NH_4Cl, EMD with acetylene black as the cathode components, and a specially treated paper as the separator. Cells of this type are best suited for applications requiring heavy intermittent or medium to heavy continuous discharge regimes. These cells also feature better low temperature performance characteristics, reduced levels of leakage, and increased hydrogen evolution.

The typical zinc anode for the Leclanche cells described above is composed of pure zinc (99.95% to 99.995%) with small amounts of both lead and cadmium to improve the mechanical handling properties. The discharge reaction at the zinc electrode in acidic media proceeds in accordance with:

$$Zn \longrightarrow Zn^{2+} + 2e^{1-} \qquad (4)$$

The standard electrode potential for reaction 4 is +0.763 V. One possible side reaction which could occur at the zinc electrode in Leclanche electrolyte (i.e., solutions containing NH_4Cl) would result in the evolution of hydrogen gas in accordance with:

$$Zn + 2\ NH_4Cl \longrightarrow ZnCl_2 \cdot 2\ NH_3 + H_2 \qquad (5)$$
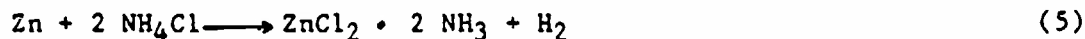
The inclusion of transition metal impurities (e.g., nickel or iron) with low hydrogen overvoltages causes the production of cathodic sites on the zinc electrode. Hydrogen would evolve rapidly at these sites with little decrease in the zinc electrode potential. Amalgamation of the zinc electrode may be effected by the reduction of small additions of mercuric chloride in the electrolyte. The electrode would then be comprised of a local electrochemical couple of zinc as the negative electrode and mercury as the positive electrode. The activation overvoltage of hydrogen on mercury is high, thereby inhibiting the corrosion rate. Alternatively, the addition of potassium dichromate to the electrolyte or to the paper separator forms a chemically resistant, protective film on zinc.[10]

A second corrosion reaction will occur in Leclanche cells if the zinc electrode is exposed to oxygen from the outside atmosphere:

$$2\ Zn + 4\ NH_4Cl + O_2 \longrightarrow 2\ ZnCl_2 \cdot NH_3 + 2\ H_2O \qquad (6)$$

The above reaction disrupts passivating films on the zinc surface and ultimately causes pitting of the cell container at the zinc-electrolyte interface. Proper sealing of Leclanche cells not only prevents oxygen access to the cell interior but also provides a means to prevent moisture loss.

Several types of manganese dioxide can comprise the active positive electrode material of the Leclanche cell. These include natural ores, chemically treated natural ores, synthetic hydrates, and electrolytic manganese dioxide, EMD.[2] Marked improvements in the cell performance characteristics, especially capacity, have been observed for cells containing EMD. EMD is prepared by electrolyzing a solution of $MnSO_4$ in sulfuric acid. The most important crystalline form for battery applications is the gamma crystal structure of EMD (ramsdellite) with the formula of $MnO_{1.94}$ to 1.96 (x H_2O),

where x is the amount of combined water. Kozawa has shown[3] that the predominant discharge reaction of MnO_2 for the Leclanche cell proceeds through a proton-electron mechanism in accordance with:

$$MnO_2 + H_2O + e^{1-} \longrightarrow MnOOH + OH^{1-} \qquad (7)$$

The reaction involves the incorporation of a proton and an electron into the original MnO_2 gamma structure of the EMD.[11] Both the proton and the electron are freely mobile in the lattuce structure. Though most of the self-discharge reactions occur at the zinc negative electrode, the manganese dioxide electrode contributes somewhat to the loss in cell capacity, particularly under elevated storage temperature conditions.[7] It is believed that a reaction will occur between the manganese dioxide and the carbon of the positive electrode to form carbon dioxide and carbon monoxide. A second possible self-discharge reaction relates to the interaction between the starch paste separator and the manganese dioxide to produce CO_2. Since CO_2 is easily soluble in the Leclanche electrolyte, no mechanical disruption of the paste separator occurs.

The zinc negative electrode produces Zn^{2+} ions in accordance with equation (4) which are in the form of complex species whose composition is dependent upon the predominant electrolyte salt species (i.e., NH_4Cl or $ZnCl_2$). The solution at the zinc electrode is highly acidic and diffuses through the separator into the MnO_2 electrode region. Since the discharge reaction at the MnO_2 electrode produces OH^{1-} ions (reaction 7) the acidic solutions from the zinc electrode produce precipitates of $Zn(NH_3)_2Cl_2$ in cells with NH_4Cl electrolyte and $ZnCl_2 \cdot 4\,Zn(OH)_4$ in cells with $ZnCl_2$ electrolyte. Under short circuit or high rate discharge conditions (i.e., when the voltage approaches zero volts), water tends to move from the MnO_2 cathode to the zinc anode rather than the migration of the acidic zinc electrode solution to the cathode. In these instances, the zinc solution is displaced to the upper air spaces of the cell and result in leakage as gas venting occurs. The crystalline reaction product of the cells containing NH_4Cl as the electrolyte precipitates at the outer area of the MnO_2 cathode and prevents the further diffusion of the zinc solution into the cathode. The precipitate formed in cells with $ZnCl_2$ electrolyte is porous and allows passage of the zinc electrode solution to the inner regions of the cathode. The hydrogen evolution rate would therefore be higher for cells containing NH_4Cl electroiyte since the highly acidic zinc solution is in intimate contact with the zinc surface. The combined effects of increased zinc corrosion and displacement of the zinc electrode solution to the upper air spaces enhance the possibility of cell leakage and cell venting in cells with NH_4Cl electrolyte. It can be seen, therefore, that cells containing $ZnCl_2$ as the electrolyte salt show less tendency for leakage.

The various types of Leclanche cells and batteries are manufactured using cylindrical and flat constructional designs. The cylindrical designs feature a bobbin construction of the MnO_2, acetylene black, and electrolyte solution in a zinc can. Electrical contact is provided by a porous carbon rod inserted into the positive electrode mixture. The separator is either a cereal paste mixture or a specially treated absorbent paper. A means to allow for the venting of gases is provided in these cells. The flat cell design is often employed in multicell assemblies and feature the use of duplex electrode structures. These

electrodes are fabricated by coating the zinc electrode surface with carbon. Batteries are then fabricated by contacting the zinc electrode of one cell with the MnO_2 cathode plate of the next cell until the desired battery voltage level is attained. This design feature results in the creation of a battery assembly with greatly increased volumetric energy densities as compared with cylindrical cell designs.

The open circuit voltages for the three types of Leclanche cells, the "standard" (NH_4Cl electrolyte), the "heavy duty" (NH_4Cl and $ZnCl_2$ electrolyte), and the "extra heavy duty" ($ZnCl_2$ electrolyte) vary from 1.5 to 1.6 V. The corresponding practical energy densities for the three types of cells are 25, 40, and 90 Wh/kg, respectively. The normal operating temperature range for the "standard" and "heavy duty" Leclanche cells is -6°C to +55°C while that for the "extra heavy duty" cells is -18°C to +50°C. The shapes of the discharge curves for the three types of zinc-manganese cells exhibit a gently sloping from initial load voltages to the typical cutoff level of 0.9 V. For specific performance data relative to the various cell sizes and types, the reader is referred to the battery engineering data guides published by the manufacturers.[12]

The major safety concerns for the zinc-manganese dioxide Leclanche systems relate to the leakage of the electrolytes and the pressure rupture of cells as a result of exposure to electrical or thermal abuse conditions. The most common effect of a sustained short circuit condition on cell behavior was described previously. In addition to the real possibility for cell leakage, cells may also exhibit either case bulging or, in extreme circumstances, a rupture.* It is interesting to note that D cells were, at one time, routinely subjected to short circuit conditions of 0.01 ohm for brief periods of time.[8] The objective of these experiments was the determination of the internal resistance values for the cells.

Though most zinc primary cell systems possess design specifications for balanced amounts of the active species or excess amounts of the positive electrode material, some cells containing a slight excess of zinc at the end of useful discharge could pose a minor safety hazard. Any excess zinc negative electrode material would then cause hydrogen evolution at the positive electrode once all the manganese dioxide was discharged. If the cell is allowed to be connected to the load, the accumulation of hydrogen could then lead to a pressure rupture or "violent disassembly" of the cell.** The occurrence of such pressure ruptures or cell leakage are not uncommon in applications containing solid state components. Following initial cell or battery usage, such devices would continue to draw current at very low rates in the "OFF" position. This could result in a pressure rupture with damage to the equipment.

The effects associated with both forced overdischarge or charge conditions on the Leclanche cells would depend upon the voltage output of the power unit and the amount of current passing through the cells. The possibility for the electrolysis of water with the generation of hydrogen and oxygen exists under

*Bright Star Industries, Materials Safety Data Sheet for Dry Cell Batteries, Private Communication, 1984.
**Mahy, T. X., Private Communication, 1984.

both abuse conditions. At high voltages, the chlorides in the cell are oxidized to form highly toxic chlorine gas. Pressure ruptures or cell leakage could result from extended charge or forced overdischarge. It is important to note that Leclanche cells can be charged to a limited extent. Indeed, recharging cells and charging devices were promoted in the mid-1920's, 1943 to 1946, and in the mid-1960's.[13] Constant current and unregulated constant potential charging methods were found to damage cells by overcharging. Constant potential charging at low rates using well regulated power supplies proved satisfactory if the charge voltage remained at 1.8 to 1.9 V. At 2.05 V, water would be decomposed and, at higher voltages, chlorine was evolved.[13]

Cells subjected to incineration conditions would undoubtedly experience pressure ruptures with the emission of toxic fumes from the oxidation of cell components. Cell leakage results in the liberation of NH_4Cl and/or $ZnCl_2$ electrolyte solutions which would cause acid burns when brought into contact with the skin.

REFERENCES

1. Heise, G. W., The Primary Battery, Volume 1, Heise G. W., and Cahoon, N. C., Js. (New York: John Wiley and Sons, 1971).

2. Huber, R., "Batteries," Volume 1, Manganese Dioxide, Kordesch, K. V, ed. (New York: Marcel Dekker, Inc., Chapter 1, 1974).

3. Kozawa, A., "Batteries," Volume 1, Manganese Dioxide, Kordesch, K. V., ed. (New York: Marcel Dekker, Inc., Chapter 3, 1974).

4. Tye, F. L., Electrochemical Power Sources, Primary and Secondary Batteries, IEE Energy Series 1, M. Barak, ed. (London: Peter Peregrinus Ltd., Chapter 3, 1980).

5. Franzese, K., and Bharucha, N., Handbook of Batteries and Fuel Cells, Linden, D., ed. (New York: McGraw-Hill Book Company, Chapter 5, 1984).

6. Brodd, R. J., Kozawa, A., and Kordesch, K. V., J. Electrochem. Soc., 125, 1978, p. 271C.

7. Cahoon, N. C., The Primary Battery, Volume II, Heise, G. W., and Cahoon, N. C., eds. (New York: John Wiley and Sons, Chapter 1, 1976).

8. Vinal, G. W., Primary Batteries (New York: John Wiley and Sons, 1950).

9. Mantell, C. L., Batteries and Energy Systems, Second Edition (New York: McGraw Hill Book Company, Chapter 6, 1983).

10. Glicksman, R., J. Electrochem. Soc., 106, 1959, p. 457.

11. Kozawa, A., and Yeager, J. F., J. Electrochem. Soc., 115, 1968, p. 1003.

12. Union Carbide Corporation, Eveready Battery Engineering Data, Volumes I (1980), II (1982), and III (1984).

13. Herbert, W. S., J. Electrochem. Soc. Electrochem. Technol., 1, 1963, p. 148.

Q. ZINC-MANGANESE DIOXIDE (ALKALINE, ALKALINE MANGANESE DIOXIDE)

$$Zn \mid KOH \mid MnO_2$$

$$Zn + 2\,MnO_2 + H_2O \longrightarrow ZnO + 2\,MnOOH \qquad [1]$$

$$Zn + 2\,MnO_2 + H_2O \longrightarrow ZnO + Mn_2O_3 + H_2O \qquad [2]$$

$$2\,Zn + 2\,KOH + 3\,MnO_2 \longrightarrow 2\,ZnO + Mn_3O_4 + 2\,KOH \qquad [3]$$
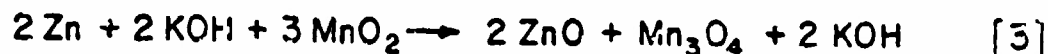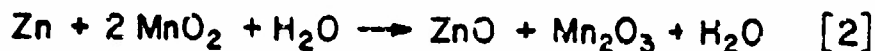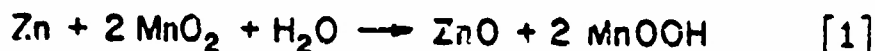
The first practical zinc-manganese dioxide alkaline cell, the "crown" cell, was developed by Herbert in the early 1950's.[1,2] The rapid progress of the zinc-alkaline battery system as a commercial success was due to improvements which included the displacement of the classical Leclanche bobbin cathode structure to a sleeve-type cathode structure at the wall of the container, the development of amalgamated zinc powder anodes in gelled electrolytes, the exclusive use of electrolytic manganese dioxide (EMD) as the positive electrode material, and the inclusion of highly conductive carbons in the cathode mixture.[1] A further achievement for the zinc-alkaline electrochemical system is the successful development of specially designed secondary cells having cycle lives up to 100.[3-5]

Detailed descriptions of the various technical aspects for the zinc-manganese dioxide alkaline system are given by Kordesch (1-3), Cahoon and Holland,[6] Tye,[7] Schumacher,[8] Brodd, Kozawa, and Kordesch,[9] and Falk and Salkind.[10]

High purity (99.8% to 99.9%) zinc with small amounts of lead (0.05%) to improve both the mechanical handling properties and corrosion resistance comprises the starting material for the preparation of zinc powder. The liquid alloy is passed in a thin stream to an air jet when it is finely dispersed or "atomized" and subsequently collected. The finely divided powder is then amalgamated with 4 to 9 percent mercury. The rigid gelled anodes are prepared by mixing KOH, the amalgamated zinc powder, sodium carboxymethylcellulose, and small amounts of zinc oxide with water. The resultant anode possesses good electronic conductivity and optimized zinc particle size.[1] The preparative method for the fabrication of porous zinc anodes requires pressing of zinc powders previously wetted by elemental mercury. The resultant void volume for these electrodes is low unless a volatile filler such as NH_4Cl is added to the starting material.[1]

The discharge reactions for amalgamated zinc electrodes in an alkaline media proceed in accordance with:[11]
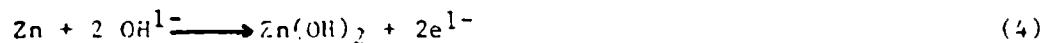
$$Zn + 2 \ OH^{1-} \longrightarrow Zn(OH)_2 + 2e^{1-} \tag{4}$$

The $Zn(OH)_2$ then dissolves in the electrolyte and eventually forms zinc oxide:

$$Zn(OH)_2 + 2 \ OH^{1-} \longrightarrow Zn(OH)_4^{2-} \tag{5}$$

and

$$Zn(OH)_4^{2-} \longrightarrow ZnO + 2 \ OH^{1-} + H_2O \tag{6}$$
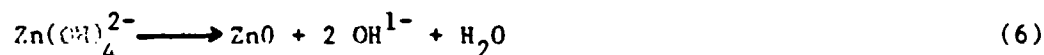
Electrode passivation will occur when the solubility limit of the discharge products in the electrolyte surrounding the zinc anode is exceeded, as given by either reaction 6 or by reaction 7:

$$Zn(OH)_2 \longrightarrow ZnO + H_2O \tag{7}$$

A summary of the zinc passivation characteristics in alkaline media is given for the zinc-mercuric oxide system.

A possible side reaction which occurs at the zinc electrode produces hydrogen and results in the wasteful corrosion of zinc:

$$Zn + 2 \ H_2O + 2 \ OH^{1-} \longrightarrow Zn(OH)_4^{2-} + H_2 \tag{8}$$
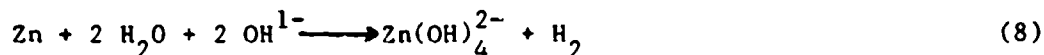
The corrosion reaction rate may be reduced significantly by increasing the hydrogen overpotential through amalgamation, the use of pure zinc starting materials, and avoidance of metal impurities of low hydrogen overvoltages (e.g., iron, nickel, etc.). Hydrogen is also evolved in cells subjected to intermittent discharge regimes and in discharged cells with excess zinc negative electrode material after the manganese dioxide is exhausted. In the former case, different sections of the zinc electrode are discharged in such a way to produce potential gradients. In the latter case, hydrogen will be evolved at the spent manganese dioxide electrode if the load remains on the cell. A continued accumulation of hydrogen can produce a pressure rupture or "violent disassembly" of the cell.*

Electrolytic manganese dioxide (EMD) is used exclusively as the active positive electrode material in zinc-alkaline cells. This material is prepared by electrolyzing a solution of $MnSO_4$ or $MnCO_3$ dissolved in about 1 M H_2SO_4.[2,12] The preferred crystal form for EMD is the gamma structure (ramsdellite) with the formula of $MnO_{1.94}$ to 1.96 $(x \ H_2O)$, where x is the amount of combined water. This form of EMD features low polarization and high voltage characteristics. A typical positive electrode is comprised of 70 percent EMD, 10 percent graphite, 2 percent acetylene black, 7 M KOH solution, and binders.

---

*Mahy, T. X., Private Communication, 1984.

Kozawa[12-14] has shown that the predominant mechanism governing the discharge reaction of EMD in alkaline media proceeds through a proton-electron mechanism in accordance with:

$$Mn + H_2O + e^{1-} \longrightarrow MnOOH + OH^{1-} \tag{9}$$
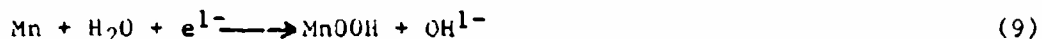
This reaction involves the incorporation of a proton and an electron into the original MnO_2 gamma structure of the EMD.[15] The positive electrode discharge potential continually changes as protons are introduced into the lattice. This is an indication that the reaction is homogeneous. The MnO_2 lattice will expand until the discharge mechanism changes. The subsequent reaction occurs heterogeneously in accordance with:[16]

$$MnOOH + H_2O + e^{1-} \longrightarrow Mn(OH)_2 + OH^{1-} \tag{10}$$
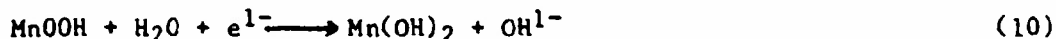
Reaction 10 occurs at too low a potential for practical use and is irreversible. Reaction 9 represents the rechargeable portion of the EMD reduction process (from MnO_2 to $MnO_{1.5}$).

Separation between the electroactive zinc anode and EMD cathode is effected through use of macroporous separators such as nonwoven cotton-cellulose, cellulose-rayon paper, and nylon.[1]

Two basic types of zinc-alkaline cells are currently manufactured: the cylindrical and the flat plate or button cell designs. In contrast to the centrally located cathode bobbin cell designs for the Leclanche cells, zinc-alkaline cylindrical cells feature an outside MnO_2 cathode and a zinc powder anode in the center of the cell. This arrangement provides for a maximum utilization of the superior performance features of the zinc-alkaline system by improving the mass transport (diffusion) properties of the cathode and by increasing the surface area of the zinc. The latter improvement is necessary to overcome the passivation tendency of the anode material.[1] The cathode material (MnO_2, graphite, acetylene black, and binders) is pressed onto the inner surface of a steel container. The separator "basket" assembly lies between the cathode and the zinc anode. Either a gelled zinc powder anode or a porous powder zinc anode is then inserted into the separator "basket." Anode current collection is provided by brass "tongues" or metal nails which lead to the negative electrode terminal at the can bottom. A safety vent is provided to avoid high internal cell pressures arising from cell exposure to electrical and thermal abuse conditions (i.e., short circuits, charging, incineration). The various venting devices include weakened case bottoms, a thinned section of the plastic cover, and a spur-tooth assembly which pierces the plastic cover. Small cells employ double O-rings or grooves in the plastic seal.

Button cells are fabricated by pressing the cathode mixture into the cell can. A macroporous separator segregates the cathode from a highly amalgamated zinc anode composite of zinc powder, gelling agent, and electrolyte. The anode cup of copper or tin clad stainless steel is then pressed onto the anode assembly. Electrical isolation between the cell can and anode cup is provided through use of a crimped nylon sealing gasket. Since the zinc anode is highly amalgamated, little gassing occurs in these cells. No vent mechanism is incorporated into these small cells.

The open circuit voltages for zinc-alkaline cells vary from 1.50 to 1.55 V. Duracell[17] MN 1300 D size cells were discharged under constant loads of 2.25, 5, and 10 ohms at 20°C. The corresponding average load voltages (to a 0.8 V load voltage cutoff level) were 1.05, 1.15, and 1.27 V, respectively. The energy densities, calculated for an average cell weight of 125 g, were 63, 85, and 102 Wh/kg for the loads of 2.25, 5, and 10 ohms, respectively. Other important performance features for the zinc-alkaline battery system are summarized below:[2,18]

1. The operating temperature range for the zinc-alkaline cells is -29° to +50°C and the recommended storage temperature range is -40°C to +50°C. At -30°C, a D cell discharged at 0.5 A will yield about 5 percent of that capacity obtained at 20°C. Cells discharged at a lesser rate of 50 mA yield approximately 30 percent of that obtained at 20°C.

2. Zinc-alkaline cells retain about 90 percent of the nominal capacity after one year storage at 20°C, 70 percent after six months storage at 50°C, and about 40 percent after two months storage at 70°C.

Attewell[19] reported the results of the electrical abuse tests of short circuit and forced overdischarge, as well as the mechanical abuse tests of crushing, penetration, and cutting open D size zinc-alkaline cells manufactured by Duracell. In addition, cells were thermally abused in flame tests. A summary of the observations are given below:

1. Three cells were short circuited through 0.015 ohm loads at both 20°C and 55°C. Cells tested at 20°C reached peak currents of 8A and a maximum temperature of 90°C during the test. No venting was observed. Those cells tested at 55°C reached peak currents of 5A and a maximum temperature of 115°C. One of the three cells vented, but "not in any spectacular manner." These tests compared the zinc alkaline, the lead-acid, nickel-cadmium, and zinc-mercuric oxide to lithium cell systems. It is interesting to note that the zinc-alkaline cells sustained the maximum current output of all the aqueous electrolyte cells.

2. Zinc-alkaline cells were also subjected to forced overdischarge tests at 20°C and 50°C under constant current conditions at the C/10 rate (1.0 A) using a sixteen volt power supply. Cells were driven into voltage reversal for a period equal to the nominal 10 Ah capacity. The zinc-alkaline cells neither vented nor exhibited any indication of pressure buildup. The maximum temperature increases were observed to be 60°C and the maximum reverse voltages were unstable at 16 V.

3. Cells subjected to crushing and cutting tests exhibited a 30°C to 50°C temperature rise caused by massive internal short circuits. Though the cells did lose electrolyte, no other external effects were observed.

4. Discharged and fresh zinc-alkaline cells were penetrated by 0.6cm steel cubes at a velocity of 200 meters per second. The net result was the creation of massive internal short circuits but no other adverse effects were noted.

5. An oxygen-propane flame was adjusted to give a cherry red spot 1
    centimeter in diameter on the cell wall of zinc-alkaline cells. Within
    two minutes, all zinc-alkaline cells "vented mildly through their
    seals". Steam and electrolyte were emitted from the cells.

Although no charging tests were performed by Attewell,[19] it would be safe
to assume that gassing would occur in zinc-alkaline cells as a result of water
electrolysis. Activation of the vent or a progressive buildup of internal cell
pressure resulting in cell bulging would then occur. If the charging rate and
voltage level were sufficiently high, a cell rupture could also occur.

REFERENCES

1. Kordesch, K. V., "Batteries," Volume 1, Manganese Dioxide, Kordesch, K. V., ed. (New York: Marcel Dekker, Inc., Chapter 2, 1974).

2. Kordesch, K. V., Handbook of Batteries and Fuel Cells, D. Linden, ed. (New York: McGraw-Hill Book Company, Chapter 7, 1984).

3. Kordesch, K., Comprehensive Treatise of Electrochemistry, Volume 3, Electrochemical Energy Conversion and Storage, Bockris, J. O'M., Conway, B. E., Yeager, E., and White, R. E., eds. (New York: Plenum Press, Chapter 6, 1981).

4. Kordesch, K. V., and Gsellmann, J., "Power Sources 7," Proc. 11th Int. Symp. Power Sources, Joint Services Electical Power Source Committee, Thompson, J., ed. (London: Academic Press, 1979), p. 557.

5. Ogawa, H., Ohira, T., Murakami, K., and Yokoyama, T., U.S. Patent No. 3,716,411, 1973.

6. Cahoon N. C., and Holland, H. W., The Primary Battery, Volume 1, Heise, G. W., and Cahoon, N. C., eds. (New York: John Wiley and Sons, Chapter 7, 1971).

7. Tye, F. L., "Electrochemical Power Sources," Primary and Secondary Batteries, IEE Energy Series I, M. Barak, ed. (London: Peter Peregrinus Ltd., Chapter 3, 1980).

8. Schumacher, E. A., The Primary Battery, Volume 1, Heise, G. W., and Cahoon, N. C., eds. (New York: John Wiley and Sons, Chapter 3, 1971).

9. Brodd, R. J., Kozawa, A., and Kordesch, K. V., J. Electrochem. Soc., 125, 1978, p. 271C.

10. Falk, S. U., and Salkind, A. J., Alkaline Storage Batteries (New York: John Wiley and Sons, 1969).

11. Armstrong, R. D., and Bell, M. F., Electrochemistry, Volume 4, Thirsk, H. R., Sr. Reporter, The Chemical Society, London, Chapter 1, 1974.

12. Kozawa, A., Batteries, Volume 1, Manganese Dioxide, Kordesch, K. V., ed. (New York: Marcel Dekker, Inc., 1974), p. 305.

REFERENCES (Cont.)

13. Kozawa A., and Yeager, E., J. Electrochem. Soc., 112, 1965, p. 960.

14. Kozawa A., and Powers, R. A., J. Electochem. Soc., 115, 1968, p. 122.

15. Kozawa, A., and Yeager, J. F., J. Electrochem. Soc., 115, 1968, p. 1003.

16. Kordesch, K., Gsellmann, J., Peri, M., Tomantschger, K., and Chemelli, R., Electrochim. Acta, 26, 1981, p. 1495.

17. "Battery Data Guide," Duracell U.S.A., Tarrytown, N.Y., 1981.

18. "Eveready Battery Engineering Data," Volume 1, Union Carbide Corporation, 1980.

19. Attewell, A., "Power Sources 9," Proc. 13th Int. Symp. Power Sources, Joint Services Electical Power Source Committee, J. Thompson, ed. (London: Academic Press, 1983), p. 473.

R. ZINC-MERCURIC OXIDE (RUBEN CELL, MERCURY CELL)

Zn | KOH | HgO

Zn | ZnSO$_4$ | HgSO$_4$ · 2 HgO

$$Zn + HgO \longrightarrow ZnO + Hg \qquad [1]$$

$$3 Zn + HgSO_4 \cdot 2HgO \longrightarrow ZnSO_4 + 2ZnO + 3Hg \qquad [2]$$

The zinc-mercuric oxide battery was developed by Samuel Ruben during the early years of World War II to provide power sources for military transceiver radios and other electronic equipment. This system fulfilled the requirements for long shelf life, storage under both low and high temperature environments, and high volumetric energy densities.[1,2] Since that time, zinc-mercuric oxide cells and batteries have found use in miniature electronic devices (e.g., hearing aids, watches, and cameras). Specially designed versions of the zinc-mercuric oxide cell were candidate power sources for implantable cardiac pacemakers.[3] Though the greatest use of the zinc-mercuric oxide system is for primary battery applications, special modifications to the design and electrode compositions enable the system to be utilized as a secondary power source.[4] However, the secondary version of the system has been found to possess a limited cycle life of about 300 shallow depths of discharge as well as a low power density capability.[4,5]

The three basic designs for zinc-mercuric oxide cells are the wound zinc/pellitized mercuric oxide flat cells, the pressed powder flat and button cells, and the pressed powder cylindrical cells. Intensive efforts have been made to produce a version of the zinc-mercuric oxide cell which would take advantage of the less costly manufacturing methods for Leclanche cells. One such attempt resulted in the development of the zinc-mercuric dioxysulfate bobbin cell.[6] The overall cell reaction is given in equation 2. This cell used a zinc can negative electrode and a positive electrode mixture of mercuric dioxysulfate (HgSO$_4$ • 2HgO) with acetylene black, a calcium carbonate buffering agent, and zinc sulfate solution. The electrolyte was a 20 percent ZnSO$_4$ • 7H$_2$O solution containing 1 percent K$_2$CrO$_4$ as an inhibitor used to limit extensive amalgamation of the zinc negative electrode by any soluble positive electrode species. The open circuit voltage for fresh AA size Leclanche type cells was 1.45 V which slowly decreased to an equilibrium value of 1.36 V after storage. The performance characteristics for these cells were obtained for AA cells under various loads from 25 to 200 ohms at 25°C. The results showed average load voltages of about 1.2 to 1.3 V and corresponding realized capacities of 1.15 to 1.43 Ah. The energy density for this system is approximately 85 Wh/kg. Though the volumetric capacity and energy density for the zinc-mercuric dioxysulfate

system was shown to be higher than the corresponding characteristics for Leclanche cells, widespread acceptance of the system has not been realized. As a result, this cell system is not commercially available at the present time.

The remainder of the discussion relative to the zinc-mercuric oxide system is concerned with the characteristics for the three basic cell designs of the primary system. The wound zinc electrode/pellitized mercuric oxide flat cell consists of a corrugated zinc metal strip wound with two layers of a porous paper. The winding is performed to provide exposed zinc surface at the top of the roll and completely enclosed zinc at the bottom of the roll. This process ensures mechanical contact of the top of the zinc roll with the top closure of the cell and a means of separation between the lower edge of the zinc roll and the mercuric oxide electrode. After winding the zinc electrode, a plastic sleeve placed over the roll provides a means of electrical isolation of the zinc from the cell case and restrains the roll from unwinding during cell assembly. The zinc electrode rolls are then soaked in the electrolyte and amalgamated. The amalgamation process requires the addition of approximately 10-13 weight percent mercury to the exposed zinc in the roll. A uniform distribution of mercury can be effected by heating the assembled cell at a minimum temperature of 55°C.[7] An inner, tinned steel container in contact with the zinc roll also is amalgamated during the heating process. This further prevents the corrosion of the zinc with attendant hydrogen evolution caused by local electrochemical cells.

The zinc electrodes in the pressed powder flat and button cell designs and the pressed powder cylindrical cell design consist of preamalgamated zinc powder (10-13 weight percent mercury) pressed to allow sufficient porosity for electrolyte absorption and nearly complete oxidation during discharge. Some pressed powder zinc electrodes may also consist of a mixture of amalgamated zinc and gelled electrolyte.[4]

The reaction of the zinc electrode in alkaline media is given by either:

$$Zn + 2\ OH^- \longrightarrow Zn(OH)_2 + 2e^{1-} \tag{3}$$

or:

$$Zn + 4\ OH^- \longrightarrow ZnO_2^{2-} + 2\ H_2O + 2e^{1-} \tag{4}$$
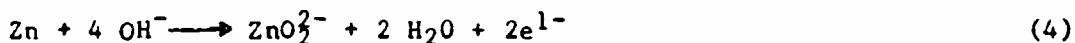
The standard potentials for equations 3 and 4 are 1.245 and 1.215 V, respectively.

One possible side reaction which could occur at the zinc electrode to produce hydrogen gas is given by:

$$2\ H_2O + 2e^{1-} \longrightarrow H_2 + 2\ OH^{1-} \tag{5}$$

The standard potential for reaction 5 is -0.828 V. It can be seen, therefore, that the zinc electrode is approximately 0.4 V more positive than the reversible hydrogen evolution potential. As a result, zinc is thermodynamically unstable in strong alkaline media and will corrode, producing hydrogen gas. The zinc negative electrode corrosion may be significantly reduced by amalgamation. This results in an increased hydrogen overpotential on the electrode. The use of

high purity zinc for the electrodes in the zinc-mercuric oxide system also contributes to the reduction of zinc corrosion.[8] Inclusion of such metal impurities as nickel or iron in the zinc electrode results in the production of cathodic sites on the zinc electrode. Hydrogen, therefore, can be evolved rapidly with little decrease in the zinc electrode potential. The addition of mercury to the zinc electrode, on the other hand, results in an electrochemical couple where zinc is the negative electrode and mercury the positive electrode. The activation overpotential of hydrogen on mercury is high and the corrosion reaction is inhibited significantly.

It is also important in zinc-mercuric oxide cells that the inner can, in contact with the zinc and electrolyte, be comprised of a metal of high hydrogen overpotential. The use of such metals as copper, lead, tin, and silver over a steel inner case top provides suitably high hydrogen overpotentials and limits the corrosion reaction of the zinc further.

The corrosion reaction at the zinc electrode may be further reduced by the addition of zinc oxide to the KOH electrolyte.[4,7] Exposure of a 0.5 g pressed pellet of zinc, in contact with a copper alloy inner can top, to a solution of 40 percent KOH saturated with ZnO showed that less than one cm^3 of hydrogen was generated after 3500 h at 60°C.[7] This gassing rate was significantly less than that observed for zinc electrodes exposed to solutions without zinc oxide.

The majority of literature references relative to anodic processes occurring at the zinc electrode have been concerned with its behavior in alkaline media.[5] Cells containing zinc negative electrodes in an acidic media do not exhibit severe rate limitations of the zinc electrode on discharge and thus have not been as extensively studied. The developmental efforts have focussed on the production of high rate primary cells containing an alkaline electrolyte; zinc passivation under such discharge conditions have been intensely investigated.[5] These investigations have resulted in much controversy.[9-19] A brief summary of the conclusions and other salient facts are given below:[5,20]

1. The dissolution of amalgamated zinc in alkaline media proceeds in a two step discharge mechanism:[18,20]

$$Zn(Hg) + 2\ OH^{1-} \longrightarrow Zn(OH)_2 + 2e^{1-} \tag{6}$$

and

$$Zn(OH)_2 + 2\ OH^{1-} \longrightarrow Zn(OH)_4^{2-} \tag{7}$$
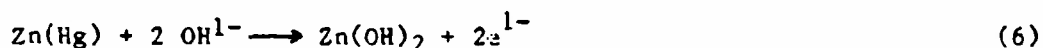
2. The capacity realized per unit area of the zinc electrode prior to passivation was found to have the maximum value for solution concentrations of 7 M KOH.[5]

3. Two types of solid films form on the zinc electrode during passivation.[5,17,18] A "Type I" film is a white, flocculent, loosely adherent film of ZnO which forms in the absence of electrolyte convection. This film is the result of the precipitation of ZnO from a supersaturated layer of zincate ions near the electrode surface. With

123

convection, a "Type II" film is found which is more compact and results in a coherent film of ZnO directly on the zinc electrode surface. The formation of this film is thought to be responsible for the creation of the passive state of zinc in alkaline media. Powers[17] showed that these Type II films also act as catalysts for hydrogen evolution. The production of hydrogen was found to disrupt the passivating film and thus cause reactivation of the zinc electrode. Powers also found that the addition of lead and tin anions (10^{-3} M) forms the respective metal films on the zinc electrode surface. These films result in the inhibition of zinc dissolution so that little ZnO precipitation occurs.

4. The efficiency of zinc electrodes in alkaline media has been shown to be maximal for electrode porosities of 80 to 85 percent.[5] The discharge product, ZnO, results in an approximately 30 percent increase in volume of the electrode during discharge. In view of the above, high efficiencies of nearly 80 percent may be obtained for thick, porous zinc electrodes. Indeed, Nagy and Bockris[21] analyzed porous zinc electrodes after discharge and found "carpet like" films within the porous structure of the electrodes. The contribution of the interior of the porous zinc electrode was found to be considerable based upon the galvanostatic measurements of Elsdale et al.[13]

5. Passivation of zinc electrodes occurs more rapidly at low temperatures.[5] For example, the limiting current densities for a zinc electrode (2% Hg) were found to be approximately 25 and 110 mA/cm^2 at temperatures of -50 and -18°C, respectively. For comparison, the limiting current density at 21°C was found to be about 340 mA/cm^2.

The mercuric oxide positive electrode consists of finely divided mercuric oxide with 5 to 10 percent graphite.[7] The addition of graphite not only provides electrical conductivity to the positive electrode but also minimizes the formation of large mercury droplets upon discharge of the cell.[4] The most important factor relative to the success of sealed zinc-mercuric oxide cells was the development of balanced cell designs. The deposition potential of hydrogen in the KOH electrolyte plus the inner container overvoltage is less than the zinc half cell potential in the KOH electrolyte. Any excess zinc negative electrode material would then cause hydrogen evolution at the positive electrode once all the mercuric oxide was discharged if the cell remained under load. The accumulation of hydrogen could then result in a pressure rupture or "violent disassembly" of the cell.* The occurrence of such pressure ruptures were noted when zinc-mercuric oxide cells were used in some devices containing solid state components. Following the initial cell or battery usage, such devices would continue to drain the power source at very low rates in the "off" position. This would also result in a pressure rupture with possible deleterious effects to equipment.*

In order to avoid the hazardous events as described above, an excess of mercuric oxide or a combination of balanced mercuric oxide with a small percentage of electrolytic manganese dioxide is used as the active positive

---

*Mahy, T. X., Private Communication, 1984.

electrode material.[1,22,23] In addition, the larger cell designs consist of a double can structure. The space between the inner and outer case provides a path for any gas produced in the cell in the event of improper cell balance or the inclusion of any impurities in the zinc electrode (e.g., nickel or iron) which would produce hydrogen gas.[2] The inner case is constructed to allow the compression of the upper part of a Neoprene gasket by the internal gas pressure. The gas is allowed to escape into the space between the inner and outer cases. The outer case is provided with a suitable gas vent for release of the hydrogen to the atmosphere. A paper sleeve between the cases absorbs any escaping electrolyte. thereby maintaining a liquid leak resistant design. With the release of the gas, the seal of the inner cell case automatically closes.

The means of separation consists of an absorbent separator material and a barrier separator. The absorbent material is necessarily resistant to the electrolyte and is composed of a felted fabric of either cotton or a synthetic which immobilizes the electrolyte solution and prevents intimate contact of the two electrode materials.[4,23] The barrier material prevents the migration of dissolved positive electrode species while remaining permeable to the KOH electrolyte. Such materials as parchment or microporous plastics next to the cathode are used to prevent internal short circuiting due to the bridging of free mercury, graphite or various semiconductive phases of zinc oxide.[4] Specially designed cells may contain a gelatinized electrolyte in place of the separator material. This electrolye is prepared by heating a 40 percent solution of KOH saturated with ZnO to 120°C and adding 4 percent sodium carboxymethyl cellulose. The barrier layer is formed on the mercuric oxide electrode surface by coating it with alkalized polyvinyl alcohol. After formation of the barrier layer, the hot electrolyte is then poured into the positive electrode container and allowed to solidify.[4,24]

The electrolyte may consist of either potassium or sodium hydroxide at concentration levels of about 40 percent by weight.[7] A saturated solution of zinc oxide (approximately 7.4 percent by weight) in the solution is added to the hydroxide solution to reduce the corrosion of zinc electrode material, as previously discussed. The use of either KOH or NaOH as the electrolyte in zinc-mercuric oxide cells depends upon the rate at which the cell or battery is to be discharged.[22] The specific conductance for the KOH electrolyte is higher than that for the NaOH electrolyte. As a result, the efficiencies for cells containing KOH are higher for cells discharged at the higher rates. For example, button cells with surface areas of about 1 cm^2 and containing either KOH or NaOH electrolytes yield 100 percent of the rated capacities up to current density values of about 0.3 mA/cm^2 at ambient temperature. At higher current densities, the efficiency of the cells containing NaOH electrolyte decrease markedly while that for cells containing KOH electrolyte remains high at rates up to about 10 mA/cm^2.[22] The normal operating temperature range for zinc-mercuric oxide cells containing KOH electrolyte is -28°C to + 54°C, while that for zinc-mercuric oxide cells containing NaOH electrolyte is -10°C to +54°C. Both types may be discharged at temperatures up to 93°C for short durations.

The open circuit voltages for zinc-mercuric oxide ls containing only mercuric oxide or a mixed mercuric oxide-manganese dioxide are 1.35 and 1.40V, respectively. The discharge characteristics for cells containing only mercuric oxide exhibit flatter discharge curves than for cells containing the mixed

positive electrode materials. Both types yield nearly equivalent capacities when discharged at the same rate. The major U.S. manufacturers or suppliers of the zinc-mercuric oxide cell system include Burgess Battery Company, Duracell International, Union Carbide (Eveready), and VARTA. Zinc-mercuric oxide cells are produced and are available in capacities ranging from 16 mAh to 28 Ah from both Duracell and Union Carbide.[22-25] Zinc-mercuric oxide batteries are commercially produced with nominal voltage levels and capacities up to 12.6 V and 0.9 Ah, respectively.[24] The major applications for the zinc-mercuric oxide system include such devices as watches, photographic equipment, electronic instruments, transceivers, and hearing aids.

In view of the fact that performance characteristics for the multitude of cells and batteries are described extensively in the technical and manufacturing literature,[1,2,4,6,7,22-25] an exhaustive description of these characteristics will not be undertaken herein. However, since safety testing was performed using a cell similar or identical to the Duracell RM12R,[26] a brief description of the operational characteristics for this cell is included. The cylindrical pressed powder RM12R cell has a nominal diameter and length of 1.58 cm and 4.97 cm, respectively, and a weight of 40 g.[23] Cells discharged at 20°C under 25 ohm loads (average rate of about 48 mA) yielded 3.5 Ah to a voltage cutoff level of 0.9 V. The energy density for these cells was 105 Wh/kg.

Zinc-mercuric oxide cells yield 85 to 90 percent of the nominal capacity of the cell after two year storage period at 20°C. Cells stored one year at 45°C retain approximately 80 percent of the nominal capacity.[23] Ruetschi[3] analyzed various self-discharge mechanisms using a medical grade (pacemaker) zinc-mercuric oxide cell as the test vehicle. Though the study specifically relates to the zinc-mercuric oxide cell, the results of the studies may be extended to other alkaline electrolyte cell systems (e.g., zinc and cadmium cells containing silver oxide and manganese dioxide as well as the cadmium-mercuric oxide system). The several self-discharge mechanisms as discussed by Ruetschi can be summarized as follows:

1. One major cause of self-discharge in zinc-mercuric oxide cells involves the dissolution of the mercuric oxide in the KOH electrolyte and subsequent oxidation of the zinc electrode by the soluble $Hg(OH)_2$ species via the reactions:

$$Hg(OH)_2 + 2e^{1-} \longrightarrow Hg + 2\ OH^- \qquad (8)$$

and

$$Zn + 2\ OH^{1-} \longrightarrow ZnO + H_2O + 2e^{1-} \qquad (9)$$

Since the zinc-mercuric oxide cells are zinc limited for safety reasons, the loss of zinc results in a corresponding loss in cell capacity.

2. Internal electrolysis loss due to the production of hydrogen at the zinc electrode and oxygen at the mercuric oxide electrode was estimated to be about 1 percent at 37°C and 0.3 percent at 22°C over a ten year period.

3. External electrolysis will occur if the battery case is exposed to an aqueous media. Since the open circuit voltage for the zinc-mercuric oxide cell is 1.35 V (decomposition of water occurring at 1.23 V or above), hydrogen will be produced on the zinc electrode terminal and oxygen on the mercuric oxide terminal if the cell is exposed to pure water. If the aqueous media should contain ions which would accelerate corrosion, the positive case material may either be corroded extensively or metallic dendrites may be formed which would bridge the positive and negative terminals. The latter would result in accelerated self-discharge. Ruetschi found that self-discharge was minimized for cells in contact with high concentrations (30-50%) of solutions containing only KOH. For example, the capacity loss of a 1.2 Ah zinc-mercuric oxide cell stored in a 50 percent KOH solution at 22°C was about 0.08 Ah after ten thousand hours while the capacity loss for cells stored in pure water was 0.7 Ah after six thousand hours. Capacity losses were significantly higher for cells stored in solutions containing various concentrations of KOH and 35 g/l NaCl. Cells stored in 50 percent KOH solutions containing the NaCl showed capacity losses of 0.2 Ah after storage of ten thousand hours while capacity losses of 1.0 Ah were observed for cells stored in a solution containing only NaCl after less than one thousand hours.

4. The degradation of organic separator materials can be enhanced due to the oxidation by dissolved mercuric oxide electrode material in the alkaline media. In addition, cell seals may degrade after storage at elevated temperatures. The influx of air into the cell would result in the oxidation of the zinc electrode and absorption of carbon dioxide by the electrolyte. The contamination of the electrolyte by CO_2 also results in significant discharge capacity losses at the zinc electrode.[27]

Safety testing has been performed upon zinc-mercuric oxide cells manufactured by Duracell International.[26] The cell size chosen for the studies was 1.6 cm in diameter and 5.0 cm long. This cell size corresponds to the cylindrical pressed powder RM12R cell offered by Duracell.[23] The nominal capacity for the RM12R cell is 3.6 Ah to a 0.9 V voltage cutoff level under a 25 ohm load at 20°C. Electrical abuse testing consisted of short circuiting three zinc-mercuric oxide through a 0.015 ohm load and forced overdischarge of three cells at the C/10 rate (i.e., 0.36 A). Both test regimens were conducted at 20°C and 55°C. The results of the short circuit test at 20°C showed that cells reached peak currents of 10 A after about eight minutes and attained the maximum cell wall temperature of 125°C after 15 minutes. The results of this test showed only case distortion. Cells short circuited at 55°C reached peak currents of 13 A after about eight minutes and attained cell wall temperatures of 190°C after 13 minutes on test. Of the three cells tested, one vented during the test but "not in any spectacular manner."[26]

Undischarged zinc-mercuric oxide cells were forced overdischarged at 20 and 50°C under constant current conditions for a period equal to the nominal capacity of the cell. The power unit used in these tests had an output voltage of 16 V. Zinc-mercuric oxide cells forced overdischarged at 0.36 A at the two test temperatures did not vent or exhibit case bulging. However, the cells did show temperature increases of about 100°C during the tests and reached unstable maximum reverse voltage levels of 16 V.

Zinc-mercuric oxide cells were also subjected to the mechanical abuse tests of crushing and cutting. Although cells exhibited temperature rises of 30 to 50°C due to massive internal short circuiting, no effects were noted other than the loss of electrolyte. Penetration of the cell case by a high velocity 0.6 cm cube also resulted in internal short circuits but "there were few spectacular or lasting effects" on the cells.[26]

Cells were subjected to localized heating (i.e., an oxygen-propane flame adjusted to give a cherry red hot spot of 1 cm diameter on the side of the cell case) for a ten minute period. Zinc-mercuric oxide cells were mounted with vents or seals facing down. All cells tested ruptured violently with expulsion of cell contents around the test facility.[26]

Specially designed zinc-mercuric oxide batteries used as power sources in an emergency submarine location beacon have experienced explosions when older batteries were discharged under conditions simulating the beacon operation.[28] The battery consisted of 30 cells connected in series to give an open circuit voltage of 40.5 V. After storage for three to four years, the battery may not have met the application requirements. As a result, a test program was developed to assess the capabilities of older batteries. During the discharge test program, two 3.5 year old batteries experienced single cell explosions. It is believed that the explosions occurred in the overdischarge of dead cells of the series string through the electrolysis of the electrolyte solvent in accordance with the reaction:

$$2 H_2O \longrightarrow 2 H_2 + O_2 \tag{10}$$

Subsequent analyses of undischarged battery packs showed that no zinc electrode material was present in dead cells while nearly 50 percent of the zinc in live cells had been consumed by the corrosion reaction. In addition, elemental mercury was found only in the positive electrode material of live cells while large amounts of mercury were found throughout the dead cells. This mercury caused internal short circuiting and oxidation of the remaining uncorroded zinc.

Based upon these observations, two possible mechanisms for the explosion were postulated by DeVries.[28] The first involves a high pressure cell rupture resulting from a fast, high pressure buildup during battery discharge. Though corrosion of up to 50 percent of the zinc electrode material would result in significant hydrogen production to cause a cell rupture if contained, the hydrogen is produced slowly over a long period of time and diffuses out of the cell before high pressures are reached. However, discharge of the battery could result in a very rapid pressure increase over the relatively short discharge period. In the two instances of single cell explosions, the hydrogen and oxygen gas was generated at times of 250 and 630 times shorter than gas formed by the corrosion of zinc.

The second possible cause of the explosions is the ignition of the hydrogen and oxygen gases produced by the electrolysis of water. Since the production of the gases necessarily dries out the cell, the ignition of the gases could occur by electrical arcing within the cell during battery discharge. Of the 24 batteries in the test program, only two cells exploded even though the other 22 batteries contained at least one dead cell. As discussed previously, significant amounts of elemental mercury were found in the dead cells examined

in this study. If a direct internal short circuit between the electrodes were formed by mercury, no electrolysis of the water or arcing could occur during the discharge period. The direct short circuit would simply act as a conductive bypass and eliminate the electrodes from the battery circuit. Therefore, the possibility does exist that no similar internal short circuit existed in the two cells which exploded.

No charging tests were reported for zinc-mercuric oxide cells or batteries. In view of the fact that forced overdischarge tests could result in the electrolysis of water in older cells, case rupture may occur in similar cells subjected to charging conditions, dependent upon cell design (seals, structural integrity, etc.) and the experimental test conditions.

REFERENCES

1. Ruben, S., J. Electrochem. Soc., 122, 1975, p. 199C.

2. Ruben, S., Comprehensive Treatise of Electrochemistry, Volume 3, Electrochemical Energy Conversion and Storage, Bockris, J. O'M., Conway, B. E., Yeager, E., and White, R. E., eds. (New York: Plenum Press, 1981), p. 234.

3. Ruetschi, P., Power Sources 7, Proc. 11th Int. Symp. Power Sources, Collins, D. H., ed. (London: Academic Press, 1979), p. 533.

4. Ruben, S., The Primary Battery, Volume I, Heise, G. W., and Cahoon, N. C., eds. (New York: John Wiley and Sons, Chapter 5, 1971).

5. McBreen, J., and Cairns, E. J., Advances in Electrochemistry and Electrochemical Engineering, Volume II, H. Gerischer and Tobias, C. W., eds. (New York: John Wiley and Sons, 1978), p. 273.

6. Ruben, S., J. Electrochem. Soc., 106., 1959, p. 77.

7. Vinal, G. W., Primary Batteries, (New York: John Wiley and Sons, Chapter 11, 1950).

8. Glicksman, R., J. Electrochem. Soc., 106, 1959, p. 457.

9. Dirkse, T. P., and Hampson, N. A., Electrochem. Acta, 16, 1971, p. 2049.

10. Hampson, N. A., Shaw, P. E., and Taylor, R., Br. Corros. J., 4, 1969, p. 207.

11. Armstrong, R. D., and Bulman, G. M., J. Electroanal. Chem., 25, 1970, p. 121.

12. Hampson, N. A., Herdman, G. A., and Taylor, R., J. Electroanal. Chem., 25, 1970, p. 9.

13. Elsdale, R. N., Hampson, N. A., Jones, P. C., and Strachan, A. N., J. Applied Electrochem., 1, 213, 1971.

14. Briggs, A. G., Hampson, N. A., and Marshall, A., Chem. Soc. Faraday Trans. II, 70, 1974, p. 1978.

REFERENCES (Cont.)

15. Ruetschi, P., J. Electrochem. Soc., 114, 1967, p. 301.

16. Powers, R. W., J. Electrochem. Soc., 116, 1969, p. 1652.

17. Powers, R. W., J. Electrochem. Soc., 118, 1971, p. 685.

18. Powers, R. W., and Breiter, M. W., J. Electrochem. Soc., 116, 1969, p. 719.

19. Devanathan, M. A. V., and Lakshmanan, S., Electrochim. Acta, 13, 1968, p. 667.

20. Armstrong R. D., and Bell, M. F., Electrochemistry, Volume 4, Thirsk, H. R., ed. (London: The Chemical Society, Chapter 1, 1974).

21. Nagy, Z., and Bockris, J. O'M., J. Electrochem. Soc., 119, 1972, p. 1129.

22. Eveready Battery Engineering Data, Union Carbide Corporation, Volume I, 1980, p. 56.

23. Duracell, Battery Data Guide for Designers, Duracell International, Tarrytown, N.Y., 1981, p. 12.

24. Crompton, T. R., Small Batteries, Volume 2, Primary Cells (New York: John Wiley and Sons, 1983), p. 59.

25. Mantell, C. L., Batteries and Energy Systems, Second Edition (New York: McGraw Hill, Chapter 9, 1983).

26. Attewell, A., "Power Sources 9," Proc. 13th Int. Symp. Power Sources, Joint Services Electrical Power Source Committee, J. Thompson, ed. (London: Academic Press, 1983), p. 473.

27. Ko, H-W., and Juang, H-K., J. Applied Electrochem., 13, 1983, p. 725.

28. DeVries, L. E., The Cause of Explosions in Old Mk 102 Mod 0 Batteries under Discharge, NTIS AD-A040976, U.S. Dept. Commerce, Springfield, VA., 1977.

S. ZINC – POTASSIUM IODATE

$$Zn \mid H_2SO_4 \mid KIO_3$$

$$5\,Zn + 2\,KIO_3 + 6\,H_2SO_4 \longrightarrow 5\,ZnSO_4 + I_2 + K_2SO_4 + 6H_2O \quad [1]$$
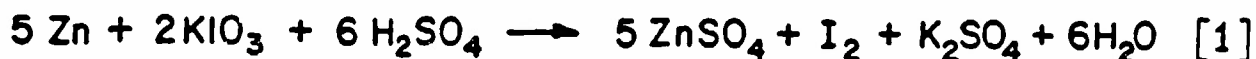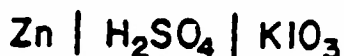
The zinc-potassium iodate primary battery system was developed and tested by the U.S. Navy at the Ordnance Test Station in Pasadena, CA.[1] The specific goal of the developmental efforts was the fabrication of a high drain rate reserve power supply for such military electronic devices as electric torpedos and other ordnance equipment. Reaction 1, above, has been shown to be the prominent reaction for cells or batteries discharged at temperatures above 25°C. However, a second reaction is dominant in the temperature range of 0°C to 25°C:

$$3\,Zn + KIO_3 + 3\,H_2SO_4 \longrightarrow 3\,ZnSO_4 + KI + 3\,H_2O \qquad (2)$$
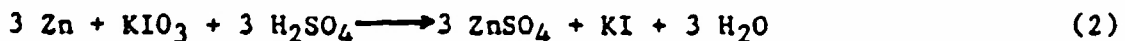
The open circuit voltage for the zinc-potassium iodate system is 1.96 V. Substitution of potassium bromate for the potassium iodate positive electrode material resulted in less desirable performance characteristics. Though cells and batteries comprised of zinc and potassium bromate were capable of being discharged at the same high rates as the zinc-potassium iodate system, the discharge curves were significantly less flat. This was an important consideration in view of the intended electronic applications for the proposed battery system. In addition, zinc-potassium bromate cells produced more hydrogen gas during discharge than zinc-potassium iodate cells.

The circular bipolar electrode for the system consisted of a zinc sheet coated on one side with a silver paint. The positive electrode matrix material of KIO_3 mixed with graphite and acetylene black is then bonded to the coated side of the zinc electrode. These electrodes may then be stacked with the zinc negative side of one electrode facing the positive side of the next electrode. Mechanical separation of approximately 0.1 cm was effected through use of gaskets and spacers on the circumference of the bipolar disc. In view of the high drain rate required of this system, no further means of separation or separator material was employed.

The reversible electrode potential of zinc in an acid media is 0.763 V for the reaction:

$$Zn \longrightarrow Zn^{2+} + 2e^-$$ (3)

Hydronium ions may be reduced in acidic media in accordance with the reaction:

$$2 H_3O^+ + 2 e^- \longrightarrow 2 H_2O + H_2$$ (4)
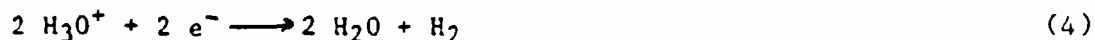
The electrode potential for equation 4 is 0.00 V. Therefore, zinc metal can undergo a corrosion reaction leading to the production of hydrogen gas in highly acidic media. Indeed, zinc is rapidly corroded in acidic solutions of pH less than 6 due to the high solubility of corrosion products in the acid.[2] It should be noted that adherent corrosion product films formed on the zinc electrode at pH values of 6 to 12.5 protect the zinc surface from severe corrosion reactions. The inclusion of impurities with low hydrogen overvoltage characteristics in the zinc electrode also results in enhanced corrosion of zinc. The impurities are essentially cathodes within the zinc electrode from which hydrogen can be produced rapidly.

The corrosion of zinc in zinc-potassium iodate cells may be represented by the anodic reaction (equation 3) and a cathodic reaction (equation 4) which proceed at the same rate for cells under open circuit conditions. The inhibition of the cathodic reaction, therefore, necessarily inhibits the anodic reaction. For zinc negative electrode electrochemical systems, the direct amalgamation of zinc or the inclusion of a mercuric compound such as $HgCl_2$ in the electrolyte produces a zinc-mercury electrochemical couple where zinc is the negative electrode and mercury is the positive electrode. The inhibition of the cathodic reaction (equation 4) is due to the high activation overpotential of hydrogen on the mercury. The corrosion reaction of the zinc is then decreased substantially. There is a limit to the amount of mercury amalgamation, however, because of the loss of desirable mechanical properties of the zinc negative electrode. Thus, some corrosion of the zinc does occur in the zinc-potassium iodate cells.

The positive electrode material for the zinc-potassium iodate system was a mixture of 57.1 percent of finely divided KIO_3, 40.8 percent graphite, and 2.1 percent of Shawinigan acetylene black with a binder of polyvinyl acetate. The above paste mixture was then applied to the silver painted side of the bipolar electrode and dried at elevated temperatures. Fabrication of the battery was accomplished by stacking the bipolar electrodes with the face of the negative electrode to the positive face of an adjacent bipolar electrode. The cell thickness was approximately 0.2 cm with an interelectrode separation of 0.1 cm.

The electrolyte for the zinc-potassium iodate system was a mixture of 8N H_2SO_4 and 0.5N HCl. The inclusion of HCl in the electrolyte was found to increase cell load voltage levels at low temperatures (i.e., to 0°C). In addition, the electrolyte contained 2 to 3 percent $HgCl_2$, in order to reduce the evolution of hydrogen at the zinc electrode.

Zinc-potassium iodate cells were discharged at various temperatures from 0°C to 65°C to determine the predominant cell reaction corresponding to either of those given in equation 1 or 2. This was accomplished by analyses of the

cell reaction products following discharge to a voltage cutoff level of 1.0 V. It was found that reaction 1 was the dominant discharge reaction scheme for cells discharged at temperatures above 25°C and that the reaction scheme given in equation 2 was dominant at the lower temperatures. The amount of zinc consumed in the corrosion reaction was found to vary from 5.1 percent at 0°C to 9.7 percent at 55°C. Further, the potassium iodate was determined to be the species most responsible for side reactions, particularly at elevated temperatures. From these data, it was concluded that the optimum operational temperature range for the system was 25°C to 30°C.

The open circuit voltage for the zinc-potassium iodate system is 1.96 V. Cells having an electrode surface area of 232 cm^2 were discharged at 28°C under constant current conditions of 24 A (current densities of about 103 mA/cm^2). The discharge duration was approximately seven minutes at an average load voltage of 1.7 V. The effect of HCl addition to the electrolyte was determined by discharging cells with and without HCl at current densities of 90 to 130 mA/cm^2. At the lower current densities, the cell load voltages were 0.15 V higher for cells containing HCl, while cell load voltages 0.30 V higher were found for cells containing HCl at the higher current densities.

A prototype primary reserve battery was fabricated to determine the performance characteristics for the zinc-potassium iodate system. The goal was the successful development of a power source for torpedo propulsion. This battery consisted of six parallel strings of 17 cells in series. Each string was designed to be discharged at 22.5 A at a voltage level of 26.5 V. Discharge of the battery resulted in an average load voltage of 26 V and an average current of 134 A (22.3 A per string). These performance values were maintained for approximately 7.3 minutes before load voltage levels decreased below the 23 V minimum. The activation time to a 20 V level was found to be 2.1 seconds for this battery. These results indicated that the energy density for the zinc-potassium iodate system was about 31.1 Wh/kg when used in such high rate applications as torpedo propulsion.

There are, however, serious deficiencies in this battery system. One of the most important requirements for torpedo propulsion is the ability to operate at sea water temperatures of -2°C. The zinc-potassium iodate battery system exhibited poor performance levels at these low temperatures. In addition, when the battery was discharged at especially high current densities, overheating of the battery took place. This resulted in the boiling and eventual violent expulsion of the electrolyte. The activated stand life of the battery can be measured in hours due to the self-discharge reactions of the KIO_3 positive electrode material, and, to a lesser extent, the zinc negative electrode. In view of these deficiencies, advanced development or manufacture of this system was not pursued.

No safety data were presented which detail the safety characteristics of the battery after testing in accordance with the electrical abuse procedures of NAVSEAINST 9310.1A. However, it should be noted that the highly corrosive electrolyte of H_2SO_4 and HCl was expelled from the battery during overheating. In addition, the electrolyte contained highly toxic mercuric chloride as a corrosion inhibitor. Hydrogen-oxygen fires or explosions could occur should the activated battery be located in a poorly ventilated area. In view of the fact that there exists no current manufacture or use of this battery

135

system, no future abuse testing is recommended. However, should the zinc-potassium iodate system become a candidate power source for Navy applications, testing in accordance with NAVSEAINST 9310.1A would be warranted due to the high rate capability of the system. Further, since many applications might require use of a battery comprised of two or more parallel strings of several cells in series, the possibility of charging and forced overdischarging would exist. The thermal management problems of a large battery might also result in the loss of electrolyte and battery operation.

REFERENCES

1. Jones, J. L., and Arranaga, A. B., J. Electrochem. Soc., 105, 1958, p. 435.

2. Glicksman, R., J. Electrochem. Soc., 106, 1959, p. 458.

T. ZINC - SILVER CHLORIDE

$$Zn \mid Mg(ClO_4)_2 \mid AgCl$$

$$Zn + 2AgCl \longrightarrow ZnCl_2 + 2 Ag \qquad [1]$$
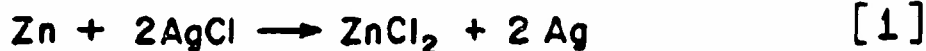
The zinc-silver chloride electrochemical system has been investigated as a power source for several applications requiring low discharge currents, operation at low temperatures after storage under severe environmental conditions, and high reliability.[1-3] Much of the modern work relative to the successful development of this system has been performed by Thorn Electronics Limited under sponsorship from the Ministry of Defence in Great Britain. The major military applications for this system include a power source candidate for air launched weapons systems,[4] a timing device to initiate detonation of explosive charges, and a power source for military electronic devices. No commercial applications for the zinc-silver chloride system exist at the present time.

Though the zinc-silver chloride system has been known for about 115 years, efforts within the past two decades have led to the successful use of the primary system for military purposes. It should be noted, however, that the system has also been intensely investigated as a fast-charging, secondary battery power supply.[5] Both the zinc negative electrode and the silver chloride positive electrode exhibit high rate charging characteristics.[6,7] The high self-discharge rate for the zinc-silver chloride system, using zinc chloride electrolyte, was found to decrease considerably by reducing the zinc chloride concentration.[5] Nonetheless, Bro and Marincic found that the corrosion of zinc led to the accumulation of hydrogen between the electrodes. This resulted in non-uniform current distribution during high charging rates. The ultimate result was the formation of dendritic zinc leading to internal short circuit conditions. It should be noted that the successful development of a fast-charging secondary battery system, based upon the cadmium-silver chloride couple, is dependent upon a dual charging process[5] (refer: cadmium-silver chloride system, Chapter 3, this work). The cadmium-silver chloride secondary system relies on the electrical charging of zinc chloride to zinc metal followed by an electrochemical exchange of the zinc by cadmium. The latter step was of much longer duration (e.g., one hour) than the electrical charging step (e.g., at the 40 C rate: 1.5 minutes).

Primary zinc-silver chloride cells as well as multicell batteries have been developed for the military in Great Britain by Thorn Electronics Limited.[1-3] Single prototype cells consisted of single discs of high purity, unamalgamated zinc and a mixture of fused silver chloride and silver on a silver current collector disc. The disc cell design included a polycarbonate case having an inner rubber gasket around the internal circumference of the cell. Interelectrode separation was effected through use of multilayers of Vilene A50 having a fiber content of 35 percent viscose rayon, 40 percent nylon, 15 percent cellulose acetate, and 10 percent Terylene. An aqueous solution of magnesium perchlorate (pH of 7.5 to 8.0) was then introduced into the cell through use of a hypodermic syringe inserted through the rubber gasket material. After filling, the fill hole was plugged, resulting in a fully assembled, sealed, unvented cell. The observed open circuit voltage was 1.05 V.

Cells of the above design[1] were stored under various environmental conditions at temperatures of -40°C to +70°C for periods of up to eighteen months and subsequently discharged at temperatures of -32°C to +50°C. The results showed that the majority of performance failures for the cells tested were the result of the loss of integrity of the polycarbonate case, particularly after exposure to high temperature storage conditions. Some deterioration in the performance characteristics were noted for cells discharged at the lower operational temperature after storage at 70°C for extended periods. In general, however, it was found that the dominant effect of storage was the slight depression of load voltage levels with no loss in realized capacity.

Further development of the zinc-silver chloride system resulted in the production of multicell battery units incorporating several significant design and electrochemical improvements.[2] Earlier results had shown that there was significant corrosion of the zinc negative electrode which resulted in the production of hydrogen. Concentrations of hydrogen gas not only led to an increase in internal pressure which could cause cell leakage but also caused a non-uniform current distribution at the electrodes. The latter produced severe polarizations particularly at low temperatures. This wasteful corrosion reaction of zinc was reduced by prior treatment of the zinc with a 2 percent solution of nitric acid and by the addition of quinoline ethiodide inhibitor to the electrolyte.

A second improvement for the system involved the replacement of the Vilene A50 separator material by a separator consisting of 70 percent Terylene and 30 percent rayon. It was found that the cellulose acetate in the Vilene A50 separator was soluble at 70°C. Upon removal of the cells from the high temperature environment, the cellulose acetate reprecipitated. Such an occurrence led to decreased separator porosity and a subsequent increase in internal cell resistance. The cellulose acetate also contributed to the corrosion of the zinc electrode. A second component of the Vilene A50, nylon, could be hydrolyzed by the $Mg(ClO_4)_2$ electrolyte. The presence of hydrolyzed nylon was also believed to contribute to the increased zinc corrosion rates.

Four cell batteries of bipolar construction and incorporating the above improvements were preconditioned at -20°C for a two week period. The batteries were then weighed and the open circuit voltages were measured. These batteries were subjected to an automatic temperature cycling regime of six hours per day

at 70°C and 18 hours per day at 35°C for four, eight, and thirteen week periods.[2] After removal from the temperature cycling chamber, the batteries were allowed to equilibrate at ambient temperatures and then conditioned at -31°C for at least 24 hours. The performance characteristics for the above test units were obtained by discharging the batteries under 100 ohm loads (30mA) at a temperature of -31°C. The results show that the open circuit voltage decreased from about 3.90 V to 3.80 V and that the average weight loss for all cells tested was 1.25 g at the end of the 13-week test period. The weight loss value was attributed to water loss of the electrolyte and represented a total battery weight loss of about 0.24 percent. The nominal capacity for these test batteries was approximately 600 mAh. The discharge results showed that average capacities and load voltages of 545 mAh and 3.04 V, respectively, were obtained at -31°C.

Similarly designed three cell batteries were tested after a ten-year storage period at ambient temperature.[3] In contrast to those batteries described above, these batteries weighed 47.9 g and possessed nominal capacities of 40 mAh. These batteries were discharged at 60°C, 20°C, and -30°C (under constant loads of either 3.3 or 12 kohms (approximately 0.80 and 0.22 mA, respectively). The discharge tests showed average realized capacities of 38, 40, and 39 mAh at 60°C, 20°C, and -30°C, respectively, for the two sets of discharge loads. The average load voltages for batteries discharged at 60°C and 20°C were 2.72 and 2.67 V, respectively. At the lowest temperature of -30°C, the average load voltages decreased to 2.52 V. No batteries exhibited evidence of leakage prior to testing. However, leakage did occur in batteries after discharge, particularly for cells discharged under the lighter 1 ad. It was found that the zinc electrodes were pitted due to local penetration initiated by corrosion reactions at metal impurity sites on the zinc. Continued erosion of these pits during battery discharge led to cell leakage if the battery remained on load for extended periods after the useful discharge ended.

The average energy densities for the above batteries discharged at -30°C to +60°C were approximately 2.1 Wh/kg. It should be noted, however, that the requirements for these batteries include high reliability after ten years storage and operation at temperatures of -30°C to +60°C after storage. In view of the above, the silver chloride positive electrode was fabricated by melt impregnation onto a sintered silver powder current collector. The resultant electrode was, therefore, essentially a non-porous glass. Higher energy densities would be expected for the zinc-silver chloride system if the positive electrode were more porous. The storability characteristics, on the other hand, would exhibit decreased shelf life with an attendant loss in capacity over long storage periods.

No safety data was reported for the zinc-silver chloride system. Though the battery has found use for military applications in Great Britain, it is believed that there exist no similar applications for this battery system in the United States military.

In view of the fact that the present zinc-silver chloride battery is, by design, a low rate power supply, short circuit testing in accordance with the procedures of NAVSEAINST 9310.1A should not result in catastrophic failure or case rupture. It should be noted that cells and batteries are sealed and do not have vent structures. Electrolysis of water could occur during either the force

overdischarge or charge tests. A pressure buildup within cells or batteries would eventually cause case rupture or a loss of integrity of the butyl rubber gasket seal. Similar results to the above would be expected for cells or batteries subjected to incineration testing.

REFERENCES

1. Ginger, D. A, Burton, J. S., Sperrin, A. D., and Wilson, J., "Power Sources 1966," Proc. Fifth Int. Symp., Joint Services Electrical Power Sources Committee, D.H. Collins, ed. (London: Pergamon Press, 1967), p. 99.

2. Dale, R. H. M., Burton, J. S., and Ginger, D. A., "Power Sources 3," Proc. Seventh Int. Symp., Power Sources, Joint Services Electrical Power Sources Committee, D.H. Collins, ed. (Newcastle Upon Tyne: Oriel Press, 1971), p. 567.

3. Fryer, A. J., Morgan, C. J., and Sinclair, T. J., Proc. Power Sources Symp. 28, 1979, p. 101.

4. Attewell A., and Tattershall, P., Proc. Power Sources Symp. 29, 1981, p. 53.

5. Bro, P., and Marincic, N., J. Electrochem. Soc., 117, 1970, p. 113.

6. Bro, P., and Marincic, N., J. Electrochem. Soc., 116, 1969, p. 1338.

7. Bro, P., and Marincic, N., J. Electrochem. Soc., 116, 1969, p. 448.

U. ZINC-SILVER OXIDE (SILVER-ZINC)

$$Zn \mid KOH \mid Ag_2O_2, Ag_2O$$

$$2\,Zn + Ag_2O_2 + 2\,H_2O \longrightarrow 2\,Zn(OH)_2 + 2\,Ag \qquad [1]$$

$$Zn + Ag_2O + H_2O \longrightarrow Zn(OH)_2 + 2\,Ag \qquad [2]$$
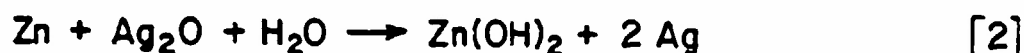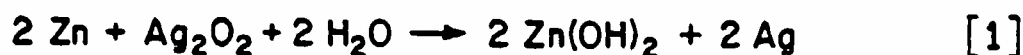
The zinc-silver oxide (silver-zinc) cell was developed by H. G. Andre and patented in 1943.[1] Primary silver-zinc cells and batteries are presently used as the power source in several U.S. military and space applications which require high energy densities at high rates. The U.S. Navy has employed the primary silver-zinc battery for torpedo propulsion, expendable antisubmarine warfare target vessels, submarines, and detonation (pyrotechnic) ignition devices. Silver-zinc batteries have also served as the principal auxiliary power supplies on U.S. missiles (e.g., rocket instrumentation, guidance, and telemetry) and space orbiting vehicles (e.g., Explorers XVII and XXXII). Small primary cells and batteries[2,3] are available on the consumer market for such applications as hearing aids, watches, and camera flash units. The focus of this discussion for the primary silver-zinc battery concerns the characteristics of large military and aerospace batteries. Several types of silver-zinc primary batteries are available for specialized military and aerospace applications. These include the manually and remotely (reserve) activated as well as custom dry-charged units with the capability of discharge at rates as high as one minute.[4]

Detailed discussions for the silver-zinc battery system are given by Fleischer and Lander[5] and Falk and Salkind.[6] The reactions at the zinc electrode in an alkaline media during cell reaction are summarized below:

$$Zn + 2\,OH^{1-} \longrightarrow Zn(OH)_2 + 2e^{1-} \qquad (3)$$

The $Zn(OH)_2$ then dissolves and forms zincate ions:

$$Zn(OH)_2 + 2\,OH^{1-} \longrightarrow Zn(OH)_4^{2-} \qquad (4)$$

The standard potential for equation 3 is 1.245 V. One possible side reaction which occurs at the zinc electrode produces hydrogen in accordance with:

$$2\,H_2O + 2e^{1-} \longrightarrow H_2 + 2\,OH^{1-} \qquad (5)$$

145

The standard potential for reaction 5 is -0.828 V. Since the zinc electrode is approximately 0.4 V more positive than the reversible hydrogen evolution potential, zinc is thermodynamically unstable in strong alkaline media and will experience corrosion. The corrosion reaction may be reduced considerably by increasing the hydrogen overpotential of zinc through amalgamation and the use of pure zinc. The zinc electrode may be amalgamated in mercuric chloride or acetate. A two percent amalgamation level results in high activation overpotentials of hydrogen on the mercury and the inhibition of the corrosion reaction. Passivation of the zinc electrode by ZnO will occur when the solubility limit for zinc species in the electrolyte at the immediate vicinity of the zinc electrode is exceeded:[7]

$$Zn(OH_2) \longrightarrow ZnO + H_2O \tag{6}$$

or

$$Zn(OH)_4^{2-} \Longrightarrow ZnO + 2\ OH^{1-} + H_2O \tag{7}$$

A summary of the zinc passivation characteristics in alkaline media is described for the zinc-mercuric oxide system.

Several methods are used to produce zinc electrodes for the silver-zinc primary cells. These include the dry, pressed powder process, the paste method, and the electrodeposition process.[6] In the pressed powder process, zinc oxide dust containing one to ten percent mercuric oxide and a binder is pressed onto a zinc or silver expanded metal screen in a mold. The porosity of the electrode can be varied for high rate discharge (80-90% porosity) or for low rate discharge (30-40% porosity). These electrodes are then electrolytically reduced in a 5 percent KOH solution. The pasting process applies a slurry of zinc oxide with a gelling agent onto a silver or copper expanded metal screen. The pasted electrode is then reduced in a 5 percent KOH solution. In the electrodeposition process, zinc is plated onto expanded metal screens from either a zinc oxide slurry or a cyanide bath. Electrodes for primary silver-zinc cells may also be fabricated by sintered powder techniques.

Similar techniques are employed to produce silver oxide electrodes for primary cells. The slurry process requires a mixture of silver oxide in water with carboxy-methylcellulose binder to be applied to an expanded silver plated screen. The electrode is then dried at 70°C. The use of these electrodes is limited to primary cells since there is poor adhesion of the silver oxide material to the grid. The silver electrode is then electroformed to Ag_2O_2 by low rate charging in 5 percent KOH solutions. A dry process technique applies chemically prepared silver oxides and binder to a silver expanded metal grid at pressures of 1560 psi to 3120 psi (11 M Pa to 22 M Pa). The most widely used procedure in the fabrication of silver electrodes is the continuous sintered powder process.

The silver oxide electrode exhibits a two step discharge in accordance with the reduction of Ag_2O_2 followed by the reduction of Ag_2O:

$$Ag_2O_2 + H_2O + 2e^{1-} \longrightarrow Ag_2O + 2\ OH^{1-} \tag{8}$$

$$Ag_2O + H_2O + 2e^{1-} \longrightarrow 2\ Ag + 2\ OH^{1-} \tag{9}$$
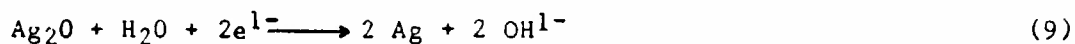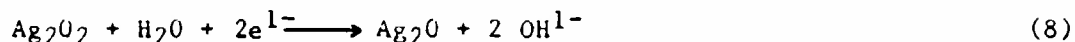
The standard potentials for reactions 8 and 9 are 0.607 and 0.345 V, respectively. It can be seen that the electrical capacity for the Ag_2O_2 species is twice that for Ag_2O. The duration of the higher load voltages associated with the discharge of Ag_2O_2 is dependent upon such factors as discharge rate, temperature, and length of stand time after activation. Silver (I) oxide, Ag_2O, is soluble in alkaline solutions.[8,9] The maximum solubility for Ag_2O of about 5×10^{-4}N occurs at concentration levels of 7 M KOH. The dissolved silver (I) oxide material diffuses to the zinc electrode and is reduced:

$$Zn + 2 \, Ag(OH)_2^{1-} \longrightarrow Zn(OH)_4^{2-} + 2 \, Ag \qquad (10)$$

The formation of metallic silver often results in the promotion of short circuits between the electrodes.

The separator system for the primary silver-zinc cell has been the object of several intensive investigations. The requirements for the separator assembly include low electrolytic resistance for cell discharge at high rates, resistance to chemical oxidation by the silver oxide, and low permeability to both the colloidal silver oxide and zinc oxide species. In addition, these separators must be thin enough to allow efficient operation at high power and energy densities.[6,10,11] Several different separator materials have been considered for use as dendristatic and argentostatic membranes. These include various types of regenerated cellulose (sausage casing, cellophane, irradiated polyethylenes, nylon, and inorganic separators). Nearest each electrode are wraps of inert, nonwoven materials to ensure proper wetting of the electrode and electrolyte retention.

The electrolyte for the silver-zinc primary cell is 7 to 10 M KOH. Some primary cell electrolytes also contain ZnO at concentrations up to 80 g per liter of solution. The inclusion of ZnO has been shown to further reduce the corrosion rate at the zinc electrode.[12]

Several designs of primary silver-zinc batteries are available for military applications. These include the manually activated system, the remotely activated (reserve) system, and the remotely activated (reserve) pile design. The manually activated silver-zinc battery provides rapid activation prior to use and an extended activated stand time than for other designs. This design also allows performance testing before actual deployment since the battery possesses some cycling capability. Remotely activated batteries essentially consist of a cell stack, an electrolyte reservoir, and a gas generation device. The latter device is activated by firing a squib or by severe setback conditions (inertia). The pressure of the gas generated upon the electrolyte reservoir will then force open metal diaphragms allowing the electrolyte to flow rapidly into the cell stack. Remotely activated batteries may also consist of a cell stack having bipolar electrodes. This design is especially desirable for fulfillment of high rate, high energy density requirements. All battery designs provide for venting.

The open circuit voltages for the silver-zinc cell are 1.86 V for the reduction of Ag_2O_2 and 1.60 V for the reduction of Ag_2O.[13] The silver-zinc cells and batteries are characterized by very high energy densities at high discharge rates. In addition, this system also exhibits long storage

life in the dry state, low self-discharge and mechanical ruggedness. Cells discharged at high rates of C to 6C at 25°C will yield realized capacities of 120 percent to 80 percent, respectively, of the nominal capacity. Under the lower discharge rates, two load voltage plateaus corresponding to reactions 1 and 2 are observed. Only one discharge plateau is seen at the higher discharge rates. The energy density values for primary cells vary from 50 Wh/kg to 200 Wh/kg depending upon rate, temperature, design, and size. Remotely activated silver-zinc batteries exhibit lower energy densities due to the inclusion of the electrolyte reservoir, activation generator, and plumbing. These energy densities are typically 15 Wh/kg to 100 Wh/kg, dependent upon similar conditions as described above. The normal operational temperatures are -40°C to 55°C for cells and manually activated batteries. Remotely activated batteries operate at 0°C to 50°C. Lower temperature operation can be achieved using heaters.

The major U.S. manufacturers of silver-zinc batteries for military and space applications are Eagle-Picher, General Electric, and Yardney Electric Corporation.

Primary silver-zinc batteries have experienced several instances of fire following inadvertent activations[14,15] or external short circuiting.* In addition, since both hydrogen and oxygen are produced during a fire or thermal runaway condition, there existed the distinct possibility for an explosion in these instances. Large amounts of toxic gases from the oxidation of cell components and plastic materials were also emitted. A study to determine the causes of spontaneous combustion of silver-zinc batteries was conducted by Britz and Thomas.[15] A summary of the findings is given below:

1. Combustion began when zinc plates, partially saturated with electrolyte, reached temperatures of 163°C or higher. When a silver positive electrode plate was then placed in contact with a partially wetted zinc plate, combustion was much more vigorous. The fire was supported by the release of oxygen from the silver electrode.

2. Spontaneous combustion was not the result of electrolyte leakage to the battery case.

3. Test performed on 33 and 350 Ah cells which were only partially filled with electrolyte did not exhibit spontaneous combustion.

4. Direct short circuiting of the zinc and silver electrode plates by a steel pin for 33 Ah cells resulted in a maximum temperature rise of 93°C. Combustion did not occur but the electrolyte boiled and both smoke and vapor was observed. The same test performed upon 350 Ah cells resulted in ignition and fire. Combustion began at the site of the short circuit.

5. The tendency for the occurrence of fires was greater for larger cells. A fire will occur after local drying of the electrode plates at the point of short circuit. The minimum temperature for plate combustion is 163°C.

---

*Yedwab, D., Private Communication, 1984.

6. Cells with nominal capacities of 33, 300, and 350 Ah were discharged at
    the high rates of 300 and 770 A, 100 to 300 A, and 35 to 300 A,
    respectively. An internal explosion was observed for the 33 Ah cell
    discharged at 770 A. Smoke was observed for the 350 Ah battery
    discharged at 300 A. It was concluded that combustion and/or an
    explosion could occur due to an overload condition. These high rates
    corresponded, in some cases, to short circuit conditions.

7. Combustion of 33 and 350 Ah cells will occur for cells placed in an
    oven at approximately 163°C. This test confirmed that combustion will
    occur when the electrode plates reach about 163°C.

8. Gas evolution tests showed that both hydrogen and oxygen are evolved
    during discharge.

Though no results were given for silver-zinc primary cells subjected to
either forced overdischarge or overcharge testing, significant amounts of both
hydrogen and oxygen would be produced under these conditions. In view of the
above results indicating that cells will spontaneously combust after electrode
plate temperatures reach about 163°C, the possibility of fires and explosions
would also exist for batteries in the overdischarge or overcharge condition,
dependent upon the discharge or charge rates. Further, the production of
hydrogen and oxygen in these cells or batteries would consume large amounts of
water. The combination of water loss with a high rate overdischarge or
overcharge condition could also result in localized heating with a resultant
fire or explosion.

REFERENCES

1. Andre, H. G., U.S. Patent No. 2, 317, 711, 1943.

2. Megahed, E-S. A., and Davig, D. C., "Power Sources 8," Proc. 12th Int. Symp. Power Sources, Joint Services Electrical Power Source Committee, J. Thompson, ed. (London: Academic Press, 1981), p. 141.

3. Crompton, T. R., "Small Batteries," Volume 2, Primary Cells (New York: John Wiley and Sons, 1983), p. 111.

4. Mantell, C. L., Batteries and Energy Systems, Second Edition (New York: McGraw Hill, 1983), p. 106.

5. Zinc-Silver Oxide Batteries, Fleischer, A., and Lander, J. J., eds. (New York: John Wiley and Sons, 1971).

6. Alkaline Storage Batteries, Falk, S. U., and Salkind, A. J., (New York: John Wiley and Sons, 1969).

7. Hampson, N. A., in reference 5, p. 51.

8. Dirske, T. P., The Primary Battery, Volume 1, Heise, G. W., and Cahoon, N. C., ed. (New York: John Wiley and Sons, 1971), p. 228.

9. Dirske, T. P., in reference 5, p. 100.

10. Falk, U., "Electrochemical Power Sources," Primary and Secondary Battery Systems, IEE Energy Series 1, Barak, M., ed. (London: Peter Peregrinus Ltd., 1980), p. 384.

11. Gregory, D. P., reference 5, p. 226.

12. Dalin, G. A., in reference 5, p. 87.

13. McBreen, J., Comprehensive Treatise of Electrochemistry, Volume 3, Electrochemical Energy Conversion and Storage, Bockris, J. O'M., Conway, B. E., Yeager, E., and White, R. E., eds. (New York: Plenum Press, 1981), p. 308.

14. Murphy, F. G., in reference 5, p. 397.

15. Britz W. J., and Thomas, C. E., Proc. Power Sources Symp. 26, 1975, p. 162.

V. ZINC-SODIUM DICHROMATE

$$Zn \mid H_2SO_4 \mid Na_2Cr_2O_7$$

$$3\,Zn + Na_2Cr_2O_7 + 7\,H_2SO_4 \longrightarrow Cr_2(SO_4)_3 + 3\,ZnSO_4 \qquad [1]$$
$$+ Na_2SO_4 + 7\,H_2O$$
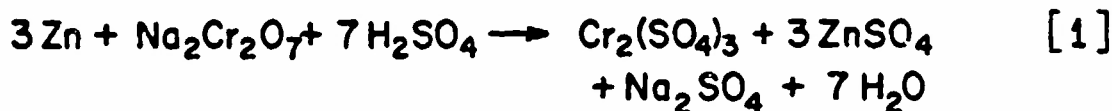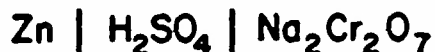
The zinc-sodium dichromate system was developed in the late nineteen sixties by Pistoia and Scrosati[1] in the effort to provide a zinc battery having power densities greater than 0.25 W/cm^2. At that time, the most desirable characteristics for a high power cell included a high open circuit voltage, low internal resistance (high electrolyte conductivity), and very low electrode polarization at high rates of discharge. Several positive electrode candidates were considered prior to the selection of the $Na_2Cr_2O_7$:

(1) $S_2O_8^{2-}/SO_4^{2-}$, $E° = 2.01$ V,

(2) Co^{3+}/Co^{2+}, $E° = 1.81$ V,

(3) MnO_4^{1-}/Mn^{2+}, $E° = 1.69$ V, and

(4) Ce^{4+}/Ce^{3+}, $E° = 1.61$ V.

When each of the above positive electrode candidates were discharged in cells containing zinc negative electrodes and sulfuric acid electrolyte, the load voltages were less than 1.0 V at current densities of about 50 mA/cm^2. The open circuit voltage for the zinc-dichromate system was found to be 2.12 V at H_2SO_4 concentrations of 4.5 M. Cells of standard design exhibited severe electrode polarizations and poor shelf life characteristics. However, it was determined that electrode polarization could be greatly decreased by circulating the electrolyte through the electrodes at an optimum operating temperature of 60°C to 75°C.

Both potassium and sodium dichromates were considered as the soluble positive electrode material in 32 weight percent of H_2SO_4 (4.5 M). The solubility of the potassium dichromate was found to be only 10 weight percent in the acid. As a result, the sodium dichromate salt was chosen as the soluble positive electrode material since dichromate concentrations of up to 20 weight percent in the sulfuric acid could be obtained. Further, the optimum concentration of sodium dichromate was 15 weight percent. Higher concentrations of the salt did not produce any further performance advantages in this system.

The reversible electrode potential of zinc in an acid environment is 0.763 V for the reaction:

$$Zn \longrightarrow Zn^{2+} + 2e^- \tag{2}$$

Similarly, hydronium ions may be reduced and produce hydrogen gas in an acid media in accordance with the reaction:

$$2H_3O^+ + 2e^- \longrightarrow 2 H_2O + H_2 \tag{3}$$

The electrode potential for the above reaction is 0.00 V. It can be seen, therefore, that zinc metal can experience a severe corrosion reaction in highly acidic media. In fact, zinc is rapidly corroded in acidic solutions of pH less than 6 due to the high solubility of corrosion products in the acid.[2] It should be noted that adherent, protective corrosion product films formed on the zinc negative electrode in solutions of pH 6 to 12.5 will protect the zinc surface from severe corrosion reactions. The films will dissolve in more acidic or more basic media, however.

For most battery applications, the zinc electrode must be of high purity or be amalgamated with mercury. Low purity unamalgamated zinc electrodes may contain impurities with low hydrogen overvoltage characteristics. Use of such electrodes result in the enhanced corrosion of zinc. These impurities act essentially as cathode materials within the zinc electrode from which hydrogen can be rapidly evolved. The corrosion of the zinc electrode in the zinc-sodium dichromate cells may be represented by the anodic reaction of equation 2 and the cathodic reaction of equation 3. These reactions proceed at the same rate for cells under open circuit conditions. The inhibition of either reaction necessarily inhibits the other reaction. For the zinc-sodium dichromate system, the zinc electrode is amalgamated. This results in a zinc-mercury electrochemical couple, where zinc is the negative electrode and mercury is the positive electrode. The inhibition of the reaction whereby the hydronium ions are reduced to produce hydrogen gas is due to the high activation overpotential of hydrogen on the mercury. The amount of hydrogen evolution on the zinc electrode, therefore, is reduced dramatically. There is, however, a mercury concentration limit relative to amalgamation of the zinc electrode. With the inclusion of large amounts of mercury, a lessening of desirable mechanical properties of the electrodes (e.g., electrodes become very brittle) is observed. In view of the above, some corrosion of the zinc does occur in zinc-sodium dichromate cells if the electrolyte is allowed to remain in contact with the electrode.

The soluble positive electrode material, a 15-weight percent solution of $Na_2Cr_2O_7$ in water was stored in a reservoir. A second reservoir contained a 32-weight percent solution of H_2SO_4. The electrical performance characteristics for this system were found to be optimum at operating temperatures of 75°C. An external heating device was avoided by mixing the soluble $Na_2Cr_2O_7$ positive electrode solution with the sulfuric acid solution prior to cell activation. The desired operating temperature of 75°C was attained, therefore, by mixing the appropriate quantities of the two solutions. The conductivity of the resultant solution was about 1.0 ohm^{-1}cm^{-1} at 75°C (versus about 0.66 ohm^{-1}cm^{-1} at 20°C). Mixing took place in a container connected to a circulation pump and fitted with means to

remove the spent solution. In addition, a pressure release valve was included in the structure of the mixing chamber to eliminate any pressure increases during mixing of the solutions or during cell operation. A pump then continuously circulated the electrolyte through the cell. At the end of the cell operation, the electrolyte was drained from the mixing chamber, thereby limiting the exposure of the zinc electrode and positive electrode current collector to the solution. Thus, the self-discharge processes were restricted only to the period of cell operation.

The experimental cell used in this study consisted of a circular amalgamated zinc plate negative electrode facing a circular graphite current collector electrode. The surface area for each electrode was 50 cm^2 and the interelectrode spacing was 0.2 cm. Separation of the electrodes was maintained through use of inert supports and gasket rings. Two factors precluded the use of any separator material for this system: 1) electrolyte circulation would be restricted and reaction products could not be efficiently removed from the interelectrode spacing and 2) the rate capability of the cell would be decreased considerably. Both factors would contribute to severe electrode polarization and decreased performance.

The open circuit voltage for the zinc-sodium dichromate system at 60°C is 2.10 to 2.12 V. Cells as described above were discharged at various current densities from 16 mA/cm^2 to 500 mA/cm^2. The performance characteristics for cells discharged at the lower current densities of 16 to 200 mA/cm^2 showed average load voltages of 1.88 V to 1.64 V, respectively. These values reflect the low internal resistance of the cell as well as the effect of continuous circulation of electrolyte. The corresponding power densities for cells discharged at current densities of 16 to 200 mA/cm^2 were 0.03 and 0.33 W/cm^2. Discharge durations for these cells varied from 0.83 to 0.17 hour, respectively.

Cells discharged at the higher current densities of 300 to 500 mA/cm^2 showed average load voltages of 1.59 to 1.00 V, respectively. The corresponding power densities for these cells ranged from 0.48W/cm^2 to 0.62 W/cm^2. The maximum power density value was observed for cells discharged at the current density of 400 mA/cm^2. It should be noted that the discharge times for these cells were 0.13 and 0.05 h over this current density range. No energy density values were given for this system since the system was not optimized relative to both volume and weight. However, in view of the fact that this system requires such external equipment as two reservoirs, a mixing chamber, and solution pump, the energy density (Wh/kg) and power density (W/kg) values would be significantly lower than many self-contained battery systems (e.g., zinc-silver oxide).

No safety data were given for the zinc-sodium dichromate system relative to the test procedures of NAVSEAINST 9310.1A. This battery has not progressed to either the advanced development or manufacturing phase at the present time. However, provision was made in the experimental cells to relieve excess pressure in the electrolyte mixing chamber caused by overheating or boiling of the solution during mixing or cell discharge. No safety vent was included in the cell chamber to account for pressure buildup in the event of an electrolyte pump malfunction.

In view of the fact that the system is not commercially available, no future testing in accordance with NAVSEAINST 9310.1A procedures is possible.

REFERENCES

1. Pistoia, G., and Scrosati, B., J. Electrochem. Soc., 117, 1970, p. 645.

2. Glicksman, R., J. Electrochem. Soc., 106, 1959, p. 458.

CHAPTER 3

SECONDARY BATTERY SYSTEMS

A. ALUMINUM-AIR   (ALUMINUM-OXYGEN)

Al | SEA WATER | O$_2$

$$4 \, Al + 3 \, O_2 + 6 \, H_2O \longrightarrow 4 \, Al(OH)_3 \qquad\qquad [1]$$

Aluminum has been studied extensively as a candidate material for negative electrodes in a number of electrochemical systems. Its advantages include low cost, availability, low equivalent weight (9.0 grams per equivalent), and safety in handling. Several problems, however, have inhibited the use of aluminum in many power source systems. Aluminum will undergo a violent chemical reaction with water in basic media and produce hydrogen (equation 2):

$$2Al + 6H_2O \longrightarrow 2Al(OH)_3 + 3H_2 \qquad\qquad (2)$$

Secondly, when reaction 2 is prevented by the formation of protective aluminum oxide films and exposed to a neutral electrolyte solution, the observed open circuit voltage is much less than the theoretical open circuit voltage, leading to a substantial loss in energy density. Activation of the aluminum-air battery results in the destruction of the oxide film with subsequent aluminum reaction with water producing rapid corrosion and pitting of the aluminum electrode.[1]

A number of attempts have been made to alloy the aluminum to produce an electrochemically active metal with reduced reactivity with water. Test cells containing aluminum electrodes alloyed with trace amounts of indium, gallium, and thallium[2,3] have exhibited high cell potentials at current densities of 30mA/cm^2. One cell containing an aluminum alloy of 0.07 percent In and 0.03 percent Ga exhibited the optimum polarization curve compared to cells of aluminum (99.5 percent) and an alloy of 0.07 percent In, 0.05 percent Ga, and 0.03 percent Ti. However, the lowest corrosion rate (7%) was observed for the

cell containing the In, Ga, and Tl alloy compared to 22 percent for the cell containing the In and Ga alloy. Aluminum alloyed with 1.2, 5.2, and 9.5 percent zinc has also been used as negative electrodes in sea water batteries.[4] The Al-Zn alloys exhibited a low self discharge rate in the slightly basic sea water (pH 8.2) and can be used for applications requiring low discharge rates. The utilization of the aluminum was approximately 67 percent in test cells.

Amalgamation of the aluminum metal results in changes in the hydrogen overvoltage and anodic polarization.[5] The higher potentials observed with amalgamated aluminum negative electrodes are attributed to the partial removal of the protective oxide film by the amalgamation process. Accordingly, the rate of corrosion is greatly increased.

Use of high purity (99.9%) aluminum (slightly amalgamated) electrodes have been reported in sea water activated aluminum-air cells.[6] The success of these cells for the large part, was due to the development of carbon-based air diffusion electrodes capable of operation in salt water conditions without protective membranes. Typically, air electrodes are composed of active carbon material with PTFE and have a nickel screen current collector.[7] However, considerable success has also been reported for air electrodes containing a platinum or platinum group metal catalyst.[8,9] More recently, macrocyclic catalysts (e.g., cobalt tetramethoxyphenylporphyrin) have been developed which replace the more expensive platinum catalysts.[10]

The electrolyte for the aluminum-air system may be 2M $NaCl$,[2,3] sea water,[4,6] a mixture of KCl and KF,[7] NaCl and NaF,[6] tap water,[10] or 6M KOH.[11,12] Various additives to the electrolyte have been investigated in an effort to reduce the aluminum corrosion reaction and to enhance the precipitation of voluminous amounts of the $Al(OH)_3$ reaction product. One of the more effective additives used to coagulate the reaction product in experimental cells was found to be 0.1M NaF combined with the addition of one gram of solid Al_2O_3 every half hour or one portion of Al_2O_3 (20 grams) at the beginning of activation.[3] In summary, however, the electrolytes and corrosion inhibitors do not fully solve the problems associated with delay at activation and corrosion.

Separators and membranes for small laboratory cells have employed Celgard,[2,3] or no separators or membranes.[6] The latter cells rely on isolating foils surrounding the aluminum electrodes. Larger electric vehicle power systems proposed by Lawrence Livermore National Laboratory and Lockheed contain an electrode separation comprised of triangular copper bars in electrical contact with the aluminum electrode and an isolation means on the opposite side in contact with the air electrode. Incoming air membranes are used to remove dust and small amounts of carbon dioxide which would have a deleterious effect on the life of the air electrodes. The exhaust air passes through a recombination catalyst to remove hydrogen produced by reaction 2 and through a moisture/heat exchanger. The moisture/heat exchanger transfers the moisture and heat contained in the exhaust air to the incoming air.

The ultimate goal in present developmental efforts by Lawrence Livermore National Laboratory is the production of an economical and reliable power source for electric vehicles and other applications. Since the aluminum-air system is,

at present, only mechanically rechargeable (i.e., removal of hydrargillate, $Al(OH)_3$, and replacement of the aluminum electrodes must be carried out periodically), additional mechanisms relative to crystallization and temporary storage of the $Al(OH)_3$, the addition of water to the cell stack, temperature control, and the battery controller are included in the total battery unit.

The theoretical open circuit voltage (OCV) for the aluminum-air cell is 2.72 V. However, because of the corrosion reaction taking place in accordance with equation 2 and the effect of protective films on the pure aluminum electrode or various alloys, the cell OCV has been observed to be between 1.5 and 2.1 V.

Small, experimental aluminum-air cells were discharged at current densities of 30 mA/cm^2. The average cell voltage was 0.75 V throughout the discharge period.[2,3] The energy density based upon the above results for single cell tests was 80 Wh/kg. It should be noted that individual cell weights contribute significantly more weight per unit energy than for a number of cells comprising a battery. One practical battery of ten cells designed for use as a electric generator was fabricated and discharged at various current densities up to 22 mA/cm.[7] The average load voltage varied from approximately 18 V at low current densities to approximately 10 V at current densities of 22 mA/cm^2. The optimum power for the above battery was found to be 40 W (current density of 17 mA/cm^2) at a battery voltage of 12 V.

The discharge characteristics have also been determined for cells containing a proprietary aluminum alloy.[13] The average cell voltages observed were 1.4 and 1.2 V at current densities of 100 and 200 mA/cm^2. No discharge performance data was available for large batteries or submodules such as those proposed for electric vehicle applications.[10] However, it was determined that the optimum operational temperature for a large battery was 60°C to 80°C. Energy densities of 300 Wh/kg and power densities up to 150W/kg were obtained for prototype modules of the system at these temperatures.

The aluminum-air electric vehicle battery is mechanically rechargeable, i.e., the $Al(OH)_3$ (hydrargillate) would be removed from the storage container and returned for reprocessing.[14] In addition, the aluminum electrodes would also be replaced on a less frequent bases (i.e., every 1600 to 3200 km). The air electrode for the system has obtained lifetimes of 500 to 1000 cycles. In order to meet the two year life expectancy goal of 1500 cycles, a period of 500 hours operating time must be achieved. As a result, newer macrocyclic catalysts are being investigated as replacements for platinum.

Aluminum-air batteries cannot be stored for significant periods of time in the activated state. The corrosion reaction (equation 2) would consume the available aluminum and, concurrently, the reaction product would agglomerate and plug the air electrode. As a result, battery systems such as those considered for electric vehicle applications require that the electrolyte be removed from the cell stack when the battery is not in use.

The major developers for practical aluminum-air batteries are Lawrence Livermore National Laboratories, Lockheed Missile and Space Company, Zaromb Research Corporation, and the Norwegian Defence Research Establishment. Further, fundamental cell level studies were carried out at the University of Bonn and the University of Belgrade.

No data relative to the specific safety testing procedures of NAVSEAINST 9310.1A have been found for the aluminum-air system in the literature. However, a number of safety considerations do exist:

1. Large volumes of hydrogen gas are generated in practical batteries under operational and storage conditions (if the electrolyte is not removed). As a consequence, the possibility of a hydrogen-oxygen explosion hazard does exist. Therefore, a hydrogen recombination device such as that previously described for the electric vehicle battery is necessary. Further, a hydrogen explosion may occur if the capacity of the recombination device is exceeded due to excess hydrogen evolution or a diminishing capability of the device.

2. The electric vehicle version of the Al-air battery has an optimum operational temperature of 60°C to 80°C. Should the temperature of the system increase, large volumes of reaction product and caustic NaOH could be expelled from the battery stack. A temperature controller such as described by Cooper[12] for the electric vehicle battery is required as well as the appropriate heating and cooling devices.

3. The battery necessarily is exposed to the external environment. As a result, the internal pressure of the system would approximate the atmospheric pressure. Therefore, rupture of the battery package is highly unlikely should the battery be subjected to the electrical abuse tests of, for example, short circuit, charge, and overdischarge.

One patent[15] describes the addition of plumbite, plumbate, or stannate in concentration levels of less than 0.2 M in the electrolyte. The functions of the additive are the inhibition of the self-corrosion of the aluminum, an increase in current efficiency, and limitation of the electrolyte temperature.

REFERENCES

1. Brodd, R. J., Kozawa, A., and Kordesch, K. V., _J. Electrochem. Soc._, 125, 1978, p. 271C.

2. Despic, A. R., Drazic, D. M., Zecevic, S. K., and Grozdic, T. D., "Power Sources 6," _Proc. Tenth Int. Symp. Power Sources_, Collins, D. H., ed. (London: Academic Press, 1977), p. 361.

3. Drazic, D. M., Despic, A. R., Zecevic, S., and Atanakovic, M., "Power Sources 7," _Proc. 11th Int. Symp. Power Sources_, Collins, D. H., ed. (London: Academic Press, 1979), p. 353.

4. Wales, C. P., Simon, A. C., and Schuldiner, S., _Electrochim. Acta_, 20, 1975, p. 895.

5. Glicksman, R., _J. Electrochem. Soc._, 106, 1959, p. 457.

6. Ritschel, M., and Vielstich, W., _Electrochim. Acta_, 24, 1979, p. 885.

7. Valand, T., Mollestad, O., and Nillson, G., "Power Sources 8," _Proc. 12th Int. Symp. Power Sources_, J. Thompson, ed. (London: Academic Press, 1981), p. 523.

8. Gross, S., _Energy Conversion_, 15, 1976, p. 95.

9. Gregory, D. P., _Metal-Air Batteries_, (London: Mills and Boon Limited, Chapter 3, 1972).

10. Cooper, J. F., _Al 2_0 Battery Development: Toward an Electric Car_, Energy and Technology Review, Lawrence Livermore National Laboratory, 1983, p. 21.

11. Zaromb, S., _J. Electrochem. Soc._, 109, 1962, p. 1125.

12. Cooper, J. F., and Littauer, E. L., _Proc. of the 13th IECEC_, American Society of Mechanical Engineers, 1978, p. 738.

13. Behrin, E., et al, _Electric and Hybrid Vehicles_, Energy Technology Review, No. 44, M.J. Cole, ed., Noyes Data Corp., Park Ridge, NJ, 1979, p. 441.

REFERENCES (Cont.)

14. Gratt, L. B., Environmental, Health and Safety Impact Analysis of An Aluminum-Air Battery for Vehicular Applications and Impact Analysis, Final Report, Volume 2, Lawrence Livermore National Laboratory, VCRL15434, 1981.

15. Katoh, M., U.S. Patent 3, 563, 1971, p. 803.

B. CADMIUM-AIR (CADMIUM-OXYGEN)

Cd | KOH | O_2

$$2\,Cd + O_2 + 2\,H_2O \rightleftharpoons 2\,Cd(OH)_2 \qquad\qquad [1]$$

The cadmium electrode possesses the stability and cycle life characteristics necessary for effective operation as demonstrated in the nickel-cadmium and silver-cadmium battery systems. In addition, cadmium has a theoretical energy density of approximately 440 Wh/kg and exhibits a low self-discharge rate. On the other hand, cadmium is of high cost compared to other negative electrode materials and is also of limited supply. The use of cadmium in a system exposed to the environment also requires nearly total removal of carbon dioxide which promotes the penetration of the separator by cadmium after several cycles. In view of the above technological and economic factors, little work has been carried out relative to the secondary cadmium-air battery system.

The cadmium-air system has been investigated by Wagner.[1] Sponge cadmium electrodes were prepared by the reduction of cadmium oxide blended with five weight percent of nickel (carbonyl) powder and five to ten weight percent of either ferric oxide or titanium oxide extenders. The mixture was pressed on a nickel Exmet grid. The completed electrode was then wrapped in separator and placed in Pellon bags.

The air electrodes (platinized active carbon) were supplied by General Electric and Leesona Moos Laboratories. No auxiliary charging electrodes were necessary since the air electrodes could be cycled. The electrolyte was 35 percent KOH or 35 percent KOH containing various additives (e.g., either carbonates or zincates). The observed open circuit voltage for freshly made cells was 1.21 V.

Test cells were cycled at the 0.2C rate to a discharge cutoff voltage of 0.0 V and a charge voltage cutoff of 1.9 V. A means to remove incoming carbon dioxide was employed to determine the effect on cycle life and capacity maintenance. The results of the testing are summarized below:

1. The capacity loss of the cadmium electrode following continuous cycling was found to be inhibited by the use of ferric oxide or titanium dioxide and the removal of carbon dioxide in the influent air. Cycling data showed that cells containing the ferric oxide and which were free of CO_2, could be deep discharge cycled up to 100 times and still

retain 75 to 80 percent of the theoretical capacity. The average load voltages were 0.7 V. A cell containing no ferric oxide and exposed to CO_2 lost 37 percent of its initial capacity in twelve cycles.

2. Cadmium penetration through the separator was found to be promoted by CO_2 and the extent of overcharge.

3. The air electrode became inactive during discharge in CO_2 free cells but not in cells containing CO_2/CO_3^{--}. It was found that the cadmium formed a soluble species which deactivated the air electrode. This effect was overcome by saturating the electrolyte with zincate ions.

4. The air-cathode exhibited a loss in electrocatalytic activity.

5. Water loss resulted from transpiration of water vapor through the pores of the air electrode and the cell vent.

6. Practical energy densities of 110 Wh/kg at the 0.1C rate and 96 Wh/kg at the 0.5C rate were obtained for the test cells. The cycle life capability for these cells was 300 cycles.

It should be noted that the cadmium-air system is not a commercially available product at the present time. Widespread use of the system is not anticipated due to the high cost and the short supply of cadmium metal.[2] In addition, the complete removal of CO_2 from the air supply would not be economically feasible. Only one practical battery comprised of cadmium-air cells was fabricated. Though the energy density values obtained were promising, 80 Wh/kg, the battery failed due to electrolyte leakage and air electrode flooding.

No safety data was presented in the technical literature for the cadmium-air system. Since the data presented herein[1] were obtained for laboratory cells enclosed in a glass reaction kettles, estimation of the safety characteristics for the system is not possible.

REFERENCES

1. Wagner, O. C., <u>J. Electrochem. Soc.</u>, <u>116</u>, 1969, p. 693.

2. Gregory, D. P., <u>Metal-Air Batteries</u>, (London: Mills and Boon Limited, 1972), p. 61.

C. CADMIUM – NICKEL(III)OXYHYDROXIDE   (NICKEL-CADMIUM, NICAD)

Cd | KOH | NiOOH

$$Cd + 2\ NiOOH + 2\ H_2O \rightleftharpoons Cd(OH)_2 + 2\ Ni(OH)_2 \qquad [1]$$

The cadmium-nickel (III) oxyhydroxide (nickel-cadmium) battery was invented and developed by Jungner and Estelle in the 1890's.[1-3] The evolution of the nickel-cadmium system has progressed through three distinct phases:[4]

1. Batteries produced during the first fifty years of this century were fabricated exclusively of nickel plated steel with pocket type plates. The active materials were contained in these thin perforated pockets. A later modification used perforated nickel plated steel tubes containing nickel flake and nickel hydroxide as the positive electrode with the standard pocket cadmium negative electrode. These batteries were used for mining vehicles, delivery vans, railway signalling, standby power, diesel engine starting, and other heavy duty industrial applications.

2. Sintered plate technology emerged at about 1950. The electrodes in these batteries consisted of perforated metal sheets or expanded metal screens onto which a powdered metal is sintered. Nickel-cadmium batteries with sintered electrode structures exhibited increased energy densities and higher rate capabilities. The applications for these nickel-cadmium batteries included the communications and electronics industries. During this period, an alternate method for electrode processing combined the electroactive materials with carbon or graphite and a binder. The resultant mixture is either pressed or pasted onto expanded metal screens. A later development allowed the electrode-position of the electrode materials onto expanded metal grids or screens.

3. Sealed nickel-cadmium cells were developed in the mid-1960's. Since both hydrogen and oxygen are generated during overcharge or overdischarge, a means to eliminate hydrogen evolution in these cells was devised. The inclusion of excess uncharged negative electrode material in both the negative and positive electrodes permitted the controlled recombination of oxygen from the positive electrode during overcharge and from the negative electrode during overdischarge. These

cells also were electrolyte-starved in order to provide only enough electrolyte to keep the electrodes and separators wet. The starved electrolyte condition provides a means for oxygen to diffuse through the separator to the negative electrode (overcharge) or to the positive electrode (overdischarge). A metal-gas-liquid three phase boundary is also required for an effective recombination reaction. Sealed nickel-cadmium batteries have found extensive use in aerospace applications, portable tools, emergency equipment, electronic devices, and appliances.

Nickel-cadmium cells are manufactured in either the vented, flooded electrolyte or the sealed, starved electrolyte designs. The electrodes for either of the two designs may be the pocket, sintered, pasted, or pressed powder types. The constructional design shapes of either type of nickel-cadmium cell are typically rectangular (plate), cylindrical (rod shaped, pressed electrodes or spirally wound sintered electrodes), or button (pressed or sintered electrodes).[5]

Vented cells are provided with a device in the lid which opens and closes during normal cell operation. Internal cell pressures of 2 psi to 10 psi (14 to 70 kPa) above atmospheric pressure are required to activate the venting mechanism.[6-10] The vent allows for the escape of hydrogen and oxygen produced during the charging process and accessibility for filling cells with electrolyte. Further, the vent restricts the escape of electrolyte and the loss of water due to evaporation. Since carbon dioxide is detrimental to the performance of nickel-cadmium cells, the vent design also limits the admission of air into the cell. Though this vent mechanism is not a safety feature per se, it does allow the escape of gases and/or electrolyte in cells subjected to the electrical abuses of overcharge and overdischarge. Both hydrogen and oxygen are vented under these conditions. The separator for vented cells typically consists of one layer of cellophane between one or more layers of nylon or polyamide material. The cellophane acts as a gas barrier to limit extensive recombination of oxygen with hydrogen at the negative plate. There does exist, however, the possibility of an oxygen-hydrogen fire or explosion in the environment outside the cells if appropriate ventilation is not provided. Excessive overcharge or overdischarge of vented cells would lead to the drying of the cell components and subsequent performance failure. Vented cells which have been short circuited could expel hot, caustic KOH electrolyte. Exposure of vented cells to elevated temperatures or incineration conditions not only would cause electrolyte expulsion but also would release toxic materials from the oxidation of cell contents and plastic case materials.

Though the remainder of the discussion for the nickel-cadmium system will be concerned with the characteristics of sealed cells, a summary of some important features for vented cells is given below:[6-10]

1. Vented nickel-cadmium cells are available in low and high rate designs with capacities up to 1200 Ah. The latter cells are also characterized by high energy densities and low internal resistances. Special sintered plate cells discharged at rates as high as 20C to a 0.6 V load voltage cutoff level yield about 50 percent of the nominal capacity. Energy densities of 20 to 35 and 15 to 25 Wh/kg are obtained for sintered and pocket vented cells, respectively.

2. Cells must be mounted upright to allow the escape of gases during overcharge and to avoid the loss of electrolyte during vent operation.

3. The operational temperature range for these cells is -20°C to +45°C using 7M KOH electrolyte. With higher KOH concentrations, the lower limit may be extended to -50°C.

4. Vented sintered plate cells may be charged using constant current, constant potential, or modified constant potential techniques in the temperature range of -55°C to 75°C.[11] Under constant current charging, the rate is usually 0.1°C to 0.2 C for 14 and 7 hours, respectively. A charge potential of 1.40 to 1.55 V per cell is used in constant potential charging procedures.

5. The charge retention characteristics for vented cells are better than for sealed cells. At least 90 percent of the nominal capacity is available after storage for either one month at 25°C or six months at -20°C. After storage at 25°C for six months, about 70 percent of the nominal capacity is realized while less than 10 percent capacity is realized after one month at 50°C.

6. The cycle life expectancy is one to two thousand deep discharge cycles to 50 percent of the rated nominal capacity. The lifetime for cells varies from two to ten years, dependent upon the application, service conditions, amount of overcharge (or overdischarge), and operational temperature.

7. Vented cells can withstand shock, vibration, and other physically abusive conditions (e.g., specifications given in MIL-B-26220).

Sintered cells first appeared in Germany during World War II, but it was not until the 1950's that the sealed version of the cell was developed.[4] Within the past two decades, this design has been the most widely manufactured type of nickel-cadmium cell. Intensive optimization studies were conducted by the National Aeronautics and Space Administration (NASA) and its subcontractors to utilize the system in several aerospace applications.[12-16]

The discharge reaction at the cadmium electrode in an alkaline solution involves the dissolution of cadmium metal as a soluble complex ion of either $Cd(OH)_4^{2-}$ or $Cd(OH)_3^{1-}$:

$$Cd + 4\ OH^{1-} \longrightarrow Cd(OH)_4^{2-} \tag{2}$$

followed by the precipitation of $Cd(OH)_2$ discharge product within the electrode matrix:[1,4,17,18]

$$Cd(OH)_4^{2-} \longrightarrow Cd(OH)_2 + 2\ OH^{1-} \tag{3}$$
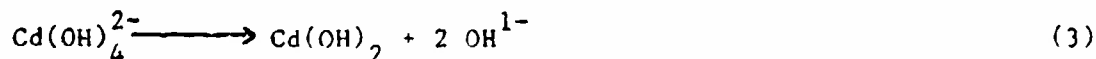
Continued precipitation of $Cd(OH)_2$ results in the reduction of the active surface area of the electrode. A thin layer of either CdO or $Cd(OH)_2$ on the cadmium metal surface is then formed and causes electrode passivation. The overall reactions at the cadmium electrode during discharge and charge are given by:

$$Cd + 2\ OH^{1-} \underset{charge}{\overset{discharge}{\rightleftarrows}} Cd(OH)_2 + 2e^{1-} \tag{4}$$
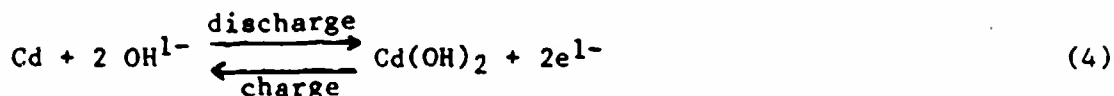
The porous sintered nickel plaque retains the cadmium negative electrode material and also serves as the current collector.[4] A section of nickel expanded metal screen is dipped into a low density aqueous nickel slurry thickened with carboxymethylcellulose. The nickel strip is then sintered in a vertical oven at about 900°C. Typical thicknesses for the resultant plaque vary from 0.6 to about 1.0 mm. The plaque is characterized by high porosities of 80 to 90 percent and high surface areas of about 0.5 m^2/g. These sintered plaques are filled with nickel nitrate using vacuum impregnation techniques. The absorbed material may then be precipitated within the pores of the sinter by electrochemical, thermal, or chemical means. The cadmium negative material at this point may be cadmium, cadmium hydroxide, or cadmium oxide, dependent upon the previous precipitation steps. Several impregnation cycles may be necessary to introduce the required amount of active cadmium material into the sintered plaque. A typical impregnation process will give 0.5 Ah/cm^3 capacity at the five hour discharge rate. These electrodes are then cycled in a KOH electrolyte to remove such impurities as nitrates, carbonates, and organic materials. At this time, the cadmium compounds are also reduced to produce the cadmium active material.

The above process produces cadmium electrodes with excess negative capacity and up to 20 percent of uncharged $Cd(OH)_2$. During cell charging, oxygen is evolved at the nickel electrode before the cadmium electrode can become fully charged. Negative cadmium electrodes with excess amounts of uncharged $Cd(OH)_2$ eliminate hydrogen evolution during normal overcharge conditions. The presence of both hydrogen and oxygen within a sealed cell would constitute a serious safety hazard. The oxygen will be evolved at the nickel electrode before the negative electrode can be reduced:

$$4\ OH^{1-} \longrightarrow O_2 + 2\ H_2O + 4e^{1-} \tag{5}$$

and

$$Cd(OH)_2 + 2e^{1-} \longrightarrow Cd + 2\ OH^{1-} \tag{6}$$

Since there exists both a limited amount of electrolyte in the cell and a suitably permeable separator assembly, the oxygen will be transferred to the cadmium electrode and will react with the cadmium metal:

$$2\ Cd + O_2 + 2H_2O \longrightarrow 2\ Cd(OH)_2 \tag{7}$$

This oxygen cycle results in the consumption of oxygen at the negative electrode with no net chemical compositional changes. The continuous charge rates for sealed cells are limited by the overcharge recombination capability of the cells. Should the recombination capability be exceeded by charging at particularly high rates, activation of a high pressure vent will occur. The recommended charging rate is 0.1 C for 14 hours. However, some specially designed cells can accept overcharge rates as high as 0.3C.[19] Nickel positive plates are fabricated by the impregnation of porous sintered nickel plaques with

a mixture of $Ni(NO_3)_2$, graphite, and $Co(NO_3)_2$. The inclusion of about ten weight percent $Co(NO_3)_2$ in the mixture results in improved capacity maintenance during cycling. During the impregnation process, cadmium hydroxide is added to the electroactive material to inhibit the generation of hydrogen at the nickel positive electrode during cell voltage reversal (overdischarge). The so-called antipolar mass (APM) of $Cd(OH)_2$ participates in an oxygen cycle during voltage reversal conditions caused by either mismatched cells or the use of multiple voltage taps in a series strings of cells. During cell voltage reversal conditions, oxygen is produced at the cadmium electrode:

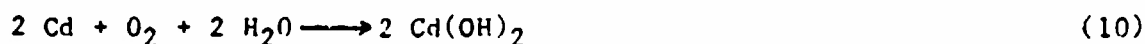$$4 \ OH^{1-} \longrightarrow O_2 + 2 \ H_2O + 4e^{1-} \tag{8}$$
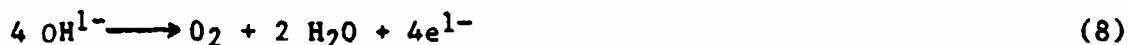
The oxygen then diffuses to the nickel electrode where some of the APM has been reduced to Cd during these reversal conditions:

$$Cd(OH)_2 + 2e^{1-} \longrightarrow Cd + 2 \ OH^{1-} \tag{9}$$

The oxygen will react with the cadmium of the nickel electrode and preclude hydrogen evolution:

$$2 \ Cd + O_2 + 2 \ H_2O \longrightarrow 2 \ Cd(OH)_2 \tag{10}$$

Several studies have been conducted to determine the charge/discharge mechanism of the nickel (III) oxyhydroxide electrode.[20-24] These reactions may be simply represented by the equation:

$$NiOOH + H_2O + e^{1-} \xrightarrow[\text{charge}]{\text{discharge}} Ni(OH)_2 + OH^{1-} \tag{11}$$
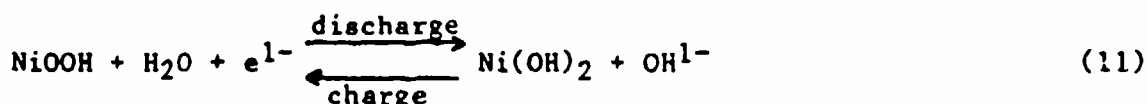
However, the above reaction does not proceed as simply as that given in equation 11 because of phenomena associated with the various phases of both charged and discharged nickel compounds, as well as the fact that the transformations do not involve exact trivalent or divalent nickel species.[4] The oxidized nickel oxyhydroxide absorbs KOH which is at least partially desorbed during discharge. In addition, both charged and discharged nickel compounds contain trapped water. For example, a possible reaction mechanism for positive electrodes containing graphite proceeds in accordance with:

$$2 \ NiOOH \cdot 0.067 \ KOH_{ads} + 0.84 \ H_2O + 2e^{1-}$$

$$\xrightarrow[\text{charge}]{\text{discharge}} 2 \ Ni(OH)_2 + 2 \ OH^{1-} + 0.067 \ KOH \tag{12}$$
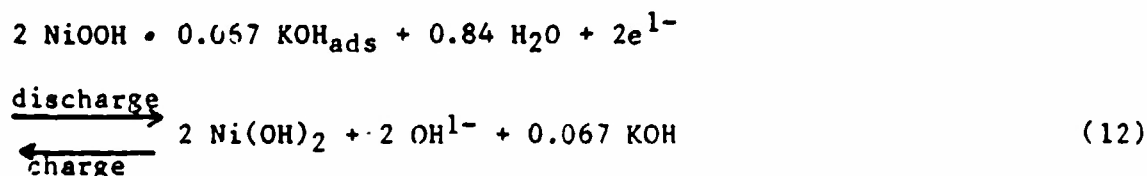
The electrolyte for sealed, sintered nickel-cadmium cells is 5.5 to 7.2 M KOH. The oxygen recombination rate decreases in cells with higher concentrations of KOH due to the decreased solubility of oxygen.[25] The addition of 18 g of LiOH per liter of the electrolyte maintains cell voltage levels in continuous cycling regimen but does not result either in increased capacities during high rate discharge or in any beneficial effects relative to charging voltage levels.

In addition to the usual requirements of low electrolyte resistance, mechanical and chemical stability over a wide temperature range, and porosity characteristics necessary to inhibit penetration by active materials, the separator for the sealed nickel-cadmium cell must also be of sufficient porosity to permit the free diffusion of oxygen to the negative electrode during overcharge. Since these cells contain only the minimal amount of electrolyte necessary for useful function, the separator must possess excellent absorbent and retention properties. In view of the above, the common separators for sealed cells are multilayers of non-woven polyamide, nylon, polypropylene or polyethylene materials (high temperature operation).

Most sealed nickel-cadmium cells are provided with a high pressure vent to relieve excessive gas pressure generated during abusive conditions (e.g., sustained overcharge or overdischarge at high rates). A resealing safety vent valve is preferred over the vent which remains open after the release of pressure. A typical resealing valve will open at a maximum internal cell pressure of about 142 psi (980 kPa). Following the pressure release, the valve would reseal the cell. Little effect on the subsequent performance characteristics would be observed. However, repeated ventings will have deleterious effects on cell life due to the drying of cell contents. The case material for sealed nickel-cadmium cells is nickel plated stainless steel. Though most cells are of the crimp seal design, some specialty cells are hermetically sealed. The glass to metal seals in these cells are resistant to the KOH electrolyte and can withstand internal pressures of up to 280 psi (1960 kPa).[10]

The open circuit voltage and theoretical energy densities for the nickel-cadmium system are 1.35 V and 218 Wh/kg.[26] Sealed cylindrical cells discharged at rates of 0.2 C,C, and 5C at 25°C yield realized capacities of 110, 100, and 75 percent of the cell nominal capacity value to a 0.9 V discharge voltage cutoff level. Typical energy density values for sealed cylindrical cells and batteries are 30 and 25 Wh/kg, respectively.[11] The corresponding values for rectangular and button cell designs are 25 and 20 Wh/kg, and 20 and 15 Wh/kg, respectively.

Sealed nickel-cadmium cells and batteries are typically charged under constant current conditions at either the 0.1C rate for 14 hours or the 0.2 C rate for 7 hours. Some specially designed cells may be charged at higher rates (e.g, 0.3C or higher). Excessive internal pressure will develop if the recombination capability of the cell is exceeded. Constant potential charging is not recommended for the sealed nickel-cadmium cell, particularly if current limiting is not provided. Charging under these conditions could lead to thermal runaway in overcharge. The recombination reaction generates significant amounts of heat during the overcharge period[27] and the cell temperature will rise if the generated heat is not transferred or radiated at the same rate as it is produced. The internal impedance will then decrease under these constant potential charging conditions.[27] The charge current will, therefore, also increase. The increased current will result in a further increase in the internal temperature which, in turn, continues to lower the impedance. Dependent upon the charger capacity, the above cycle would continue until the negative plate is fully charged. At this point, hydrogen would be generated. Since oxygen is not recombined under these conditions, excessive internal pressures will be produced.

170

Sealed nickel-cadmium cells and batteries were subjected to the electrical abuse tests of forced overdischarge, overcharge, and short circuit. Cell voltage reversal tests were conducted using aerospace nickel-cadmium batteries in the effort to determine whether the useful life could be extended by deep discharge reconditioning. Such reconditioning would result in some cell voltage reversals and the production of hydrogen at the positive electrode. The cells were discharged under constant current conditions at the C/100 to C/300 rates.[33,34,36] The results for these tests indicated that internal short circuits were formed which limited the hydrogen pressure buildup in the cell. These internal shorts were found to be reversible with subsequent charging of the cells. The rate of hydrogen recombination under subsequent open circuit conditions was monitored to determine the safe waiting period before cell charging (with production of O_2 in overcharge) could commence. No internal shorting was observed for cells overdischarged at the C/5 rate. No hazardous events were reported for these tests.

Spirally wound D nickel-cadmium cells were forced overdischarged under constant current conditions at the C/10 (0.4A) rate at 20°C and 50°C.[37] The duration of the reversal period was ten hours. The results showed a 10°C temperature rise and a stable reverse voltage of 1.5 V. None of these cells exhibited signs of excessive pressures.

Overcharge testing of a nickel-cadmium space-qualified battery pack at the C/3 rate showed that a massive internal short circuit could be created.[38] The localized hot spot penetrated through several plates in each direction. It should be noted that no hazardous condition was reported for this test.

A fully charged 22 cell battery was trickle charged at 0.5A in a vacuum chamber at 10^{-5} mm for an extended period.[39] The initial temperature of the battery was 1°C. During the test, the battery temperature was supposed to be maintained at 22°C through use of either a heater or cooler. It was later found that the battery was isolated from both the heater and cooler. As a result, several cells experienced an explosion and all the cells were unsealed. Subsequent analysis of the test showed that the battery had reached temperatures between 216°C and 230°C. It was determined that the battery could not reach the elevated temperatures solely through the heating due to trickle charge conditions. It is believed that, since the self-discharge characteristics for the nickel-cadmium cell increase considerably at elevated temperatures, the energy from the self-discharge resulted in a further temperature increase until a catastrophic runaway condition occurred.

Spirally wound D cells were short circuited through a 0.015 ohm load at 20°C and 55°C.[37] Average peak currents of 55 and 35 A were observed at 20°C and 55°C, respectively. Cell wall temperatures reached 90°C for the first set of cells at the lower initial temperature and 105°C for the cells tested at 55°C. All cells remained unchanged in appearance.

The spirally wound D cells were also mechanically abused by crushing to one half the original diameter and by cutting the cells in half.[37] No external effects were observed. Cell wall temperatures, however, did increase 30 to 50°C caused by massive internal short circuiting. Fresh and discharged cells were also punctured by 0.6 cm cubes fired at 200 m/sec. All nickel-cadmium cells were short circuited but "there were few spectacular or lasting effects."[37]

Additional characteristics of sealed nickel-cadmium cells are summarized below:

1. Constant current charging is normally performed at temperatures of 5°C to 45°C. The oxygen recombination rate at lower temperatures is decreased markedly and excessive gas pressures would develop. Charge acceptance at elevated temperatures is poor.[11]

2. Cells may be charged at higher rates ("fast charge") using pressure and temperature sensing devices. Charging would be terminated at preset values for temperature and/or pressure.

3. The charge retention characteristics for sintered, sealed cells are poorer than those for vented cells. Cells stored for one month at 25°C and 6 months at -20°C will yield 65 and 80 percent of the nominal capacity. Less than ten percent capacity would be obtained for cells stored for six months at 25°C or one month at 50°C. The self-discharge rate is greatly increased at temperatures above 30°C. At storage temperatures of less than 0°C, the self-discharge rate is low.

4. The cycle life for sealed nickel-cadmium cells is about 500 to 1000 cycles to 60 to 80 percent of the nominal capacity at a 50 percent depth of discharge.

The sealed nickel-cadmium cell has found use in several aerospace, commercial, and consumer applications. The success of this system can be attributed in part to the long life characteristics. After a period of time, however, these cells will fail. Several studies[28-32] have been conducted to determine the failure mechanisms for sealed nickel-cadmium cells. Some of these mechanisms are summarized below:

1. Impurities such as carbonate and nitrate ions promote corrosion of the sintered nickel plaque.

2. The nickel electrode will physically expand as a function of the number of cycles and depth of discharge. The nickel electrode will then experience loss of active material ("shedding").

3. The reduction of the $Cd(OH)_2$ APM material during voltage reversal can lead to the growth of cadmium dendrites and eventual internal short circuits. During subsequent charging, the dendrites are oxidized. No long term effects on cell performance is observed after the dendrites are oxidized.

4. Cadmium will migrate from the interior of the negative electrode, through the separator, and to the nickel electrode. Internal short circuiting could then occur.

5. Some of the electrolyte will leave the separator during cycling and enter the electrode matrices. This condition increases cell resistance, accelerates cadmium migration, and decreases electrode utilization.

Thermal abuse testing of nickel-cadmium D cells was conducted by positioning an oxypropane flame to produce a cherry red area of about 1 cm diameter on the cell wall for a period of ten minutes or until all thermal events had been completed. One nickel-cadmium cell vented through its seal at the one minute mark of the test. The other two cells experienced case bulging with subsequent rupture and generation of steam.[37] Incineration testing of nickel-cadmium cells in accordance with NAVSEAINST 9310.1A procedures would, at the minimum, cause rapid expulsion of hot electrolyte. Cell rupture may also occur. It should be noted that rapid oxidation of cell contents would generate toxic materials.

REFERENCES

1. Milner, P. C., and Thomas, U. B., Advances in Electrochemistry and Electrochemical Engineering, Volume 5, C.W. Tobias and P. Delehey, eds. (New York: Interscience, 1967), p. 2.

2. Bergstrom, S., J. Electrochem. Soc., 99, 1952, p. 248C.

3. Atkinson, G. S., Electrochem. Technol., 4, 1966, p. 431.

4. Salkind, A. J., Farrell, D. T., Jr., and Hedges, A. J., J. Electrochem. Soc., 125, 1978, p. 314C.

5. Von Sturm, F., Comprehensive Treatise of Electrochemistry, Volume 3, Electrochemical Energy Conversion and Storage, Bockris, J. O'M., Conway, B. E., Yeager, E., and White, R. E., eds. (New York: Plenum Press, 1981), p. 393.

6. Nickel-Cadmium Battery, Application Engineering Handbook, J.C. Grant, ed., General Electric Company, No. GET-3148A, Gainesville, FL., 1975.

7. Eveready Battery Engineering Data, Nickel-Cadmium, Volume IV, Union Carbide Corporation, Danbury, CT., 1983.

8. Crompton, T. R., Small Batteries, Volume 1, Secondary Cells (New York: John Wiley and Sons, 1983).

9. Mantell, C. L., Batteries and Energy Systems, Second Edition (New York: McGraw Hill, 1983), p. 195.

10. Falk, S. U., and Salkind, A. L., Alkaline Storage Batteries (New York: John Wiley and Sons, 1969).

11. Falk, U., Electrochemical Power Sources, Primary and Secondary Batteries, IEE Energy Series I, M. Barak, ed. (London: Peter Peregrinus Ltd., Chapter 5, 1980).

12. Halpert, G., Electrolyte Concentration Changes During Operation of the Nickel-Cadmium Cell, NASA TMX-70977, 1975.

13. Halpert, G., and Webster, W. H., Jr., Secondary Aerospace Batteries and Battery Materials, A Bibliography, 1923-1968, NASA SP-7027, 1969.

14. Halpert, G., Nickel-Cadmium Battery Test Project - Relationship Between Operation, Life and Failure Mechanism, Volume III, Analysis of the Cells and Components, NASA TM X63550, 1969.

15. Scott, W. R., and Rusta, D. W., Sealed Cell Nickel-Cadmium Battery, Applications Manual, NASA Reference Publication 1062, 1979.

16. McCullum, J., Thomas, R. F., and Waite, J. H., Accelerated Testing of Space Batteries, NASA SP-323, 1973.

17. Yoshizawa, S., and Takehara, Z., Electrochim. Acta, 5, 1961, p. 240.

18. Will, F. G., and Hess, H. J., J. Electrochem. Soc., 120, 1973, p. 1.

19. Crompton, T. R., Small Batteries, Volume 1, Secondary Cells (New York: John Wiley and Sons, Chapter 2, 1982).

20. Bourgault, P. L., and Conway, B. E., Can. J. Chem., 38, 1960, p. 1557.

21. Conway, B. E., and Bourgault, P. L., Can. J. Chem., 37, 1959, p. 292.

22. Casey, E. J., Dubois, A. R., Lake, P. E., and Moroz, W. J., J. Electrochem. Soc., 112, 1965, p. 371.

23. Barnard, R., Randell, C. F., and Tye, F. L., J. Applied Electrochem., 10, 1980, p. 127.

24. Barnard, R., Randell, C. F., and Tye, . L., J. Applied Electrochem., 10, 1980, p. 109.

25. Reference 10, p. 611.

26. McBreen, J., "Comprehensive Treatise of Electrochemistry," Volume 3, Electrochemical Energy Conversion and Storage, Bockris, J. O'M., Conway, B. E., Yeager, E., and White, R. E., eds. (New York: Plenum Press, 1981), p. 308.

27. Salkind, A. J., and Duddy, J. C., J. Electrochem. Soc., 109, 1962, p. 360.

28. Gross, S., Energy Conversion, 11, 1971, p. 39.

29. Gross, S., Proc. of the 16th IECEC, American Society of Mechanical Engineers, 1981, p. 177.

30. McDermott, P. P., Proc. Power Sources Symp. 28, 1979, p. 109.

31. Zimmerman, A. H., and Effa, P. K., Short Circuit Formation During NiCd Cell Reversal, NTIS AD-A117912, U.S. Dept. Commerce, Springfield, VA, 1982.

32. Bauer, P., and Lurie, C., DSCS II Battery Anomaly Investigation Satellites 9437 and 9438, Final Report, NTIS AD-A087390, U.S. Dept. Commerce, Springfield, VA, 1980.

33. Hwang, W. C., Poston, T. M., and Badcock, C. C., Proc. of the 16th IECEC, American Society of Mechanical Engineers, 1981, p. 187.

REFERENCES (Cont.)

34. Hwang, W., The 1981 Goddard Space Flight Center Battery Workshop, NASA Conference Publication 2217, 1982, p. 271.

35. Badcock, C., The 1980 Goddard Space Flight Center Battery Workshop, NASA Conference Publication 2177, 1981, p. 355.

36. Ritterman, P., The 1980 Goddard Space Flight Center Battery Workshop, NASA Conference Publication 2177, 1981, p. 343.

37. Attewell, A., Power Sources 9, Proc. 13th Int. Symp. Power Sources, Joint Services Electrical Power Source Committee, J. Thompson, ed. (London: Academic Press, 1981), p. 473.

38. Scott, W., The 1980 Goddard Space Flight Center Battery Workshop, NASA Conference Publication 2177, 1981, p. 229.

39. Sense, K., The 1980 Goddard Space Flight Center Battery Workshop, NASA Conference Publication 2217, 1982, p. 189.

D. CADMIUM – SILVER CHLORIDE

$$Cd \mid CdCl_2 , NaClO_4 , ZnCl_2 \mid AgCl$$

$$Cd + 2AgCl \rightleftharpoons CdCl_2 + 2Ag \qquad [1]$$

The cadmium-silver chloride secondary battery was investigated by Bro and Marincic[1] at P. R. Mallory and Company (Duracell International). The primary objective of the work was the development of a power source which could be charged at rates of 30 C to 90 C, where C is the one hour rate. In addition to the primary objective, a second condition for the sealed system required that no gas be evolved during the high charging rates. It was found that negative electrodes resulting from the deposition from concentrated salt solutions of the negative electrode material produced electrodes of higher rate capabilities than those electrodes formed by charging cells containing the solid reaction products of the negative electrode. Preliminary efforts involved the investigation of the zinc-silver chloride system (refer: Chapter 2, Zn/AgCl) as a possible candidate for a secondary power source. The choice of the electrodes was based upon the high rate charging characteristics of both the zinc and silver chloride electrodes. The zinc-silver chloride system was found to possess high self-discharge characteristics on storage. Though the self-discharge rate could be reduced by decreasing the zinc chloride electrolyte concentration, it was subsequently found that zinc corroded in the acidic zinc chloride electrolyte in cells. The hydrogen gas bubbles resulted in non-uniform current distribution. When zinc-silver chloride cells were charged, these non-uniform current distributions led to dendritic formation with subsequent internal short circuiting of cells on charging.

In view of the above deficiencies for the zinc-silver chloride system, Bro and Marincic then sought to develop the cadmium-silver chloride system. Cadmium possesses several desirable characteristics necessary for use in a secondary battery system. These include high charging rate capability, a low reversible potential, and a high hydrogen overvoltage. Cells containing cadmium chloride as the electrolyte were found to yield varied discharge efficiencies, however. It was found that the cadmium chloride altered the structure of the silver chloride positive electrode material to a powder which lost contact with the supporting current collector. The rate of production of powdered silver chloride was reduced by limiting the cadmium chloride concentration to less than 0.1 M. However, with such low concentrations of cadmium-chloride, the system could not be charged at the desired high rates.

The solution to the above dilemma involved the adaptation of a dual charging process for the system. By judicious choice of the $ZnCl_2$ concentration to yield the desired high charging rates and a concentration of $CdCl_2$ which would result in a concentration of 0.1 M after the charging period, the following charging scheme proceeded by:

$$ZnCl_2 + 2e^{1-} \longrightarrow Zn + 2\ Cl^{1-} \tag{2}$$

and

$$2\ Ag + 2\ Cl^{1-} \longrightarrow 2\ AgCl + 2e^{1-} \tag{3}$$

$$Zn + CdCl_2 \longrightarrow Cd + ZnCl_2 \tag{4}$$

Reactions (2) and (3) show the results of electrical charging of the system. Following the cessation of the charging period, an electrochemical exchange reaction (4) occurs which led to the formation of the cadmium negative electrode. The charging process, reactions (2) and (3), could be completed within a brief period of time (for example, at the 40C rate, cells were fully charged after 90 seconds). The electrochemical exchange reaction (4), on the other hand, proceeded much more slowly, typically lasting for 40 to 60 minutes. Discharge of the cell immediately following the electrical charging process resulted in higher cell load voltages than those observed for the pure cadmium electrode.

Cells which were fabricated using parallel plate designs having equal negative and positive electrode surface areas and interelectrode spacings of 0.4 cm failed due to zinc dendrite formation after a few cycles. Efforts then were directed toward a cell design using negative electrodes of twice the surface area in order to eliminate or limit the interelectrode short circuits. These cells also failed due to dendrite formation after a few charge-discharge cycles.

A cylindrical cell design using a centrally located silver rod as the positive electrode current collector and an outer cadmium cylinder as the negative electrode current collector proved to be an adequate solution to the problems noted for the parallel plate design. This cell design also possessed two special features necessary for the successful operation of the system. The first was the inclusion of shaped end baffles to reduce the edge effects occurring during charging of the negative electrode. The second consisted of an absorber used to decrease the intensity of electrolyte convective flows during charging. These convective flows resulted in non-uniform current densities at the electrodes and premature failure of the cell.

The electrolyte for the above cell system consisted of 2.0 M $ZnCl_2$, 1.5 M $NaClO_4$ and that amount of $CdCl_2$ (0.365 M) necessary to yield a concentration of 0.1 M $CdCl_2$ or less at the end of the dual charging process. The inclusion of $NaClO_4$ was found to be required to increase the conductivity of the electrolyte solution.

The observed open circuit voltage immediately after charging was 1.05 V, the expected cell potential for the zinc-silver chloride system. However, the open circuit potential decreased to that for the Cd/AgCl couple (0.75 V) after approximately 40 to 60 minutes following charging. The charge-discharge performance characteristics were determined for the cadmium-silver chloride system at 25°C. Cells were charged under constant current conditions of 2A (40

C rate) to 4A (80 C rate) to a final nominal capacity of 50 mAh. For example, cells charged at the 40 C rate exhibited constant voltage levels of about 2 V for the first 60 seconds of charge. The voltage levels then increased to approximately 5 V during the final 30 seconds of charge. Bro and Marincic postulated that the abrupt increase in charging voltage was the result of increased resistances of the AgCl positive electrode film and the diffusion layer at that electrode which had become depleted in charge carriers.[1]

Cells having nominal capacities of 50 mAh were discharged at the 2C rate (100 mA). The results show a load voltage plateau of about 0.75 V for the first three minutes of discharge followed by a long load voltage plateau at 0.6 V for the remainder of the nearly 30 minute discharge period. The cell was discharged to a load voltage level of about zero volts and subsequently charged. The average percent charge recovery for cells charged at the lower rate of 40C (2.0A) was 97 percent over ten cycles while that observed for cells charged at the higher rate of 80C (4.0A) was about 94 percent.

The storability characteristics were measured by charging cells and allowing them to remain at open circuit at 25°C for various periods of time prior to discharge. The results showed an initial self-discharge rate of 0.5 mAh per day for the first 30 days of storage. It was further found that the initial rate decreased significantly for storage periods longer than thirty days. For example, approximately 60 percent of the initial capacity remained after 90 days storage. The observed high initial self-discharge rate was believed to be the result of the interaction of the $CdCl_2$ remaining after the dual charging process with the silver chloride positive electrode material, producing powdered silver chloride which lost contact with the silver current collector. The projected shelf life characteristics for uncharged cells was predicted to be of long term, particularly if the current collector for the negative electrode was replaced by a silver substrate.

The ultimate goal for the system was the development of a sealed system which could be charged at exceptionally high rates. In view of the fact that the zinc electrode resulting from the electrical charging remains active for about one hour before electrochemical exchange with cadmium is completed, measurement of the hydrogen evolution for this cell showed that approximately $10^{-4} cm^3$ per hour of hydrogen was accumulated. It was concluded that a significant amount of hydrogen would not be evolved unless the cell was subjected to extended cycling. In addition, because zinc metal is being oxidized for a one hour period after charging (equation 4), the evolution of hydrogen would be further reduced. Therefore, it was concluded that this system did not need vent structures.

Since the cells described herein possessed non-porous electrodes, the cells could only be charged to low capacity values. As a result, the energy densities for the 50 mAh cells were found to be about 2.0 Wh/kg. It should be noted, however, that these cells were charged at especially high rates with no gas evolution. Similar charging of conventional secondary systems would undoubtedly result in excessive gas evolution and, perhaps, the precipitous decrease of energy densities to values comparable to the Cd/AgCl system.

No safety data was given for the cadmium-silver chloride system which detailed results for sealed cells subjected to either the electrical abuse tests or the incineration test given in NAVSEAINST 9310.1A. Extended charging,

particularly at the rates cited, could lead to excessive gas evolution due to the electrolysis of water with a resultant cell case rupture. Similar results could be obtained should the cell be forced overdischarged by a constant current supply for extended periods or by a series string of cells. Incineration of sealed cells with no vent structures could also result in cell case rupture, the extent of which would be dependent upon the mechanical strength of the welds, etc. The discharge characteristics for 50 mAh cells of the cadmium-silver chloride system showed that 2 C rates yielded approximate capacities of 48 to 50 mAh at load voltages of 0.6 V. In addition, Bro and Marincic further showed that the discharge overvoltage for these cells discharged at currents of 20 to 100 mA varied linearly and that the impedance was about 1.5 ohms. It would be expected, therefore, that the cell would rapidly polarize when subjected to short circuit conditions. This would probably not result in a hazardous situation.
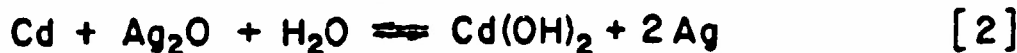
Cells or batteries of the cadmium-silver chloride system have not been produced commercially. Therefore, no future testing in accordance with procedures of NAVSEAINST 9310.1A is presently anticipated. However, should the system become of importance to the Navy, testing in accordance with modified procedures of NAVSEAINST 9310.1A would be warranted.

REFERENCES

1. Bro, P., and Marincic, N., J. Electrochem. Soc., 117, 1970, p. 131.

E. CADMIUM-SILVER OXIDE

$$Cd \mid KOH \mid Ag_2O_2 , Ag_2O$$

$$2\ Cd + Ag_2O_2 + 2\ H_2O \rightleftharpoons 2\ Cd(OH)_2 + 2\ Ag \qquad [1]$$

$$Cd + Ag_2O + H_2O \rightleftharpoons Cd(OH)_2 + 2\ Ag \qquad [2]$$

Secondary cadmium-silver oxide (silver-cadmium) batteries were first produced by Jungner for electric vehicle propulsion applications in 1900. It was not until after the late 1950's, however, that the system found limited use in such applications as portable appliances, satellites, and recoverable antisubmarine warfare target vessels. This system combines the cycle life characteristics of the nickel-cadmium battery with energy density values closely approaching those for the silver-zinc battery. The silver-cadmium system also exhibits high charge retention, resistance to mechanical stress, and nonmagnetic properties.[1-4] The silver-cadmium system does not, however, exhibit the high rate discharge characteristics of either the nickel-cadmium or the silver-zinc systems. The most important disadvantage of the silver-cadmium battery is the high cost of both the silver and cadmium electrode materials. It is this fact which limits the widespread use of these in military, space, and commercial applications.

Vented and sealed silver-cadmium cell designs are currently manufactured in the United States. Vented cells are provided with a venting device in the lid which opens at low internal pressures of 2 psig to 10 psig (14 kPa to 70 kPa) above atmospheric pressure. The venting device allows for the escape of gases formed during charging and accessibility for filling cells with electrolyte. The vent prevents the escape of the electrolyte and the loss of water due to evaporation. Since carbon dioxide is detrimental to the performance characteristics of cells, the vent must also minimize the admission of air into the cell. Though this vent mechanism is not a safety feature per se, it does allow the escape of gases and/or electrolyte in cells which have been subjected to the electrical abuses of overdischarge and overcharge. Both hydrogen and oxygen are vented under these conditions. The possibility of a fire or explosion would exist if proper ventilation is not provided. Excessive overdischarge and overcharge of the vented silver-cadmium cells would lead to the drying out of the cells and subsequent failure. Cells subjected to short circuit conditions expel hot, caustic KOH electrolyte. Incineration of vented

183

silver-cadmium cells not only would result in the expulsion of the KOH electrolyte but also would release toxic materials caused by the rapid oxidation of the cell contents.

Though the remainder of the discussion for the silver-cadmium system will focus on the characteristics of sealed silver-cadmium cells, the performance, storability, and charging properties of vented cells may be summarized below:[5]

1. The major U.S. manufacturers of vented silver-cadmium cells and batteries are Eagle-Picher and Yardney Electric Corp. Cells are available in nominal capacities of 0.1 Ah to 300 Ah.

2. The open circuit voltage is 1.40 to 1.42 V. Energy densities of 48 to 75 Wh/kg are obtained for these cells depending upon temperature, discharge rate, and charging conditions.

3. Cycle life is dependent upon the depth of discharge. For example, 200 to 300 cycles would be obtained for cells deep discharged to depths of 75 to 95 percent and over 600 cycles would be obtained for cells shallow discharged to depths of 25 to 50 percent.

4. The wet shelf and dry storage life are 3 years and about 5 years, respectively.

5. The optimum operating temperature range is -21°C to +50°C. Operation at lower temperatures is possible through use of heating devices.

6. The wet storage temperature range is -47°C to 73°C and the dry storage temperature range is -60°C to +73°C.

7. The suggested charge duration is 10 h to 20 h under either constant current or constant potential charging conditions. The charging process is completed when a sharp voltage increase at 1.6 V is observed. A charge retention of over 80 percent of the nominal capacity is obtained after three months storage at ambient temperature.

8. Optimum performance characteristics for vented cells are achieved when cells are situated in the upright position.

Sealed silver-cadmium cells are produced in flat plate, cylindrical, pile, and button cell designs.[1] The cadmium negative electrode can be fabricated using several methods:

1. Pasting cadmium oxide, cadmium powder or cadmium hydroxide onto a silver or nickel grid.

2. Electrodeposition of the cadmium metal onto a nickel expanded metal screen.

3. A porous plaque is prepared by sintering powdered nickel onto an expanded metal screen. The plaque is then impregnated in a solution of $Cd(NO_3)_2$. After removal from the solution, the $Cd(NO_3)_2$ is converted to $Cd(OH)_2$ by thermal, chemical, or electrolytic decomposition.

During the cell charging process, oxygen is evolved at the silver electrode and hydrogen is evolved at the cadmium electrode. The presence of both gases would constitute a serious problem in sealed silver-cadmium cells. Though the gases may be recombined using a catalytic device, negative electrodes with an excess amount of uncharged $Cd(OH)_2$ may be used to avoid hydrogen evolution during overcharge. Oxygen will be evolved at the silver electrode before all the negative electrode material can be reduced:

$$4\ OH^{1-} \longrightarrow O_2 + 2\ H_2O + 4e^{1-} \tag{3}$$
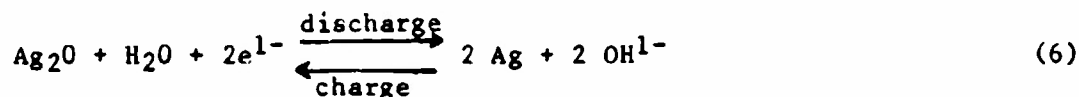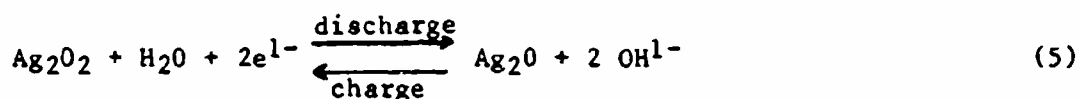
If there exist both a limited amount of KOH electrolyte in the cell and a suitable porous separator assembly, the oxygen will be transferred to the cadmium electrode where it will react with the excess cadmium metal:

$$2\ Cd + O_2 + H_2O \longrightarrow 2\ Cd(OH)_2 \tag{4}$$

The net effect is the consumption of oxygen at the negative electrode with no chemical compositional changes within the cell. It should be emphasized, however, that overcharging silver-cadmium cells should not be continued at rates higher than about C/200 since most semipermeable membranes (e.g., cellulose or cellophane) used to restrict silver migration from the positive electrode do not allow the efficient transport of oxygen to the negative electrode during overcharge.

Silver oxide positive plates may be fabricated by impregnation of a porous sintered nickel plaque with silver compounds followed by electrolytic or thermal decomposition, sintering silver powder onto an expanded silver or nickel metal screen, or by pasting silver oxides onto expanded metal grids followed by sintering.[1] The reactions at the silver electrode are given by:

$$Ag_2O_2 + H_2O + 2e^{1-} \underset{charge}{\overset{discharge}{\rightleftarrows}} Ag_2O + 2\ OH^{1-} \tag{5}$$

$$Ag_2O + H_2O + 2e^{1-} \underset{charge}{\overset{discharge}{\rightleftarrows}} 2\ Ag + 2\ OH^{1-} \tag{6}$$

Both hydrogen and oxygen are generated at the silver and cadmium electrodes, respectively, during cell voltage reversal (overdischarge). The generation of hydrogen at the silver electrode can be eliminated by including an antipolar mass of $Cd(OH)_2$ in the silver electrode material. Thus, during cell voltage reversal, oxygen is produced at the cadmium electrode:

$$4\ OH^{1-} \longrightarrow O_2 + 2\ H_2O + 4e^{1-} \tag{7}$$

Meanwhile, the antipolar mass of $Cd(OH)_2$ at the silver electrode is reduced to cadmium metal, thereby precluding the evolution of hydrogen:

NSWC TR 84-302

$$Cd(OH)_2 + 2e^{1-} \longrightarrow Cd + 2\ OH^{1-} \tag{8}$$

The oxygen then establishes an oxygen cycle with the cadmium metal of the silver electrode before any hydrogen can be evolved at the silver electrode:

$$2\ Cd + O_2 + 2\ H_2O \longrightarrow 2\ Cd(OH)_2 \tag{9}$$
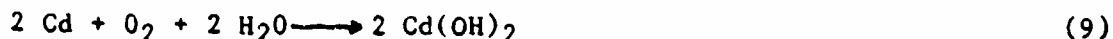
Sealed silver-cadmium cells containing the charge reserve of $Cd(OH)_2$ in the cadmium electrode[6] and the antipolar mass in the silver electrode have been described in the literature.[6,7] It is not known whether these gas recombination mechanisms are still in use with sealed silver-cadmium cells produced at the present time.

The electrolyte for the silver-cadmium sealed cell is about 10 M KOH.[1] Sealed cells normally contain only that amount of electrolyte necessary to be absorbed by the separator and electrodes. This electrolyte condition allows the free diffusion of oxygen gas to the cadmium electrode during overcharge. It should be noted that more electrolyte can be added to those sealed cells used for special applications in which the charging is closely controlled. The additional amount of electrolyte results in more complete utilization of the active materials. The high concentration of the electrolyte is necessary for two reasons: silver migration from the positive was found to be at a minimum at these concentration levels and the cellophane separator is not readily oxidized in 10 M KOH solutions but is rapidly oxidized in solutions of lower concentrations.

The separator assembly consists of absorbent materials such as cellulose or felted nylon which are placed next to the electrodes to ensure proper wetting and a number of layers of such film separator materials as cellophane, ion exchange membranes, and Visking. The latter separators are employed to minimize the migration of silver species to the negative electrode.

Most sealed silver-cadmium cells are provided with a high pressure vent to relieve excessive gas pressures generated during abusive conditions (e.g., overcharge at very high rates or sustained overdischarge). A resealing safety vent valve is preferred over the vent which remains open after the release of pressure. One example of a resealing valve will open at a maximum internal cell pressure of about 142 psi (980 kPa). Following the release of pressure, the valve would reseal the cell with little effect on the performance characteristics of the cell. The case materials for the silver-cadmium cells can be either plastic materials with epoxy resin potting or stainless steel cans. The glass to metal seals used in the cell are resistant to KOH and can withstand internal cell pressures of up to 280 psi (1960 kPa).[1]

The open circuit voltages for the silver-cadmium cell are 1.41 V and 1.15 V, respectively, for the reactions given in equations 1 and 2. Sealed cells containing highly porous sintered silver electrodes were discharged at various rates to a 0.60 V voltage cutoff level at room temperature. The nominal capacity for these cells was about 7.5 Ah. Realized capacities of 6.5, 7.5 and more than 8 Ah were obtained for discharge rates of 2C (15A), C (7.5A), and 0.5C (3.8A), respectively. Though the above specially fabricated cells exhibited two load voltage plateaus corresponding to the reduction of Ag_2O_2, the

performance curves for cells discharged at high rates may not exhibit the load voltage plateau corresponding to the reduction of Ag_2O_2. In addition, only the load voltage plateau for the reduction of Ag_2O is observed for cells which have previously been charged at rates of C/50 or lower. The typical energy densities for sealed silver-cadmium cells and batteries are 44 and 35 Wh/kg for discharges at the C rate. Other performance characteristics are summarized below:[1]

1. Sealed silver-cadmium cells may be charged using either constant current or constant potential/modified constant potential methods. Constant current charging is typically achieved at the 0.05C to 0.10C rate until a cell voltage of 1.60 to 1.65 is reached. The voltage limit for modified constant potential charging is 1.60 V. In contrast to several alkaline systems, the silver-cadmium sealed cells may be charged efficiently at low temperatures.

2. The charge retention for sealed cells is about 85 percent after six months storage at room temperature.

3. The cycle life of sealed silver-cadmium cells is significantly better than for vented cells. Over 500 cycles may be obtained for cells/batteries at low depths of discharge. Cycle lives of 4000 to 10,000 are predicted for batteries discharged to 45 to 25 depths of discharge, respectively. A total lifetime of two to three years can be expected for these cells.

4. The most common modes of failure include the deterioration of the separator by dissolved silver species and the increase in internal cell pressures.

5. The sealed silver-cadmium cell is resistant to severe mechanical abuse and environmental conditions.

Sealed silver-cadmium cells are manufactured in the United States by Yardney Electric Corporation, Eagle-Picher Company, and the Electric Storage Battery (ESB) Incorporated.

No data was presented which describe the results of such electrical abuse testing as short circuit, forced overdischarge, or overcharge. Both hydrogen and oxygen may be generated in sealed cells subjected to prolonged overdischarge (cell voltage reversal) and overcharge conditions if the oxygen recombination capability of the cells is exceeded. It has been noted that effective recombination capability is limited to rather low rates under both conditions. Increased internal cell pressures then would develop which, dependent upon the cell vent operational characteristics, could lead to a violent expulsion of gases and hot KOH electrolyte. Should the vent not function properly or if no venting mechanism is present, the pressure increase could lead to a violent case rupture. The escaping hydrogen and oxygen could then react to create a fire or explosion. The use of constant potential charging techniques could also lead to a thermal runaway condition. If a sealed cell experiences a temperature increase during charging, the internal resistance of the cell would decrease and the charge current would increase. This cycle would continue until the onset of thermal runaway. If the oxygen recombination capability is exceeded to the

extent of preventing complete charging of the cadmium electrode, hydrogen would be generated. The cell could then experience cell case rupture or violent venting dependent on the vent characteristics, as previously described.

Incineration of sealed silver-cadmium cells would at least cause the rapid expulsion of hot electrolyte. Under worst conditions (i.e., no venting), the cell case would rupture. Rapid oxidation of the cell contents would also generate toxic materials.

REFERENCES

1. Falk, S. U., and Salkind, A. J., <u>Alkaline Storage Batteries</u> (New York:
    John Wiley and Sons, 1969).

2. Salkind, J., and Pearlman, E., <u>Batteries and Electric Cells, Secondary</u>,
    Encyclopedia Chem. Tech., Third Edition, 1978, p. 629.

3. Falk, U., <u>Electrochemical Power Sources</u>, Primary and Secondary Batteries,
    IEE Energy Series 1, M. Barak, ed. (London: Peter Peregrinus Ltd., 1980),
    p. 380.

4. Salkind, A. J., Farrell, D. T., Jr., and Hedges, A. J., <u>J. Electrochem.
    Soc.</u>, <u>125</u>, 1978, p. 311C.

5. Crompton, T. R., <u>Small Batteries</u>, Volume 1, Secondary Cells (New York:
    John Wiley and Sons, 1982), p. 177.

6. Gale, R. J., "Power Sources 1966," <u>Proc. Fifth Int. Symp.</u>, Joint Services
    Electrical Power Source Committee, Collins, D. H., ed. (London: Pergamon
    Press, 1967), p. 411.

7. Howard, P. L., <u>Electrochem. Technol.</u>, <u>1</u>, 1963, p. 272.

F. HYDROGEN (LaNi$_5$H$_6$) - AIR

$$LaNi_5H_6 | KOH | O_2$$

$$2 LaNi_5H_6 + 3 O_2 \rightleftharpoons 2 LaNi_5 + 6 H_2O \qquad [1]$$

The hydrogen-oxygen electrochemical couple possesses the highest theoretical energy density of approximately 3652 Wh/kg for any battery system known. However, the successful development of a practical hydrogen-oxygen cell system has not been achieved, due principally to the cross leakage of the two gasses.[1] Indeed, practical energy density values of only 44 to 110 Wh/kg have been realized for this secondary system. In addition, low open circuit voltages of approximately 0.9 V have been observed (compared to the theoretical value of 1.229 V). Successful use of the hydrogen electrode has been attained for the hydrogen-nickel (III) oxyhydroxide (nickel-hydrogen) system,[2-6] and, to a lesser extent, the hydrogen-silver oxide (silver-hydrogen) system.[7,8] A critical limitation for both systems relative to more widespread commercialization and usage is the requirement for a pressure vessel for hydrogen containment. The vessel adds significantly to both the cell weight and its volume. In view of the above, recent efforts have shown the practicality for hydrogen storage on the interstitial sites of such metal lattices as LaNi$_5$[9-12] and partially substituted LaNi$_5$.[13] The advantages gained through use of metal hydrides include cell volume/weight reduction and design simplification.
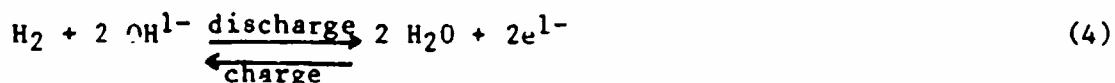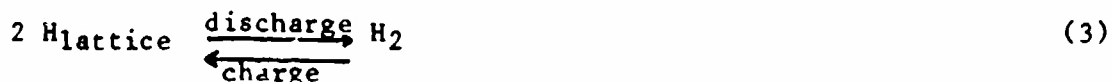
The use of such metal hydrides as negative electrodes has been extended to the hydrogen-oxygen system.[14] In view of the fact that optimized, efficient electrodes have not yet been developed, however, the hydride-oxygen system has not progressed beyond the research and development stages. Nonetheless, preliminary efforts have shown that the system does indeed look promising as a power source for such applications as electric vehicle propulsion.

Analysis of the fully charged hydride electrode showed that up to 6.6 hydrogen atoms were contained per formula unit of the LaNi$_5$ alloy. At equilibrium pressures of less than about 2.5 atm (253 k Pa), however, the hydrogen is desorbed from the hydride lattice according to:

$$2 H_{lattice} \longrightarrow H_2 (g) \qquad (2)$$

The recombination rate of desorbed hydrogen atoms is slow in the 5 N KOH electrolyte but can be increased at elevated temperatures. At temperatures of 60°C, an equilibrium pressure of 9.9 atm (1000 k Pa) is required to prevent the desorption of the hydrogen from the lattice. The realized capacities for unpressurized cells, therefore, are significantly less than those obtained from cells pressurized at or above the equilibrium pressure.[14] In view of the above, research has focussed on the partial substitution of Ni by either Mn or Al in the LaNi$_5$ alloy in order to find a more stable hydride having a significantly lower equilibrium pressure requirement. In addition, the resultant hydride composite must also absorb high amounts of hydrogen. Substitution of aluminum and manganese for nickel in the LaNi$_5$ alloy have resulted in several hydride electrode candidates with equilibrium pressure requirements of less than 1 atm while maintaining high hydrogen absorption. Sarradin et al.[14] reported that such alloys as LaNi$_{4.5}$Mn$_{0.5}$ require equilibrium pressures of about 1 atm (101.3 k Pa). The capacity of the above alloy was found to be about 380 Ah/kg. At elevated temperatures, the realized capacities were also found to be significantly higher for the alloys containing manganese. At 40°C, the capacity for the LaNi$_{4.5}$Mn$_{0.5}$ alloy was about 360 Ah/kg while that for the LaNi$_5$ electrode was less than 40 Ah/kg.

The negative LaNi$_5$ electrode is fabricated by bonding the alloy with Teflon and pressing the mixture onto an expanded nickel screen. The reactions occurring at the negative electrode are given by:

$$2 \text{ H}_{\text{lattice}} \xrightleftharpoons[\text{charge}]{\text{discharge}} \text{H}_2 \tag{3}$$

$$\text{H}_2 + 2 \text{ OH}^{1-} \xrightleftharpoons[\text{charge}]{\text{discharge}} 2 \text{ H}_2\text{O} + 2\text{e}^{1-} \tag{4}$$

The potential for reaction 4 is -0.828 V.

Several reversible air electrodes were investigated in the effort to find a positive electrode of high cycle life and low polarization characteristics at high current densities. Of the candidate air electrodes, thermochemically treated carbon black samples were used in these preliminary studies.[14] It should be noted that all air electrodes exhibited low polarization characteristics up to 30 cycles at current densities of 20 mA/cm^2. However, significant polarization of the electrode did occur at higher cycles. The reaction at the positive electrode is given by.

$$2 \text{ H}_2\text{O} + \text{O}_2 + 4\text{e}^{1-} \xrightleftharpoons[\text{charge}]{\text{discharge}} 4 \text{ OH}^{1-} \tag{5}$$
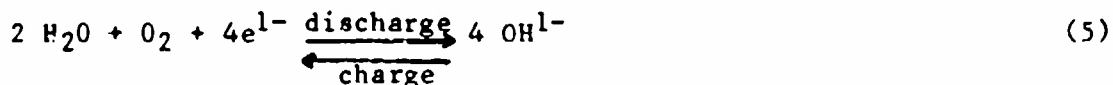
Th equi ium potential for the electrode is +0.401 V. The measured electrode potential, however, was 0.15 to 0.25 V less than the equilibrium potential.

Experimental cell design employed two reversible air positive electrodes on either side of a single LaNi$_5$ electrode. No data was reported for cells using the alloys containing either manganese or aluminum. The observed open circuit voltage for the test cells was about 1.05 V, compared to the theoretical open circuit voltage of 1.229 V. Cells discharged at current densities of 40 mA/cm^2 showed an average load voltage of approximately 0.7 V. The energy densities

for these cells were found to be about 100 Wh/kg. No further details relative to the performance or lifetime characteristics were given.

Several technical problems must be resolved before successful development and commercialization of this system can occur. A significant amount of work must be performed to optimize the air electrode relative to increased energy density, resistance to deterioration after extended cycling, and rate capability. Negative hydride electrodes must be developed which are more stable at elevated temperatures and still maintain the electrochemical characteristics. It should be further noted that auxiliary equipment must also be added before the system can be employed for large-scale applications. In addition to the necessity for pressurizing cells, devices to remove carbon dioxide from the air must be included. Contamination of the KOH electrolyte by CO_2 would result in decreased performance characteristics.[15] The inclusion of such devices in the design of the system would lead to lower energy density values.

No safety data was presented which detailed the results of such electrical abuse testing as short circuit, forced overdischarge, charge, or incineration. Since the hydride-air system does possess several problem areas which inhibit its development, it does not appear that commercially produced cells and batteries will be available for evaluation in U.S. Navy applications for some time. No safety testing is recommended at this time.

REFERENCES

1. Kordesch, K., Comprehensive Treatise of Electrochemistry, Volume 3, Electrochemical Energy Conversion and Storage, J. O'M. Bockris, B.E. Conway, E. Yeager, and R.E. White, eds. (New York: Plenum Press, 1981), p. 161.

2. Dunlop, J. D., and Stockel, J. F., J. Energy, 6, 1982, p. 28.

3. Dunlop, J. D., Giner, J., van Ommering, G., and Stockel, J. F., U.S. Patent No. 3,867,199, 1975.

4. Giner, J., and Dunlop, J. D., J. Electrochem. Soc., 122, 1975, p. 4.

5. Klein, M., and George, M., Proc. Power Sources Symp. 26, 1975, p. 18.

6. Kordesch, K. V., and Cieszewski, S. J., "Power Sources 6," Proc. Tenth Int. Symp. Power Sources, Joint Services Electrical Power Source Committee, D.H. Collins, ed. (London: Academic Press, 1977), p. 249.

7. Antoine, P., and Fougere, P., "Power Sources 7," Proc. 11th Int. Symp. Power Sources, Joint Services Electrical Power Sources Committee, Collins, D. H., ed. (London: Academic Press, 1979), p. 285.

8. Holleck, G. L., Turchan, M. J., Shuker, F. S., DeBiccari, D. J., and Offenhartz, P. O'D., "Power Sources 7," Proc. 11th Int. Symp. Power Sources, Joint Services Electrical Power Source Committee, Collins, D. H., ed. (London: Academic Press, 1979), p. 271.

9. Holleck, G. L., Driscoll, J. R., and Paul, B., Proc. Power Sources Symp. 29, 1981, p. 228.

10. Earl, M. W., and Dunlop, J. D., Proc. Power Sources Symp. 26, 1975, p. 24.

11. Markin, T. L., Bridger, N. J., Bennett, R., and Dell, R. M., Proc. Power Sources Symp. 28, 1979, p. 136.

12. Markin, T. L., Bennett, R., Gridger, N. J., and Dell, R. M., "Power Sources 8," Proc. 12th Int. Symp. Power Sources, Joint Services Electrical Power Source Committee, J. Thompson, ed. (London: Academic Press, 1981), p. 445.

13. Goualard, B. J., and Fougere, P., The 1982 Goddard Space Flight Center Battery Workshop, NASA Conference Publication 2263, 1983, p. 347.

REFERENCES (Cont.)

14. Sarradin, J., Bronoel, G., Percheron-Guegan, A., and Achard, J. C., "Power Sources 7," Proc. 11th Int. Symp. Power Sources, Joint Services Electrical Power Source Committee, D.H. Collins, ed. (London: Academic Press, 1979), p. 345.

15. Ko, H-W., and Juang, H-K., J. Applied Electrochem., 13, 1983, p. 725.

G. HYDROGEN-NICKEL(III)OXYHYDROXIDE (NICKEL-HYDROGEN)

H_2 | KOH | NiOOH

$$H_2 + 2\ NiOOH \rightleftharpoons 2\ Ni(OH)_2 \qquad\qquad [1]$$

The successful development of the hydrogen-nickel (III) oxyhydroxide (nickel-hydrogen) battery system was the result of the efforts by Dunlop, Van Ommering, and Stockel at COMSAT Laboratories and Giner, Perry, and Swette at Tyco Laboratories in the early 1970's.[1-4] The specific intent of these investigations was to provide a more reliable, long life and lightweight efficient power source alternative to the cadmium-nickel (III) oxyhydroxide (nickel-cadmium) space battery.[1] The sealed nickel-hydrogen system is a hybrid battery which uses the nickel (III) oxyhydroxide positive electrode developed for the aerospace nickel-cadmium batteries and the platinum black negative electrode developed for hydrogen-oxygen fuel cells. The advantages of this system also include higher energy and power densities when compared to such conventional secondary systems as the nickel-cadmium, lead-lead dioxide (H_2SO_4), and zinc-silver oxide cell systems.[5]

The basic design of the nickel-hydrogen container consists of a cylindrical pressure vessel with hemispherical end caps. Electrical feedthrough terminals are insulated using either ceramic to metal seals or plastic compression seals (i.e., Ziegler seals). The container may be fabricated from Inconel 718 or nickel plated steel. Since the hydrogen pressure varied from about 41 atm (4150 k Pa) for fully charged cells used in both the NTS-2 (Navigation Technology Satellite-2) and the INTELSAT V (International Telecommunications Satellite) to about 7 atm (709 k Pa) for cells discharged to 1.0 V, the container vessel must provide a significant safety margin. The burst strengths for the Inconel 718 vessels used in the above cells was found to be 160 atm (16200 k Pa). This provided a four to one safety factor for the fully charged cell.[6] Recent work has shown that the safety margin could be lowered to a ratio of two to one. Indeed, a 50 Ah high pressure cell design has been fabricated and tested which has a maximum pressure of 68 atm (6890 k Pa) with a ratio of 2.5:1 for the safety margin. By decreasing the safety margin, a corresponding reduction in weight and volume may be obtained.[1]

The negative electrode designs for the nickel-hydrogen cell were modified versions of previously developed hydrogen electrodes for H_2-O_2 alkaline fuel cells and secondary metal-air systems.[1,7,8] Typically, the electrode/current collector consists of a Teflon bonded platinum catalyzed carbon layer on a fine mesh, nickel expanded metal screen. Hydrogen diffusion to the negative electrode is enhanced by placing a Teflon gas diffusion mesh on the back side of the electrode. The hydrophobic Teflon layer prevents electrolyte entrainment during the charging process. The typical concentration of the platinum catalyst in the carbon layer varies from one to three percent.

The positive nickel (III) oxyhydroxide electrodes are prepared by electrochemical impregnation using the process developed at Bell Laboratories.[9-14] The electrode plaque of nickel screen and nickel powder (e.g., Inco 287) is prepared using a dry sintering process. The resultant porosity for the plaque varies from 78 to 82 percent. The plaque is electrochemically impregnated in a bath containing 1.6 to 1.8 M $Ni(NO_3)_4$ and 0.1 to 0.2 M $Co(NO_3)_2$ in a 45 percent solution of ethanol. This process required pH levels of 3.0 at temperatures of about 75°C.[11] The typical current density for the impregnation process is 0.05 A/cm^2. The impregnation process results in a loading level of 1.50 g to 1.75 g per cubic centimeter of plaque void volume. The formation of the positive electrode required repeated cycling in a 20 percent KOH solution at 25°C. Current densities of 0.07 A/cm^2 are employed in the first two discharge-charge cycles. The final discharge cycle in the process is performed at a current density of 0.01 A/cm^2 for 20 minutes. After the electrodes are rinsed, dried, and weighed, they are subjected to an electrical test of 20 cycles comprised of a 1.2 h charge at the C rate and a discharge at the C rate to -0.2 V. The electrodes are then subjected to a charge regime of 16 h at the C/10 rate followed by a discharge at the C/2 rate to -0.2 V. Acceptance of the electrodes for use in nickel-hydrogen space cells is determined by the measured capacities, weight loss, and stress testing.[11] Experimental cells using positive electrodes fabricated by the Bell Laboratories process have achieved 8,000 cycles at deep depths of discharge.[10]

Various separator materials have been evaluated during the development of the nickel-hydrogen cell system. The candidate separator materials have included Nylon, polypropylene, fuel cell grade asbestos, potassium titanate, and Zircar.[1,4-7,15-17] The separator in the nickel-hydrogen cell must permit the free passage of ions and retain the electrolyte but may also allow the passage of free oxygen during the overcharge period. Since both hydrogen and oxygen are present during the overcharge period, the two gases may react violently in the presence of the platinum catalyst. The reaction can occur through non-woven separators and result in melted areas of Nylon separators. Complete failure of cells due to cell stack thermal pressures have been noted. The use of ceramic based separators would not only prevent the development of an internal short circuit but would also retain oxygen within the cell stack and prevent the drying out of the cell. Asbestos and potassium titanate separators also prevent the generation of hot spots since a very rapid mixing of oxygen with the hydrogen atmosphere of the cell would occur.[15,16] Since fuel cell grade asbestos possesses such desirable properties as wettability and resistance to both high temperature environments and degradation in concentrated KOH solutions, most of the nickel-hydrogen cells designed for space applications have employed it as the preferred separator. It should be noted, however, that

alternative separator materials, including the ceramic cloths, may replace
asbestos, due to environmental and health hazards associated with the handling
of asbestos in manufacture.

The major causes of electrolyte loss within the nickel-hydrogen cell stack
are the displacement of the 30 percent KOH electrolyte by gases and the
evaporation/condensation of electrolyte due to temperature differentials between
the cell stack and the walls of the pressure vessel.[17] The former electrolyte
loss mechanism was found to only occur during the first few cycles and enough
electrolyte remained within the cell stack for efficient operation of the cell.
The evaporation/condensation of the electrolyte resulted in a noted decrease in
the performance characteristics during extended cycling. Alleviation of this
problem was obtained by either wrapping the cell stack with a non-woven Nylon
wick[15] or by ensuring that the separators were of sufficiently large enough
diameter to contact the cell walls, previously coated with yttrium-stabilized
zirconium oxide.[17] In either case, the wettability of the wicking material
must be significantly less than that of the separator material or the cell stack
may experience electrolyte starvation.

Two designs for the conventional nickel-hydrogen cell have been employed.
The first design requires a cell stacking construction of a Teflon hydrogen gas
diffusion mesh, the platinized carbon-hydrogen electrode, a
separator-electrolyte matrix, two nickel (III) oxyhydroxide electrodes in a
back-to-back configuration, a separator-electrolyte matrix, a second platinized
carbon-hydrogen electrode, and a Teflon gas diffusion mesh.[5] The second
design requires a cell stacking arrangement of an opposite configuration to the
first design: two back-to-back platinized carbon-hydrogen electrodes separated
by a Teflon diffusion mesh, separators, and nickel (III) oxyhydroxide electrodes
at the ends of the cell stack.[18] Recent efforts have focussed on advanced
nickel hydrogen cell designs which employ bipolar electrodes and common pressure
vessels.[19,20]

One critical limitation of the nickel-hydrogen system is the requirement of
a pressure vessel which comprises a significant amount of the total battery
weight. A reliable, low cost method for hydrogen storage must be successfully
developed before practical use of the battery could be made in non-space
applications.[21] The safety factors relative to the ratio of vessel burst
strength to the maximum internal gas pressure would be necessarily high in such
commercial applications as electric vehicle propulsion.[18] In view of the
above, recent results have shown the practicality of storing hydrogen on
interstitial sites of such metal lattices as $LaNi_5$.[22-25] Analysis of the
fully charged hydrided electrode material was found to contain 6.6 H atoms per
$LaNi_5$. Use of the metal hydride as the source of hydrogen gas for the
negative electrode in nickel-hydrogen cells has resulted in dramatic decreases
in internal cell pressure. For example, an experimental nickel-hydrogen cell
containing the metal hydride exhibited maximum operating pressures of about 7
atm (710 k Pa) while maximum operating pressures of the same cell without the
hydride exhibited internal pressures of 24 atm (2430 k Pa).[23] It should be
noted that the absorption of H_2 in the $LaNi_5$ lattice is an exothermic
process (7.2 kcal/mol H_2) which results in higher pressures than expected at
the end of the charging process. With optimization of the heat transfer
characteristics between the hydride and cell constituents, such advantages as
cell volume reduction, simplification of design and significantly lower hydrogen
pressures could ensure acceptance for several commercial applications.

The open circuit voltage and theoretical energy density for conventional nickel-hydrogen cells are 1.358 V and 390 Wh/kg, respectively.[26] Since the performance characteristics for cells and batteries have been extensively reviewed,[1,5-8,16,17] only one example will be discussed here.[8] A cell of nominal capacity of 50 Ah was charged at the C/5 rate (10A) for a period of six hours, corresponding to an overcharge capacity of 10 Ah. The cell was then discharged at the C/2 rate (25 A). The realized capacity to a 1.0 V cutoff level was about 53 Ah. The cell was then forced discharged and remained in voltage reversal at the 25 A rate for 0.5 h. The pressure profile for this cycle showed a steady increase in pressure from 6 atm (608 k Pa) at the beginning of the charge to 34 atm (3440 k Pa) at the end of the charging period. The pressure remained constant during the overcharge. When the cell was discharged, the pressure decreased linearly to a value of about 6 atm (608 k Pa) at a cell voltage of 0 V and remained constant at that value during the cell voltage reversal period. Very little difference in practical energy densities for the nickel hydrogen is observed for cells and batteries discharged at high rates. For example, energy densities of 45-50 Wh/kg are obtained for optimized cells discharged at the C/2 rate while only slightly lower values of 35 to 40 Wh/kg are obtained for satellite batteries.[27]

The operational temperature range for the nickel-hydrogen system is -20 to +65°C.[26] Very little difference in realized capacity is noted for cells discharged from temperatures of 0°C to +40°C, but significant capacity losses of more than 25 percent result from discharge at -10°C.[5] The self-discharge characteristics for the cell show losses of 20 percent of the full capacity after an open circuit stand of 24 hours and a 40 percent loss after 100 hours.

Nickel-hydrogen cells were continuously cycled using the following charge/discharge regime: charge for 34 minutes at the C/1.5 rate to a 30 percent overcharge followed by discharge for 26 minutes at the C/1.5 rate to a 26.8 percent depth of discharge.[5] The number of cycles for the five cells tested varies from 468 to more than 5000 cycles before reaching discharge voltages below 1.0 V. Cells may be charged using either constant current sources, constant voltage power supplies, or voltage versus temperature level charge techniques.[28]

The nickel-hydrogen cell system was developed in the United States with major funding from INTELSAT (COMSAT Laboratories) and the U.S. Air Force (Aero Propulsion Laboratory, Wright-Patterson Air Force Base). Major participants in the development program include Eagle-Picher, Energy Research Corporation, Tyco Laboratories, Hughes Aircraft Company, Western Electric Company, Marcoussis Laboratories (France), TRW Incorporated, EIC Corporation, Naval Research Laboratories, Lockheed Missiles and Space Company, Yardney Electric Division, Union Carbide Corporation, Bell Laboratories, McDonnell Douglas Corporation, and Ford Aerospace and Communications Corporation.

The electrical abuse testing of short circuit, forced overdischarge and prolonged overcharge have been performed for nickel-hydrogen cells. A fully charged, lightweight cell with a nominal 25 Ah capacity was short circuited through a set of relays.[29] The total resistance for the short circuit was 2.6 X 10^{-3} ohms. The cell voltage, short circuit current, cell pressure, and temperatures at various locations on the cell were monitored and recorded throughout the test. Immediately upon application of the short circuit, the

cell voltage dropped to about 1.1 V and remained at that voltage for
approximately 7.5 minutes. A second load voltage plateau was observed at about
0.75 V for the next two minutes. The voltage then decreased to zero volts at
the 12 minute mark. The initial cell pressure was about 28.6 atm (2890 k Pa)
which decreased linearly to about 6.8 atm (689 k Pa) at the 9.5 minute mark.
The pressure then remained constant for the remainder of the test period. The
average short circuit current for the cell was more than 200 A during the first
7.5 minutes of the test and gradually decreased to a low value at the end of the
test. It is interesting to note that a realized capacity of 25 Ah was obtained
during the initial 7.5 minutes under short circuit conditions. The maximum
temperature of about 180°C was observed on the relay case while a temperature of
about 130°C at the cell terminal was noted. A capacity test on the cell showed
an identical realized capacity as that obtained prior to the short circuit test.
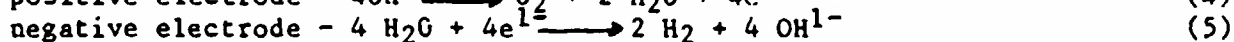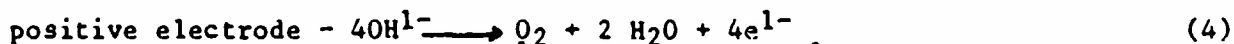
One important safety feature of the nickel-hydrogen system is the ability
to tolerate overcharge at high rates with no ill effects relative to performance
or safety characteristics.[4,5,8,10,18] The nickel-hydrogen cell is positive
electrode limited on charge due to the unlimited supply of water at the hydrogen
electrode. During normal cell operation, the reactions at the positive
electrode are:

$$Ni(OH)_2 + OH^{1-} \quad \underset{\text{discharge}}{\overset{\text{charge}}{\rightleftharpoons}} \quad NiOOH + H_2O + e^{1-} \tag{2}$$
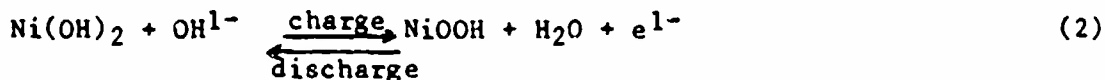
and the reactions at the negative electrode are:

$$2 H_2O + 2e^{1-} \quad \underset{\text{discharge}}{\overset{\text{charge}}{\rightleftharpoons}} \quad H_2 + 2 OH^{1-} \tag{3}$$
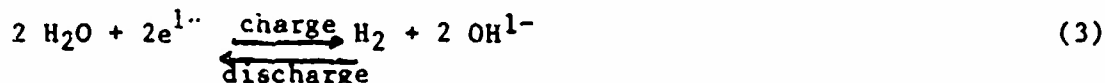
On overcharge, oxygen is evolved at the positive electrode after all the nickel
material has been charged and hydrogen continues to be evolved at the negative
electrode at the same rate as the oxygen evolution:

$$\text{positive electrode} - 4OH^{1-} \longrightarrow O_2 + 2 H_2O + 4e^{1-} \tag{4}$$
$$\text{negative electrode} - 4 H_2O + 4e^{1-} \longrightarrow 2 H_2 + 4 OH^{1-} \tag{5}$$

The overall reaction during overcharge is given by:

$$2 H_2O \longrightarrow 2 H_2 + O_2 \tag{6}$$

The oxygen will then chemically recombine with hydrogen at the catalyzed
negative hydrogen electrode to form water in accordance with:
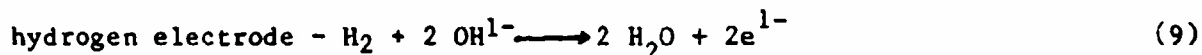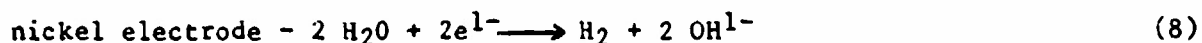
$$2 H_2 + O_2 \longrightarrow 2 H_2O \tag{7}$$

The recombination rate is rapid so that the total oxygen concentration is
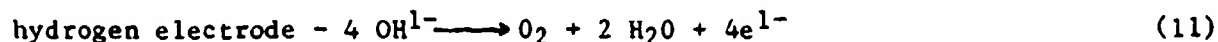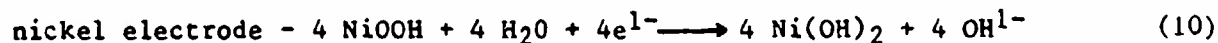limited to about 0.10 to 0.15 percent at 25°C and about 0.20 percent at
-25°C.[30]

Overcharge tests were performed for both cells[5] and batteries.[6]
Nickel-hydrogen cells were overcharged at the C/10 rate to a level in excess of
1.7 times the nominal capacity. The temperature of the cell decreased slightly
during the initial 10-hour charge period. Since nearly all of the power to the

cell in the overcharge regime is dissipated as heat, the temperature increased
only about 5°C during the overcharge period. The increased temperature is also
the result of the exothermic recombination reaction between evolved H_2 and
O_2 to form water. A battery comprised of fourteen 35 Ah cells in series was
subjected to a thermal vacuum cycle in which the battery was discharged under
constant power conditions (average current, 21 A) for one hour, charged at 3.7 A
for 6.5 hours, and finally trickle charged at 0.6 A for 4.5 hours.[6] After the
discharged capacity of 21 Ah was restored to the battery, an abrupt temperature
increase of about 6°C was observed at the beginning of the overcharge period.
No hazardous conditions were reported for any nickel-hydrogen cells or batteries
subjected to prolonged overcharge conditions although thermal management
provisions must be considered. In addition, hydrogen pressures will increase
during overcharge but the maximum observed pressures will be significantly less
than the designed burst strength of the pressure vessel.

Protection against hazardous conditions as a result of prolonged
overdischarge is achieved in the nickel-hydrogen system by introducing an excess
amount of hydrogen in the cell. The cell then becomes positive electrode
limited. Hydrogen will be produced at the positive electrode during voltage
reversal and will then be consumed at the negative electrode as in the normal
course of discharge:

$$\text{nickel electrode} - 2\ H_2O + 2e^{1-} \longrightarrow H_2 + 2\ OH^{1-} \tag{8}$$

$$\text{hydrogen electrode} - H_2 + 2\ OH^{1-} \longrightarrow 2\ H_2O + 2e^{1-} \tag{9}$$

The positive electrode limited cell can be operated continuously in cell voltage
reversal with no net change in the amount of water and operating
pressure.[8,10] In the event that cell voltage reversal does occur in cells
which are negative electrode limited, the nickel electrode will continue to
discharge and oxygen gas will be evolved at the hydrogen electrode:

$$\text{nickel electrode} - 4\ NiOOH + 4\ H_2O + 4e^{1-} \longrightarrow 4\ Ni(OH)_2 + 4\ OH^{1-} \tag{10}$$

$$\text{hydrogen electrode} - 4\ OH^{1-} \longrightarrow O_2 + 2\ H_2O + 4e^{1-} \tag{11}$$

The net result would be an increase in cell pressure and the possibility of a
violent reaction between the two gases in the presence of the platinum
catalyst. Complete failure of cells due to cell stack thermal events with
attendant development of high internal pressures have been noted.[15,16]

Nickel-hydrogen cells of the positive limited design were forced
overdischarged at the 0.73 C rate for 0.5 h after entering voltage
reversal.[29] The reversal voltage remained constant at about -0.19 V for the
duration of the test. It should be noted that no instances of any hazardous
conditions for positive limited cells subjected to overdischarge conditions were
reported.

Negative limited cells were also forced overdischarged at the same rates
but for much shorter durations than those described for the positive limited
cells.[29] The negative limited cell was obtained by removing 30 percent of the
hydrogen from the cell. This cell was then subjected to a discharge at the
0.73C rate for only five minutes after entering voltage reversal. The end of

discharge voltage observed for this cell was -0.36 V. The cell was refilled
with hydrogen and cycled. A second reversal test of five minutes at the 0.73 C
rate was performed on the above cell after 60 percent of the hydrogen was
removed. As in the first test, the end of discharge voltage observed for the
cell was -0.33 V. The cell was then disassembled and examined for component
damage. No observable damage to the cell or its components were found. It
should be emphasized, however, that the time in cell voltage reversal was of
short duration. Prolonged cell reversal tests using these negative limited
cells could result in hazardous conditions. It is for this reason that all
nickel-hydrogen cells are of the positive-limited design.

No data was presented which detail the results of incineration testing for
nickel-hydrogen cells. Since the maximum internal pressure of the cells are as
high as 41 atm (4153 k Pa) and a typical burst strength of the pressure vessel
is 160 atm (16,200 k Pa), a safety factor (i.e., the ratio of pressure vessel
burst strength to maximum cell pressure) of approximately 4 exists for some cell
designs. However, it should be noted that sufficiently high internal pressures
could be produced in cells exposed to the incineration conditions given in
NAVSEAINST 9310.1A to result in violent cell rupture. In the event that either
the ceramic to metal seals or the Ziegler seals should leak under incineration
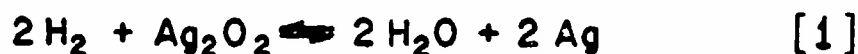conditions, a hydrogen-air fire or explosion could occur.

REFERENCES

1. Dunlop, J. D., and Stockel, J. F., *J. Energy*, 6, 1982, p. 28.

2. Miller, L., *The 1980 Goddard Space Flight Center Battery Workshop*, NASA Conference Publication 2177, 1981, p. 391.

3. Miller, L., *Proc. of the 16th IECEC*, American Society of Mechanical Engineers, 1981, p. 200.

4. Dunlop, J. D., Giner, J., van Ommering, G., and Stockel, J. F., U.S. Patent No. 3,867,199, 1975.

5. Giner, J., and Dunlop, J. D., *J. Electrochem. Soc.*, Electrochem. Science and Technol., 122, 1975, p. 4.

6. Dunlop, J. D., van Ommering, G., and Earl, M. W., "Power Sources 6," *Proc. Tenth Int. Symp. Power Sources*, Joint Services Electrical Power Source Committee, Collins, D. H., ed. (London: Academic Press, 1977), p. 231.

7. Kordesch, K. V., and Cieszewski, S. J., "Power Sources 6," *Proc. Tenth Int. Symp. Power Sources*, Joint Services Electrical Power Source Committee, D.H. Collins, ed. (London: Academic Press, 1977), p. 249.

8. Klein, M., and George, M., *Proc. Power Sources Symp. 26*, 1975, p. 18.

9. Beauchamp, R., U.S. Patent No. 3,653,967, 1972.

10. Dunlop, J. D., *The 1982 Goddard Space Flight Center Battery Workshop*, NASA Conference Publication 2263, 1983, p. 389.

11. Bleser, C., *The 1981 Goddard Space Flight Center Battery Workshop*, NASA Conference Publication 2217, 1982, p. 471.

12. Dyer, C., *The 1981 Goddard Space Flight Center Battery Workshop*, NASA Conference Publication 2217, 1982, p. 459.

13. Rodgers, H. H., Dalton, P. J., and Tinker, L. A., *The 1980 Goddard Space Flight Center Battery Workshop*, NASA Conferene Publication 2177, 1981, p. 431.

14. Bleser, C. A., and Scherer, M. D., *Proc. Power Sources Symp. 30*, 1983, p. 111.

REFERENCES (Cont.)

15. Levy, E., Jr., Rogers, H. H., McGrath, R. J., and Wittman, A., Nickel Hydrogen Energy Storage For Satellites, NTIS No. AD-A006427, U.S. Dept. Commerce, Springfield, VA, 1974.

16. Levy, E., Jr. and Rodgers, H. H., Nickel Hydrogen Energy Storage For Satellites, NTIS No. AD-A012303, U.S. Dept. Commerce, Springfield, VA, 1975.

17. Rodgers, H. H., Krause, S. J., and Levy, E., Jr., Proc. Power Sources Symp. 28, 1979, p. 142.

18. Gross, S., Energy Conversion, 15, 1976, p. 95.

19. Perez, F., The 1982 Goddard Space Flight Center Battery Workshop, NASA Conference Publication 2263, 1983, p. 481.

20. Chireau, R. F., and Berchielli, A. S., Proc. Power Sources Symp. 29, 1981, p. 230.

21. Salkind, A. J., Farrell, D. T., Jr., and Hodges, A. J., J. Electrochem. Soc., 125, 1978, p. 311C.

22. Holleck, G. L., Driscoll, J. R., and Paul, B., Proc. Power Sources Symp. 29, 1981, p. 228.

23. Earl, M. W., and Dunlop, J. D., Proc. Power Sources Symp. 26, 1975, p. 24.

24. Markin, T. L., Bridger, N. J., Bennett, R., and Dell, R. M., Proc. Power Sources Symp. 28, 1979, p. 136.

25. Markin, T. L., Bennett, R., Bridger, N. J., and Dell, R. M., "Power Sources 8," Proc. 12th Int. Symp. Power Sources, Joint Services Electrical Power Source Committee, J. Thompson, ed. (London: Academic Press, 1981), p. 445.

26. McBreen, J., Comprehensive Treatise of Electrochemistry, Volume 3, Electrochemical Energy Conversion and Storage, Bockris, J. O'M., Conway, B. E., Yeager, E., and White, R. E., eds. (New York: Plenum Press, 1981), p. 309.

27. Goualard, B. J., and Fougere, P., The 1982 Goddard Space Flight Center Battery Workshop, NASA Conference Publication 2263, 1983, p. 347.

28. Mackowski, M. J., Proc. of the 16th IECEC, American Society of Mechanical Engineers, 1981, p. 216.

29. Stadnick, S., The 1981 Goddard Space Flight Center Workshop, NASA Conference Publication 2217, 1982, p. 525.

30. Rogers, H. H., The 1981 Goddard Space Flight Center Battery Workshop, NASA Conference Publication 2217, 1982, p. 513.

H. HYDROGEN-SILVER OXIDE (SILVER-HYDROGEN)

$$H_2 \mid KOH \mid Ag_2O_2, Ag_2O$$

$$2 H_2 + Ag_2O_2 \rightleftharpoons 2 H_2O + 2 Ag \qquad [1]$$

$$H_2 + Ag_2O \rightleftharpoons H_2O + 2 Ag \qquad [2]$$

The electrical power demands of satellites have historically required the use of such secondary battery systems as the cadmium-nickel (III) oxyhydroxide (nickel-cadmium) and the zinc-silver oxide (silver-zinc). Since the nickel-cadmium battery was necessarily limited to low depths of discharge, the practical energy densities were correspondingly low. The life of the silver-zinc battery is limited due to the solubility of the zinc electrode.[1] In view of the above, the successful development of an alternative power source, the hydrogen-nickel (III) oxyhydroxide (nickel-hydrogen) secondary system, was carried out by COMSAT Laboratories and Tyco Laboratories and others[2-5] in the early 1970's. This battery has shown energy density improvements of up to 60 percent greater than the nickel-cadmium system. A further improvement in energy density was more recently obtained by replacing the nickel (III) oxyhydroxide positive electrode of the nickel-hydrogen system by the more highly energetic silver oxide electrode developed for the zinc-silver oxide and cadmium-silver oxide batteries to create the hydrogen-silver oxide system.[6] The negative electrode is still comprised of the platinized carbon black electrode used in the nickel-hydrogen cell (the H_2-O_2 alkaline fuel cell negative electrode).

The basic design of the silver-hydrogen cell container consists of a cylindrical pressure vessel with hemispherical end caps. Electrical feedthrough terminals are insulated using either ceramic to metal seals or Ziegler plastic compression seals. The Inconel pressure vessel must provide a significant safety margin in view of the fact that maximum internal hydrogen pressures of about 35 to 40 atm (3550 k Pa to 4050 k Pa) are produced in the fully charged cell.

The negative electrode/current collector typically consists of a Teflon bonded, platinum-catalyzed carbon layer on a fine mesh, nickel expanded metal screen. Hydrogen diffusion to the electrode is enhanced by placing Teflon picks on the Teflon coated, hydrophobic side of the electrode.[6] This layer prevents electrolyte entrainment during the charging process.

The positive silver oxide electrode is prepared by sintering a fine silver powder onto a fine mesh, expanded nickel, or silver metal screen.[1,6] The sintering process requires heating at temperatures of 650°C for short time periods and results in the bonding of the silver particles together and to the expanded metal screen. Silver connecting tabs are then hot forged to the electrode after shaping to the desired size.

The major area for the improvement of silver-hydrogen cells is the selection of a separator assembly which would prevent the migration of silver ion, serve as a reservoir of 40 percent KOH electrolyte, exhibit chemical stability in the electrolyte, and maintain mechanical strength for the battery life.[6] Since no single separator possesses all of the above properties, a separator using multilayers of different separator materials must be employed. The use of common argentistatic membranes such as the cellulose-based Visking and grafted polyethylene films result in poor electrolyte transport properties.[7] Other candidate materials for the separator have included Cellophane, Polypropylene, asbestos, potassium titanate, zirconia, and an inorganic-organic (I.O.) separator developed by NASA-Lewis Research Center. The I.O. separator material is a plastic bonded zirconia ceramic on one side of a fuel cell-grade asbestos separator which was impregnated by low concentrations of polyphenylene oxide. In one cell design,[1] both the I.O. separator and an asbestos separator were used in a silver-hydrogen cell: the I.O. separator was placed against the silver oxide electrode with the zirconia ceramic side facing the hydrogen electrode and the asbestos separator was placed between the I.O. separator and the hydrogen electrode. Both the asbestos and the I.O. separator served as electrolyte reservoirs while also functioning as a mechanical barrier to silver ion migration and a chemical barrier to fix the silver ions. The use of such non-oxidizable separators also prevents the development of internal short circuits and hot spots during the overcharge period.

Though several designs for the conventional silver-hydrogen system are possible, the stack cell design of the nickel-hydrogen system seems to be preferred. This cell arrangement requires a cell stacking construction of two platinized carbon-hydrogen electrodes back to back and separated by a gas diffusion screen, a separator-barrier-electrolyte matrix on each side of the hydrogen electrodes, and a silver oxide electrode at either end of the stack assembly.[7]

Perhaps the most critical limitation of the silver-hydrogen system relative to widespread commercialization and usage of the battery is the requirement of a pressure vessel. A reliable, low cost method for hydrogen storage must be developed before practical use of the battery could be made in non-space applications. For example, the safety factors for the vessel would be necessarily high for such applications as electric vehicle propulsion.[8] In view of the above, recent efforts have shown the practicality of storing hydrogen on interstitial sites of such metal lattices as $LaNi_5$ and $La_{0.8}Ce_{0.2}Ni_5$.[9] Analysis of a fully charged, hydrided $LaNi_5$ electrode showed that up to 6.6 H atoms per $LaNi_5$ could be stored. The use of the metal hydride as the source of hydrogen gas for the negative electrode would result in a dramatic reduction in internal cell pressure with attendant decreases in cell volume and weight.

The observed open circuit voltages for the silver hydrogen cell are 1.38 and 1.12 V, respectively, for the H_2-Ag_2O_2 and H_2-Ag_2O electrochemical couples.[10] Silver-hydrogen cells of a nominal capacity of 25 Ah were cycled at 20°C. During charge at rates of 0.05, 0.2, and 0.5 C, two distinct cell voltage plateaus are noted. The first plateau corresponds to the oxidation of silver to Ag_2O in accordance with the reaction,

Step 1: $2 \text{ Ag} + 2 \text{ OH}^{1-} \longrightarrow Ag_2O + H_2O + 2e^{1-}$ (3)
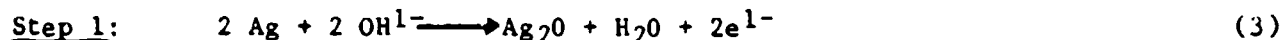
and the second step corresponds to the oxidation of Ag_2O to Ag_2O_2 in accordance with the reaction,

Step 2: $Ag_2O + 2 \text{ OH}^{1-} \longrightarrow Ag_2O_2 + H_2O + 2e^{1-}$ (4)
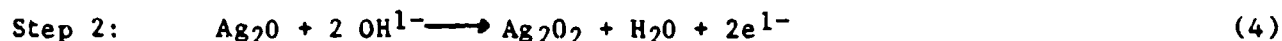
Typical cell voltage values of 1.40, 1.30, and 1.23 V are obtained for reaction 3 for cells charged at the 0.5, 0.2 and 0.05 C rates. Cell voltage values of 1.70, 1.60, and 1.55 V were observed for reaction 4 for cells similarly charged at the 0.5, 0.2 and 0.05 C rates.[6] Hydrogen is simultaneously generated at the catalyzed carbon electrode:

$2 H_2O + 2e^{1-} \longrightarrow H_2 + 2 \text{ OH}^{1-}$ (5)

The performance curves for the above cells show two plateaus for cells discharged at the lower rates. For cells discharged at rates of 0.5 C or higher, the first discharge plateau becomes nearly non-existent. Average cell voltage values of 1.23, 1.36, and 1.42 V are obtained during the first step of discharge at the 0.5, 0.2 and 0.05 C rates. The second discharge step exhibited corresponding load voltages of 1.07, 1.11 and 1.17 V. The practical energy densities for the silver-hydrogen cell and batteries are 65 to 80 and 50-60 Wh/kg, respectively.[9] Comparison of the energy density values for the silver-hydrogen system to those for the nickel-hydrogen system show average energy density increases of nearly 45 percent for the silver-hydrogen cells and batteries.
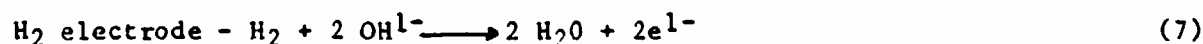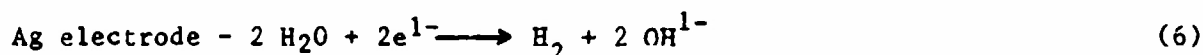
Silver-hydrogen 25 Ah cells were charged at 20°C at the 0.05 C and 0.5 C rates and subsequently discharged at the 0.2 C rate.[6] The results showed a linear cell pressure increase from about 4 atm (405 k Pa) to 31.6 atm (3200 k Pa) during the charge and overcharge periods for cells charged at the 0.05 C rate. The pressure remained constant during a one-hour cell open circuit and decreased linearly as the cell was discharged at the 0.2 C rate. However, cells discharged at the higher rate exhibited a non-linear pressure increase during the two-hour charge and one-hour overcharge period. The pressure increased from 4 atm (405 k Pa) to a maximum of about 37 atm (3750 k Pa) at the end of overcharge. The pressure decreased during the one-hour cell open circuit and stabilized at the same value noted for the cells described above. This stabilization of the pressure is the result of cell cooling after the overcharge period. Discharge of both sets of cells at the 0.2 C rate yielded identical realized capacities of more than 25 Ah.

The operational temperature range for silver-hydrogen cells and batteries is -20°C to +80°C.[10] The charge retention characteristics for the system show capacity losses of about 25 percent and 13 percent for cells stored at 20 and 0°C for fifty days. Practical cells using the NASA inorganic-organic separators

have successfully completed more than 1000 deep discharge cycles.[7] As with the nickel-hydrogen system, charging may be performed using constant current or constant voltage sources as well as voltage versus temperature level charge techniques.[11]

The major research and development efforts for the silver-hydrogen system are sponsored by United States Air Force (Aero Propulsion Laboratories, Wright-Patterson Air Force Base), NASA (Lewis Research Center), and the European Space Agency. Major participants in the above programs include EIC Corporation, Energy Research Corporation, and SAFT.
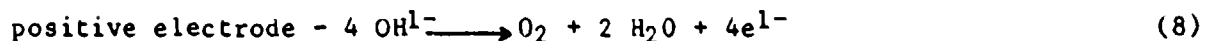
The safety characteristics for the silver-hydrogen system have not been as thoroughly investigated as those for the nickel-hydrogen system (Chapter 3). No data was presented which detail the results for either cell short circuit or forced overdischarge tests. In view of the fact that the silver-hydrogen cells are positive electrode limited (i.e., an excess amount of hydrogen is introduced into the cell), hydrogen will be produced at the positive (silver) electrode during voltage reversal and will then be consumed at the negative (hydrogen) electrode as in the normal course of cell discharge:[7]

$$Ag \text{ electrode } - 2 H_2O + 2e^{1-} \longrightarrow H_2 + 2 OH^{1-} \qquad (6)$$

$$H_2 \text{ electrode } - H_2 + 2 OH^{1-} \longrightarrow 2 H_2O + 2e^{1-} \qquad (7)$$

It can be seen that the positive electrode limited silver-hydrogen cell can be operated continuously in cell voltage reversal with no net change in internal pressure or water content.

The results of short circuit tests performed using 25 Ah nickel-hydrogen cells showed that currents as high as 200 A could be maintained for more than seven minutes. The internal cell pressures decreased from 28.6 atm (2890 k Pa) to about 6.8 atm (689 k Pa) during the twelve minute test. Cell terminal temperatures increased to a maximum value of 130°C. The cells, which were then cycled, yielded realized capacities identical to those obtained prior to the short circuit tests. Extension of these short circuit results for the nickel-hydrogen system to the silver-hydrogen system may be possible. However, the silver oxide electrode is significantly more energetic and does possess a higher energy density than the nickel (III)-oxyhydroxide electrode. In consideration of the above, higher short circuit currents and cell temperatures could be generated. The short circuit test, therefore, should be performed to determine the effects of the different electrodes on the safety characteristics.

Since the silver-hydrogen cell is positive electrode limited (there exists an unlimited supply of water at the hydrogen electrode), tolerance to overcharge conditions at high rates would be expected and no ill effects relative to subsequent performance or safety characteristics would occur. During normal cell charging, the reactions at the positive electrode are given by equations 3 and 4 and the reaction at the negative electrode is given by equation 5. In overcharge, oxygen will be generated at the positive electrode after all the silver material has been charged. Hydrogen would continue to be generated at the negative electrode at the same rate as the oxygen evolution:

positive electrode - $4\ OH^{1-} \longrightarrow O_2 + 2\ H_2O + 4e^{1-}$ (8)

negative electrode - $4\ H_2O + 4e^{1-} \longrightarrow 2\ H_2 + 4\ OH^{1-}$ (9)

The overall reaction during overcharge is given by:

$$2\ H_2O \longrightarrow 2\ H_2 + O_2 \tag{10}$$
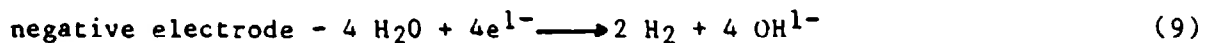
The oxygen will then recombine chemically with the hydrogen at the platinum catalyzed carbon electrode to form water:

$$2\ H_2 + O_2 \longrightarrow 2\ H_2O \tag{11}$$

The recombination rate is rapid. It is expected that the total oxygen concentration in the cell will be limited to about 0.1 to 0.2 percent, as in the case for nickel-hydrogen cells.[7,12] No hazardous conditions were reported for any silver-hydrogen cells or batteries subjected to prolonged overcharge conditions. It should be noted that thermal management for cells or batteries in the overcharge condition must be considered. In addition, the internal pressure will increase during overcharge but will be significantly less than the designed burst strength of the pressure vessel.

No data was given which detail the results of incineration testing for silver-hydrogen cells or batteries. Since the internal pressure of the cells may be as high as 40 atm (4050 k Pa) and a typical burst strength may be 160 atm (16,200 k Pa), a safety factor of four exists for some cell designs. It should be noted that the current trends may result in lighter pressure vessels with lower burst strengths. In either case, sufficiently high internal pressures could be generated in cells or batteries exposed to a fire or the incineration conditions given in NAVSEAINST 9310.1A resulting in a violent cell rupture. In the event that either the ceramic to metal seals or the Ziegler plastic compression seals should fail, a hydrogen-air fire or explosion could occur.

REFERENCES

1. Charkey, A., and Klein, M., Proc. Power Sources Symp. 28, 1979, p. 145.

2. Dunlop, J. D., and Stockel, J. F., J. Energy, 6, 1982, p. 28.

3. Miller, L., The 1980 Goddard Space Flight Center Battery Workshop, NASA Conference Publication 2177, 1981, p. 391.

4. Miller, L., Proc. of the 16th IECEC, American Society of Mechanical Engineers, 1981, p. 220.

5. Dunlop, J. D., Giner, J., van Ommering, G., and Stockel, J. F., U.S. Patent No. 3,867,199 (1975).

6. Antoine, P., and Fougere, P., "Power Sources 7," Proc. 11th Int. Symp. Power Sources, Joint Services Electrical Power Source Committee, Collins, D. H., ed. (London: Academic Press, 1979), p. 285.

7. Holleck, G. L., Turchan, M. J., Shuker, F. S., DeBiccari, D. J., and Offenhartz, P. O'D., "Power Sources 7," Proc. 11th Int. Symp. Power Sources, Joint Services Electrical Power Source Committee, Collins, D. H., ed. (London: Academic Press, 1979), p. 271.

8. Gross, S., Energy Conversion, 15, 1976, p. 95.

9. Goualard, B. J., and Fougere, P., The 1982 Goddard Space Flight Center Battery Workshop, NASA Conference Publication 2263, 1983, p. 347.

10. McBreen, J., Comprehensive Treatise of Electrochemistry, Volume 3, Electrochemical Energy Conversion and Storage, Bockris, J. O'M., Conway, B. E., Yeager, E., and White, R. E., eds. (New York: Plenum Press, 1981), p. 309.

11. Mackowski, M. J., Proc. of the 16th IECEC, American Society of Mechanical Engineers, 1981, p. 216.

12. Rogers, H. H., The 1981 Goddard Space Flight Center Battery Workshop, NASA Conference Publication 2217, 1982, p. 513.

I. IRON-AIR (IRON-OXYGEN)

Fe | KOH | O_2

$$2 Fe + O_2 + 2 H_2O \rightleftharpoons 2 Fe(OH)_2 \qquad [1]$$
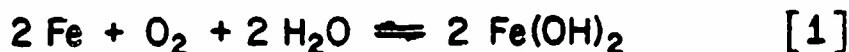
The iron-air secondary battery system is a particularly attractive power source candidate for electric vehicle propulsion due to its high theoretical energy density and low active material costs. Significant advances in iron-air technology have been made within the past decade relative to the improvement in the iron electrode[1-4] and the development of bifunctional air electrodes.[5-7] The replacement of hand pasted iron electrodes by sintered iron powder electrodes resulted in more complete utilization of the active material with increased realized capacities and lower discharge polarization characteristics. Since unifunctional electrodes only possessed the capability of oxygen reduction in accordance with the reaction,

$$O_2 + 2 H_2O + 4e^{1-} \longrightarrow 4 OH^{1-} \qquad (2)$$

such third electrodes as nickel were required during the charging process. The use of the third electrode resulted in a reduction of cell voltages and increases in both cell weights and volumes.[7] In addition, the unifunctional electrode deteriorated under open circuit conditions during cell charging. The use of bifunctional air electrodes in the iron-air cell not only permits the reduction of oxygen (reaction 2) but also allows the oxidation of the hydroxyl ion according to:

$$O_2 + 2 H_2O + 4e^{1-} \underset{\text{charge}}{\overset{\text{discharge}}{\rightleftharpoons}} 4 OH^{1-} \qquad (3)$$
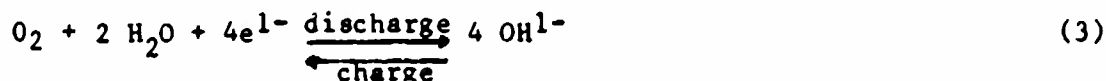
The classical manufacturing processes for the fabrication of either flat plate or hand pasted iron electrodes are given by Falk and Salkind,[8] Mantell,[9] Vinal,[10] and Andersson.[11] Recent manufacturing techniques developed by Westinghouse[12] and the Swedish National Development Company,[4] have produced sintered iron electrodes with improved performance and surface area characteristics. Typically, the iron negative electrode is a sintered iron powder on an expanded iron screen substrate.

The half cell reaction for the initial discharge of the iron electrode is given by:

$$Fe + 2\ OH^{1-} \longrightarrow Fe(OH)_2 + 2e^{1-} \tag{4}$$

Further discharge of the iron electrode would result in the formation of either $Fe(OH)_3$[3] or Fe_3O_4.[14] Such discharge beyond the first step (reaction 4) produces a large decrease in cell load voltage. In addition, high charging rates are required and a significant amount of capacity is lost over a few cycles for iron electrodes discharged to the higher oxidation state. Therefore, it is necessary to carefully regulate the cell discharge regime in order to avoid the complete discharge of the iron electrode.

The iron negative electrode undergoes a self-discharge corrosion reaction under open circuit conditions:[14-16]

$$Fe + 2\ H_2O \longrightarrow Fe(OH)_2 + H_2 \tag{5}$$

The above reaction will occur spontaneously ($E = -0.05$ V) since pure iron electrodes have low hydrogen overpotentials. Though this corrosion reaction is the predominant mode of cell capacity loss, self-discharge may also occur through the chemical oxidation of iron by oxygen. Further, large amounts of hydrogen are produced during cell charging:

$$2\ H_2O + 2e^{1-} \longrightarrow H_2 + 2\ OH^{1-} \tag{6}$$
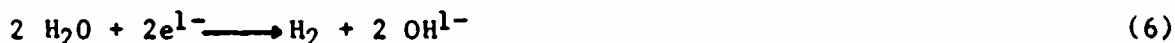
As a result, the energy efficiencies for the iron-air cell are low with typical values of less than 50 percent. The evolution of hydrogen during charge also results in heat generation which causes water loss from the KOH electrolyte. Provision for electrolyte cooling, gas recombination, heat exchange, and hydrogen detection/ separation must be considered to minimize possible safety hazards attendant with cell charging.

The bifunctional air positive electrode must withstand oxygen evolution during the charging process without deleterious effects to either the catalyst or the electrode structure.[17] Westinghouse[5,7] produces a carbon-based air electrode by a wet pasting process using a tungsten carbide catalyst (2 mg/cm^2) with Teflon as both the binder and hydrophobic agent. The use of a hydrophobic agent such as Teflon permits the diffusion of air to the cell interior while restricting the loss of KOH electrolyte from the cell. A second type of bifunctional air electrode is fabricated using porous nickel electrode structures with coarse and fine pore characteristics.[4,6,17] Inclusion of a silver catalyst[6] or transition metal oxide catalyst[17] in the fine pore nickel layer aids in the reduction of oxygen during discharge. During charge, the effect of oxygen evolution is the displacement of electrolyte from the fine pore nickel layer with oxygen evolution occurring in the coarse nickel layer.

The electrolyte consists of 5 M KOH (approximately 22 weight percent) with an additive of LiOH at concentration levels of 0.2 to 1.0 M. The inclusion of LiOH improves the utilization of the iron electrode. It is believed[3] that the lithium ion is incorporated into the iron electrode and results in improved ionic conductivity of the $Fe(OH)_2$ product. Iron electrodes discharged in a KOH-LiOH electrolyte showed capacity increases of more than 30 percent compared

to similar iron electrodes discharged in pure KOH solutions.[18] Further, the addition of FeS to the electrolyte was found to reduce the self-discharge characteristics at the iron electrode by increasing the hydrogen overpotential.

Several technical problem areas must be overcome before the iron-air system can be considered as a viable power source for electric vehicle propulsion:

1. Voluminous amounts of hydrogen are evolved during the charging process. In view of the above, a recombination catalyst (e.g., Pt on Al_2O_3) or device must be included at the top of the cell in order to avoid a serious hydrogen-oxygen explosion. This is especially important for closed systems[6] which rely on an oxygen storage tank-compressor assembly. In addition, hydrogen gas sensors may be required between the cell and the storage tank-compressor assembly to avoid the introduction of H_2 into the pressurized oxygen tank.

2. The inclusion of carbon dioxide with the air or oxygen supply results in premature pore blockage and poor performance characteristics.[19] A method for CO_2 removal, therefore, must be included for iron-air batteries.

3. Thermal management problems arise in iron-air batteries, particularly during charging. In view of the above, the most effective method for heat control would be electrolyte circulation.[17]

4. During charging, the evolved oxygen would contain significant amounts of water. Therefore, a condensor-evaporator accessory may be required for water management purposes in closed systems.

The theoretical open circuit voltage for the iron-air cell is 1.278 V. The discharge polarization characteristics for hypothetical Westinghouse iron-air cells[7] at current densities of 25 to 100 mA/cm^2 would exhibit load voltages of 0.93 to 0.72 V, respectively. An improvement in cell load voltage of about 0.06 V is observed for cells supplied with pure oxygen. The theoretical energy density for the iron-air system is 716 Wh/kg.[20] Prototype cells yeild energy densities of about 80 to 90 Wh/kg at the five hour rate and 55 to 65 Wh/kg at the one hour rate. Additional characteristics for iron-air cells are summarized below:

1. The operational temperature range is typically 25 to 60°C. The poor performance characteristics at low temperatures are due to the formation of passivating films on the iron electrode.[21]

2. The energy efficiency for the system is about 30 percent to 50 percent.[20] A cycle life of more than 1000 cycles is expected for fully optimized electric vehicle batteries.

3. Charging of prototype cells and batteries was accomplished under constant current conditions.

The Department of Energy sponsors the research, development, and engineering programs at Westinghouse. The work in Sweden is sponsored by the Swedish National Development Company and the Swedish Board for Technical Development.

No data was presented which described the effects of the electrical abuse testing as prescribed in NAVSEAINST 9310.1A. In view of the fact that iron-air electric vehicle batteries have not been fully developed or extensively tested, an assessment of the safety characteristics is not possible. Consideration must be made for thermal management (electrolyte circulation) and water loss during battery operation. The most critical safety concern is the production of large amounts of hydrogen gas during cycling. Though some hydrogen is generated during discharge and open circuit conditions, the majority of the hydrogen is produced during charge and overcharge. The energy efficiency during charge is about 30 to 50 percent. Since both hydrogen and oxygen are produced during charge, overcharge, and overdischarge conditions, the possibility of a hydrogen-oxygen fire or explosion does exist in the absence of an efficient, reliable recombination device. Because hydrogen does exhibit a broad flammability range in air, the possibility of a fire or explosion is increased and extended in pure oxygen within the cell. In addition, cell rupture could occur due to the increased pressure created by the gases within closed systems, depending on cell design and materials.

No testing was described which detailed the results of incineration testing of iron-air batteries. It should be noted that the maximum operating temperature is 60°C. The effect of high temperature exposure of the closed iron-air battery could be a thermal runaway condition with possible case rupture or expulsion of hot electrolyte.

REFERENCES

1. Cnobloch, H., "Power Sources 5," Proc. Ninth Int. Symp. Power Sources, Joint Services Electrical Power Source Committee, D.H. Collins, ed. (London: Academic Press, 1975), p. 261.

2. Lindstrom, O., "Power Sources 5," Proc. Ninth Int. Symp. Power Sources, Joint Services Electrical Power Source Committee, D.H. Collins, ed. (London: Academic Press, 1975), 283.

3. Va ;ie, P.R., and Tseung, A. C. C., Electrochim. Acta, 21, 1976, p. 299.

4. Anderson, B., and Ojefors, L., "Power Sources 7," Proc. 11th Int. Symp. Power Sources, Joint Services Electrical Power Source Committee, D.H. Collins, ed. (London: Academic Press, 1979), p. 329.

5. Roberts, R., Electrotechnology, Volume 2, Ouellette, R. P., Ellerbusch, F., and Cheremisinoff, P. N., eds. (Ann Arbor, Michigan: Ann Arbor Science, 1978), p. 366.

6. Burssell, M., "Power Sources 8," Proc. 12th Int. Symp. Power Sources, Joint Services Electrical Power Source Committee, J. Thompson, ed. (London: Academic Press, 1981), p. 513.

7. Bryant, W. A., Liu, D. T., and Buzzelli, E. S., Proc. Power Sources Symp. 28, 1979, p. 152.

8. Falk, S. U., and Salkind, A. J., Alkaline Storage Batteries (New York: John Wiley and Sons, 1969).

9. Mantell, C. L., Batteries and Energy Systems, Second Edition (New York: McGraw Hill, 1983), p. 187.

10. Vinal, G. W., Storage Batteries (New York: John Wiley and Sons, 1940), p. 76.

11. Anderson, F. C., J. Electrochem. Soc., 99, 1952, p. 244C.

12. Yao, N. P., Christianson, C. C., Elliott, R. C., and Miller, J. F., Proc. Power Sources Symp. 29, 1981, p. 247.

13. Salkind, A. J., Venuto, C. J., and Falk, S. U., J. Electrochem. Soc., 111, 1964, p. 493.

REFERENCES (Cont.)

14. Falk, U., Electrochemical Power Sources, Primary and Secondary Batteries, IEE Energy Series 1, M. Barak, ed. (London: Peter Peregrinus Ltd., 1980), p. 356.

15. Hersch, P., Trans. Faraday Soc., 51, 1955, p. 1442.

16. Ojefors, L., Electrochim Acta, 21, 1976, p. 263.

17. Hart, A. B., and Webb, A. H., "Power Sources 6," Proc. Tenth Int. Symp. Power Sources, Joint Services Electrical Power Sources Committee, D.H. Collins, ed. (London: Academic Press, 1977), p. 627.

18. Hills, S., J. Electrochem. Soc., 112, 1965, p. 1048.

19. Kordesch, K., Comprehensive Treatise of Electrochemistry, Volume 3 Electrochemical Energy Conversion and Storage, J. O'M. Bockris, B.E. Conway, E. Yeager, and R.E. White. eds. (New York: Plenum Press, 1981), p. 159.

20. McBreen, J., Comprehensive Treatise of Electrochemistry, Volume 3, Electrochemical Energy Conversion and Storage, J. O'M. Bockris, B.E. Conway, E. Yeager, and R.E. White, eds. (New York: Plenum Press, 1981, p. 308.

21. Ojefors, L., J. Electrochem. Soc., Electrochem. Science and Technol., 123, 1976, p. 1139.

J. IRON(III) – CHROMIUM(II) (REDOX)

$$Fe^{+3} \mid HCl \mid Cr^{+2}$$

$$Fe^{+3} + Cr^{+2} \rightleftharpoons Fe^{+2} + Cr^{+3} \qquad [1]$$
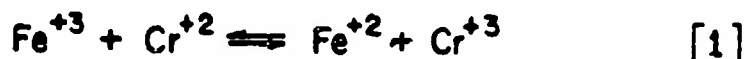
The concept for REDOX electrochemical systems is based upon cell reactions in which the reactant and product species are completely soluble metal ions which exist in two oxidation states. These systems use inert carbon current collectors and highly selective membranes which prevent the cross diffusion of the metal ions but allow the passage of anions.[1] The ideal REDOX cell would be comprised of two solutions of the same transition metal species in different oxidation states.[2] One such system which has been extensively investigated by K.D. Beccu at Battelle (Geneva) is the $Cr^{2+}-Cr^{3+}/Cr^{3+}-Cr_2O_7^{2-}$ REDOX cell.[3] Much of the developmental efforts, however, have focussed on the study of those REDOX cell systems which utilize the ionic species of two different metals. Examples for these systems include the $Fe^{2+}-Fe^{3+}/Sn^{2+}-Sn^{4+}$, the $Ti^{3+}-Ti^{4+}/Fe^{2+}-Fe^{3+}$, and the $Fe^{2+}-Fe^{3+}/Cr^{2+}-Cr^{3+}$ electrochemical couples.[3,4]

With sponsorship from the Department of Energy and the Agency for International Development, NASA-Lewis Research Center has developed a prototype iron-chromium REDOX energy storage system for use in conjuction with either solar photovoltaic or wind turbine electrical generating systems. Such a complete system would constitute an independent (or "stand alone") power supply for applications in remote geographical areas or in situations where this system is the most economical choice. Lead-acid batteries were tested as the energy storage system in the demonstration phases of the program at Schuchuli, Arizona and Tangaye, Upper Volta.[5] Several disadvantages of the lead-acid batteries were noted in these initial test programs. These included cost, reliability, maintenance, charge control, and life.[1] In view of the above, the iron-chromium REDOX battery is presently a candidate for field testing in applications such as those described.

The basic design of the iron-chromium REDOX system consists of the cell or series of cells, two storage tanks for the positive and negative electrode solutions, and two circulating pumps.[1] The current collectors are carbon felts compressed between a thin carbon bipolar plate and the ion exchange membrane. The porous carbon flow through electrode on the chromium side of the

cell must be catalyzed. The ion exchange membrane is produced by the polymerization of vinylbenzylchloride and dimethylaminoethylmethacrylate (CDL-A5-27.5NP). The purpose of the membrane is to restrict the cross diffusion of the reactant metal ions but allow the free diffusion of the anions. The 0.035 cm thick membrane is located between the two carbon current collectors. The basic cell design, therefore, consists of the bipolar plate, the carbon electrode, a gasket, a flow plate with inlet and exit ports, the ion exchange membrane, a second flow plate, gasket, the second carbon electrode, and a second bipolar plate. These cells may then be stacked to form a series connected battery. Trim cells are positioned at the end of the cell stack and automatically provide higher voltage levels when necessary. These cells can be removed from the electrical circuit when the higher voltages are not required.

A one-kilowatt (12 k Wh) solar array iron-chromium prototype battery (120 V) would consist of four cell stacks of 39 cells each with ten trim cell packs of six cells each. The volume for each reactant solution of either 1 M $FeCl_2/2N$ HCl or 1 M $CrCl_2/2$ N HCl would be about 700 liters. Though one liter of each reactant theoretically contains 26.8 Ah of capacity, only about one half this capacity is realized due to mass transport problems encountered within each reactant solution towards the end of the discharge or charge. In addition, a gradual loss of the active species occurs through cross diffusion at the membrane. Other considerations relative to the effective operation of this prototype battery are summarized:[1]

1. The rate of charge is controlled by selective use of the trim cells.

2. Separate charging and discharging stacks are used since charged solutions are returned to the same tanks from which the discharge stack assembly would draw the reactant fluids. The charge efficiency is about 70 percent.

3. The depth of discharge range is a function of the reactant flow rate, power requirements of the pumps, and shunt currents. A wide variation in the concentrations of oxidized or reduced species exists over the discharge range. These concentrations can be regulated by changing the reactant flow rates. For example, the flow requirements double when the concentrations of the reactant species are halved.

4. The electrode reactions are:

$$Fe^{3+} + e^{1-} \xrightleftharpoons[\text{charge}]{\text{discharge}} Fe^{2+} \tag{2}$$

and

$$Cr^{3+} + e^{1-} \xrightleftharpoons[\text{discharge}]{\text{charge}} Cr^{2+} \tag{3}$$

The theoretical open circuit voltage for the REDOX cell is 1.196 V. However, the open circuit voltage of the REDOX system varies as a function of the depth of discharge since these electrode reactions are heterogeneous phase reactions. For example, the open circuit voltages are 1.195, 1.075, and 0.955 V at the 10, 50, and 90 percent depth of discharge levels, respectively.

5. The only permanent loss in capacity is due to the cross diffusion of reactant species across the membrane. For the membrane used in this REDOX cell,[1] the cross diffusion rate is 12×10^{-6} g Fe per hour per cm^2 initially (i.e., the diffusion rate across the membrane into an iron-free solution). The predicted decrease in capacity due to this loss mechanism is about 10 percent in ten years, 30 percent in 30 years, and 45 percent in 110 years.

6. The theoretical energy density for the iron-chromium REDOX cell is about 100 to 120 Wh/kg.[6,7] However, the practical energy densities obtained using prototype REDOX cells are less than 30 Wh/kg at both the one and five hour discharge rates. These values are about equal to those obtained for the lead-acid system. In view of the above, the use of the REDOX system for applications other than load levelling (e.g., satellites,[7] etc.) does not appear practical.

7. The operational temperature range for the iron-chromium REDOX system is 0 to 100°C.[6]

8. Very large volumes of the reactant species are required for effective operation. This would be a distinct disadvantage if only the electrical performance of the battery is considered. However, it should be noted that the system could also be utilized as a heat storage device when coupled with a solar photovoltaic system.[6]

Because no field testing has been reported for practical iron-chromium REDOX batteries, an evaluation of the safety/hazards characteristics relative to the abuse testing procedures given in NAVSEAINST 9310.1A is not possible at this time. However, a recent study[8] has assessed the safety characteristics of a six kWh iron-chromium REDOX battery and compared them to other candidate battery systems. All batteries considered were of the six kWh design. The rankings given were on a scale of one to ten with a value of ten signifying the most safe system. The iron-chromium REDOX system achieved the highest value of nine. The report specifically stated that the REDOX battery offered "the least health and safety problems." In addition, it was pointed out that the battery operated at ambient temperature and that it contained "no hazardous substances." The reliability of the REDOX battery, however, is limited by both the plumbing and the control systems.

REFERENCES

1. Hagedord, N. H., and Thaller, L. H., "Power Sources 8," <u>Proc. 12th Int. Symp. Power Sources</u>, Joint Services Electrical Power Source Committee, J. Thompson, ed. (London: Academic Press, 1981), p. 227.

2. Douglas, D. L., and Birk, J. R., <u>Annual Review of Energy</u>, Volume 5, Hollander, J. M., Simmons, M. K., and Wood, D. O., eds. (Palo Aito, California: Annual Reviews Inc., 1980), p. 61.

3. Hart, A. B., and Webb, A. H., "Power Sources 6," <u>Proc. Tenth Int. Symp. Power Sources</u>, Joint Services Electrical Power Source Committee, Collins, D. H., ed. (London: Academic Press, 1977), p. 627.

4. Iammartino, N. R., <u>Chem. Eng.</u>, <u>82</u>, 1975, p. 48.

5. Rosenblum, L., Bifano, W. J., Hein, G. F., and Ratajczak, A. F., <u>Photovoltaic Power Systems for Rural Areas of Developing Countries</u>, NASA Scientific and Technical Information Branch, NASA No. TM-79097, 1979.

6. McBreen, J., <u>Comprehensive Treatise of Electrochemistry</u>, Volume 3, Electrochemical Energy Conversion and Storage, Bockris, J. O'M., Conway, B. E., Yeager, E., and White, R. E., eds. (New York: Plenum Press, 1981), p. 309.

7. Marcoux, L., and Marsh, R., <u>Proc. Power Sources Symp. 29</u>, 1981, p. 194.

8. Podder, A., and Kapner, M., <u>Analysis of Batteries for Use in Photovoltaic Systems, Final Report</u>, Volume 1, Department of Energy, DOE/ET/25201-1, 1981.

K. IRON – NICKEL(III)OXYHYDROXIDE   (NICKEL-IRON, EDISON CELL)

Fe | KOH | NiOOH

$$Fe + 2\,NiOOH + 2\,H_2O \rightleftharpoons 2\,Ni(OH)_2 + Fe(OH)_2 \qquad [1]$$

The iron-nickel (III) oxyhydroxide (nickel-iron) battery was developed by Jungner in Sweden and Edison in the United States at the turn of the Twentieth Century.[1-3] The major applications for this system included vehicle traction, railroad car lighting, and railroad signalling. The use of the nickel-iron battery declined considerably after 1960 because of the development of a low cost, tubular plate lead-acid battery. Westinghouse Electric Corporation, however, did continue investigations of the nickel-iron system and developed processes for the manufacture of nontubular nickel and iron electrodes.[1] With the passage of the Electric and Hybrid Vehicle Research, Development and Demonstration Act of 1976, there was renewed interest in the nickel-iron system for meeting near-term electric vehicle propulsion requirements. Both the nickel-iron and nickel-zinc systems possess theoretical energy densities (263 and 345 Wh/kg, respectively) between those of lead-acid (175 Wh/kg) and such advanced candidate electric vehicle propulsion systems as sodium-sulfur (760 Wh/kg) and lithium/aluminum-iron disulfide (650 Wh/kg). In view of the above, intense efforts by both Westinghouse and Eagle-Picher Industries, Inc., in the United States have resulted in the design, fabrication, and testing of full sized nickel-iron cells and modules.

The classical manufacturing processes for the preparation of either flat plate or sintered iron negative electrodes are given by Falk and Salkind,[4] Mantell,[5] Vinal,[6] and Anderson.[2] Recent manufacturing techniques developed by Westinghouse have produced iron electrodes with improved porosity and surface area characteristics.[1] These electrodes are prepared by pressing iron oxide paste into a steel wool matrix and sintering the material at an elevated temperature in a hydrogen reducing atmosphere. Eagle-Picher uses an iron electrode developed by the Swedish National Development Company. This plate electrode is a sintered iron powder on an expanded iron screen substrate.[7]

The initial half cell reaction for the discharge of the alkaline iron electrode is given by:

$$Fe + 2\,OH^{1-} \longrightarrow Fe(OH)_2 + 2e^{1-} \qquad (2)$$

Further discharge of the electrode would result in the formation of either $Fe(OH)_3$[8] or Fe_3O_4.[9] Such discharge beyond the first Fe (II) step produces a 0.2 V decrease in cell load voltage. In addition, higher charging rates are required and a significant amount of capacity is lost over a number of cycles for iron electrodes discharged to the higher oxidation state. Therefore, the iron electrode discharge may be limited to reaction 2 by designing practical nickel-iron cells with excess iron capacity.

The iron negative electrode in the nickel-iron cell undergoes a corrosion reaction[10-12] in accordance with:

$$Fe + 2 H_2O \longrightarrow Fe(OH)_2 + H_2 \tag{3}$$

Reaction 3 will occur spontaneously (E = - 0.05 V) since the pure iron electrode has a low hydrogen overpotential. Though the corrosion reaction is the predominant mode of self-discharge in nickel-iron cells, self-discharge may also occur through oxidation of iron by oxygen from the electrolyte and cell free space following charge, the decomposition of the nickel (III) oxyhydroxide, and from cell leakage. All self-discharge processes result in high initial capacity losses of about 1.5 percent per day for cells on open circuit stand.[10]

Because of the low overvoltage of hydrogen on the pure iron electrode, large amounts of hydrogen are produced during battery charging:

$$2 H_2O + 2e^{1-} \longrightarrow H_2 + 2 OH^{1-} \tag{4}$$

As a result, the energy efficiency of the iron negative electrode is low compared to the lead-acid battery. Typical charge acceptance efficiencies of 50 to 60 percent are observed for the electric vehicle nickel-iron battery compared to a 75 percent charge acceptance efficiency for the lead-acid battery.[13] The evolution of large amounts of hydrogen is also accompanied by significant heat generation which further results in water loss from the electrolyte. In view of the above, provision for electrolyte cooling, venting and gas recombination devices, heat exchangers and hydrogen separation must be considered to minimize the safety hazards associated with hydrogen production and attendant thermal management problems during charging. Westinghouse has developed a circulating electrolyte management system which either may be installed with the battery on the electric vehicle or may be included only with the battery charging unit.[14,15]

The nickel (III) oxyhydroxide positive electrode may be produced by either electrochemical impregnation or pasting processes. Westinghouse employs a nickel coated steel wool current collector to increase the surface area and porosity. Eagle-Picher, on the other hand, uses a 0.20 to 0.24 cm thick porous, sintered nickel plaque prepared by the "double pass" method. The plaque is then electrochemically impregnated with the active positive electrode material at loading densities of about 1.6 g/cm^2.[7] Another electrode preparative technique is the pressed powder method used by VARTA.[16] A mixture of $Ni(OH)_2$ containing cobalt and cadmium, graphite, and Teflon is pressed onto plates and connected to two layers of expanded nickel screen. The inclusion of the cobalt and cadmium additives in the positive electrode results in higher charge efficiencies. All nickel-iron cells are positive electrode limited in order to reduce the possibility of the discharge of the iron electrode beyond the Fe^{2+} state. During charging, oxygen is evolved at the nickel electrode in accordance with the reaction:

$$4 \ OH^{1-} \longrightarrow O_2 + 2 \ H_2O + 4e^{1-} \tag{5}$$

Optimization of the nickel-iron battery for applications such as electric vehicle propulsion which require high energy densities has necessitated the replacement of spacers as the means of electrode separation by thin sheets of porous polyvinylchloride (PVC) film. Since the nickel (III) oxyhydroxide electrode exhibits a tendency to swell, disintegration and loss of contact with the current collector will occur after initial cycling. Thus, the positive electrode requires a uniform pressure on the entire electrode area. This is accomplished through use of the separator and an external clamping device which may also serve as a state-of-charge indicator.[17] The indicator/clamping device relies on the pressure characteristics of the nickel-iron cell or battery during various operational stages. For example, the pressure will gradually decrease to minimum values during charging due to a decrease in the amount of the more voluminous discharge products. The partially or fully discharged nickel-iron cell will exhibit higher or the maximum pressure values, respectively. During cell discharge, a linear relationship between pressure and capacity exists. A nonlinear relationship exists during charge, however.

The electrolyte consists of approximately 4.5 M (20 weight percent) KOH with a LiOH additive at concentration levels of 0.2 to 2.0 M. The inclusion of LiOH improves the utilization of both the iron and nickel electrodes. It is believed[8] that the lithium incorporated into the iron electrode as Li^{1+} results in the improved ionic conductivity of the $Fe(OH)_2$ lattice. Iron electrodes discharged in a KOH-LiOH electrolyte showed capacity increases of more than 30 percent compared to the iron electrodes discharged in the pure KOH electrolyte.[18] Similar beneficial effects of LiOH addition have been observed for the positive nickel (III) oxyhydroxide electrode.[19] Significant capacity increases of more than 20 percent have been observed for the positive electrode in cells containing electrolyte with 2 M LiOH. The most important effect of the LiOH addition is the increase in the cycle life characteristics for the nickel-iron system. Cells containing the electrolyte may attain more than 2000 cycles before the capacity of the nickel electrode decreases to one-half the nominal value. Cells which contained pure KOH electrolyte achieved 100 cycles. Some nickel-iron cells may also contain sulfur, iron sulfide, or potassium sulfide in the electrolyte.[3,8,16,17] The addition of sulfur results in the activation of the iron oxides with subsequent breakdown of passivating layers on the iron surface. The electrode, therefore, is kept in an active state.[3] Vassie[8] found that the self-discharge (corrosion) of the iron electrode is decreased by the addition of FeS due to an increased hydrogen overpotential at the electrode.

The present nickel-iron cell designs for electric vehicle (EV) applications differ markedly from the classical designs described by Vinal,[6] Falk and Salkind,[4] and Mantell.[5] The nickel-iron battery must provide a sufficient increase in energy density to compete effectively with such other near term electric vehicle propulsion candidates as the nickel-zinc and the Improved State-of-the-Art (ISOA) lead-acid batteries. In view of the above, several changes in the basic design of the nickel-iron system were made. These changes included the use of lighter cell container materials, reduced amounts of excess electrolyte, and the elimination of some inactive material in electrodes. Though the reduction in the amount of electrolyte does correspond to a significant weight saving, hydrogen evolution during charge consumes large

amounts of water from the electrolyte. Therefore, significant attention must be directed toward maintaining electrolyte levels for the safe and efficient operation of the battery. VARTA,[16,17] on the other hand, installs gas recombination devices on each cell. The recombination device consists of a supported palladium catalyst reactor which recombines the hydrogen and oxygen generated during charging. The lifetime of the above recombination device is about one year in the nickel-iron cell.[17]

The open circuit voltage for the nickel-iron cell is 1.37 V. The performance characteristics were obtained for Eagle-Picher prototype 280 Ah nickel-iron cells designed for electric vehicle applications.[7] The cells, which were 6.9 cm wide, 18 cm long, and 27 cm high, weighed 7.1 kg. After being charged at the C/4 (65 A) rate, these cells were discharged under constant current conditions at rates of C/6 to 1.3 C (45 to 360 A). Realized capacities of 280 Ah or higher were obtained for the cells discharged at the lower rates of 45 and 90 A to a 1.0 V voltage cutoff level. Lower realized capacities of 270 to 240 Ah were obtained for cells discharged at the 180 and 360 A rate, respectively. The corresponding energy density values for these cells varied from 37 to 50 Wh/kg.

The Department of Energy (DOE) and Argonne National Laboratories (ANL) jointly sponsor the research, development and engineering programs of candidate battery systems suitable for near term electric vehicles.[1] The three candidate systems tested in this program were:[20] the Improved State-of-the-Art (ISOA) lead-acid (Globe, Exide, and Eltra), the nickel-zinc (Energy Research Corp., Exide, and Gould), and the nickel-iron (Westinghouse and Eagle-Picher). Both Eagle-Picher and Westinghouse supplied 80 and 90 cell nickel-iron batteries for testing at the Jet Propulsion Laboratory under this program.[21] The features and results for the Eagle-Picher VNF 300 batteries are summarized below:

1. The battery weights were 595 kg and 670 kg for the 80 and 90 cell (300 Ah nominal capacity) batteries, respectively.

2. There was no provision for handling gases produced during charge. Each cell was vented to the atmosphere and required separate maintenance.

3. The battery was charged at a constant current of 60 A to 120 percent of the discharged capacity. All nickel-iron batteries were discharged within ten minutes following recharge due to self-discharge considerations.

4. The internal resistance was significantly higher than that for the ISOA lead-acid battery. This resulted in large voltage drops with attendant battery heating.

5. The energy efficiency for the battery was about 60 percent. This resulted in the evolution of 2300 liters of H_2 per cycle (900 liters for the ISOA lead-acid).

6. The capacity was found to be insensitive to the discharge rate. This battery achieved the highest energy densities (38 Wh/kg) for any battery in these tests.

7. The capacity losses on open circuit stand following charging were found to be 3.1 percent after 0.5 h, 12 percent after 24 h, and 15 percent after 67 h.

8. The battery consumed 1.7 l of water each cycle (2300 l H_2 released each cycle).

9. The self-heating for the battery was 14 and 5.2°C to battery depletion and to the 50 percent discharge level, respectively. The temperature increases noted during recharge after complete and partial discharge were 9 and 7°C, respectively.

10. The primary failure[20] modes were found to be nickel electrode swelling, electrolyte starvation, and pore blockage.

The features and results for the Westinghouse nickel-iron battery are summarized below:

1. The weight for the 80 cell battery was 607 kg.

2. An electrolyte management system (EMS) was provided. The main functions of the EMS were to control the battery temperature, to separate gasses from the electrolyte and safely vent them to the atmosphere, to provide excess electrolyte during charging, to prevent overpressure in the system, to isolate the electrolyte from the atmosphere (prevent carbonation), and to provide single access for water and electrolyte replenishment.

3. The battery was charged at 70 A until the voltage reached 157 V. The current was then allowed to taper. Charging terminated when cells attained 300 Ah.

4. The energy efficiency was about 39 percent and resulted in the evolution of 2600 liters of hydrogen per cycle.

5. The internal resistance of the battery was significantly higher than that for the 180A lead-acid (resistive heating).

6. The Westinghouse battery exhibited the lowest energy density for any of the systems tested. Significant voltage drops were observed especially during the vehicle acceleration tests (cell voltages of 0.5 V during acceleration and 1.0 V during cruise or idle tests).

7. The capacity losses on open circuit stand following charging were found to be 4.0 percent after 0.5 h, 13.6 percent after 24 h, and 27.1 percent after 72 h.

8. The self-heating on discharge for the battery was about 22°C to battery depletion.

9. The primary failure modes were found to be electrolyte leakage, cell case cracking, and cell rupture.

Additional characteristics for nickel-iron cells and batteries are summarized below:

1. The operational temperature range for the system is typically 0 to 45°C although useful capacity can be obtained for batteries discharged at low temperatures and at low rates (e.g., 50 percent realized capacity at the C/8 rate at -18°C).[9] The poorer performance characteristics at low temperatures are due to the formation of passivating films on the iron electrode.[22]

2. Ventilation must be provided to nickel iron batteries when discharged at elevated temperatures or to depths of discharge greater than 80 percent.

3. Charging of the nickel-iron battery may be accomplished with constant current, constant potential, or taper charging units. It should be noted that charging at rates higher than 0.2 C could result in overheating and possible thermal runaway.

4. The lifetime for the nickel-iron battery is from 7 to 25 years, depending on usage. A cycle life of 2000 to 4000 deep discharge cycles are routinely obtained from this battery system.

5. One of the most important advantages of the nickel-iron system is the ability to withstand severe mechanical and electrical abuse.

6. Prior to long-term storage, nickel-iron batteries are deep discharged and subsequently stored in the short circuited state.

The nickel-iron battery system has historically enjoyed the reputation of extreme high tolerance to such electrical abuse as short circuit, overdischarge, and overcharge.[3,4,10] Indeed, terms such as "virtually foolproof electrically" and "non destructible" are applied to the nickel-iron battery relative to both the electrical safety characteristics and mechanical stability of the system.[3] Though the above descriptions specifically relate to the "first generation" nickel-iron batteries produced from 1900 to 1970, the above terms may be generally applied to the present nickel-iron batteries considered for electric vehicle propulsion. It should be noted, however, that the modern nickel-iron battery was optimized relative to both energy density and rate capability. The requirement for weight reduction of the battery has resulted in the replacement of the steel case by plastic materials such as polyethylene, etc.[16] As a consequence, the nickel-iron battery may not presently possess the structural characteristics required for severe mechanical abuse or the high pressures encountered during charging.

No data was presented which described the effects of short circuiting nickel-iron cells or batteries. However, Eagle-Picher 280 Ah cells were discharged under constant current conditions at the 1.3 C rate (360 A) at ambient temperature.[7] The realized capacity and average cell voltage for the test were 240 Ah and 1.09 V, respectively. The discharge rate corresponds to a load of approximately 3×10^{-3} ohms. This resistance value is significantly less than the maximum resistance value of 10×10^{-3} ohms prescribed in the short circuit test procedure of NAVSEAINST 9310.1A.

Though no specific tests were performed to determine the safety/hazards characteristics for nickel-iron cells subjected to forced overdischarge procedures, electric vehicle propulsion cells were inadvertently overdischarged during performance evaluation tests.[21] A battery consisting of 90 discharged cells was assembled with 42 cells installed backwards. The battery was then charged at the C/4 (70 A) rate for four hours. All 42 cells were driven to negative voltage levels before the installation error was discovered. Subsequent testing of the 42 cells revealed that there was no discernible decrease in capacity or effect on the cycling characteristics.

Extensive overcharge testing was not reported for the nickel-iron electric vehicle propulsion batteries. It should be noted that, under some charging conditions (i.e., constant potential or constant current at rates greater than 0.2C), the battery may experience thermal runaway with the expulsion of hot, corrosive KOH electrolyte through either the venting devices or the case. The most critical safety concern is the production of large amounts of hydrogen gas during cycling. Though some hydrogen is generated during discharge, the majority of hydrogen is produced during charge and overcharge. The amounts of hydrogen produced for the Eagle-Picher and Westinghouse electric vehicle batteries were 2300 and 2600 liters, respectively, per cycle. In the former case, the Eagle-Picher battery accepted most of the charge for the first 3.5 hours of charging and experienced increases in both the gas evolution rate and temperature during the last 1.5 hours of charging.[21] The Westinghouse battery began to evolve significant amounts of hydrogen after only 0.5 hour of charging. Since both hydrogen and oxygen are produced during charge and overcharge conditions, the possibility of a hydrogen-oxygen fire or explosion does exist. Because hydrogen exhibits a broad flammability range in air, the possibility of a fire or explosion is increased and extended with the presence of oxygen within the cell. In addition, cell rupture may occur due to the increased internal pressure created by the gasses.

No testing was described which detail the results of incineration testing of nickel-iron batteries. It should be noted that the recommended maximum operating temperature is 45°C. The effect of high temperature exposure of the present nickel-iron battery could lead to a breakdown of the PVC separator and massive internal short circuiting. The battery would then enter a thermal runaway condition with possible case rupture and expulsion of the electrolyte.

A study has been completed which assessed the relative safety of a number of conventional and advanced battery systems.[23] All batteries considered were of a 6 k Wh design and were evaluated on a scale of one to ten (ten signifying the most safe battery system). The "Redox" iron-chromium system was ranked highest at a value of nine. The lead-acid, nickel-iron, nickel-zinc, and zinc-ferrocyanide systems were classified as eight. The ambient temperature systems of lead-acid, nickel-zinc and nickel-iron are "proven to be safe." The report does note that the reliability of the lead-acid and nickel-iron systems is also high at a value of nine (second only to the nickel-hydrogen system) but the performance can be damaged by exposure to either overdischarge or overcharge conditions.

REFERENCES

1. Yao, N. P., Christianson, C. C., Elliott, R. C., and Miller, J. F., Proc. Power Sources Symp. 29, 1981, p. 247.

2. Anderson, F. C., J. Electrochem. Soc., 99, 1952, p. 244C.

3. Gross, S., Energy Conversion, 15, 1976, p. 95.

4. Falk, S. U., and Salkind, A. J., Alkaline Storage Batteries (New York: John Wiley and Sons, 1969), p. 95.

5. Mantell, C. L., Batteries and Energy Systems, Second Edition (New York: McGraw Hill, 1983, p. 187.

6. Vinal, G. W., Storage Batteries (New York: John Wiley and Sons, 1940), p. 76.

7. Hudson, R., and Broglio, E., Proc. Power Sources Symp. 29, 1981, p. 259.

8. Vassie, P. R., and Tseung, A. C. C.; Electrochim. Acta, 21, 1976, p. 299.

9. Salkind, A. J., Venuto, C. J., and Falk, S. U., J. Electrochem. Soc., 111, 1964, p. 493.

10. Falk, U., Electrochemical Power Sources, Primary and Secondary Batteries, IEE Energy Series 1, M. Barak, ed. (London: Peter Peregrinus Ltd., 1980), p. 356.

11. Hersch, P., Trans. Faraday Soc., 51, 1955, p. 1442.

12. Ojefors, L., Electrochim. Acta, 21, 1976, p. 263.

13. Collie, M. J., Electric and Hybrid Vehicles, Energy Technology Review No. 44, M.J. Collie, ed. (Park Ridge, New Jersey: Noyes Data Corporation, 1979), p. 181.

14. Feduska, W., and Voill, R. E., Battery Design and Optimization, The Electrochemical Society Softbound Proceedings Series, S. Gross, ed., 79-1, 1979.

15. Hill, R. E., Rosey, R., and Voill, R. E., Proc. Power Sources Symp. 28, 1979, p. 149.

REFERENCES (Cont.)

16. Lexow, K. W., Kramer, G., and Oliapuram, V. A., "Power Sources 8," Proc. 12th Int. Symp. Power Sources, Joint Services Electrical Power Source Committee, J. Thompson, ed. (London: Academic Press, 1981), p. 389.

17. Lexow, K. W., Kramer, G., and Oliapuram, V. A., Proc. Power Sources Symp. 29, 1981, p. 256.

18. Hills, S., J. Electrochem. Soc., 112, 1965, p. 1048.

19. Falk, S. U., and Salkind, A. J., Alkaline Storage Batteries (New York: John Wiley and Sons, 1969), p. 613.

20. Chemical Engineering Division Annual Technical Report, 1981, Argonne National Laboratories, Report No. ANL-82-23, Dept. of Energy No. DE82019248, 1982, p. 40.

21. Hewitt, R., and Bryant, J., Testing of the Eagle-Picher Nickel-Iron, the Globe ISOA Lead-Acid, and the Westinghouse Nickel-Iron Batteries for Electric Vehicle Propulsion, U.S. DOE Contract AI01-78CS54209, Dept. of Energy No. DE83-003283, Jet Propulsion Laboratory, Pasadena CA, 1982.

22. Ojefors, L., J. Electrochem. Soc., Electrochem. Science and Technol., 123, 1976, p. 1139.

23. Poddes, A., and Kapner, M., Analysis of Batteries for Use in Photovoltaic Systems, Final Report, Volume 1, Department of Energy, DOE/ET/25201-1, 1981.

L. IRON-SILVER OXIDE

$$Fe \mid KOH \mid Ag_2O_2, Ag_2O$$

$$3\,Fe + 2\,Ag_2O_2 + 4\,H_2O \rightleftharpoons Fe_3O_4 \cdot 4\,H_2O + 4\,Ag \qquad [1]$$

The iron-silver oxide secondary battery was developed recently by Buzzelli at Westinghouse to provide a high energy density power source alternative to the zinc-silver oxide battery.[1] The tendency of the zinc electrode in the zinc-silver oxide system to undergo shape change during cycling limits the life of the battery. The replacement of the zinc electrode by an iron electrode was believed to not only alleviate the problems associated with the zinc negative electrode but to also maintain the high energy and power densities while increasing the cycle life at deep discharge. Though the present applications of the iron-silver oxide battery are limited to use as an emergency power source in high altitude balloon telecommunications systems, the fully developed system may fulfill the requirements of several future U.S. Navy applications.

The electrochemical reaction given in equation 1, above, represents the complete discharge reaction for the cell. The formation of either Fe_3O_4[2] or $Fe(OH)_3$[3] as the final discharge product is not advantageous for long cycle life. Such a discharge produces a significant decrease in cell load voltage. In addition, higher charging rates are required and significant losses in capacity are observed for iron electrodes discharged to the higher oxidation state. The initial discharge reaction for this system is given by:

$$Fe + Ag_2O_2 + H_2O \longrightarrow Fe(OH)_2 + Ag_2O \qquad (2)$$
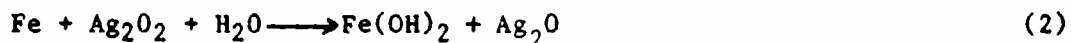
The theoretical open circuit voltage for the above reaction is 1.484 V. Further discharge of the iron-silver oxide cell results in a second discharge step in accordance with:

$$Fe + Ag_2O + H_2O \longrightarrow Fe(OH)_2 + 2\,Ag \qquad (3)$$
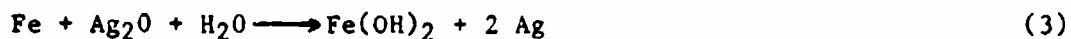
The theoretical open circuit voltage for reaction 3 is 1.222 V. The extent of cell discharge is limited to reaction 3 by designing practical iron-silver oxide cells with excess iron capacity.

The iron negative electrode in the cell will experience a corrosion reaction which results in the production of hydrogen:[4-6]

$$Fe + 2 H_2O \longrightarrow Fe(OH)_2 + H_2 \qquad (4)$$

Reaction 4 will occur spontaneously (E = -0.05 V) since pure iron electrode material has a low hydrogen overpotential. This corrosion reaction represents the predominant mode of self discharge in iron-silver oxide cells. However, other self-discharge processes can occur within the cell.[5] The oxidation of iron by oxygen from the electrolyte and from the atmosphere of the cell free space can also occur. In addition, oxygen species may also be present from the decomposition of the silver oxide positive material and from cell leakage.

Since there exists a low overvoltage of hydrogen on the pure iron electrode, large amounts of hydrogen are produced during cell charging:

$$2 H_2O + 2e^{1-} \longrightarrow H_2 + 2 OH^{1-} \qquad (5)$$

As a result, the energy efficiency of the negative electrode is low compared to other systems such as the lead-acid battery.[7] For example, charge acceptance efficiencies of 50 to 60 percent are typical values for iron electrode systems. Charge acceptance efficiencies of more than 75 percent are observed for the lead-acid battery.[7]

No specific details relative to the preparation of the iron negative plate electrodes were given.[1] The cells contained seven iron plates with the dimensions 8.9 cm X ' ' cm. Five of the iron electrodes were 0.22 cm thick and were positioned betwec che silver positive electrodes. Two iron electrodes of 0.14 cm thickness comprised the outer negative electrode plates.

The six positive silver electrode plates were 8.6 cm high X 15.2 cm wide X 0.12 cm thick. The total surface area for the silver electrode in these cells was 1564 cm^2. Details relative to the preparation of these electrodes were also not given. The separator consisted of multilayered polypropylene with three layers of microporous sheets 0.003 cm thick between four layers of a 0.015 cm thick nonwoven mat. The separator assembly was formed into a heat-sealed envelope which surrounded the iron electrodes.

The electrolyte for the iron-silver oxide cell was 7 M KOH containing 15 grams of LiOH per liter. The addition of LiOH to the electrolyte results in the improvement in the utilization of the iron electrode. It is believed that the incorporation of lithium into the iron electrode as Li^{1+} results in the improved ionic conductivity of the Fe(OH)$_2$ lattice.[3] Capacity increases of more than 30 percent were observed for iron electrodes discharged in KOH electrolyte containing LiOH.[8] Similar beneficial effects are not obtained for the silver oxide electrode.[9]

The open circuit voltage for the iron-silver oxide cell is 1.48 V. The performance characteristics for 140 Ah cells were obtained after an initial charge cycle required to form the silver oxide electrode.[1] Cells were charged under constant current conditions at a current density of 16 mA/cm^2. The two charging voltage plateaus corresponded to the formation of Ag$_2$O at 1.6 V and Ag$_2$O$_2$ at 1.75 V. The charging mode was continued into the overcharge state

for an extended period. Hydrogen was evolved at the iron electrode in accordance with reaction 5 and oxygen was evolved at the silver electrode in accordance with the reaction:

$$4 \ OH^{1-} \longrightarrow O_2 + 2 \ H_2O + 2e^{1-} \tag{6}$$

The cells were allowed to stand on open circuit for one hour prior to discharge. The performance characteristics were then obtained for cells discharged at the 10 A (C/14 rate, 6.4 mA/cm^2), 45 A(C/3 rate, 29 mA/cm^2), and 80 A (C/1.75 rate, 51 mA/cm^2) rates to a 100 percent utilization of the silver electrode. The discharge curves show two distinct load voltage plateaus for the reduction of Ag_2O_2 and Ag_2O respectively. The realized capacities for cells discharged at the 10 A, 45 A, and 80 A rates were 152, 147, and 142 Ah, respectively, to a load voltage cutoff level of 0.9 V. The corresponding energy density values were 106, 97, and 87 Wh/kg. The open circuit voltage for discharged cells was 1.2 V.

Other features of the iron-silver oxide system are summarized below:

1. The self-discharge current for the 140 Ah cells was 30 mA. This value corresponded to a loss of about 0.7 Ah per day (0.5 percent of the nominal capacity).

2. Capacity maintenance may be accomplished by either constant current float charging at low rates (e.g., 0.25 A) or by periodic pulse charging (e.g., 4 A for one hour per day). Both charging methods result in equivalent capacity retention.

3. The operational temperature range of the iron-silver oxide cell is -18 to 80°C. It should be noted that an auxiliary heating system is required for effective operation at the lower temperatures. The poorer performance characteristics observed for unheated cells at the lower temperatures are due to the formation of passivating films on the iron electrode.[10]

4. The wet life of the system was observed to be more than one year if periodic cycling was performed.

5. The cycle life for the iron-silver oxide system exceeded 150 cycles at a 100 percent depth of discharge of the silver oxide electrode.

Specific details relative to the design and construction of the iron-silver oxide cells were not reported.[1] Such design features as vent structures, fusing, thermal and electrolyte management measures, and control devices for the gases produced during overcharge and overdischarge would be necessary to accurately assess the safety features of the system. No data was presented which described the effects of short circuit testing of the iron-silver oxide cells or batteries. However, 140 Ah cells were discharged under constant current conditions at the C/1.75 rate (80 A) at ambient temperatures. The realized capacity and average cell load voltage for the test were 142 Ah and 1.00 V, respectively. The discharge rate corresponded to a constant resistive load of approximately 12.5×10^{-3} ohms. This resistive value is only slightly higher than the maximum resistance value of 10×10^{-3} ohms prescribed in the short circuit test procedure of NAVSEAINST 9310.1A.

Iron-silver oxide cells were overdischarged at high and low rates to the point of cell voltage reversal and gas evolution at the electrodes (i.e., hydrogen evolution at the silver oxide electrode and oxygen evolution at the iron electrode). No effect relative to either the safety or to the capacity for any of these test cells was observed.

Iron-silver oxide cells were routinely charged under constant current conditions of 25 A for eight hours.[1] Since the nominal capacity for the cells was 140 Ah, the duration of the overcharge period was more than two hours at a voltage of 1.90 V. Both hydrogen and oxygen were evolved during this time. No deleterious effects relative to safety or to cell performance were obtained for cells subjected to this charge regime. However, since both hydrogen and oxygen are produced during overcharge and overdischarge conditions, the possibility of a hydrogen-oxygen fire or explosion does exist. Because hydrogen possesses a broad flammability range in air, the probability of a fire or explosion is increased and extended for oxygen enriched atmospheres.

No testing was reported which describe the results of incineration tests with iron-silver oxide cells or batteries. The effect of high temperature exposure of the cells could lead to a breakdown of the separator material and massive internal short circuiting accompanied by thermal runaway. Depending on the cell design characteristics, the thermal runaway condition could result in case rupture and expulsion of hot, corrosive KOH electrolyte through the cell closure.

REFERENCES

1. Buzzelli, E. S., *Proc. Power Sources Symp. 28*, 1979, p. 160.

2. Salkind, A. J., Venuto, C. J., and Falk, S. U., *J. Electrochem. Soc.*, 111, 1964, p. 493.

3. Vassie, P. R., and Tseung, A. C. C., *Electrochim. Acta*, 21, 1976, p. 299.

4. Falk, U., *Electrochemical Power Sources*, Primary and Secondary Batteries, IEE Energy Series 1, M. Barak, ed. (London: Peter Peregrinus Ltd., 1980), p. 356.

5. Hersch, P., *Trans. Faraday Soc.*, 51, 1955, p. 1442.

6. Ojefors, L., *Electrochim. Acta*, 21, 1976, p. 263.

7. Collie, M. J., *Electric and Hybrid Vehicles*, Energy Technology Review No. 44, M.J. Collie, ed. (Park Ridge, New Jersey: Noyes Data Corporation, 1979), p. 181.

8. Hills, S., *J. Electrochem. Soc.*, 112, 1965, p. 1048.

9. Falk, S. U., and Salkind, A. J., *Alkaline Storage Batteries* (New York: John Wiley and Sons, 1969), p. 619.

10. Ojefors, L., *J. Electrochem. Soc.*, Electrochem. Science and Technol., 123, 1976, p. 1139.

M. LEAD-LEAD DIOXIDE (LEAD ACID)

$$Pb \mid H_2SO_4 \mid PbO_2$$

$$Pb + PbO_2 + 2H_2SO_4 \rightleftharpoons 2PbSO_4 + 2H_2O \qquad [1]$$

The lead-lead dioxide-sulfuric acid (lead-acid) secondary battery system was first demonstrated and patented in 1860[1,2] by G. Plante. Significant developments from that time to the present include the production of pasted plates by Foure in 1881 and Tudor in 1883,[2,3] lead-antimony grids by Sellon in 1881,[1,3] the "double-sulfate reaction scheme" by Gladstone and Tribe in 1882,[2,3] tubular plate construction in the period 1890 to 1910,[2,3] the lead-calcium alloy grid by Haring and Thomas in 1935, and sealed and maintenance free lead-acid batteries in the period of 1970 to the present.[3]

Detailed descriptions for the lead-acid battery system are given by Bode,[1] Ruetschi,[2] Salkind, Mayer, and Linden,[3] Kordesch,[4] Burbank, Simon, and Willihnganz,[5] Carr and Hampson,[6] Barak,[7] Smith,[8] and Vinal.[9]

The lead-lead dioxide-sulfuric acid cell is comprised of a highly porous, spongy lead negative electrode, a lead dioxide positive electrode, and a solution of dilute sulfuric acid as the electrolyte. Various types of separators have been used in the lead-acid battery. These include specially treated wood (before 1940), microporous plastics (polyvinylchloride, polyethylene, and polypropylene), resin treated cellulose, glass wool, and rubber.[3,8,10]

The electrochemically active materials are supported upon grid structures comprised of lead alloys. Pure lead electrodes are only employed in cells of special designs such as the sealed lead acid cell[11] and the Bell Telephone cylindrical lead-acid reserve battery.[12] The addition of four to twelve weight percent antimony to pure lead improves both the mechanical properties (e.g., increased rigidity) and the casting characteristics. Antimony has been shown to impart several effects on the PbO_2 positive electrode by lowering the oxygen overvoltage and preventing the loss of PbO_2 by "shedding." However, antimony is oxidized during overcharge conditions[7] and by the PbO_2 in the positive plate.[13] This latter effect contributes significantly to the self-discharge of the positive electrode. Most of the dissolved antimony is subsequently reduced at the lead negative electrode. Since the hydrogen overpotential is less than that for pure lead, a self-discharge reaction with

239

the evolution of hydrogen will occur. During subsequent charging, metallic antimony will react to form stibine, SbH_3 at voltages above 2.45 V:[7,14]

$$Sb + 3 H^{1+} + 3e^{1-} \longrightarrow SbH_3 \qquad (2)$$

The remainder of the antimony in the lead negative electrode severely inhibits the charge acceptance at the electrode which creates the need for extended overcharge conditions. Extended overcharge of lead-acid cells causes loss of water by electrolysis and accelerates grid attack. Grid assemblies containing reduced amounts of antimony (less than four percent Sb) must be combined with arsenic (0.2%) and/or tin (0.5%) to produce electrodes with favorable microstructure characteristics,[5] increased corrosion resistance, and favorable casting characteristics. It should be noted that arsenic will produce arsine, AsH_3, in a reaction similar to equation 2, above.

An alternative lead-calcium grid material was developed by Bell Laboratories for use in early float type standby batteries.[15] At the present time, lead-calcium (0.08%) grids with small amounts of tin (0.5%) find application in the maintenance-free (MF) lead-acid battery. The main advantage for the lead-calcium grid relates to the high corrosion resistance with significantly less gassing during charge conditions and the reduced requirements for water additions. It should be noted, however, that premature battery failures could result from active material shedding, high resistances between the grid and active material,[7] and abnormal grid growth behavior.[16]

With the exception of sealed lead-acid cells/batteries, only two types of electrode structures are currently in use, the pasted plate and the tubular plate designs.[2] Typically, pasted plates are prepared by mixing appropriate amounts of "grey oxide" (60 to 70 percent beta-lead oxide, PbO, and 40 to 30 percent lead) with water, sulfuric acid, and additives to a uniform consistency and applied to the grid structures by mechanical or manual techniques. Specific additives (expanders) to the lead negative electrode paste material include lamp black,[17] barium sulfate,[17-22] and lignosulfonate salts.[18,20-23] The effect of these expanders is to increase the porosity of the lead material, to improve the charge/discharge reactions, and to enable more uniform distribution of the reaction product throughout the electrode.[7] Additives to the lead oxide positive electrode paste material include silica gel or fibrous materials (wood pulp and synthetic plastics), and sand.[7] These materials act to increase the porosity. The resultant electrodes are cured, electrochemically formed (charged) in a dilute solution of sulfuric acid, and dried. The lead electrode is a light gray sponge while the lead oxide electrode is maroon. Tubular plate electrodes consist of porous tubes of glass or polyester fibers filled with oxidized lead with appropriate additives. Current collection for the tubes comprising the plate is effected by using a lead alloy wire. The assembled plates are then charged in dilute sulfuric acid. This results in the formation of sponge lead negatives and lead dioxide positives.

The discharge reaction at the negative electrode proceeds by the dissolution of lead followed by the precipitation of lead sulfate in accordance with:

$$Pb \longrightarrow Pb^{2+} + 2e^{1-} \qquad (3)$$

and

$$Pb^{2+} + SO_4^{2-} \longrightarrow PbSO_4(s) \tag{4}$$

The standard potential for the combined equations 3 and 4 is -0.3588 V. Hydronium ions will be reduced in acidic media to form hydrogen according to the reaction:

$$2 H_3O^{1+} + 2e^{1-} \longrightarrow 2 H_2O + H_2 \tag{5}$$

The standard potential for equation 5 is 0.00 V. It can be seen, therefore, that hydrogen will be evolved under all open circuit conditions, the amount of which is dependent upon the hydrogen overvoltage on the lead. Cells containing pure lead or lead-calcium alloys exhibit low hydrogen generation rates due to the high hydrogen overvoltage while cells containing lead-antimony alloys exhibit high hydrogen generation rates.

The fully charged lead oxide positive electrode is comprised of a mixture of alpha-PbO_2 (orthorhombic columbite structure) and beta-PbO_2 (tetragonal rutile structure).[6] The relative amounts of alpha-PbO_2 and beta-PbO_2 change during normal cell cycling. Alpha-PbO_2 will discharge to $PbSO_4$ and be converted to beta-PbO_2 with subsequent charging. Continued cycling results in a coating of beta-PbO_2 over a composite of both PbO_2 forms. The electrode content of both forms reach an equilibrium value after several cycles.[5] It is important to note that PbO_2 is a non-stoichiometric compound. The true composition of the compound is generally accepted as varying from $PbO_{1.95}$ to $PbO_{1.98}$,[6] but some investigators believe that the lead oxide compound is $PbO_{1.80}$ to $_{1.98}$ $(OH)_{0.11}$ to $_{0.26}$.[5]

The discharge reaction at the positive electrode proceeds by the dissolution of lead oxide, PbO_x (where x varies from 1.95 to 1.98) followed by the precipitation of lead sulfate in accordance with:

$$PbO_2 + 4 H^{1+} + 2e^{1-} \longrightarrow Pb^{2+} + 2 H_2O \tag{6}$$

and

$$Pb^{2+} + SO_4^{2-} \longrightarrow PbSO_4(s) \tag{7}$$
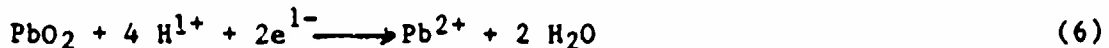
The standard potential for the combined equations 6 and 7, is +1.682 V. Water will be oxidized in acidic media to form oxygen according to the reaction:

$$2 H_2O \longrightarrow O_2 + 4 H^{1+} + 4e^{1-} \tag{8}$$

The standard potential for reaction 8 is -1.229 V, or about 0.45V below that for the lead oxide positive electrode. Oxygen evolution will then occur, dependent upon the acid concentration and impurity level (e.g., antimony, silver, cobalt, etc.).

The theoretical open circuit voltage for the cell reaction between lead and lead dioxide in acidic media is appoximately 2.04 V. However, the open circuit voltage varies with the concentration of the sulfuric acid. It can be seen from equation 1 that sulfuric acid does indeed participate in the cell reaction and

ie, for all practical purposes, an electrochemically active material. Thus, the open circuit voltage for the lead-acid cell will also be dependent upon the concentration of the acid. For example, the normal concentration of H_2SO_4 in a fully charged Starting, Lighting, and Ignition (SLI) cell is 1.28 g/cm^3 (485 g H_2SO_4 per liter). The open circuit voltage for the cell is 2.12V. As cell discharge proceeds, the acid will be consumed and the open circuit voltage will decrease. At 50, 25, and 0 percent state of charge levels, the open circuit voltages are, respectively, 2.03, 2.00, and 1.96 V. These values may be predicted by the equation:[24]

$$E = density (g/cm^3) + 0.84 \qquad (9)$$

Under normal conditions, the state of charge for the lead-acid cell may be easily obtained by measuring the electrolyte density. However, sulfuric acid may be consumed extensively during the corrosion process which forms $PbSO_4$ (one type of "sulfation"). The addition of more electrolyte to the cell under these conditions will lead to higher acid concentrations upon charging. Increased acid concentrations above the recommended level result in more vigorous corrosion reactions.[9] The most common type of sulfation relates to the formation of large, electrochemically inactive crystals of $PbSO_4$ as a consequence of extended storage of the battery in the discharged state, the unnecessary addition of sulfuric acid to the electrolyte, cell operation at elevated temperatures, and undercharging.[9] In some cases, sulfation may be remedied by cycling the cell/battery at low rates using pure water.

Several classes of lead-acid batteries are currently manufactured throughout the world. These include the portable (SLI, deep cycle traction, maintenance-free and sealed) and the stationary (load levelling, emergency lighting, and telephone standby power sources) battery types. The most important features for each of the above are summarized below:

1. **Automotive SLI battery:** The six and twelve volt batteries possess thin electrode plates to provide high discharge rates required during automotive starting operations. The energy densities are typically 28 to 48 Wh/kg or 50 to 100 Wh/1 which are higher than for any other class of lead acid batteries.[4] Other features include:[3,4,7]

    a. Operational temperature range: -40°C to +60°C
    b. Recommended temperature range: +21°C to 32°C
    c. Storage temperature (wet): -40°C to 46°C
    d. Self-discharge rate (wet): 5 to 11 percent per month
    e. Cycle life: 150 to 250 cycles
    f. Electrolyte density: 1.28 g/cm^3
    g. Operation at elevated temperatures produces accelerated corrosion rates
    h. The ordinary duty cycle requires a shallow depth of discharge (20 percent)
    i. Charging is accomplished by voltage regulated and temperature compensation techniques. The charging voltage for a 12V battery is 14.4 V with a recommended trickle charge rate of C/100.

2. <u>Deep cycle traction</u>: These lead-acid batteries are employed in such applications as mine locomotives, golf carts, electric vehicles, submarines, and aircraft. The energy densities for these lead-acid batteries are 19 to 24 Wh/kg and 60 to 85 Wh/l at the six hour discharge rate. Special wrapping of the PbO_2 positive electrode assembly provides longer cycle life characteristics by reducing shedding of the active material during some abusive operating conditions. Other features include:[3,4,7]

   a. Operational temperature range: -18°C to +43°C
   b. Recommended discharge temperature: 21°C to 43°C
   c. Storage temperature (wet): -1°C to +25°C
   d. Self discharge rate (wet): 7 to 10 percent per month
   e. Cycle life: 1000 to 2000
   f. Electrolyte density: 1.28 g/cm^3

   Special consideration must be made for the Improved State-of-the-Art (ISOA) electric vehicle battery.[25-27] Three battery manufacturers, Eltre, ESB, and Globe Union, submitted lead-acid batteries to Argonne National Laboratory for testing under electric vehicle conditions. The Globe Union ISOA lead-acid battery featured a circulating electrolyte.[25] Test results showed an energy density of 41 Wh/kg, a power density of 118 W/kg, and a cycle life of 250 cycles (80 percent of the rated capacity at the 3 h discharge rate) for this battery.

   The largest lead-acid traction batteries are used for submarine propulsion, lighting, and instrumentation during submersion. A typical battery may be comprised of 4 parallel strings of 112 cells in series and possess capacities of 5000 to 12000 Ah (up to 2.7 MWh). To avoid the possibility of exposure to highly toxic stibine, SbH_3 and arsine AsH_3, the grid materials are fabricated from a lead-calcium alloy. These grids also provide a benefit by maintaining low hydrogen evolution. Special cooling for the batteries is accomplished by circulating water through the busbar plates. Since hydrogen evolution generally promotes electrolyte mixing, the reduced rates of hydrogen evolution tend to produce electrolyte stratification in these cells. Tubular air lift pumps are therefore required for uniform electrolyte compositions.

3. <u>Maintenance-free</u>: This variation of the SLI battery employs calcium-lead or low antimony grid alloys which drastically reduce the rate at which water is electrolysed during overcharge or extended overcharge conditions. In addition, the design for this battery requires electrolyte flooding and the use of smaller electrode plates. Retention of the lead dioxide active material by wrapping the plates with separator material avoids the risk of internal short circuits brought about by shedding. It is important to note that this battery design does include a flame arrestor vent device to release gas in the event of an uncontrollable pressure rise. Some manufacturers of the maintenance-free batteries employ a gelled electrolyte of sulfuric acid and sodium silicate. Hydrogen and oxygen gas evolution is minimized by using special charging equipment which terminate the charge at the onset of gasing.

4. **Sealed cells:** The following design considerations characterize the sealed lead-acid (SLA) cell:

a. The grids are either lead-calcium alloy or pure lead which possess high hydrogen overvoltages.

b. The cells contain limited amounts of electrolyte (either an aqueous solution or a gel) and an excess amount of the negative electrode material.[28] In view of the fact that oxygen will vary rapidly react with lead at the surface, oxygen diffusion to the negative electrode is enhanced considerably by limiting the amount of electrolyte. The reaction proceeds accordingly:

$$2\ Pb + 2\ H_2SO_4 + O_2 \longrightarrow 2\ PbSO_4 + 2\ H_2O \tag{10}$$
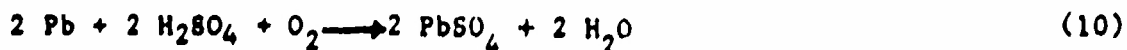
The reaction of hydrogen at the positive plate is slow compared to the recombination rate for oxygen but does proceed in accordance with:

$$PbO_2 + H_2SO_4 + H_2 \longrightarrow PbSO_4 + 2\ H_2O \tag{11}$$
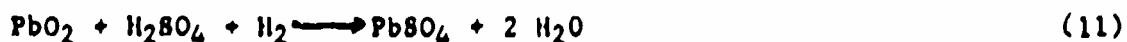
c. SLA cells possess venting devices which open at pressures of approximately 4 atmospheres (400 kPa). Such pressures would develop if the recombination capabilities for reactions 10 and 11 were exceeded. This would occur if the cell were overcharged at rates above C/3.

d. The two types of SLA cells which are currently manufactured are the spirally wound and prismatic designs.

e. The addition of phosphoric acid to the electrolyte improves the cycle life for SLA cells.[29]

f. The cycle life expectancy varies from 250 to 300 cycles for depths of discharge equal to 80 percent of the rated capacity. The cycle life for cells discharged to only 25 percent depths is 1500 cycles.

5. **Stationary batteries:** Various applications for these batteries include load levelling,[30,31] emergency lighting, and telephone standby power systems.[12] Cells comprising the stationary batteries contain particularly robust components, an excess of electrolyte to minimize maintenance, and positive limited electrodes. During overcharge conditions, positive electrode grid corrosion does occur. The result is a grid growth so that specific designs allow for certain amounts of growth within the cell. Too much grid expansion causes loss of the active material from the electrode.

The selection of the charging method is dependent upon such factors as battery type, service conditions, number of cells comprising the battery, charging facilities, and the time allotted for charging.[3] It is important to avoid charge voltages greater than the gassing voltages of the cell (2.384). When all of the discharged capacity is returned to the cell, the charging current should be decreased to a value of 5 A per 100 Ah of rated capacity.

Several charging methods are currently employed relative to lead-acid batteries: constant current, modified constant current, constant current with progressively decreasing rates, constant potential, modified constant potential (with constant finishing rate, constant initial current, or constant initial and final rate), taper charging, pulse charging, trickle charging, and float charging.[3,7] In view of the fact that cells in a series string may not be exactly balanced, some cells receive a greater degree of overcharge than other cells. Sustained and consistent undercharging results in the depletion of some cells which could lead to cell voltage reversal and plate buckling. These conditions may be alleviated to some degree by subjecting the battery to an "equalization charge." This procedure involves extended charging beyond the limits of the normal charging regime and usually requires up to six hours additional charging at the finishing rate.

The most important safety concern relative to lead-acid batteries concerns the production of potentially explosive H_2-air or H_2-O_2 gas mixtures by the electrolysis of water during overcharge conditions. The evolution of oxygen at the positive PbO_2 electrode is given by the combined reactions:

$$PbO_2 + 4\ H^{1+} + 4e^{1-} \longrightarrow Pb + 2\ H_2O \tag{12}$$

and

$$2\ H_2O \longrightarrow O_2 + 4\ H^{1+} + 4e^{1-} \tag{13}$$
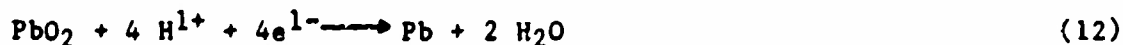
Hydrogen will be evolved at the negative Pb electrode in accordance with:

$$2\ H^{1+} + 2e^{1-} \longrightarrow H_2 \tag{14}$$

Gas mixtures of hydrogen and oxygen/air are explosive when the concentration of hydrogen is in the range of 4 to 76 percent by volume.[32] Hydrogen gas may also be evolved by the corrosion reaction with lead at the lead negative and the local action of antimony on the negative electrode. Oxygen may also be formed as a result of the chemical decomposition of PbO_2.[7] The explosion reaction between the two gases is usually initiated by a spark or static electricity. Most nonsealed cells possess flame arrestors in the vent cap assembly to prevent ignition of the gas mixture within the cells.

Gas mixtures can be controlled by using fuel-cell type hydrogen oxygen recombination devices (HORD). The gases are allowed to contact a platinum catalyzed carbon fuel cell located in large vent plug structures. Though small fuel cell HORD devices are in use in small lead-acid batteries, much of the effort for the development of HORDs have been concerned with large load levelling systems.[33] A second method for the control of explosive gas mixtures relates to the use of silver-catalyzed carbon auxiliary electrodes. Such electrodes are connected to the negative electrode plates and reduce oxygen immediately, thus precluding the evolution of hydrogen at the negative electrode. Sealed cells rely on the direct recombination of O_2 at the negative electrode and H_2 at the positive electrode, as previously discussed.

In view of the fact that lead-acid cells have very low internal impedances, such cells possess the capability of yielding high discharge rates when subjected to heavy loads, such as those attendant with external short

circuiting. The heat generated by the batteries could cause fires and severe burns to personnel. Expulsion of sulfuric acid electrolyte would also cause chemical burns.

Lead-acid cells/batteries subjected to incineration conditions would result in electrolyte expulsion and the evolution of toxic gases from the plastic components of the battery.

Cell voltage reversal conditions occur when cells of limited capacity are overdischarged by cells of greater capacity. The net result is the creation of electrode plates containing both positive (PbO_2) and negative (Pb) materials. Such electrodes are subject to strong local corrosion reactions which lead to the evolution of gases and the rapid consumption of the sulfuric acid electrolyte. No data was found which detail any hazardous events as a result of voltage reversal testing.

Specific safety testing has been performed using spirally-wound, sealed lead-acid D cells manufactured by Gates.[34] The results for these tests are summarized below:

1. Cells short-circuited through 0.015 ohm loads at 25 and 55°C exhibited peak currents of 75 and 65A in less than 0.5 minutes followed by rapid polarization. The corresponding maximum cell case temperatures were 57 and 90°C after 7 to 9 minutes. Cells short circuited at 25°C showed some case distortion while those at 55°C did not lose any electrolyte.

2. Cells were overdischarged under constant current conditions at the C/10 rate for a period equal to the nominal cell capacity at 20 and 50°C. Cells overdischarged under the above conditions (0.25 A) exhibited maximum temperature increases of 10°C and maximum, stable reverse voltages of 2.0 V. No venting or excessive pressure buildup was observed.

3. Cells which were mechanically abused by either cutting by a steel knife or by penetration by a steel cube at 200 meters per second exhibited no rise in temperature (cutting) or internal short circuiting (penetration).

4. Incineration of cells using an oxygen-propane flame adjusted to give a cherry red spot 1 cm in diameter resulted in the incineration of plastic case materials and the melting of the electrode structures.

The chemical hazards related to the lead-acid cell/battery relates to the production of stibine, SbH_3 and arsine, AsH_3 in those cells and batteries which use lead-antimony grid assemblies.[14] The presence of these gases is of major concern for applications requiring battery use in confined environments (e.g., electric vehicles, submarines, stationary load levelling facilities. etc.). Though the amounts of stibine produced is 20 to 50 times more than that for arsine, both are extremely toxic. For example, exposure to 250 ppm of arsine for 0.5 h has been shown to be fatal. Similar toxic characteristics are also expected for stibine.[35,36] Acute inhalation exposure to either or both compounds would lead to abdominal pain, red cell breakdown, and eventual death due to kidney failure. The exposure limits allowed under OSHA guidelines are

0.1 and 0.05 ppm for stibine and arsine, respectively.[14] It can be seen, therefore, that proper ventilation of the battery charging area is important not only to dissipate the evolved hydrogen gases but also to avoid or minimize contact with stibine and arsine.

REFERENCES

1. Bode, H., Lead Acid Batteries, Translated by Brodd, R. J., and Kordesch, K. V. (New York: John Wiley and Sons, 1977).

2. Ruetschi, P., J. Power Sources, 2, 1977/1978, p. 3.

3. Salkind, A. J., Mayer, G. E., and Linden, D., Handbook of Batteries and Fuel Cells, Linden, D., ed. (New York: McGraw-Hill Book Company, Chapters 14 and 15, 1984).

4. Kordesch, K. V., Batteries, Volume 2, Lead-Acid Batteries and Electric Vehicles (New York: Marcel Dekker Inc., 1977).

5. Burbank, J., Simon, A. C., and Willihnganz, E., "The Lead Acid Cell," Advances in Electrochemistry and Electrochemical Engineering, Volume 8, C.W. Tobias, ed. (New York: Wiley-Interscience, 1971).

6. Carr, J. P., and Hampson, N. A., Chem. Rev., 72, 1972, p. 679.

7. Barak, M., Electrochemical Power Sources, Primary and Secondary Batteries, IEE Energy Series 1, M. Barak, ed. (London: Peter Peregrinus Ltd., Chapter 4, 1980).

8. Smith, G., Storage Batteries (London: Sir Isaac Pitman and Sons, 1964).

9. Vinal, G. W., Storage Batteries (New York: John Wiley and Sons, 1940).

10. Dafler, J. R., J. Electrochem. Soc., Electrochem. Sci. and Technol., 125, 1978, p. 833.

11. Bullock, K. R., and McClelland, D. H., J. Electrochem. Soc., Electrochem. Sci. and Technol., 123, 1976, p. 327.

12. American Telephone and Telegraph Company, Inc., Bell System Tech. J., 1970, p. 49.

13. Lander, J. J., J. Electrochem. Soc., 99, 1952, p. 339.

14. Loutfy, R. O., and Varma, R., Procedures for Safe Handling of Off-Gases from Electric Vehicle Lead Acid Batteries During Overcharge, Argonne National Laboratory, ANL/CNSV-TM-28 (1980).

REFERENCES (Cont.)

15. Henderson, M., _Electronics and Power_, 23, 1977, p. 491.

16. Mao, G. W., Larson, J. G., and Rao, P., _J. Electrochem. Soc._, Electrochem. Sci. and Technol., 120, 1973, p. 11.

17. Zachlin, A. C., _J. Electrochem. Soc._, 98, 1951, p. 325.

18. Hampson, N. A., and Lakeman, J. B., _J. Electroanal. Chem._, 119, 1981, p. 3.

19. Duttmann, J. F., and Harner, H. R., _J. Electrochem. Soc._, 101, 1954, p. 533.

20. Simon, A. C., Caulder, S. M., Garlusky, P. J., and Pierson, J. R., _J. Electrochem. Soc._, 121, 1974, p. 463.

21. Simon, A. C., Caulder, S. M., Garlusky, P. J., and Pierson, J. R., _Electrochim. Acta_, 19, 1974, p. 739.

22. Brennan, M. P. J., and Hampson, N. A., _Electroanal. Chem._, 48, 1973, p. 465.

23. Mahato, B. K., _J. Electrochem. Soc._, 124, 1977, p. 1663.

24. Berndt, D., _Comprehensive Treatise of Electrochemistry_, Volume 3, Electrochemical Energy Conversion and Storage, Bockris, J. O'M., Conway, B. E., Yeager, E., and White, R. E., eds. (New York: Plenum Press, Chapter 12, 1981).

25. Andrew, M. G., and Weinlein, C. E., _IEEE Transactions on Vehicular Technology_, VT-32, 1983, p. 21.

26. Yao, N. P., Christianson, C. C., and Lee, T. S., _Proc. Power Sources Symp._ 29, 1981, p. 261.

27. Yanni, L. A., Jr., _IEEE Transactions on Vehicular Technology_, VT-32, 1983, p. 74.

28. Hammel, R. O., _Handbook of Batteries and Fuel Cells_, Linden, D., ed. (New York: McGraw-Hill Book Company, Chapter 15, 1984).

29. Amlie, R. F., Weissman, E. Y., Morehouse, C. K., and Qureshi, N. M., _J. Electrochem. Soc._, Electrochem. Sci. and Technol., 119, 1972, p. 568.

30. Maskalick, N. J., _Proc. Amer. Power Conf._, 41, 1979, p. 1049.

31. Choi, K. W., and Yao, N. P., _J. Electrochem. Soc._, Electrochem Sci. and Technol., 125, 1978, p. 1011.

32. Simmons, R. F., and Wolfhard, H. G., _Trans. Faraday Soc._, 15, 1211, 1955, cited in R.G. Zalosh and S.N. Bajpai, "Comparative Hazard Investigation for a Zinc-Bromine Load Leveling Battery," Final Technical Report, EPRI Project 1198-4, Factory Mutual Research Corporation, Norwood, MA, 1980.

REFERENCES (Cont.)

33. <u>Fabrication and Testing of a Prototype Gas Recombination Device for Utility Lead Acid Cells</u>, Final Report, Argonne National Laboratory ANL/ OEPM-80-8, 1980.

34. Attewell, A., "Power Sources 9," <u>Proc. 13th Int. Symp. Power Sources</u>, Joint Services Electrical Power Source Committee, J. Thompson, ed. (London: Academic Press, 1983), p. 473.

35. Levvy, G. A., <u>J. Exp. Physiol.</u>, 34, 1947, p. 47.

36. Muehreke, R., and Pirani, C. L., <u>Ann. Intern. Med.</u>, 68, 1968, p. 853.

N. SODIUM-SULFUR

$$Na \, | \, \beta''\text{-}Al_2O_3 \, | \, S$$

$$Na \, | \, Na^+ Glass \, | \, S$$

$$2 \, Na + 3 \, S \rightleftharpoons Na_2S_3 \qquad [1]$$

The basic concept for the use of a solid ceramic as the electrolyte for the secondary sodium-sulfur battery system was announced by J. T. Kummer and N. Weber of the Ford Motor Company in 1967.[1-3] Patent approval for this sodium-sulfur electrochemical system was granted in 1968.[4] At approximately the same time, C. Levine of Dow Chemical Company independently developed glass fibers as an alternative solid electrolyte for the sodium-sulfur battery.[5] Several major programs are currently devoted to the development of the sodium-sulfur battery with efforts focussed upon load leveling, electric vehicle propulsion, and railroad applications. The principal developers in the United States are Ford Aerospace and Communications Corporation (electric vehicle and load leveling, supported by the Department of Energy), General Electric Company (load leveling, supported by the Electric Power Research Institute and GE), and Dow (load leveling, supported by DOE and Dow).[6] The major European developers are British Rails (railroad applications, supported by the Departments of Environment and Transportation), Chloride Silent Power (electric vehicle, supported by the Central Electricity Generating Board and Chloride Silent Power), Brown, Boveri and Cie AG (electric vehicle, supported by the West German Government and Brown, Boveri), and Compagnie Generale d'Electricite (basic research, supported by the French government, the Electric Power Research Institute, and the General Electric Company). Sodium-sulfur electric vehicle battery development is also carried out at Yuasa Battery Company in Japan.[6]

The sodium-sulfur cell primarily consists of molten sodium and sulfur as the negative and positive electrode materials, respectively. Separation is effected by either the beta "-alumina ceramic electrolyte (cell operating temperature: 350°C) or the sodium ion conducting glass (cell operating temperature: 300°C). Other sodium ion electrolyte materials, most notably the sodium zirconium phosphosilicates (NASICON, $Na_{1+x} \, Zr_2 \, Si_x \, P_{3-x} \, O_{12}$), have been developed which exhibit higher conductivities at lower temperatures.[7,8] In view of the fact that present technology favors the use of beta "-alumina and the conductive glass as the electrolytes for the sodium-sulfur system, this discussion will focus on the cell designs incorporating these materials.

Beta"-alumina, a sodium aluminate of the approximate composition $Na_2O \cdot 6Al_2O_3$, is a layer structure consisting of hexagonal blocks of aluminum and oxygen atoms in a spinel formation which alternate with a layer of sodium ions.[7,9] The sodium ions, situated in planes perpendicular to the C-axis of the crystals, provide the sodium ion conduction in two dimensions. This material possesses a high defect structure and is not stable at temperatures above 1550°C. The addition of Li_2O and/or MgO in small quantities (e.g., less than 1 weight percent) acts to stabilize the beta "-alumina structure and permits the preparation of a high density polycrystalline ceramic required for battery use.[9] The conductivities of the various beta"-alumina compositions used by the various sodium-sulfur battery developers vary from about 0.1 to 0.6 $ohm^{-1}cm^{-1}$ at temperatures of 300 to 350°C. For comparison, the conductivity of sulfuric acid in lead-lead dioxide batteries at 25°C is about 0.2 $ohm^{-1}cm^{-1}$.[10]

Beta "-alumina ceramic tubes are fabricated by either isostatically pressing a spray dried powder or by electrophoretic deposition methods.[9,11] In the former process, a mixture of alpha alumina, sodium hydroxide, lithium hydroxide, and water are ball milled into a slurry. This slurry is then spray dried to produce a fine powder. The powder is isostatically pressed at 35 kpsi (240 MPa) into the green tubes. The tubes are then sintered at elevated temperatures up to 1620°C. Electrophoretic preparation methods use a beta-alumina (various compositions of $Na_2O.5.33 Al_2O_3$ to $Na_2O \cdot 11 Al_2O_3$) starting material to which MgO or Li_2O is added.[11] The mixture is fused, cooled, and milled to yield powders with surface areas of 2 m^2/g. The powders are suspended in an organic solvent containing an organic acid. The charging process entails the adsorption of positively charged species on the powder from the acid. Beta "-alumina tube formation takes place on a negatively charged metal rod.[11] The resultant tubes are sintered at a temperature of about 1850°C.

Beta"-alumina tubes are typically sealed to either an alpha-alumina tube or an alpha-alumina collar through use of proprietary glasses. Hermetic cell closure is effected by glass to metal seals, thermocompression seals, soft metal gasketing with radial compression rings, or, in the case of experimental glass cells, graded glass sealing directly to the alpha-alumina.[9,12] It is important to note that two distinct cell designs employing beta "-alumina tubes currently exist:

1. The original design for the sodium-sulfur cell required that the sodium be retained within the beta"-alumina tube and a sodium reservoir. This so-called Central Sodium Design is employed by Ford and General Electric in the United States and Brown, Boveri and Cie in West Germany. The sodium and sulfur containers are comprised of stainless steel (Ford) or a mild steel (G.E.). In addition, a coating of chromium on the sulfur container surface is required to minimize the corrosive effects of the sodium sulfide species.[10,13,14] The transition metal sulfides produced in the container corrosion process reduce the amount of sulfur available for the electrochemical reaction, adversely affect the transport properties at the beta"-alumina/sulfur electrode interface, and could cause loss of contact between the stainless steel container and the electronically conducting graphite felt matrix.[14] The overall effect is the gradual loss of capacity

on cell cycling. The graphite felt matrix (WDF graphite or various pitch based Thornels) provides not only electronic conduction within the sulfur electrode but also the reaction sites for discharge and charge.

An important safety feature for the central sodium design consists of a stainless steel protective tube or a sodium insert within the beta"-alumina electrolyte which extends into the sodium reservoir.[12] This elongated, funnel-shaped device functions as a liquid sodium control in the event of catastrophic failure of the solid ceramic electrolyte. Only that amount of liquid sodium sufficient to maintain the cell reaction is provided to the sodium/electrolyte interface. A sodium wick, located between the safety tube and the inside of the electrolyte tube, allows for sufficient wetting of the sodium/beta"-alumina interface. It can be seen, therefore, that, in the event of a fracture of the ceramic tube, only a limited amount of sodium will react chemically resulting in significantly lower temperature excursions above the operating temperature.

2. The second design for the sodium-sulfur cell also uses beta "-alumina as the electrolyte material but the sulfur electrode is positioned inside the tube while the sodium is outside the tube. Chloride Silent Power and British Rails developed this cell design which is used exclusively in all their programs.[5,15,16] Recently, Brown, Boveri and Cie have reported some success using the central sulfur concept with multi-electrolyte tube cells.[17] The chief advantage of the central sulfur design relates to the alleviation of cell container corrosion problems attendant with the central sodium design. Only the current collector in the sulfur electrode is, therefore, subject to corrosion.[5] One corrosion-resistant current collector rod is comprised of an aluminum core with an exterior of niobium doped rutile.[5] It should be noted that central sulfur cells do not possess as high gravimetric or volumetric energy densities and electrochemical efficiencies as for the central sodium cells.[16]

The design of these cells requires the use of a pressurized sodium reservoir by incorporating a thin can of aluminum ("pressure can") under inert gas pressure. The entire reservoir assembly is enclosed within the cell case. The sodium reservoir is separated from the beta"-alumina tube by a carbon felt restrictor plate. Hames and Tilley[16] have set forth three safety principles relative to this specific design:

a. Separation of the reactants - the gap between the beta "-alumina and the cell case is minimized to about 0.15 cm. Most of the sodium is stored in the aluminum pressure can.

b. Restriction of sodium flow - the gap between the aluminum pressure can and the cell case is minimized. Should the pressure can melt, the sodium flow would be restricted by the carbon felt restrictor plate.

c. Protection of the cell case from sodium polysulfide corrosion
after cell (electrolyte) failure - a lining of Grafoil between
the electrolyte and cell case protects the cell case material
(mild steel) from rapid corrosion.

3. The third design for the sodium-sulfur cell uses a multitude of hollow
glass fibers as the solid electrolyte.[7,9,12,18,19] The electrolyte
is a sodium borosilicate glass with the composition of $Na_2O \cdot B_2O_3 \cdot$
$2 SiO_2$ with 0.16 NaCl. The inclusion of NaCl in the composition
increases the ionic conductivity and acts to prevent crystal-
lization.[9] The typical hollow fiber (with a closed end) has an
outside diameter of 70 microns (7×10^{-3} cm), an inside diameter of
50 microns (5×10^{-3} cm), a wall thickness of 10 microns (1×10^{-3}
cm), and a length of about 10 cm. The conductivity of the glass is
approximately 5×10^{-5} $ohm^{-1}cm^{-1}$ at 300°C, a particularly low
value when compared to the beta "-alumina.

The basic design of the Dow hollow fiber sodium-sulfur cell consists of
thousands of the hollow fibers bonded to a glass tubesheet. The glass
tubesheet allows the separation of the sodium reservoir from the sulfur
chamber while simultaneously permitting the free access of the sodium
to the inside of each fiber. The glass composition of the tubesheet is
8 weight percent Na_2O with the remainder B_2O_3.[18] The expansion
coefficient of this glass compares closely to that for the electrolyte
glass.

The current collector for sulfur electrode consists of an aluminum
sheet of about 1×10^{-3} cm thick, sputter-coated with about a 400
angstrom thickness of molybdenum for corrosion protection.[19] The
aluminum current collector is then either interwoven between adjacent
rows of fibers or spirally wound among the glass fibers. The glass
fiber/aluminum current collector strip can then be wound on a mandrel.
A paste of powdered tubesheet glass is applied to the open tube end
portion of the wound assembly. The solvent of the paste is evaporated
and the glass powder is fused into a solid glass tubesheet disc.[18]
An aluminum sodium reservoir is subsequently attached to the glass
tubesheet. This assembly is fitted into a stainless steel can and
filled with sodium and sulfur.

The optimum current density for the hollow glass fiber cell is about 2
mA/cm^2. In view of the fact that such cells possess large surface
areas and nearly 100 percent coulombic efficiencies, the voltaic
efficiencies determine the overall energy efficiency of the system.
Typically, the charge voltage is 2.18 V and the discharge voltage is
1.98 V. It can be seen that the overall energy efficiency would be 91
percent if all the sodium polysulfides were converted to sulfur. As is
the case with beta"-alumina sodium sulfur cells, one hundred percent
conversion to sulfur is not possible in practical cells. For the Dow
glass fiber electrolyte cells, a complete charge is defined as the
production of the two-liquid phase having an approximate composition of
$Na_2S_5 + 10 S$.[18]

The sodium and sulfur react electrochemically to produce various sodium sulfide species in accordance with the reaction:

$$2\ Na + X\ S \longrightarrow Na_2\ S_x \qquad\qquad (2)$$
$$(x = 2,3,4,5.2)$$

At the beginning of cell discharge, the sulfur electrode contains only a single phase of liquid sulfur embedded in the current collector matrix. The reaction produces a sodium sulfide species, as in equation 2, which is sparingly soluble in the sulfur phase. As discharge proceeds, a separate liquid phase of sodium polysulfide with the stoichiometric composition of $Na_2S_{5.2}$ appears. Thus, after a short discharge period, two liquid phases are present in the cell: liquid sulfur saturated with a sodium polysulfide species and a sodium polysulfide species, $Na_2S_{5.2}$ comprised of Na_2S_5 and Na_2S_6.[7,9] As the discharge is continued, more of the sodium polysulfide phase is produced until all the sulfur is consumed. There now exists a single polysulfide phase of $Na_2S_{5.2}$ (78.3 weight percent sulfur). Further discharge will result in the production of a sodium sulfide species, Na_2S_4, which is a mixture of Na_2S_2, Na_2S_4, and Na_2S_5.[7] The cell may be discharged further until the solubility limit of Na_2S_2 (melting point: 482°C) is reached.[20] The precipitation of Na_2S_2 at the beta"-alumina or glass electrolyte surface limits further realization of useful electrochemical energy. The sodium sulfide composition at the end of normal discharge is Na_2S_3. The cell open circuit voltage at any discharge point in the two-liquid phase region is invariant at 2.078 V. As the reaction of the single phase of $Na_2S_{5.2}$ proceeds, the open circuit voltage decreases linearly until the sodium sulfide, Na_2S_3, is produced. The open circuit voltage at this discharge stage will remain at 1.782 V.[12] A depth of discharge of 100% for the sodium-sulfur cell corresponds to the formation of Na_2S_3.[9] The theoretical energy density for the reaction leading to the formation of Na_2S_3 is 760 Wh/kg.[12]

The physical properties of the various chemical components of the sulfer electrode dictate many of the operational parameters for the sodium-sulfer battery system. For example, pure sulfur possesses poor electrical conductive properties at 300 and 350°C (conductivities of approximately 8×10^{-12} and 40×10^{-12} $ohm^{-1}cm^{-1}$, respectively), high viscosity values (approximately 22 and 5 poise at 300 and 350°C, respectively), and vapor pressures of approximately 50 mm (6.7 kPa) at 300°C and 150 mm (20 kPa) at 350°C.[20] The boiling point for sulfur is 444°C.[9] The melting points for the sodium sulfide species, Na_2S_5, Na_2S_4, Na_2S_3, Na_2S_2, and Na_2S are, respectively, 264 ± 10, 285, 230, 482, and 1170°C.[9] In order to achieve full utilization for the discharge reaction to Na_2S_3, the operating temperature must be well above 285°C, the temperature below which Na_2S_4 will precipitate from the single phase liquid. The upper temperature limit is restricted by the boiling point of sulfur and the need to maintain comparatively low vapor pressure values to avoid sulfur condensation in cooler parts of the cell structure away from the reaction site.

As the sodium sulfur cell is charged, Na_2S_3 is oxidized to higher sulfide species (i.e., Na_2S_4, Na_2S_5). However, when the composition of the sulfide species is equal to or greater than that of $Na_2S_{5.2}$ charging is carried out in the two liquid phase region of $Na_2S_{5.2}$ and sulfur saturated with $Na_2S_{5.2}$. The formation of sulfur in this part of the charging cycle

may lead to premature cell polarization if sufficient mass transport of sodium sulfides to the electrolyte surface is not achieved. This inability to charge significantly into the two phase region severely limits the realization of high specific energies. No other aspect of sulfur electrode research has received as much attention as has the need to improve the mass transport properties at the graphite felt/electrolyte interface. Several approaches have been made in the effort to achieve nearly complete conversion of sodium sulfide species to elemental sulfur:

1. Alteration of the wetting characteristics of the graphite felts,[21,22] the use of carbon species of different resistivities,[23,24] and the addition of alumina fibers to the graphite felt matrix.[5]

2. The addition of 0.8 mol percent of tetracyanoethylene, C_6N_4, to the sulfur electrode to improve sulfur conductivity,[25] the addition of selenium,[26] and the inclusion of alpha-alumina adjacent to the electrolyte.[9]

3. The incorporation of channels in the graphite felt matrix.[9]

The primary safety concern for the sodium-sulfur battery system relates to the uncontrolled chemical reaction between liquid sodium and sulfur at cell operating temperatures of 300 to 350°C or higher. The occurrence of such a reaction could lead to cell case rupture, fires, and explosions. The development of stainless steel protective tube inserts for the beta"-alumina electrolyte in central sodium designs, the restriction of free access of the reactants by designing central sulfur cells in accordance with the three safety principles set forth by Hames and Tilley, and the use of either a sodium porous glass frit immobilizer cup or a ceramic sodium flow restrictor for hollow glass fiber cells[19,27] have contributed significantly to the reduction of this safety hazard.

Fracture of the beta "-alumina or hollow glass fiber electrolytes may occur as a result of applied mechanical stresses, temperature cycling (freeze/thaw), stresses resulting from the precipitation of solid sodium sulfides (Na_2S_2) at the electrolyte following overdischarge conditions, and the stresses associated with high internal resistances arising from extended overcharge conditions leading to the formation of non conductive sulfur at the electrolyte surface. It is important to note that an overdischarge condition in sodium-sulfur cells is considered as extended cell discharge beyond the formation of the Na_2S_3 species. Given below are the safety test results for the three sodium-sulfur cell designs, central sodium (Ford, G.E., and Brown, Boveri and Cie AG), central sulfur (British Rails and Chloride Silent Power), and the Dow hollow glass fiber cell design:

1. Central sodium design

Specific safety testing at Brown, Boveri and Cie[28,29] using 50 Ah Na/S cells resulted in the following observations:

a. The destruction of a hot cell using mechanical methods results in fire and the emission of toxic gases.

b. The exposure of cells to high temperature environments lead to seal leakage with fire and the emission of toxic gases if the temperature is more than 200°C above the operating temperature.

c. Cells may be overcharged to about 30 V with no hazard occurrence. At higher voltages, explosions and fires occur.

d. A short circuit test showed that the cell temperature would increase about 100°C. No safety hazard occurred and the cells remained sealed.

e. The direct mixture of liquid sodium and sulfur resulted in a very violent reaction.

f. In other tests at Brown, Boveri and Cie,[25] the electrolyte was fractured intentionally by a high charge in cells with no means for sodium flow restriction. Such cells exhibited temperature excursions in excess of 1000°C. Similar tests performed upon cells with sodium flow restriction showed temperature increases of only 100°C for cells with 25 percent of the sodium available for reaction and only 50°C for cells with 12 percent of the sodium available.

Forced overdischarge tests at Compagnie Generale d'Electricite[30] showed that the electrolyte will fracture due to the mechanical strains imposed by the precipitation of solid Na_2S_2. Solid Na_2S_2 formed when the cell is discharged beyond the sodium sulfide composition of Na_2S_3.

2. Central sulfur design

Safety testing of 100 Ah sodium-sulfur cells fabricated in accordance with the safety design principles of Hames and Tilley resulted in the following observations:[16,31,32]

a. Discharged cells were deliberately failed by imposing a high charge rate. None of the 50 cells ruptured, although two cells exhibited temperatures up to 700°C.

b. A "dead short" circuit test resulted in currents of 200A for 20 minutes. The cell temperatures rose to about 650°C during the test period. No cell ruptures were observed.

c. Exposure of the cells to high temperature environments showed that cell rupture could occur at temperatures greater than 750°C.

d. Less than one percent of the more than 200 safety tests showed that cells reached temperatures of 800°C or higher.

3. Dow hollow fiber cell

Dow sodium-sulfur 40 Ah cells fabricated with a sodium immobilizer and a ceramic flow restrictor have been deliberately failed by shorting and by

mechanical impact.[19,27] No significant exotherms or case ruptures were observed for these tests.

When 40 Ah cells were short circuited, the internal cell temperature increased from 300°C to 370°C. The short circuit current for these cells attained maximum values of 34 A after 3 minutes. Cells operated normally following short circuit testing.

Discharge beyond the sodium sulfide, Na_2S_3, leads to glass fiber breakage and shortened cell life.

A major concern for the Dow hollow fiber cell relates to the release of sufficient heat during the reaction between sodium and sulfur to cause the aluminum foil current collector to melt. The reaction between aluminum and sulfur would, in turn, initiate a reaction between the sulfur species and the stainless steel case. This reaction, with a corresponding buildup of sulfur vapor pressure with increased temperature, could cause case rupture.

Liquid sodium was injected directly into the sulfur electrode chamber of a 40 Ah cell maintained at 300°C. The results showed only a 140°C temperature increase for a four gram injection of sodium. However, when an eight gram injection of sodium was introduced into a second cell, the internal temperature rose to more than 1000°C. Further sodium injection experiments were performed using a screw feeder to control the amount of sodium more accurately. Injections of 1.5 g batches of sodium were introduced at seven minute intervals. The results for the first two injections showed normal (i.e., 70°C) temperature increases followed by a return to 300°C. The third injection exhibited a temperature event to 1000°C. It was concluded that sodium reacts nonuniformly.

Sodium-sulfur cell case ruptures occurring at operating temperatures of 300 to 350°C or at abuse test temperatures up to 800°C will release highly toxic, aggressive fumes.[20] Sulfur will decompose and oxidize at elevated temperatures to form SO_2 and SO_3 gases. The reaction of sodium sulfides with moisture or water in the atmosphere will produce highly toxic hydrogen sulfide, H_2S. In addition, liquid sulfides and polysulfide species could react explosively in the presence of strong oxidizing materials.

REFERENCES

1. Kummer, K. T., and Weber, N., "A Sodium-Sulfur Secondary Battery," Proc. SAE Automotive Engineering Conference, Detroit, MI., No. 670179, SAE Trans., 76, 1968, p. 1003.

2. Weber, N., and Kummer, J. T., Proc. Advanced Energy Conversion Engineering ASME Conference, 1967, p. 913.

3. Kummer, J. T., and Weber, N., Proc. Power Sources Symp. 21, 1967, p. 37.

4. Kummer, J. T., and Weber, N., U.S. Patent No. 3,404,035, 1968.

5. Jones, I. W., Phil. Trans. R. Soc. Lond. A, 302, 1981, p. 339.

6. Douglas, D. L., and Birk, J. R., Annual Review of Energy, Volume 5, Hollander, J. M., Simmons, M. K., and Wood, D. O., eds. (Palo Alto, California, Annual Reviews Inc., 1980), p. 79.

7. Cairns, E. J., Comprehensive Treatise of Electrochemistry, Volume 3, Electrochemical Energy Conversion and Storage, Bockris, J. O'M., Conway, B. E., Yeager, E., and White, R. E., eds. (New York: Plenum Press, Chapter 11, 1981).

8. Goodenough, J. B., Hong, H. V.-P., and Kafalas, J. A., Mat. Res. Bull., 11, 1976, p. 203.

9. Sudworth, J. L., Electrochemical Power Sources, Primary and Secondary Batteries, IEE Energy Series 1, M. Barak, ed. (London: Peter Peregrinus Ltd., Chapter 6, 1980).

10. Asher, J. A., and Bast, J. A., Proc. Power Sources Symp. 29, 1981, p. 181.

11. Fally, J., Lasne, C., Lazennec, Y., LeCars, Y., and Margotin, P., J. Electrochem. Soc., Electrochem. Sci. and Technol., 120, 1973, p. 1296.

12. Rizzo, R. A., Towle, W. L., and McClanahan, M. L., Handbook of Batteries and Fuel Cells, D. Linden, ed. (New York: McGraw Hill Book Company, Chapter 32, 1984).

13. Bones, R. J., and Markin, T. L., J. Electrochem. Soc., Electrochem. Sci. and Technol., 125, 1978, p. 1587.

REFERENCES (Cont.)

14. Dunn, B., Breiter, M. W., and Park, D. S., J. Applied Electrochem., 11, 1981, p. 103.

15. Bird, J. M., Tilley, A. R., and Sudworth, J. L., Proc. of the 13th IECEC, Society of Automotive Engineers, 1978, p. 685.

16. Hames, M. D., and Sudworth, J. L., Proc. IEE, 126, 1979, p. 1157.

17. Knoedler, R., and Krapf, R., J. Power Sources, 10, 1983, p. 263.

18. Levine, C. A., Proc. of the Tenth IECEC, American Society of Mechanical Engineers, 1975, p. 621.

19. Levine, C. A., Proc. of the 16th IECEC, American Society of Mechanical Engineers, 1981, p. 823.

20. Janz, G. J., Murphy, R. M., et al., "Physical Properties Data Compilations Relevant to Energy Storage," II Molten Salts: Data on Single and MultiComponent Salt Systems, National Bureau of Standards, NSRDS-NBS 61, part II, U.S. Dept. Commerce, U.S. Govt. Printing Office, Washington, DC, 1979.

21. Janz, G. J., and Murphy, R. M., J. Electrochem. Soc., 125, 1978, p. 1605.

22. Janz, G. J., Spiak, W. A., and Murphy, R. M., J. Applied Electrochem., 10, 1980, p. 789.

23. Mennicke, S., Proc. Power Sources Symp. 30, 1983, p. 48.

24. Mitoff, S. P., Breiter, M. W., and Chatterji, D., Proc. of the 12th IECEC, American Society of Mechanical Engineers, 1977, p. 359.

25. Fischer, W., Solid State Ionics, 3/4, 1981, p. 413.

26. Bauer, R., Haar, W., Kleinschmager, H., Weddigen, G., and Fischer, W., J. Power Sources, 1, 2, 1976/1977.

27. Levine, C. A., Development of a Sodium-Sulfur Battery by Electric Utilities and for Vehicular Propulsion, Final Report, DOE/ET/25103-TI, Dow Chemical Company, Midland, MI, 1981.

28. Knoedler, R., Proc. of the 17th IECEC, American Society of Mechanical Engineers, 1982, p. 552.

29. Knoedler, R., Lecture Notes in Physics, 172, 1982, p. 160.

30. Fally, J., Lasne, C., Lazennec, Y., and Margotin, P., J. Electrochem. Soc., Electrochem. Sci. and Technol., 120, 1973, p. 1292.

REFERENCES (Cont.)

31. Seeds, A. D., Wright, M. L., and Hames, M. D., "Power Sources 8," Proc. 12th Int. Symp. Power Sources., J. Thompson, ed. (London: Academic Press, 1981), p. 323.

32. Hames, M. D., Hartley, D. G., and Hudson, N. H., "Power Sources 7," Proc. of the 11th Int. Symp. Power Sources, D.H. Collins, ed. (London: Academic Press, 1979), p. 743.

O. ZINC-BROMINE

$$Zn \mid ZnBr_2 \mid Br_2$$

$$Zn + Br_2 \rightleftharpoons ZnBr_2 \qquad [1]$$

The zinc-bromine cell system was first described by Koosen in 1884[1] and patented by Bradley in 1885 and 1889.[2] The development of a practical zinc-bromine secondary battery was hindered by the inability to limit the self-discharge reaction as a result of the rapid diffusion of the highly soluble bromine to the zinc electrode surface and the short cycle life caused by internal short circuiting attendant with the formation of zinc dendrites.[3,4] A third factor which inhibited the development of the zinc-bromine battery relates to the corrosive nature of bromine resulting in the requirement for high cost metal cell components and electrodes such as ruthenized titanium.[5,6] Research and development efforts since the mid-1970's have led to the reduction of the above deleterious effects to acceptable levels by utilizing a flowing electrolyte concept, limiting the bromine solubility through complexation with quaternary ammonium compounds, restricting the diffusion of bromine to the zinc electrode by using semipermeable/cation exchange membranes, and controlling zinc morphology by carefully limiting both the charge current densities and the amount of deposited zinc. The quality of the zinc deposit is also enhanced by periodically discharging all remaining zinc metal after the load voltage cutoff level has been reached.

The zinc-bromine battery system was initially developed by Exxon and Gould, Inc. with major sponsorship from both the Electric Power Research Institute (EPRI) and the Department of Energy (DOE). The work at Exxon focussed upon the development of an electric vehicle power source system while the emphasis at Gould stressed the development of an electric utility load levelling system.[6] In 1981, Energy Research Corporation acquired the zinc-bromine battery technology from Gould, Inc. At the present time, three organizations are involved in zinc-bromine battery development work: Exxon, Energy Research Corporation, and GEL, Inc.[7] Both Exxon and Energy Research are supported with funding from DOE and EPRI. GEL, Inc. is funded privately.

The state-of-the-art Exxon zinc-bromine battery system is comprised of a cell stack containing bipolar elements of conductive "carbon plastic" bordered by non-conductive plastic material.[5] The Gould-Energy Research Corporation bipolar design utilizes a carbon electrode bonded into plastic frames. On one

side of this carbon electrode is a smooth carbon surface (zinc electrode substrate) while the other side possesses a carbon felt as the bromine electrode substrate.[7] The preferred separator for both design concepts is microporous Daramic although a great deal of success has been observed with the perfluorosulfonic acid membrane, Nafion.[8] Such separators are assembled into plastic frames containing the electrolyte manifolds which direct the flow of the two electrolytes to the appropriate electrode surfaces. A grid assembly between the separator and the zinc side of the bipolar element is used to prevent contact between the zinc deposit and the separator/frame assembly. These assembled bipolar elements are positioned so that the zinc electrode side of one bipolar element faces the bromine electrode side of a second bipolar element with a sep' tor positioned between the two electrodes. The above stacking process is continued and results in the creation of a series connected cell stack of the appropriate voltage level. A single-sided zinc or bromine end plate is located at the respective terminals of the series string.

The zinc-bromine battery is comprised of the cell stack, two electrolyte flow systems with a storage tank and pumps for the zinc negative and bromine positive electrodes, and a storage/transfer system for free bromine. The electrolyte for the battery is 3M $ZnBr_2$, 1M of a quaternary ammonium salt, and supporting electrolytes. The most prominent quaternary ammonium salts used as bromine complexing agents are tetramethyl ammonium bromide, N-ethyl N-methylmorpholinium bromide, and trioctyl methyl ammonium chloride.[9] The electrolyte also contains 4 mol/l KCl as the supporting electrolyte which results in a significant increase in solution conductivity and a reduction in solution viscosity.[5,10]

As the zinc-bromine battery is charged under constant current conditions, zinc is deposited onto the negative electrode substrate. It is believed[5] that the combined effects of flowing electrolyte system and the quaternary ammonium salt result in a smooth deposit of zinc and the elimination of dendritic zinc growth. The bromine generated on the positive electrode reacts with the quaternary ammonium salt to form a dense liquid phase which separates out in the positive electrolyte storage compartment. On discharge, a separate pump within the positive electrolyte storage unit forces the complexed bromine into the bulk aqueous electrolyte phase. The resultant solution is then directed into the positive electrode side of the cell stack. The electrochemical reaction between zinc and bromine produces zinc bromide and electrochemical energy.

The discharge/charge reactions at the zinc electrode in acidic media proceed in accordance with:

$$Zn \xrightarrow[\text{charge}]{\text{discharge}} Zn^{2+} + 2e^{1-} \qquad (2)$$

The zinc deposit is thermodynamically unstable in strong acid (particularly at pH values of less than 2) and will experience a corrosion reaction accompanied by hydrogen gas evolution:

$$Zn + 2 H_3O^{1+} \longrightarrow Zn^{2+} + 2 H_2O + H_2 \qquad (3)$$
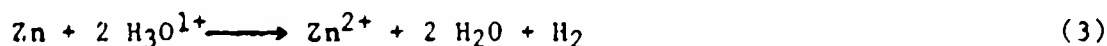
The evolved hydrogen would be carried from the negative electrode side of the microporous membrane into the negative electrolyte storage unit.[9] The accumulation of large amounts of hydrogen in the unit could cause a hydrogen-air explosion. It should be noted that, unlike the zinc-chlorine battery system (Chapter 3), the possibility for a hydrogen-halogen explosion does not present as great a hazard in the zinc-bromine battery system.[9] The accumulation of explosive gaseous mixtures of H_2 and air, H_2 and Br_2, and H_2, Br_2, and air may result from either an insufficient amount of bromine vapor required to recombine with hydrogen in the negative electrolyte storage unit or a failure of the hydrogen-bromine catalytic recombiner. Data[11] cited by Zalosh[9] indicate that hydrogen-air mixtures are flammable at hydrogen concentrations of 4 to 76 mol percent and hydrogen-bromine mixtures are flammable at hydrogen concentrations of 15 to 65 mol percent. Pressures exceeding 100 psig (greater than 700 k Pa) would undoubtedly be greater than the burst strength of the container vessel. It is predicted[9] that a significant blast wave and possible shrapnel damage would result from such an explosion hazard. In addition, significant amounts of bromine vapor could be released to the atmosphere if the protective tray and shield did not confine the positive electrolyte solution (electric vehicle battery).

The zinc electrode exhibits low polarization characteristics during both charge and discharge.[8] For example, the overpotentials at the zinc electrode comprised of reticulated vitreous carbon was found to be -0.030 V and +0.050 V for charge and discharge tests, respectively, at current densities of 40 mA/cm^2. The formation of dendritic or nodular zinc growths may be controlled to some degree by electrolyte circulation, the use of quaternary ammonium salts, limiting the charge current densities and the amount of zinc deposited on the electrode, and periodically short circuiting the cell at the end of discharge to ensure smooth deposits. However, electrochemical short circuits may be created in bipolar assemblies having a common electrolyte. A common ionic path in the electrolyte manifold would not only lead to poor energy efficiencies due to the existence of shunt currents but also could lead to zinc growth in the electrolyte manifold, thus causing severe problems with electrolyte flow. Exxon has developed techniques which provide a protective current in the manifold assembly system.[10,12,13] The net effect is the elimination of the harmful shunt currents.

The charge/discharge reactions at the bromine electrode substrate proceed in accordance with:

$$2 \; Br^{1-} \xrightarrow[\text{discharge}]{\text{charge}} Br_2 + 2e^{1-} \tag{5}$$

It should be noted that the bromine does exist as tribromide and pentabromide ions:[3,8,15]

$$Br_2 + Br^{1-} \longrightarrow Br_3^{1-}, \; K = 14\text{-}16 \tag{6}$$

and

$$2 \; Br_2 + Br^{1-} \longrightarrow Br_5^{1-}, \; K = 40 \tag{7}$$

The species produced in accordance with reactions 6 and 7 would then complex with the quaternary ammonium compound and flow into the bromine storage unit. The bromine electrode also exhibits low polarization characteristics during cell cycling. For example, the overpotentials at the electrode substrate (reticulated vitreous carbon foam coated with graphite) was found to be +0.025 V and -0.022 V for charge and discharge tests, respectively, at current densities of 40 mA/cm^2.[8]

The open circuit voltage and theoretical energy density for the zinc-bromine cell are 1.828 V and 428 Wh/kg.[15] Design specifications for a 10 kWh electric vehicle bipolar battery module required 78 cells connected in series.[14] The active surface area for each unit cell was 1200 cm^2 with a zinc electrode capacity density of 90 mAh/cm^2 (high power, electric vehicle cell design). The battery unit was discharged under constant current conditions at current densities of 20 mA/cm^2. The results showed a gently sloping load voltage plateau until approximately 80 percent of the zinc electrode material was expended. At that point, the load voltage decreased dramatically to less than 100 V. The unit was charged under constant current conditions of 20 mA/cm^2 for a period of time equivalent to a 30 percent overcharge. The voltage versus time plot exhibited a linear relationship with a slightly positive slope. The data showed coulombic efficiencies (the ratio of the discharge capacity to the charge capacity) of more than 80 percent and voltaic efficiencies (the ratio of the average load voltage to the average charge voltage) of 87 percent. The energy efficiency for this prototype electric vehicle module would then be approximately 70 percent (voltaic efficiency X coulombic efficiency). The energy densities for high power and high energy state-of-the-art designs are 55 to 60 Wh/kg and 75 to 80 Wh/kg, respectively.[14] Other performance features are summarized below:

1. Charging is accomplished through use of constant current devices preset to deliver charge for a specified length of time.[10]

2. The projected cycle lives for the Exxon electric vehicle battery consist of more than 1400 shallow cycles at discharge capacity densities of 5 to 30 mAh/cm^2, more than 400 deep cycles at random capacity densities of 60 mAh/cm^2, and more than 500 cycles at random discharge regimes.[14]

3. The operating temperature range for the zinc-bromine battery is 0 to 50°C.[15]

4. Low capacity losses would be expected for a battery unit on open circuit stand in the absence of electrolyte circulation. It should be noted, however, that significant losses would be expected if the electrolyte pumps are operational.

5. The pH of the electrolyte must be maintained in the range of 2 to 4. Excessive hydrogen evolution would occur at pH values of less than 2 while porous zinc deposits would occur as a result of charging at pH values higher than 4.[9,10]

266

No safety data were presented which detailed the electrical abuse tests of short circuit, forced overdischarge, or excessive overcharge conditions. However, in view of the fact that short circuit tests were conducted upon battery cells and modules of the zinc-chlorine system (Chapter 3) which also employs a circulating electrolyte, similar tests using zinc-bromine cells and batteries should show high short circuit values for only a brief period of time with the pumps off. With electrolyte circulation, the short circuit current could be maintained for significantly longer time periods. Subsequent performance testing showed no immediate deleterious effects for the zinc-chlorine battery after both short circuit conditions.

Electrolysis of water would eventually occur during severe overcharge and overdischarge conditions.[16] In both cases, significant amounts of oxygen and hydrogen would be evolved at the appropriate electrodes in both circumstances. It can be seen, therefore, that there would exist the possibility for a hydrogen-oxygen fire or explosion if the capability of the H_2 recombination device in the negative electrolyte storage unit was exceeded and oxygen was present. Under less severe conditions, it is believed that overcharge and overdischarge will not damage the battery.[16]

The major safety concern for the zinc-bromine system relates to the accidental release of significant amounts of bromine to the environment in the event of case rupture.[9,17] Zalosh at Factory Mutual Research Corporation conducted tests to determine the extent of the bromine hazard. Spill tests performed using the complexes formed between bromine and three representative quaternary ammonium salts showed vapor pressures in the range of 24 to 120 mm Hg (3 to 16 kPa). The physiological effects caused by exposure to various concentrations of bromine are summarized below:[18]

1. Throat irritation   : 0.3 ppm
2. Lacrimation   : less than 1 ppm
3. Odor threshold   : 1.5 to 3.5 ppm
4. Severe respiratory irritation : 10 ppm
5. Dangerous for short exposure : 40 to 60 ppm
6. Rapidly fatal   : 1000 ppm

The release of bromine to the atmosphere could result from case rupture caused by the failure of control devices (e.g., the H_2/Br_2 recombination reactor), mechanical abuse from external sources (e.g., electric vehicle crashes), or incineration conditions (e.g., garage fires or fires following an electric vehicle accident). The test results conducted by Zalosh[9] showed that transient bromine concentrations of 50 ppm at 70°C would exist for 8 to 21 meters downwind for the three bromine complexes of the study. The danger zone would range from 10 to 27 meters for spill tests conducted at 30°C. It is important to note that no testing has been conducted to determine the crashworthiness of the zinc-bromine battery in practical electric vehicles. The evolution of bromine during battery fires would be expected to lessen the fire hazard.

REFERENCES

1. Heise, G. W., The Primary Battery, Volume 1, Heise, G. W., and Cahoon, N. C., eds. (New York: John Wiley and Sons, 1971), p. 43.

2. Bradley, C. S., U.S. Patents 312,802 (1885) and 409,448 (1889), cited by J. McBreen, in "Comprehensive Treatise of Electrochemistry", Volume 3, Electrochemical Energy Conversion and Storage, J. O'M. Bockris, B.E. Conway, E. Yeager, and R.E. White, eds. (New York: Plenum Press, 1981), p. 322.

3. Will, F. G., Proc. of the 12th IECEC, American Society of Mechanical Engineers, 1977, p. 250.

4. Barnartt, S., and Forejt, D. A., J. Electrochem. Soc., 111, 1964, p. 1201.

5. Malachesky, P. A., Bellows, R. J., Einstein, H., Grimes, P., Kantner, E., Newby, K., and Young, A., Developments in Electric and Hybrid Vehicles P-105, Society of Automotive Engineers, Warrendale, PA, 1982, p. 1.

6. Douglas, D. L., and Birk, J. R., Annual Review of Energy, Volume 5, Hollander, J. M., Simmons, M. K., and Wood, D. O., eds. (Palo Alto, California: Annual Reviews, Inc., 1980), p. 84.

7. Kalhammer, F., EPRI Journal, Jan/Feb 1984, p. 58.

8. Will, F. G., "Power Sources 7," Proc. 11th Int. Symp. Power Sources, Joint Services Electrical Power Source Committee, D.H. Collins, ed. (London: Academic Press, 1979), p. 313.

9. Zalosh, R. G., and Bajpai, S. N., Comparative Hazard Investigation For A Zinc-Bromine Load Levelling Battery, Final Technical Report, PRI Project RP 1198-4, Factory Mutual Research Corporation, Norwood, MA, 1980.

10. Trowle, W. L., and Rizzo, R. A., Handbook of Batteries and Fuel Cells, Linden, D., ed. (New York: McGraw Hill Book Company 1984), p. 29-3.

11. Simmons, R. F., and Wolfhard, H. F., Trans. Faraday Soc., 15, 1955, cited in reference 9, p. 1211.

12. Zahn, M., Grimes, P., and Bellows, R. J., U.S. Patent No. 4,197,196, 1980, cited in reference 5.

REFERENCES (Cont.)

13. Grimes, P., Zahn, M., and Bellows, R., U.S. Patent No. 4,312,735, 1982, cited in reference 14.

14. Bellows, R. J., Grimes, P., Einstein, H., Kantner, E., Malachesky, P., and Newby, K., _IEEE Transactions of Vehicular Technology_, VT-32, 1983, p. 26.

15. McBreen, J., _Comprehensive Treatise of Electrochemistry_, Volume 3, Electrochemical Energy Conversion and Storage, Bockris, J. O'M., Conway, B. E., Yeager, E., and White, R. S., eds. (New York: Plenum Press, 1981) p. 322.

16. Lim, H. S., Lackner, A. M., and Knechtli, R. C., _J. Electrochem. Soc._, _Electrochem. Sci. and Technol._, 124, 1977, p. 1154.

17. Collie, M. J., ed., _Electric and Hybrid Vehicles_, Energy Technology Review, no. 44, Noyes Data Corporation, Park Ridge, N.J., 1979, p. 415.

18. American Industrial Hygiene Association, _Hygiene Guide Series_, Bromine, 1978, cited in reference 9.

P. ZINC-CHLORINE

$$Zn \mid ZnCl_2 \mid Cl_2$$

$$Zn + Cl_2 \rightleftharpoons ZnCl_2 \qquad [1]$$
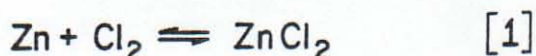
The zinc-chlorine cell system was first described by Upward in 1876[1] and patented by Pearce in 1887.[2] The practical development of the system was hindered by the inability to safely control and store toxic chlorine gas. Though relatively safe storage of chlorine on activated charcoal had been proposed for such high temperature fused salt cells as the lithium-chlorine system,[3] no effective method of chlorine control for ambient temperature aqueous cell systems was found until the early 1970's. In 1973, P.C. Symons at Oxy Metal Finishing Corporation patented a method for storing chlorine as solid chlorine hydrate for use in the secondary zinc-chlorine battery.[4] The feasibility of the battery, therefore, is dependent upon the formation of the solid chlorine clathrate-type compound in accordance with the reaction:

$$Cl_{2(aq)} + X\ H_2O \longrightarrow Cl_2 \cdot X\ H_2O_{(s)} \qquad (2)$$
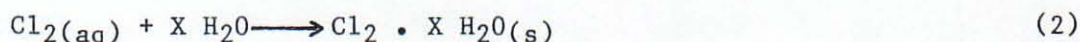
where X varies from about 6 to 10. This advanced secondary battery has been exclusively developed by Energy Development Associates (a Gulf & Western Company) for utility load levelling and electric vehicle applications. The developmental work for the utility load levelling battery was jointly funded by the Electric Power Research Institute (EPRI), the Department of Energy (DOE), and Energy Development Associates (EDA), while the electric vehicle battery development has been jointly funded by DOE and EDA.[5]

The basic cell design for the zinc-chlorine battery consists of two graphite bipolar bus bar plates which serve to hold and to space high density graphite zinc electrode substrates and highly porous graphite chlorine electrode substrates.[6] Each bus bar plate is grooved on both sides to retain the zinc electrode plates on one side, as in the teeth of a comb, and the chlorine electrodes on the other. These assembled bus bars are then positioned so that the zinc electrode side of one bus bar plate intermeshes with the chlorine electrode side of the second bus bar plate, forming an alternating negative and positive electrode array. The above process is continued and results in the creation of a series connected cell stack of the appropriate projected voltage level. A single-sided zinc or chlorine end bus plate is located at the respective terminals of the series string.

The negative electrode substrate is typically comprised of dense graphite plates of Union Carbide ATJ or EBP grade materials.[7] These graphites exhibit high coulombic efficiencies, low polarization characteristics, and high capacity densities. However, since both graphites are relatively expensive and contribute significantly to the total cost of the zinc-chlorine battery, studies at EDA were conducted to evaluate and qualify several alternate low cost graphites for use in the battery. Graphite grade CLD was found to compare favorably to the ATJ material when tested in a prototype battery design.[7]

The discharge/charge reactions at the zinc electrode in acidic media proceed in accordance with:

$$Zn \xrightarrow[\text{charge}]{\text{discharge}} Zn^{2+} + 2e^{1-} \tag{3}$$

Zinc is thermodynamically unstable in strong acid and will experience a corrosion reaction accompanied by hydrogen gas evolution:

$$Zn + 2 H_3O^{1+} \longrightarrow Zn^{2+} + 2 H_2O + H_2 \tag{4}$$
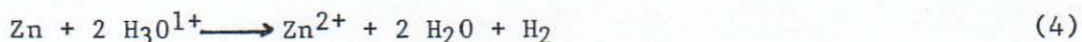
The corrosion reaction is enhanced if transition metal impurities such as iron, copper, and nickel are present in the electrolyte.[8] Studies at EDA have also shown that the degradation products which resulted from the activation of the porous graphite chlorine electrode in HNO_3 solutions at high temperatures significantly contributed to corrosion and hydrogen gas evolution. The elimination of the problems attendant with these impurities may be effected by thoroughly rinsing cells after fabrication or by using alternate electrolytical activation methods.[6] A related mechanism leading to further zinc corrosion with hydrogen evolution concerns the oxidation of the chlorine electrode during normal cell operation.[9] Graphite will be oxidized in accordance with the reaction:

$$C + 2 Cl_2 + 2 H_2O \longrightarrow CO_2 + 4 HCl \tag{5}$$
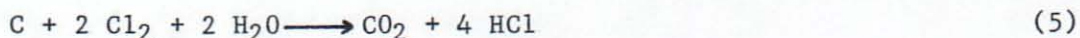
Zinc could then react with the HCl produced and generate hydrogen as in reaction 4, above. Since the reaction of chlorine with the porous graphite substrate is slow, it is believed that the life for the chlorine porous graphite electrode will meet or exceed the ten year goal.[5]

The zinc electrode exhibits low polarization characteristics during both discharge and charge.[10] For example, the overpotentials at the zinc electrode (ATJ graphite) were found to be -0.050 V and +0.040 V for charge and discharge tests, respectively, at current densities of 22 mA/cm^2. However, the zinc produced during charging may result in the formation of dendritic or nodular growths which could cause short circuiting, accelerated self-discharge, and low coulombic efficiencies. Such deposits were typically found to occur at the electrode edges[7] and at the junction of the electrode with the intercell bus bar plate.[11] The formation of these dendrites may be reduced by "masking" the zinc plate edges and junction areas with a coating of Kynar resin and graphite[7] and reducing electrolyte leakage paths between cells.[11] Other methods to control the formation of dendrites include the addition of amine compounds[12] and such inorganic compounds as thallium chloride to the electrolyte.[13] Though both types of additives minimize dendrite formation,

NSWC TR 84-302

present technology exclusively employs the inorganic additives. Dendrite formation may also be minimized by periodically discharging all remaining zinc after the load voltage cutoff level has been reached.[14] This is usually accomplished by electrically short circuiting the battery.

The chlorine electrode is comprised of two porous graphite plates (e.g., Union Carbide PG 60) which have been machined in such a way to create an inner void space when the two sections have been bonded together.[6,7] Provision is made for the fitting of electrolyte feeder tubes into the resulting compartment and for the escape of the chlorine gas during charging. The discharge/charge reactions at the chlorine electrode proceed in accordance with:

$$Cl_2 + 2e^{1-} \xrightarrow[\text{charge}]{\text{discharge}} 2 Cl^{1-} \tag{6}$$

Discharge at the chlorine electrode proceeds in accordance with a two-step mechanism:[15]

$$Cl_2 + e^{1-} \longrightarrow Cl_{ads} + Cl^{1-} \tag{7}$$

and

$$Cl_{ads} + e^{1-} \longrightarrow Cl^{1-} \tag{8}$$

with the latter reaction being the rate determining step. Chlorine electrodes of "as received" porous graphite exhibit particularly high polarization during both discharge and charge. In view of the above, two methods have been employed to reduce the polarization of the porous electrode. The first procedure required heating the electrodes at 115°C in nitric acid for periods of 10 to 13 days.[6] Investigations of electrodes treated by the above process showed overpotentials of +0.12 V and -0.20 V for the charging and discharging processes, respectively, at current densities of 22 mA/cm^2.[10] The second technique is performed using fully assembled cells.[7] These cells are charged for only a few hours with a one percent solution of $ZnCl_2$ flowing through the cell assembly. The polarization characteristics for these porous chlorine electrodes are significantly less than for those treated with nitric acid.[7]

A second, more important self-discharge mechanism in the zinc-chlorine system concerns the chemical reaction between the zinc at the negative electrode and chlorine dissolved in the electrolyte.[16] This process occurs during charge and discharge of the battery but is most detrimental during open circuit stand following charging. The chlorine produced by the decomposition of the chlorine hydrate in the latter instance will migrate to the cell stack and react with the zinc. After a short period of time (e.g., hours), the open circuit voltage will drop to 0 volts with the electrolyte circulation pumps off. An auxiliary power source must be employed to initiate electrolyte flow under these circumstances.[19] Correspondingly, the open circuit voltage will be intermediate between 0 and the open circuit voltage when the pumps are operational. Under this condition, very little capacity would be realized.[9] The solubility of chlorine in the electrolyte varies from about 0.01 to 0.03 M under atmospheric pressure conditions[10] and may be reduced significantly by decreasing the pressure in the battery cell stack. Under practical operational

273

conditions, the cell stack pressure is maintained under partial vacuum conditions.[6,7] For example, values for cell stack pressures under charge and discharge conditions are typically 70 to 90 kPa and 50 to 75 kPa, respectively.[7,11]

Studies at EDA have shown that the optimum electrolyte for the zinc-chlorine battery system is 2.5 M $ZnCl_2$ containing KCl and NaCl as supporting electrolytes.[7] The pH of the solution is about zero. The selection criteria for the choice of supporting electrolyte concentrations included high conductivity, low chlorine solubility, high electrochemical energy efficiency, and high (greater than 200 mAh/cm^2) capacity densities.[7] Three electrolyte solutions were found to meet or exceed the requirements for 70 percent electrochemical energy efficiency and for greater than 200 mAh/cm^2 capacity densities: 2.5 M $ZnCl_2$ with 2.0 M KCl, 2.5M $ZnCl_2$ with 4.0 M KCl and 1.0 M NaCl, and 2.5 M $ZnCl_2$ with 3.0 M KCl and 2.0 M NaCl.[7] No separator is employed in the zinc-chlorine battery.

The zinc-chlorine secondary battery is comprised of the cell stack, an electrolyte storage unit (sump), and the chlorine hydrate storage unit.[6,7] Prior to initial operation, the zinc-chlorine battery unit is in the fully discharged state, i.e., the battery does not contain either elemental zinc or chlorine as chlorine hydrate but only contains the concentrated $ZnCl_2$ electrolyte. This safety feature avoids the risk of hazardous conditions during handling and installation. During constant current charging, the $ZnCl_2$ is electrolyzed with zinc deposited on the dense graphite electrodes and chlorine evolved on the porous graphite electrodes. The chlorine is then pumped from the gas space of the cell stack into the chlorine hydrate storage unit while the electrolyte is returned to the sump. The chlorine reacts with water (load leveling) or electrolyte (electric vehicle) refrigerated to temperatures of 0 to 10°C to form chlorine hydrate in accordance with reaction 2. The reaction of chlorine with water is exothermic with a heat of formation of -18.6 kcal/mol (77.8 kJ/mol) for the compound $Cl_2 \cdot 8H_2O$.[17] In view of the above, the chlorine hydrate storage unit is continuously refrigerated during the charging process. As charging proceeds, the hydrate is filtered and eventually forms a solid block. It is interesting to note that the resultant chlorine hydrate may be handled with bare hands without injury.[18] Under complete charge conditions, the $ZnCl_2$ concentration in the electrolyte is about 0.5 to 1.0 M.

On discharge, the chlorine hydrate at a maximum temperature of 9.6°C is decomposed by heating with warm electrolyte circulated through the storage unit or by heat exchange with the sump. Since the chlorine hydrate storage unit gas pressure is higher than that for the cell stack, the return of electrolyte containing dissolved chlorine to the cell stack is facilitated in the electric vehicle battery.[17] For the load leveling battery, chlorine is forced from the storage unit to the electrolyte in close proximity to the porous graphite chlorine electrode. In either case, the electrochemical reaction between zinc and chlorine occurs which releases both electrical energy and significant amounts of heat.[7] The heat is then transferred to the chlorine hdyrate storage unit to bring about further decomposition of chlorine hydrate. As discharge proceeds, $ZnCl_2$ is formed in the electrolyte until, at the end of discharge, the original 2.5 M $ZnCl_2$ concentration is restored.

Several important differences exist between the electric vehicle and load leveling zinc-chlorine battery as developed by EDA. These differences arise from the necessity to minimize the battery weight while maintaining high power densities for the electric vehicle battery and to maximize the energy efficiency for the load leveling battery.[19] In view of the above, the electric vehicle battery uses the battery electrolyte in the formation of the chlorine hydrate rather than a separate store of pure water as in the load leveling battery design. The use of separate water storage in the load leveling battery, however, provides a more efficient means for refrigeration during the charging process. The electric vehicle battery does not possess the means for refrigeration on board the vehicle. The refrigeration device is included with the charging equipment. In addition, one less heat exchange unit is required for the electric vehicle battery since hydrate decomposition may be effected by pumping electrolyte from its storage unit directly into the hydrate storage unit.[19] In comparison, the load leveling battery requires that warm electrolyte be pumped through titanium tubing in the storage unit. Maximum power densities are further obtained in the electric vehicle battery by fabricating unit cells with a minimum interelectrode separation of about 0.20 cm. The interelectrode separation for load leveling cells is about 0.33 cm. This greater interelectrode separation results in higher energy efficiencies.[19]

The zinc-chlorine battery system possesses several operational and safety features which aid in the effective operation of the battery and the prevention of hazard-related conditions. These devices and design features are summarized below:

1. An inert gas separation and rejection device consists of a chlorine-chlorine electrochemical cell which separates gases other than chlorine from the battery atmosphere and vents them to the external atmosphere. The presence of such gases as CO_2, CO, and O_2 from the degradation of the porous chlorine electrode are deleterious to battery performance, reduces the partial pressure of chlorine, and decreases the solubility of chlorine in the electrolyte.

2. Hydrogen will react explosively with chlorine when hydrogen concentration levels in chlorine are greater than about 18 percent.[9,20] The occurrence of explosions would result in only mild pressures being developed but detonations of hydrogen-chlorine gas mixtures result in pressure increases of more than 2000 psi (13800 kPa) within a few milliseconds.[20] Such high pressures would undoubtedly result in the rupture of the polyvinyl chloride-lined fiberglass container vessel for the zinc-chlorine battery. Irradiation of a H_2-Cl_2 gas mixture by ultraviolet radiation at 3500 angstroms has been shown to safely remove the hydrogen by forming HCl.[20] In view of the above, one design consideration for the zinc-chlorine battery included the use of UV lights to facilitate the combination of free hydrogen with Cl_2. Though UV lamps have been exclusively employed in zinc-chlorine batteries to date, the present UV reactor lasts for approximately two months and is dependent upon an outside power source. Recent work at EDA has focussed upon the development of a self-powered tritium light as a back up reactor to the UV fluorescent lights.[7,9]

3. Other safety designs for the zinc-chlorine system include one way relief valves for the escape of all Cl_2 into an external vessel containing a chlorine absorbent such as ammonia in water[21] or caustic soda[22] in the event of overpressure, external Cl_2 gas detection devices,[9] phototransducer detectors to indicate failure of the hydrogen reactor, pressure transducers to monitor below ambient pressures in the cell stack, and temperature sensors located in both the electrolyte and hydrate storage units as well as at ultraviolet hydrogen reactor. Several fault detection and safety shutdown mechanisms have also been included in the battery controller design.[9]

The open circuit voltage and theoretical energy density values for the zinc-chlorine cell are 2.12 V and 826 Wh/kg, respectively.[8] Design specifications for a 104 MWh load leveling battery plant require 36 parallel strings of 44 battery modules connected in series.[6] EDA refers to this design concept as the "Mark 4." Each module ("FC + 5") consists of ten cells in series with an open circuit voltage of 21.2 V and a nominal capacity of 3300 Ah. The estimated average discharge voltage for the module is 20.0 V. The energy design goal for the module would then be approximately 66 kWh. Charging would be performed under constant current density/constant voltage conditions at 544 A (33 mA/cm^2) for seven hours (3808 Ah) and 21.8 V (2.18 V per cell). The module could then be discharged under constant current conditions of 659 A (40 mA/cm^2) for five hours at an average load voltage of 20.0 V (2.00 V per cell). It can be seen that the coulombic and voltaic efficiencies are 86.5 percent (i.e., 3295 Ah/3808 Ah X 100%) and 91.7 percent (i.e., 20.0/21.8 X 100%) for the module. The electrochemical energy efficiency, the product of the coulombic and voltaic efficiencies, is 79.4 percent. At the end of the discharge period, about 1.7 percent of the zinc remains undischarged. To ensure uniform plating on subsequent charging, this unused zinc is removed by externally shortcircuiting the module while slowly circulating the electrolyte. No energy density or weight values were given for this module. An electric vehicle preproduction zinc-chlorine battery consisting of two parallel strings of 30 cells in series and weighing 636 kg was developed to power a four passenger vehicle.[19] The overall dimensions for the battery were 229 cm X 56 cm x 19 cm. This battery achieved over 200 charge/discharge cycles in vehicle testing. The maximum energy delivered by the battery was 41 kWh[19] corresponding to an energy density of 64 Wh/kg and a power density of 59 W/kg.[19]

Extensive safety testing and analysis have been reported for the zinc-chlorine battery system.[6,7,9,13,17,22] Short circuit tests were performed using a 45 kWh battery module comprised of ten cells in series.[7] These tests not only concerned the safety aspects relative to the occurrence of external short circuits but also determined the feasibility of employing the short circuit as a method to bypass defective modules in a series string, thus avoiding the complete elimination of the string from the battery. Though nine tests were conducted with the electrolyte pump off, one module was short circuited with the electrolyte pump in operation for 30 seconds. The test results for modules without electrolyte circulation showed peak short circuit currents of 9200 A after 0.004 second. The current decreased rapidly to a value of 400 A at the 15-second mark. At the conclusion of these tests, voltage recovery was observed to be very slow. The peak short circuit current for the module with electrolyte circulation was also observed to be 9200 A. However, the decrease in the current was considerably less (i.e., at the end of the 30

second test, the observed short circuit current was 1200 A). Subsequent performance testing using these modules showed no immediate deletereous effects. In fact, slight improvement in efficiencies were noted.[7]

Though no specific data was reported whioh described the results of forced overdischarge testing of zinc-chlorine cells or batteries, EDA[7] has stated that "the zinc-chlorine battery does not suffer performance-wise in subsequent charge-discharge cycles because of overdischarge". In overdischarge, all zinc would be reacted and only chlorine would be evolved at the dense graphite electrode (zinc substrate).

As in the case for overdischarge testing, no data was presented describing the results for prolonged overcharge conditions. However, it is believed that internal short circuiting would occur due to extensive formation of zinc dendrites.[6,7] It should also be noted that no hazards or long term performance losses have been reported for zinc-chlorine cells, modules, or battery units with extensive dendritic or nodular zinc growths.

The major safety concern for the zinc-chlorine system relates to the accidental release of chlorine gas in the event of battery case rupture.[7,9,17,22] Chlorine is neither flammable nor explosive under normal conditions, but the gas is highly toxic. The physiological effects caused by exposure to various concentrations of chlorine are summarized below:[23]

1. Slight irritation after long term exposure: 1 ppm

2. Detectable odor limit: 0.02 to 3.5 ppm

3. Coughing: 30 ppm

4. Dangerous if exposure 30 minutes or more: 40-60 ppm

5. Unbearable in 1 minute: 100 ppm

6. Fatal for most animals after a few deep breaths: 1000 ppm

The release of chlorine to the atmosphere would result from case rupture caused by the failure of control devices (e.g., the H_2/Cl_2 reactor), mechanical abuse from external sources (e.g., electric vehicle crashes or rupture of load leveling modules at an electric storage facility), or incineration conditions (e.g., garage fires or exposure to high temperature environments). It should be emphasized that, in addition to the safety features already discussed for the zinc-chlorine system, several intrinsic safety features relative to the release of chlorine lessen the hazard:[6,7,9,17,22]

1. The solid chlorine hydrate will remain within the hydrate storage unit in the case for a minor case rupture. The escape of chlorine to the atmosphere will be slow.

2. Large load leveling batteries would be comprised of several hundred modular units. It can be seen, therefore, that only a restricted amount of chlorine would escape. For example, one design[6] for a 100 MWh battery plant requires 36 strings of 44 modules connected in series. The total amount of chlorine required for battery operation would be about 73180 kg. However, single modules only contain 46.2 kg of Cl_2.

3. A severe rupture of the module case would result in a complete hydrate spill onto the area surrounding the scene. Even under these circumstances, the chlorine release would be slowed since the hydrate decomposes at 9.6°C. Decomposition would also be affected by the ambient temperature, heat transfer characteristics, hydrate form (solid or slush), and the amount of contact area.

Chlorine hydrate spill tests conducted by Zalosh at Factory Mutual Research Corporation[17] showed that transient chlorine concentrations of 100 ppm would exist 23 meters downwind of a complete spill onto a 30 to 38°C surface. These conditions simulated the total loss of the hydrate from a 50 kWh electric vehicle battery. It is important to note that no testing has been performed which determined the crashworthiness of the battery in practical electric vehicles. Similar testing for zinc-chlorine load leveling modules has not been reported.

(·

REFERENCES

1. Heise, G. W., The Primary Battery, Volume 1, Heise, G. W., and Cahoon, N. C., eds. (New York: John Wiley and Sons, 1971), p. 43.

2. Pearce, J. E., U.S. Patent NO. 356, 261, cited by D.L. Douglas and Birk, J. R., Annual Review of Energy, Volume 5, J.M. Hollander, Simmons, M. K., and D.O. Wood, eds. (Palo Alto, California: Annual Reviews, Inc., 1980), p. 74.

3. Werth, J., and Zeitner, E. J., Jr., Proc. of the Second IECEC, American Society of Mechanical Engineers, 1967, p. 927.

4. Symons, P. C., U.S. Patent No. 3,713,888, 1973.

5. Douglas, D. L., and Birk, J. R., Annual Review of Energy, Volume 5, Hollander, J. M., Simmons, M. K., and Wood, D. O., eds. (Palo Alto, California: Annual ' views, Inc., 1980), p. 75.

6. Energy Development Associates, ' velopment of the Zinc-Chlorine Battery for Utility Applications, EPRI EM 1u51 Interim Report, Electric Power Research Institute, Palo Alto, CA, 1979.

7. Energy Development Associates, Development of the Zinc-Chloride Battery for Utility Applications, EPRI EM-1417 Interim Report, Electric Power Research Institute, Palo Alto, CA, 1980.

8. McBreen, J., Comprehensive Treatise of Electrochemistry, Volume 3, Electrochemical Energy Conversion and Storage, J. O'M. Bockris, B. E. Conway, E. Yeager, and R. E. White, eds. (New York: Plenum Press, 1981), p. 321.

9. Argonne National Laboratory, Preliminary Safety Analysis of the Zinc Chlorine Electric Vehicle Battery, Argonne National Laboratory ANL/CNSVTM-84, 1981.

10. Jorne, J., Kim, J. T., and Kralik, D., J. Applied Electrochem., 9, 1979, p. 573.

11. Clubb, R. D., Warde, C. J., and Carr, P., Proc. Power Sources Symp. 29, 1981, p. 192.

12. Doe, J. B., Batteries and Electric Cells, Secondary, Encylcopedia Chem. Tech., Third Edition, 1978, p. 664.

REFERENCES (Cont.)

13. Poddes, A., and Kapner, M., Analysis of Batteries for Use in Photovoltaic Systems, Final Report, Volume 1, Department of Energy, DOE/ET/25201-1, 1981.

14. Cairnes, E. J., Energy and Chemistry, R. Thompson, ed., Royal Society of Chemistry, Special Publication No. 41, 1981, p. 261.

15. Kim, J. T., and Jorne, J., J. Electrochem. Soc., Electrochem. Sci. and Technol., 124, 1977, p. 1473.

16. Kim, J. T., and Jorne, J., J. Electrochem. Soc., Electrochem. Sci. and Technol., 125, 1978, p. 89.

17. Zalosh, R. G., Bajpai, S. N., Short, T. P., and Tsui, R. K., Chlorine Hazard Evaluation for the Zinc-Chlorine Electric Vehicle Battery, Final Technical Report, Factory Mutual Corporation, COO-5088-1, Norwood MA, 1980.

18. Unnewehr, L. E., and Nasar, S. A., Electric Vehicle Technology, (New York: John Wiley and Sons, 1982), p. 74.

19. Carr, P., Warde, C. J., Lijoi, A., and Brummet, B. D., Proc. Power Sources Symp. 30, 1983, p. 99.

20. Eichelberger, W. C., and Hartford, W. W., Electrochem. Technol., 5, 1967, p. 104.

21. Mitra, S., J. Power Sources, 8, 1982, p. 359.

22. Bechtel Corporation, Engineering Design and Cost Analysis of Chlorine Storage Concepts for a Chlorine Load Leveling Battery, NTIS No. PB 262016, U.S. Dept. Commerce, Springfield, VA, 1975.

23. Fieldner, A. C., Katz, S. H., and Kinnsy, S. P., Gas Masks for Gases Met in Fighting Fires, Bureau of Mines Technical Paper 248 (1921), not presently available: data cited in Reference 17.

Q. ZINC-LEAD DIOXIDE

$$Zn \mid H_2SO_4 \mid PbO_2$$

$$Zn + PbO_2 + 2\,H_2SO_4 \rightleftharpoons PbSO_4 + ZnSO_4 + 2H_2O \qquad [1]$$

The substitution of zinc for lead in the lead-lead dioxide sulfuric acid battery system was attempted in 1843. The advantages of a zinc negative electrode in this system include higher operating voltages, lighter weight, and high rate capability.[1] Indeed, this system was used for streetcar propulsion in New York about 1887. The zinc-lead dioxide system produces a soluble reaction product, $ZnSO_4$, and an insoluble reaction product, $PbSO_4$, in accordance with equation 1. However, zinc is rapidly corroded in the sulfuric acid electolyte. Heavy amalgamation of the zinc and the copper current collector for the zinc electrode alleviated the corrosion problems somewhat but resulted in zinc electrodes of poor mechanical strength. The chief disadvantage of the zinc-lead dioxide system, however, was the poor charging characteristics of the zinc electrode in the sulfuric acid electrolyte. It was found that smooth zinc deposits were obtained at either the initial stages of the charge process or for a few charge-discharge cycles. Eventually, however, a mossy, nonadherent zinc deposit would be obtained at the end of the first charging period or after several cycles.[1,2] Though mossy zinc deposits are not in themselves detrimental to cell operation, the mossy zinc deposits could promote zinc electrode shape change, densification, and dendrite formation in zinc secondary systems. In view of the above difficulties relative to the zinc electrode, the zinc-lead dioxide sulfuric acid battery is now considered only as a reserve primary system.

Much of the developmental work relative to the zinc-lead dioxide primary reserve battery was performed by The Electric Storage Battery Company.[3] The chief goal of this work was the production of prototype batteries for many military applications. The negative electrode was a thin sheet of high purity zinc amalgamated with mercury. The positive electrode consisted of a lead alloy grid filled with PbO_2 similar to the positive electrodes of the lead-lead dioxide sulfuric acid battery. The separator material was a combination of a woven plastic screen with a porous paper.

The concentration of the sulfuric acid electrolyte varied from 35 to 50 weight percent. The higher concentrations were found to increase the efficiency of the lead dioxide electrode and increase the polarization of the zinc

electrode. The lower sulfuric acid concentrations produced the opposite effects. Optimum performance characteristics were obtained using a sulfuric acid concentration between 35 and 50 weight percent.

The open circuit voltage for the zinc-lead dioxide system was 2.5 V, approximately. Prototype cells were discharged at current densities of 10 to 240 mA/cm^2 to a voltage cutoff level of 1.6 V. The corresponding capacities, based upon the electrode surface area, were 20 mAh/cm^2 to 11 mAh/cm^2, respectively. The maximum energy densities varied from 108 to 78 Wh/kg for cells discharged at current density values of 137 to 207 mA/cm^2, respectively.

The zinc-lead dioxide primary reserve system suffers from a number of disadvantages relative to effective operation for military applications. The two most prominent disadvantages are poor performance characteristics at low temperatures and high hydrogen gas evolution accompanied by zinc corrosion. Indeed, the lower temperature limit for effective operation is 25°C or higher.[3] Even though the system possesses such advantages as high operating voltages at high current densities, low cost, and good storability characteristics, the only known application was for ship lifeboat radio systems.[4]

Recently, the zinc-lead dioxide system has been investigated as a direct secondary battery replacement for the lead-lead dioxide sulfuric acid system.[5] In contrast to the zinc-lead dioxide system described above, this zinc-lead dioxide system used a saturated, neutral solution of sodium sulfate and zinc sulfate as the electrolyte. Several advantages were found for the zinc-lead dioxide cells when compared to similarly constructed lead-lead dioxide sulfuric acid cells. The zinc based system is lighter and its discharge characteristics show gradual decreases in voltage rather than the abrupt voltage decreases observed for the lead-lead dioxide system. In addition, the zinc system yields higher energy densities during discharge and operates at higher voltage levels. However, the open circuit voltage levels for the zinc-lead dioxide system decreases following charging, from about 2.57 V immediately after charging to the 2.00 V level twelve hours after charging. This indicated a faster self-discharge process between the lead dioxide and the electrolyte[5] for the zinc-lead dioxide system than for the lead-lead dioxide sulfuric acid system. In summary, the zinc-lead dioxide system does not exhibit a definite superiority over the conventional lead-lead dioxide system at the present. This zinc system has not yet reached the advanced prototype or production phases of development.

Attempts have also been made to adapt the primary zinc-lead dioxide cell to an alkaline electrolyte system.[6] Spirally wound and bobbin C-size cells were used in the investigation. For comparison purposes, Leclanche C-size cells were similarly tested. The optimum electrolyte for these zinc-lead dioxide cells was found to be a solution of 8M ammonium hydroxide, NH_4OH, and 1M zinc chloride, based upon a high specific conductivity of 0.13 ohm^{-1}cm^{-1}, a low solubility of the PbO_2, and a low corrosion rate for zinc of 1.3 g/cm^2/day. Spirally wound C cells exhibited open circuit voltages of 1.52 V. Cells were discharged at 0.2, 0.6, and 1.0 A to a voltage cutoff level of 0.75 V. The corresponding utilization of the lead dioxide electrodes were found to be 61, 44, and 25 percent respectively, based upon the cell reaction:

$$Zn + PbO_2 \longrightarrow ZnO + PbO \tag{2}$$

Bobbin cells containing soluble ammonium bicarbonate, NH_4HCO_3, in the lead dioxide matrix were tested versus zinc-manganese Leclanche C cells. The inclusion of the soluble NH_4HCO_3 was used to provide increased porosity in the lead dioxide positive electrode matrix. The open circuit voltage for these cells increased to 1.8 V, due to the inclusion of the NH_4HCO_3. Cells discharged under constant loads of four ohms to a 0.75 V cutoff level yielded discharge times of 3.9 and 1.9 hours for the zinc-lead dioxide and zinc-manganese dioxide cells, respectively. It should be noted, however, that the average weight of a Leclanche C cell is about 40 grams and that for the zinc-lead dioxide C cell is 71 grams. In view of this weight differential, the energy density values were identical (i.e., about 151 Wh/kg). Several other disadvantages were noted for the alkaline zinc-lead dioxide system: 1) the electrolyte freezing point was -10°C; poor low temperature performance would be expected, 2) the electrolyte is significantly more corrosive than the Leclanche electrolyte, and 3) the high vapor pressure of the electrolyte precludes the use of cell designs employing vent structures. No commercialization of the alkaline zinc-lead dioxide system is presently planned. The work relative to the investigation of the alkaline zinc-lead dioxide system was performed at P.R. Mallory and Company, Inc. (Duracell International).

In view of the fact that no viable commercialization of the zinc-lead dioxide battery systems (sulfuric acid, neutral salt, or alkaline electrolytes) is presently taking place, no recommendation relative to safety testing cells or batteries is given. Further, no safety data relative to NAVSEAINST 9310.1A were presented for the zinc-lead dioxide system with the various electrolytes in the literature. It should be noted, however, that copious amounts of hydrogen were evolved from cells under both open circuit and operating conditions. Storage of activated cells or discharge of cells in unventilated areas could result in hydrogen-air fires or explosions.

REFERENCES

1. Vinal, G. W., _Primary Batteries_ (New York: John Wiley and Sons, 1950), p. 302.

2. McBreen, J., and Cairns, E. J., _Advances in Electrochemistry and Electrochemical Engineering_, Volume Eleven, H. Gerischer and Tobias, C. W., eds. (New York: John Wiley and Sons, 1978), p. 317.

3. Schlotter, W. J., _J. Electrochem. Soc._, 99, 1952, p. 205C.

4. Barak, M., _IEE Reviews_, 117, 1970, p. 1568.

5. Abdo, M. S. E., and Fahidy, T. Z., _J. Applied Electrochem._, 12, 1982, p. 225.

6. Rao, M. L. B., _J. Electrochem. Soc._, 120, 1973, p. 855.

R. ZINC – NICKEL(III)OXYHYDROXIDE   (NICKEL-ZINC)

Zn | KOH | NiOOH

$$Zn + 2\,NiOOH + 2\,H_2O \rightleftharpoons Zn(OH)_2 + 2\,Ni(OH)_2 \qquad [1]$$
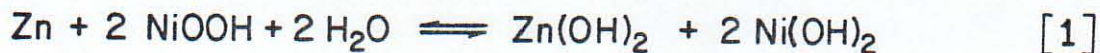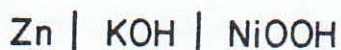
The first descriptions for the zinc-nickel (III) oxyhydroxide (nickel-zinc) and the nickel-iron systems were made around 1900 by Jungner, Edison, and de Michalowski.[1,3] The basic patents for practical nickel-zinc batteries, however, were obtained by Drumm in the early 1930's.[4] The first applications for nickel-zinc batteries included train propulsion and lighting in Ireland. Interest in this system declined considerably until the early 1960's when Russian investigators reported improvements in the energy density and cycle life characteristics. With passage of the Electric and Hybrid Vehicle Research, Development, and Demonstration Act of 1976, there was renewed interest in the nickel-zinc system for meeting near term electric vehicle propulsion requirements in the United States. Both nickel-zinc and nickel-iron systems possess theoretical energy densities (345 and 263 Wh/kg, respectively) between that of the lead-acid (175 Wh/kg) and such advanced systems as sodium-sulfur (760 Wh/kg) and lithium/aluminum-iron disulfide (650 Wh/kg). In view of the above, intense efforts by ESB, Energy Research Corporation, Gould, Eagle-Picher, and Yardney in the United States have resulted in the design, fabrication, and testing of full sized nickel-zinc prototype electric vehicle batteries.[2]

The discharge reactions at the zinc electrode in alkaline solution proceeds as follows:

$$Zn + 2\,OH^{1-} \longrightarrow Zn(OH)_2 + 2e^{1-} \qquad (2)$$

The $Zn(OH)_2$ dissolves in the electrolyte and forms zinc oxide:[5]

$$Zn(OH)_2 + 2\,OH^{1-} \longrightarrow Zn(OH)_4^{2-} \qquad (3)$$

and

$$Zn(OH)_4^{2-} \longrightarrow ZnO + 2\,OH^{1-} + H_2O \qquad (4)$$

Passivation of the zinc electrode occurs when the solubility limit of the discharge products surrounding the electrode or within the electrode matrix is exceeded. Zinc oxide films are formed in accordance with reaction 4, above, or by reaction 5

$$Zn(OH)_2 \longrightarrow ZnO + H_2O \tag{5}$$

A summary of the passivation characteristics for zinc electrodes in strong alkaline media is given for the zinc-mercuric oxide system, Chapter 2.

Zinc is thermodynamically unstable in strong alkaline solutions and will experience a corrosion reaction accompanied by hydrogen gas evolution. Hydrogen will be reduced in accordance with the reaction:

$$2 H_2O + 2e^{-1} \longrightarrow H_2 + 2 OH^{1-} \tag{6}$$

The standard potentials for reactions 2 and 6 are 1.245 and -0.828 V, respectively. The corrosion reaction may be significantly reduced by increasing the hydrogen overpotential of the zinc through amalgamation and the use of pure zinc electrodes. Amalgamation of the zinc electrode for the nickel-zinc system is typically accomplished by adding various amounts of mercuric oxide to the zinc or zinc oxide mixture prior to electrode fabrication. The substitution of bismuth trioxide and cadmium oxide for mercury in nickel-zinc cells has been shown to significantly reduce hydrogen evolution and increase cycle life.[6] In addition, Himy[7] has found that binary mixtures of cadmium, lead, indium, and thallium oxides or hydroxides not only reduce the zinc corrosion reaction but also act as extenders in preventing densification of the zinc electrode material.

The electrodeposition of zinc from the electrolyte is a two step process:[8]

$$Zn(OH)_4^{2-} \longrightarrow Zn(OH)_2 + OH^{1-} \tag{7}$$

and

$$Zn(OH)_2 + 2e^{1-} \longrightarrow Zn + 2 OH^{1-} \tag{8}$$

The zinc produced in accordance with reaction 8 may be either mossy or dendritic dependent upon the charge current density, potential, and zincate ion concentration in the vicinity of the zinc electrode matrix.[9] Mossy zinc is formed at low current densities (e.g., 4 to 20 mA/cm^2), low overpotentials (below 75 mV), and in solutions of sufficient zincate ion concentration.[8,9] If the current density and the potential are increased or the zincate concentration is reduced, zinc dendrite formation will occur. Dendritic zinc could grow through the separator material and cause catastrophic short circuiting or accelerated self-discharge. A second mode of failure for the zinc electrode relates to the loss of electrode porosity and effective surface area by the agglomeration of zinc and the migration of zinc from the sides and top of the electrode to the center ("shape change"). During charging, dendritic zinc grows preferentially at the top and edges of the electrode and mossy zinc is deposited over a layer of ZnO at the center of the zinc plate. The growth of dendritic zinc is enhanced by the depletion of the $Zn(OH)_4^{2-}$ species as the zinc electrode experiences shape change. The use of KOH electrolyte satured with ZnO reduces the severity of $Zn(OH)_4^{2-}$ concentration effects during charging. The suppression of zinc electrode shape change has been investigated for a number of secondary zinc electrochemical systems.[10,11] The effects of current distribution differences at the zinc electrode and high convective flow

286

rates were found to substantially contribute to the "shape change" phenomenon. One approach to alleviate the problem uses zincate ion complexation agents such as $Ca(OH)_2$. The addition of $Ca(OH)_2$ to the zinc electrode composition has been found to inhibit zinc dissolution.[6,8]

Several methods to control zinc dendrite formation and electrode shape change by mechanical means have been attempted. Vibration of the zinc electrode during the charging process results in a small degree of turbulence in the electrolyte layer immediately surrounding the zinc electrode and stirring of the bulk electrolyte.[12] The net effect of this charging method is the production of a smooth, adherent zinc layer over the total area of the zinc electrode surface. Further advantages of vibrating the electrode include higher utilization of the zinc active material and the inclusion of the vibrating mechanism with the off-vehicle charging equipment.[2] A second approach uses a rotating shutter assembly situated on either side of a zinc electrode between two nickel oxyhydroxide electrodes.[13] Shutter operation during charging not only stirs the electrolyte but also subjects the zinc electrode to a pulse charging process. As a result, both dendrite formation and shape change are thus avoided to a great extent. In view of the design considerations for the latter method, the shutter assembly is not presently under consideration for electric vehicle nickel-zinc cells.

The development of sealed nickel-zinc cells for electric vehicle and other applications has been pursued by several investigators.[2,6,14-18] During cell overcharge conditions, oxygen is evolved at the nickel oxyhydroxide electrode and hydrogen may be evolved at the zinc electrode. The presence of both gases in large quantities would constitute a serious safety hazard in nickel-zinc cells. A violent rupture could occur due to excessive pressure or the spontaneous reaction of the two gases. Provision must be made, therefore, to inhibit the production of hydrogen or to recombine hydrogen and oxygen in these cells. Two approaches have been employed to promote recombination:

1. Negative electrodes with excess amounts of uncharged negative electrode material, ZnO or $Zn(OH)_2$, may be used to inhibit hydrogen evolution during overcharge conditions. Oxygen will then be evolved at the nickel oxyhydroxide electrode before all the negative electrode material can be reduced:

$$4 \ OH^{1-} \longrightarrow O_2 + 2 \ H_2O + 4e^{1-} \tag{9}$$

If there exists both a limited amount of electrolyte in the sealed cell and a suitable porous separator assembly, the oxygen will be transferred to the zinc electrode where it will react with the excess zinc metal:

$$2 \ ZN + O_2 + 2 \ H_2O \longrightarrow 2 \ Zn(OH)_2 \tag{10}$$

It should be noted that overcharging sealed nickel-zinc cells at rates higher than C/200 should be avoided. Most semipermeable separator membranes which are required to prevent zinc dendrite penetration do not allow efficient transport of oxygen to the negative electrode during overcharge conditions. As a result, recombination rates for the oxygen cycle are significantly lower than for the sealed nickel-cadmium

cells in which such semipermeable membranes are not required. No provision is made for the inclusion of an antipolar mass (APM) of uncharged zinc at the nickel oxyhydroxide electrode to promote recombination of oxygen during cell voltage reversal conditions.

2. In view of the poor oxygen recombination characteristics as noted above, a silver/mercury catalyzed oxygen fuel cell electrode may be connected directly to the zinc electrode.[17] In addition, since hydrogen is evolved during the corrosion reaction and is not recombined at the nickel oxyhydroxide electrode, platinum catalyzed electrodes may be connected to the nickel electrode[6] to avoid internal pressure buildup.

Several methods are used to produce zinc electrodes for secondary nickel-zinc cells. These include the dry, pressed powder process, the paste method, electrodeposition, and sintered powder techniques.[1-3,6,14-18] In the pressed powder process, zinc oxide powder containing mercuric oxide with other additives and binders such as carboxymethylcellulose or Teflon is pressed upon expanded zinc metal screen. After pressing to acquire desired electrode porosity characteristics, the electrodes are electrolytically reduced in a dilute KOH solution. The pasting process applies a zinc oxide/gelling agent slurry onto an expanded metal screen. The zinc oxide is dried and subsequently reduced in a 5 percent KOH solution. In the electrodeposition process, zinc is plated onto expanded metal screens from either a zinc oxide slurry or a cyanide bath. The sintered powder technique uses a plaque of sintered nickel powder on an expanded metal screen which is impregnated in a zinc solution. The resultant zinc compound may then be converted to ZnO or $Zn(OH)_2$ by thermal, chemical, or electrolytic decomposition techniques. The dried precursor electrode may then be converted to zinc metal in a formation process.

Though nickel positive electrodes may be fabricated using standard sintered plaque and pocket plate electrode fabrication techniques, a less expensive and simpler manufacturing process employs a pressed powder method. A mixture of $Ni(OH)_2$ containing additives as well as graphite and a Teflon binder is pressed onto plates which are connected to two layers of expanded nickel screen.[2,19,20] The inclusion of cobalt and/or cadmium additives in the mixture results in higher charge efficiencies and capacity maintenance.[17]

The electrolyte for the nickel-zinc cell is typically 7 to 11 M KOH saturated with ZnO (80 g per liter). The use of ZnO not only reduces the severity of $Zn(OH)_4^{2-}$ concentration effects during the cell charging process, but also inhibits the corrosion of the zinc electrode.[21] The addition of small amounts of lithium hydroxide to the electrolyte is believed to increase the capacity of the nickel oxyhydroxide electrode.[21]

The role of the separator assembly is crucial to the effective operation of the nickel-zinc cell. The requirements for the separator include low electrolytic resistance, low permeability to zinc or zinc oxide species, and resistance to increased thickening of the zinc electrode.[22] The separator must also act as electrolyte absorption reservoirs. In view of the above, several different separator materials have been considered for use as dendristatic membranes. These include various types of regenerated cellulose such as sausage casing, cellophane, and methylcellulose, Borden polyvinyl

alcohol (PVA), NASA inorganic-organic coated asbestos, PVA coated Dynel, polypropylene, and irradiated polyethylene. Multilayers of one or more of the above separators or various modifications of these separators are usually compressed between inert, nonwoven nylons which serve to provide both proper wetting of the electrodes and electrolyte retention.

Nickel-zinc batteries are being considered as power sources for such applications as electric vehicle propulsion, missiles, aircraft starting, remotely piloted vehicles, and military control systems.[2,23-27] The major developers/manufacturers of the nickel-zinc battery in the United States are Eagle-Picher, Energy Research Corporation (ERC), Electric Storage Battery (ESB), Gould, and Yardney Electric Corporation.

Though most present applications use the vented cell design, sealed nickel-zinc cells have been developed which have exhibited exceptionally favorable cycle life characteristics.[6] The vented design necessarily requires larger, heavier cell containers to allow the escape of electrolyte-free gases through the vent during normal operation. These cells also require the periodic addition of water or electrolyte due to water loss during overcharge. In view of the fact that vented nickel-zinc cells possess higher rate capabilities than sealed cells, the construction requirements for current collection necessitate the use of heavier components. Since the charge efficiency for the nickel oxyhydroxide electrode is significantly less than that for the zinc electrode, an overcharge of about 30 percent is required to restore full charge to the positive electrode. This results in a charge imbalance between the two electrodes. At the higher charging potentials, additional zinc will be plated out from the ZnO reservoir in the electrolyte. In order to restore the original ZnO to the electrolyte, vented cells must be periodically discharged to 0.0 V. Sealed nickel-zinc cells with oxygen recombination electrodes, on the other hand, may be continuously overcharged under constant current conditions at the maximum recombination rates of the fuel cell electrode. During overcharge, oxygen is generated at the nickel oxyhydroxide electrode in accordance with:

$$4 \ OH^{1-} \longrightarrow O_2 + 2 \ H_2O + 4e^{1-} \tag{11}$$

The oxygen will then react at the recombination electrode which is electrically connected to the zinc electrode:

$$O_2 + H_2O + 4e^{1-} \longrightarrow 4 \ OH^{1-} \tag{12}$$

and the zinc electrode is subsequently discharged:

$$2 \ Zn + 4 \ OH^{1-} \longrightarrow 2 \ Zn(OH)_2 + 4e^{1-} \tag{13}$$
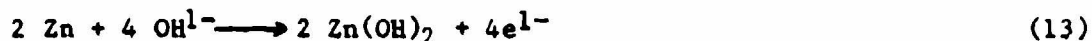
The above overcharge condition may be maintained continuously if the overcharge rate does not exceed the recombination rate. Hydrogen is evolved during both open circuit and cell voltage reversal conditions. The inclusion of a platinum catalyzed fuel cell electrode at the nickel oxyhydroxide electrode facilitates hydrogen recombination and avoids excessive pressures in sealed cells.[6] Sealed cells with no provision for hydrogen recombination must rely on the diffusion of the gas through such sealing materials as epoxy resins.[17]

The open circuit voltage and theoretical energy density for nickel-zinc cells are 1.73 V and 345 Wh/kg, respectively.[18] Vented cells having a nominal capacity of 100 Ah and weighing 2.73 kg were discharged at the 0.22 C, 0.65 C, and 1.40 C rates to a voltage cutoff level of 1.3 V.[17] The corresponding realized capacities obtained for these cells were 130, 117, and 105 Ah at average load voltages of 1.70, 1.60, and 1.48 V, respectively. It can be seen that the energy densities for these cells vary from about 57 to 81 Wh/kg. Additional characteristics for vented cells are summarized below:

1. The operational temperature range for the nickel-zinc system is -40 to +65°C. At the lower temperatures, the realized capacities and load voltages are significantly less than those obtained at 25°C. For example, 45 Ah aircraft batteries discharged at 25°C at rates of 0.44 C (20A) and 11.1 C (500A) yielded realized capacities of 53 and 42 Ah, respectively.[24] Similar performance testing for cells discharged at -29°C yielded realized capacities of 28 and 6 Ah.

2. Nickel-zinc cells are typically charged using constant current, constant potential with current limitation, and float charging techniques.[1]

3. Nickel-zinc cells retain approximately 70 percent of the initial capacity after one month open circuit storage at 25°C.[1] Cells stored at elevated temperatures exhibit severe capacity losses while good capacity retention is observed for cells stored at low temperatures.

4. The cycle life for nickel-zinc cells is dependent upon the depth of discharge, charging method and rate, and use conditions. In general, the cycle life for vented cells is about 150 to 200 deep discharge cycles. Approximately 40,000 cycles were obtained using cells discharged under pulse conditions to only a 5 percent depth of discharge.[17]

Sealed, cylindrical nickel-zinc cells have recently been fabricated in the AA, C, and D sizes.[6] The discharge performance characteristics for C cells with nominal capacities of 1.5 Ah were obtained at 25°C to a load voltage cutoff level of 1.0 V. The results for the constant current discharge of these cells at rates of 0.2 C (0.3A) to 1.33 C (2.0A) showed corresponding realized capacities of 1.5 Ah to 1.0 Ah. These values indicate that the energy densities varied from 20 to 36 Wh/kg. Other features for these sealed cells are summarized below:

1. Sealed nickel-zinc cells are charged under a pulsing constant current condition at rates of about 0.2 C. Overcharge of these cells may be eliminated entirely through use of an open circuit voltage sensing technique.[6]

2. Sealed C cells typically retain about 70 percent of the initial capacity after storage under open circuit conditions for one month at 25°C. Storage at 0°C for one month results in only a 10 percent capacity loss while nearly 50 percent capacity is lost after one month at 45°C.

3. The cycle life for sealed C cells was shown to be about 380 cycles when cells were charged using the open circuit sensing method.[6]

Specific testing for vented nickel-zinc cells in accordance with the electrical and thermal abuse procedures given in NAVSEAINST 9310.1A was not reported. It should be noted that a venting mechanism is provided in these cells which opens and closes during normal cell operation. This vent allows for both the escape of hydrogen and oxygen gases produced during the charging process and accessibility for filling cells with required amounts of water. Though the vent mechanism is not a safety feature per se, it does allow the escape of gases and/or electrolyte in cells subjected to the electrical abuses of overcharge or overdischarge. Both hydrogen and oxygen are vented under these conditions. There does exist, however, the possibility of an oxygen-hydrogen fire or explosion in the environment outside the cells if appropriate ventilation is not provided. In addition, excessive overcharge or overdischarge of vented nickel-zinc cells would result in the drying of the cell and subsequent performance failure. Vented cells which have been short circuited could expel hot, corrosive KOH electrolyte. Exposure of vented cells to elevated temperatures or incineration conditions not only would cause electrolyte expulsion but would also release toxic materials caused by the oxidation of cell contents and plastic case materials.

A study which assessed the relative safety of a number of conventional and advanced battery systems has recently been reported.[28] All batteries considered in this study were of a 6 kWh design and were evaluated on a scale of one to ten (ten signifying the most safe battery system). The "Redox" iron-chromium system was ranked safest at a value of nine. The lead-acid, nickel-iron, nickel-zinc, and zinc-ferricyanide were classified at a value of eight. The ambient temperature systems of lead-acid, nickel-zinc, and nickel-iron are "proven to be safe". This report also noted that, of all systems tested, the nickel-zinc system possessed the lowest reliability due to separator failure, zinc dendrite formation, and zinc electrode shape change failure modes.

No data was presented which detailed the results of such electrical abuse testing as short circuit, forced overdischarge, or prolonged high rate overcharge for sealed nickel-zinc cells. Both hydrogen and oxygen would be generated in cells subjected to prolonged overdischarge (cell voltage reversal) and overcharge conditions if the oxygen and hydrogen recombination capabilities of the cell were exceeded. It has been noted that the oxygen and hydrogen recombination capability is limited to low rates if no oxygen and hydrogen auxiliary electrodes are incorporated into the cell structure. Increased cell pressures would develop, which, dependent upon the structural features of the cell, could lead to either a violent expulsion of gases and hot KOH or a violent case rupture. The escaping gases could then react to create a fire or explosion hazard. The use of constant potential charging techniques with no provision for current limitation at the end of charge could lead to a thermal runaway condition.

Incineration of sealed nickel-zinc cells would, at the least, cause rapid expulsion of hot electrolyte. Under the worst conditions, the cell case would rupture. Rapid oxidation of cell contents would generate toxic materials.

REFERENCES

1. Falk, U., Electrochemical Power Sources, Primary and Secondary Batteries, IEE Energy Series 1, M. Barak, ed. (London: Peter Peragrinus Ltd., 1980), p. 391.

2. Yao, N. P., Christianson, C. C., Elliott, R. C., and Miller, J. F., Proc. Power Sources Symp. 29, 1981, p. 247.

3. Falk, S. U., and Salkind, A. J., Alkaline Storage Batteries (New York: John Wiley and Sons, 1969), p. 188.

4. Charlip, S., and Lerner, S., Proc. of the Fifth IECEC, American Society of Mechanical Engineers, 1, 1970, p. 56.

5. Hampson, N. A., Zinc-Silver Oxide Batteries, Fleischer, A., and Lander, J. J., eds. (New York: John Wiley and Sons, 1969), p. 51.

6. Sato, Y., Kanda, M., Niki, H., Veno, M., Murata, K., Shirogami, T., and Takamura, T., J. Power Sources, 9, 1983, p. 147.

7. Himy, A., and Wagner, O. C., Proc. Power Sources Symp. 28, 1979, p. 167.

8. Gaines, L., J. Electrochem. Soc., 116, 1969, p. 61C.

9. Oswen, H. G., and Blurton, K. F., Zinc-Silver Oxide Batteries, Fleischer, A., and Lander, eds. (New York: John Wiley and Sons, Chapter 6, 1971).

10. Choi, K. W., Hamby, D., Bennion, D. N., and Newman, J., J. Electrochem. Soc., 123, 1978, p. 1628.

11. McBreen, J., J. Electrochem. Soc., 119, 1972, p. 1620.

12. von Kruaenstierne, O., "Power Sources 6," Proc. Tenth Int. Symp. Power Sources, Joint Services Electrical Power Source Committee, Collins, D. H., ed. (London: Academic Press, 1977), p. 303.

13. McCoy, L. R., Proc. of the Tenth IECEC, American Society of Mechanical Engineers, 1975, p. 1131.

14. Reasbeck, P., Phil. Trans. R. Soc. Lond. A, 302, 1981. p. 351.

REFERENCES (Cont.)

15. Wagner, O. C., Almerini, A., and Smith, R. L., Proc. Power Sources Symp. 29, 1981, p. 237.

16. Wagner, O. C., Almerini, A., and Smith, R., Proc. Power Sources Symp. 30, 1983, p. 116.

17. Charkey, A., Proc. of the Tenth IECEC, American Society of Mechanical Engineers, 1975, p. 1126.

18. McBreen, J., Comprehensive Treatise of Electrochemistry, Volume 3, Electrochemical Energy Conversion and Storage, Bockris, J. O'M., Conway, B. E., Yeager, E., and White, R. E., eds. (New York: Plenum Press, 1981), p. 314.

19. Lexow, K. W., Kramer, G., and Oliapuram, V. A., Power Sources 8, Proc. 12th Int. Symp. Power Sources, Joint Services Electrical Power Source Committee, J. Thompson, ed. (London: Academic Press, 1981), p. 389.

20. Klein, M., U.S. Patent No. 3,898,099, 1975.

21. Falk, S. U., and Salkind, A. J., Alkaline Storage Batteries (New York: John Wiley and Sons, 1969), p. 619.

22. Lundquist, J. T., Jr., J. Membrane Science, 13, 1983, p. 337.

23. Dappert, D., Nickel-Zinc Batteries for RPV Applications, NTISAD-A 115843, U.S. Dept. Commerce, Springfield, VA, 1982.

24. Brown, R. A., Krinman, L. R., and Bishop, W. S., Proc. Power Sources Symp. 28, 1979, p. 157.

25. Klein, M., and Leo, A., Proc. Power Sources Symp. 29, 1981, p. 244.

26. Brown, R. A., and Cloyd, J. S., Proc. Power Sources Symp. 29 1981, p. 240.

27. Schiffer, S. V., Proc. Power Sources Symp. 30, 1983, p. 114.

28. Puddas, A., and Kapner, M., Analysis of Batteries for Use in Photovoltaic Systems, Final Report, Volume 1, Department of Energy, DOE/ET/25201-1, 1981.

S. ZINC-SILVER OXIDE (SILVER-ZINC)

$$Zn \mid KOH \mid Ag_2O_2, Ag_2O$$

$$2\,Zn + Ag_2O_2 + 2\,H_2O \rightleftharpoons 2\,Zn(OH)_2 + 2\,Ag \qquad [1]$$

$$Zn + Ag_2O + H_2O \rightleftharpoons Zn(OH)_2 + 2\,Ag \qquad [2]$$
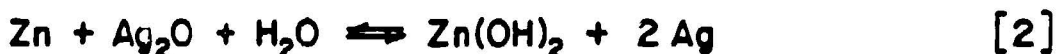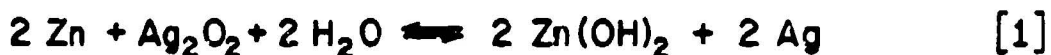
The zinc-silver oxide (silver-zinc) system was developed by H. Andre at Yardney Electric during the 1930's and was patented in 1943.[1,2] The secondary silver-zinc battery yields the highest energy and power densities of any aqueous secondary system in common use at this time. Silver-zinc cells and batteries have found use in several military and aerospace applications. The U.S. Navy has employed the secondary battery for practice torpedo propulsion, submarines, recoverable antisubmarine warfare targets, noiseless combat units, and detonation devices. Silver-zinc secondary batteries have also served as power sources for radio transceivers, rockets, and night vision scopes in the U.S. Army. Sealed cells and batteries have experienced wide usage in such aerospace applications as Explorer XXXII, the Mariner spacecraft, the Titan II, the Viking lander, and others. Several types of military and aerospace silver-zinc cells and batteries are available.[3] These include: high and low rate designs available as dry charged/dry uncharged, wet charged/wet uncharged (vented), and sealed units.

Detailed technical discussions for the secondary silver-zinc battery are given by Fleischer and Lander[4] and Falk and Salkind.[5] The discharge reaction scheme at the zinc electrode in alkaline media is given by:

$$Zn + 2\,OH^{1-} \longrightarrow Zn(OH)_2 + 2e^{1-} \qquad (3)$$

The $Zn(OH)_2$ then dissolves in the electrolyte and eventually forms zinc oxide:[6]

$$Zn(OH)_2 + 2\,OH^{1-} \longrightarrow Zn(OH)_4^{2-} \qquad (4)$$

and

$$Zn(OH)_4^{2-} \longrightarrow ZnO + 2\,OH^{1-} + H_2O \qquad (5)$$

Electrode passivation will occur when the solubility limit of the discharge products in the electrolyte surrounding the electrode is exceeded, as given by either reaction 5 or by reaction 6:

$$Zn(OH)_2 \longrightarrow ZnO + H_2O \tag{6}$$

A summary of the zinc passivation characteristics in alkaline media is described for the zinc-mercuric oxide system.

A possible side reaction which occurs at the zinc electrode produces hydrogen in accordance with:

$$2\ H_2O + 2e^{1-} \longrightarrow H_2 + 2\ OH^{1-} \tag{8}$$

The standard potentials for reactions 3 and 8 are 1.245 V and −0.828 V. It can be seen that zinc is thermodynamically unstable in strong alkaline solution and will experience corrosion accompanied by the evolution of hydrogen gas. The corrosion reaction may be reduced significantly by increasing the hydrogen overpotential through amalgamation and the use of pure zinc electrodes. Amalgamation of the zinc electrode for secondary silver-zinc cells is accomplished by adding various amounts of mercuric oxide to the zinc or zinc oxide mixture. A two percent amalgamation level results in high activation overpotentials for hydrogen evolution on the mercury and the inhibition of the corrosion reaction. The substitution of binary mixtures of cadmium, lead, indium and thallium oxides or hydroxides for mercury in secondary silver-zinc has been shown to reduce hydrogen evolution and to act as extenders in preventing densification of the zinc electrode material.[7]

The electrodeposition of zinc from the alkaline electrolyte is a two step process:[8]

$$Zn(OH)_4^{2-} \longrightarrow Zn(OH)_2 + 2\ OH^{1-} \tag{9}$$

and

$$Zn(OH)_2 + 2e^{1-} \longrightarrow Zn + 2\ OH^{1-} \tag{10}$$

The zinc produced in accordance with reaction 10 may be either mossy or dendritic dependent upon the charge current density, potential, and zincate ion concentration in the vicinity of the zinc electrode.[9] Mossy zinc is formed at low current densities (4-20 mA/cm^2), low overpotentials (below 75mV), and in solutions of sufficient zincate ion concentration.[8,9,10] If the current density and potential are increased or the concentration of zincate ion is reduced, zinc dendrite formation occurs. The dendritic zinc would grow through the separator material and cause catastrophic short circuiting or accelerated self-discharge. A second failure mechanism of the zinc electrode relates to the loss of electrode porosity and surface area by the agglomeration of zinc and the migration of zinc from the sides and top of the electrode to the center and bottom ("shape change"). During charging, dendritic zinc preferentially grows at the top and edges of the electrode and mossy zinc is deposited over a layer of ZnO at the center and bottom of the zinc plate. Growth of dendritic zinc is enhanced by the depletion of the $Zn(OH)_4^{2-}$ species as the zinc electrode

experiences shape change. The use of KOH electrolyte saturated with ZnO reduces the severity of $Zn(OH)_4^{2-}$ concentration effects during the charging process.

The suppression of zinc electrode shape change has been intensely investigated.[11,12] The effects of current distribution differences at the zinc electrode and high convective flow rates were found to substantially contribute to the zinc material redistribution from the plate edges to the center. Several approaches to alleviate the problem of zinc electrode shape change include: the addition of surfactants to the electrolyte,[13] the incorporation of iron compounds (e.g., $Fe(OH)_2$ and Fe_2O_3) in the periphery of the separator material,[14,15] and the use of zincate ion solubility depressants such as $Ca(OH)_2$.[8]

Several methods are used to produce zinc electrodes for secondary silverzinc cells.[5] These include the dry, pressed powder process, the paste method, the electrodeposition process, and sintered powder techniques. In the pressed powder process, zinc oxide dust containing specified amounts of mercuric oxide and a binder such as carboxymethylcellulose is pressed upon an expanded zinc or silver metal screen. The porosity of the zinc matrix can be varied for high rate discharge (80-90% porosity) or for low rate discharge (30-40% porosity).

These electrodes are then electrochemically reduced in a 5 percent KOH solution. The pasting process applies a zinc oxide/gelling agent slurry onto a silver expanded metal screen. The zinc oxide is subsequently reduced in a 5 percent KOH solution. In the electrodeposition process, zinc is plated onto expanded metal screens from either a zinc oxide slurry or a cyanide bath. The sintered powder technique uses a plaque of sintered nickel powder on an expanded metal screen. The plaque is then impregnated in a zinc bath. The zinc compound is converted to $Zn(OH)_2$ or ZnO by thermal, chemical, or electrolytic decomposition.

The silver oxide electrode exhibits a two step discharge in accordance with the initial reduction of Ag_2O_2 followed by the reduction of Ag_2O:

$$Ag_2O_2 + H_2O + 2e^{1-} \longrightarrow Ag_2O + 2\ OH^{1-} \tag{11}$$

$$Ag_2O + H_2O + 2e^{1-} \longrightarrow 2\ Ag + 2\ OH^{1-} \tag{12}$$
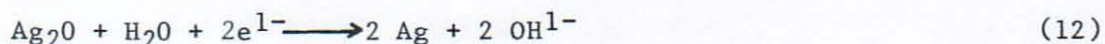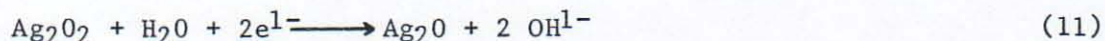
The standard potentials for reactions 11 and 12 are 0.607 and 0.345 V, respectively. It can be seen that the electrical capacity for Ag_2O_2 is twice that for Ag_2O. The duration of higher load voltages associated with the reduction of Ag_2O_2 is dependent upon such factors as discharge rate, temperature, length of wet stand time, and the charging rate (e.g., for charging currents of C/50 or less, the higher discharge voltage plateau is not observed). Silver (I) oxide Ag_2O is soluble in alkaline solutions.[16,17] The maximum solubility for Ag_2O, is about $5 \times 10^{-4}N$ occurs at KOH concentrations of 7M. The dissolved silver (I) oxide species diffuses to the zinc electrode and is reduced:

$$Zn + 2\ Ag(OH)_2^{1-} \longrightarrow Zn(OH)_4^{2-} + 2\ Ag \qquad\qquad (13)$$
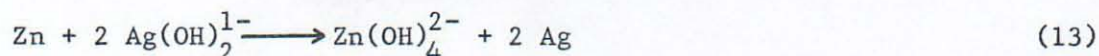
After repeated charge-discharge cycling, dendritic silver could penetrate separator materials and cause short circuits between electrodes.

During charge, the formation of Ag_2O and Ag_2O_2, proceeds in the reverse for reactions 12 and 11, respectively. Silver (I) oxide crystallizes randomly on the silver substrate followed by the growth of Ag_2O_2 as a distinct second phase on the surface of Ag_2O layer.[8] The positive silver electrode exhibits poor charge acceptance characteristics, particularly at low temperatures.[18] Efforts to improve cycling characteristics have included the sintering of silver electrodes using silver of small particle size and silver alloys with small concentrations of lead, palladium, and other metals.[19,20] The effect of the alloyed metals was the preferential etching of the silver electrode surface upon dissolution of the Pd or Pb. However, it was found that Pd lowered the hydrogen overvoltage at the zinc electrode and caused extensive corrosion and gassing. Lead, on the other hand, was also found to be beneficial relative to the formation of the zinc metal during charge.[8]

Silver oxide electrodes for secondary cells are produced by sintered powder techniques or by pressing chemically prepared silver oxides onto expanded metal screens. Of the two processes, the most widely used is the continuous sintered powder process. Chemically prepared silver oxides (Ag_2O_2) and a suitable binder are applied to a silver expanded metal screen at pressures of 1560 to 3120 psi (11 MPa to 22 MPa). The resultant electrodes have the advantage in that nearly all the electroactive material can be utilized.[1]

In no other secondary aqueous system is the role of the separator assembly as crucial to the effective operation as it is with the silver-zinc battery. The requirements for the separator assembly include: low electrolytic resistance for cell discharge at high rates, resistance to chemical oxidation by the silver oxides, and low permeability to both the colloidal silver oxide and zinc/zinc oxide species. In addition, these separators must be thin enough to allow efficient operation for high power and energy density applications.[5,21,22] Several different separator materials have been considered for use as dendristatic and argentostatic membranes. These include various types of regenerated cellulose such as sausage casing, cellophane and methylcellulose, Permion films (polyethylene acrylic, acid graft), Borden polyvinyl alcohol, electrolytical deposition of $Ca(OH)_2$ onto the silver electrode,[23] blends containing polyphenylquinoxaline polymers,[24] fuel cell grade asbestos,[25] and potassium titanate.[26] Multilayers of one or more of the above separators are usually compressed between inert, nonwoven materials which serve to provide both proper wetting of the electrodes and electrolyte retention.

The electrolyte for the silver-zinc secondary cell is 7 to 11 M KOH saturated (80 g per liter) with ZnO. The use of ZnO not only reduces the severity of $Zn(OH)_4^{2-}$ concentration effects during cell charging, but also inhibits the corrosion rate at the zinc electrode.[10]

The basic cell design characteristics for the secondary silver-zinc battery differ markedly from those for the primary cell. The most important difference is the elimination of excess electrolyte by the use of separator materials which swell considerably when wetted with electolyte. The result is tightly packed cell elements which limit the shape change failure mode during cycling. Loose packing promotes the redistribution of zinc active material to the center of the plates. Cycle life is also enhanced by the following factors:[18] low depths of discharge, high concentrations of ZnO in the electrolyte, a KOH concentration level of 11 M, low HgO content, increased numbers of plates, and operation at temperatures of 20°C to a maximum of about 40°C.

The open circuit voltages for the silver-zinc secondary cell are 1.86 V for the reduction of Ag_2O_2 and 1.60 V for the reduction of Ag_2O.[27] As previously discussed, several types of low and high rate silver-zinc designs are available for military and aerospace applications. This discussion focusses on the dry charged and sealed cell designs. The dry charged silver-zinc battery is filled with electrolyte immediately before operation. This procedure is particularly advantageous for applications which require extremely high discharge rates. For example, cells or batteries may be deep discharged at rates as high as 20C at 25°C.[1] Under high rate discharge conditions of C to 6C, cells would yield energy densities of 40 to 100 Wh/kg and have operating lives of six months. As the discharge rate and depth of discharge increase, however, the cycle life decreases dramatically (e.g., 20 cycles). In contrast, low rate cells deep discharged at the 0.1C rate will yield energy densities of 70-130 Wh/kg and have a cycle life of 100-300 cycles with an extended operating life of 12 to 18 months. The realized capacities for high rate silver-zinc secondary cells discharged at rates of C to 6C vary from 120 percent to 80 percent of the nominal cell capacity. The characteristics for the silver-zinc battery are summarized below:

1. Cells are normally charged under constant current conditions at the 0.1C rate. Charge efficiencies of about 90 percent are obtained under the above condition. Charging should be terminated when a voltage of 1.98 V is reached to avoid overcharge conditions.

2. The charge retention for secondary cells is about 80 to 95 percent under open circuit conditions for one year. These values vary as a function of manufacturer, storage temperature, and cell design.

3. The total wet life is about one to two years for low rate designs and about six months for high rate designs.

4. The silver-zinc system is mechanically rugged relative to shock, vibration and acceleration.

5. The major U.S. manufacturers of secondary silver-zinc cells and batteries are Yardney Electric and Eagle Picher at this time. Former developers/manufacturers include Gould Marathon Battery Company, Mallory (Duracell International), Energy Research Corporation, and the Electric Storage Battery Company (ESB).

During cell charging, oxygen is evolved at the silver electrode and hydrogen is evolved at the zinc electrode. The presence of both gases in large quantities would constitute a serious hazard in secondary silver-zinc cells, particularly the hermetically sealed aerospace cell.[28,29] Indeed, a violent rupture or explosion could occur dependent upon case strength. Provision must be made, therefore, to recombine the hydrogen and oxygen in these cells. Two methods have been extensively used to promote recombination:

1. Negative electrodes with excess amounts of uncharged negative electrode material, $Zn(OH)_2$ or ZnO, may be used to avoid hydrogen during overcharge. Oxygen will be evolved at the silver electrode before all the negative electrode material can be reduced:

$$4 \ OH^{1-} \longrightarrow O_2 + 2 \ H_2O + 4e^{1-} \tag{14}$$

Since there exists a limited amount of electrolyte in the cell, oxygen will be transferred to the zinc electrode where it will react with the excess zinc metal:

$$2 \ Zn + O_2 + H_2O \longrightarrow 2 \ Zn(OH)_2 \tag{15}$$

The net effect is the consumption of O_2 at the zinc electrode with no chemical compositional changes within the cell. No similar provision is made for overdischarge conditions in these cells.

2. The use of fuel cell recombination cells and electrodes within the sealed cell promotes the following reactions during overcharge (or overdischarge) conditions:

$$O_2 + 2 \ H_2O + 4e^{1-} \longrightarrow 4 \ OH^{1-} \tag{16}$$

and

$$2 \ H_2 + 4 \ OH^{1-} \longrightarrow 4 \ H_2O + 4e^{1-}$$

This fuel cell device exhibits especially high recombination rates (e.g., the device can recombine the oxygen generated on continuous overcharge at the 2C rate).

Silver-zinc batteries have experienced several instances of fire following inadvertent activation[29,30] or external short circuiting.* Since both hydrogen and oxygen are produced during a fire or thermal runaway condition, the possibility for an explosion, particularly for sealed cells, would exist. In these incineration conditions, large amounts of toxic gases from the oxidation of cell components and plastic materials were also emitted. A study to determine the causes for the spontaneous combustion of cells was conducted.[30] The findings are summarized below:

---

*Yedwab, D., Private Communication, 1984, p. 282.

1. Combustion began when partially wetted zinc plates reached temperatures of 163°C or higher. When a silver positive plate was placed in contact with a partially wetted zinc plate, combustion was much more vigorous. This fire was supported by the release of oxygen from the silver electrode.

2. Direct short circuits of the zinc and silver plates by a steel pin for 33 Ah cells resulted in the evolution of smoke and vapor and a maximum temperature rise of 93°C. The same test performed upon 350 Ah cells resulted in ignition and fire. Combustion began at the site of the short circuit.

3. The tendency for the occurrence of ignition and fires was greater for large cells. A fire erupted after local drying of the electrode plates at the point of the short circuit. The minimum temperature for plate combustion was found to be 163°C.

4. Cells with nominal capacities of 33, 300, and 350 Ah were discharged at the overload rates of 300 and 770 A, 100 to 300 A, and 35 to 300 A, respectively. An internal explosion was observed for the Ah cell discharged at 300 A. It was concluded that combustion and/ or an explosion could occur due to an overload condition. These high discharge rates corresponded to short circuit conditions in some cases.

5. Combustion of 33 and 350 Ah cells occurred if cells were placed in an oven at 163°C.

6. Gas evolution tests showed that both hydrogen and oxygen were produced during discharge.

Though no specific data were presented for silver-zinc secondary cells subjected to extended overcharge or overdischarge conditions, Lander[18] and Carson[28] both indicated that explosions would occur if a means of gas recombination in gas filled sealed cell designs was not provided and the sealed cells continued to be cycled. Both hydrogen and oxygen would be generated in either the overcharge or overdischarge abuse tests. In view of the results relative to the spontaneous combustion tests,[30] the possibility of fires or explosions would also exist for vented cells and batteries in the overdischarge or overcharge condition, dependent upon the discharge/charge rates, thermal characteristics, and design. Further, the production of gases in these cells and batteries would consume large amounts of water. The combination of water loss with high rates of overdischarge or overcharge could also result in localized heating and fires or explosions.

REFERENCES

1. Von Sturm, F., Comprehensive Treatise of Electrochemistry, Volume 3, Electrochemical Energy Conversion and Storage, Bockris, J. O'M., Conway, B. E., Yeager, E., and White, R. !., eds. (New York: Plenum Press, 1981), p. 407.

2. Andre, H., U.S. Patent No. 3,517,711.

3. Mantell, C. L., Batteries and Energy Systems, Second Edition (New York: McGraw Hill, 1983), p. 110.

4. Zinc-Silver Oxide Batteries, Fleischer, A., and Lander, J. J., eds. (New York: John Wiley and Sons, 1971).

5. Falk, S. U., and Salkind, A. J., Alkaline Storage Batteries, (New York: John Wiley and Sons, 1969).

6. Hampson, N., A., in reference 4, p. 51.

7. Himy, A., end Wegner, O. C., Proc. Power Sources Symp. 28, 1979, p. 167.

8. Gaines, L., J. Electrochem. Soc., 116, 1969, p. 61C.

9. Oswin, H. G., and Blurton, K. V., in reference 4, Chapter 6.

10. Dalen, G. A., in reference 4, Chapter 7.

11. Choi, K. W., Hamby, D., Bennion, D. N., and Newman, J., J. Electrochem. Soc., 123, 1978, p. 1628.

12. McBreen, J., J. Electrochem. Soc., 119, 1972, p. 1620.

13. Keralla, J. A., and Lander, J. J., Electrochem. Technol., 6, 1968, p. 202.

14. Poa, S.-P., and Wu, C. H., J. Applied Electrochem., 8, 1978, p. 491.

15. Poa, S.-P., and Wu, C. H., J. Applied Electrochem., 8, 1978, p. 427.

16. Dirkse, T. F., The Primary Battery, Volume 1, Heise, G. W., and Cahoon, N. C., eds. (New York: John Wiley and Sons, 1971, p. 228.

17. Dirkse, T. V., in reference 4, p. 100.

REFERENCES (Cont.)

18. Lander, J. J., in Reference 4, Chapter 33.

19. Malachesky, P., and Jasinski, R., J. Electrochem. Soc., 114, 1969, p. 1239.

20. Malachesky, P., and Jasinski, R., J. Electrochem. Soc., 114, 1967, p. 1258.

21. Falk, U., "Electrochemical Power Sources," Primary and Secondary Batteries, IEE Energy Series I, M. Barak, ed. (London: Peter Peregrinus Ltd., 1980), p. 384.

22. Gregory, D. P., in reference 4, p. 226.

23. Hamlen, R. P., McQuade, J. M., and Siwek, E. G., Electrochem. Technol., 6, 1968, p. 83.

24. Angres, I. A., Duffy, J. V., and Kilroy, W. P., Proc. Power Sources Symp. 28, 1979, p. 162.

25. Lear, J. W., and Imamura, M. S., Proc. of the 12th IECEC, American Society of Mechanical Engineers, 1977, p. 311.

26. Charkey, A., Proc. Power Sources Symp. 26, 1975, p. 87.

27. McBreen, J., Comprehensive Treatise of Electrochemistry, Volume 3, Electrochemical Energy Conversion and Storage, Bockris, J. O'M., Conway, B. E., Yeager, E., and White, R. E., eds. (New York: Plenum Press, 1981), p. 308.

28. Carson, W. N., Jr., in reference 4, p. 445.

29. Murphy, F. G., in reference 4, 393.

30. Britz, W. J., and Thomas, C. E., Proc. Power Sources Symp. 26, 1975 p. 162.

CHAPTER 4

CONCLUSIONS AND RECOMMENDATIONS

This study was conducted to determine the safety characteristics for twenty-two primary and nineteen secondary non-lithium battery systems. The specific intention of the present work was the collection and correlation of data for the non-lithium systems relative to the electrical and thermal abuse test procedures prescribed in NAVSEAINST 9310.1A[1] for lithium cells and batteries. The three presently required safety-related tests are short circuiting, forced overdischarge, and incineration. It should be noted that a fourth safety test may be incorporated into NAVSEAINST 9310.1A test procedures to evaluate the safety characteristics associated with electrically charging a cell or series string of cells.* In view of the above, this study also detailed the safety and hazards characteristics associated with electrically charging non-lithium primary cells/batteries and overcharging non-lithium secondary cells/batteries. The scope of this work is not limited to the specific tests given above but is extended to further include specific safety related issues unique to each non-lithium primary and secondary system. Details relative to cell chemistry, electrical performance characteristics, design considerations, etc., are given in the text to provide the reader with a clear and comprehensive background.

The non-lithium primary and secondary battery systems in this study may be classified into three groups: (a) systems which are not commercially available at the present time and are not likely to be developed in the future, (b) systems which are presently available, and (c) systems which are actively being developed for future applications. This summary will be concerned with those systems which are of current interest to the U.S. Navy and other U.S. military organizations as well as with those emerging systems which show promise as future power sources for the U.S. Navy and other U.S. military organizations. Also included in the summary is a brief synopsis of relevant chemical or environmental hazards which may arise from exposure of the system to the active components as a result of abusive conditions, leakage, or an accidental mechanical rupture. Incineration of cells will, in general, result in oxidation of cell components with the emission of toxic fumes (plastics, metals, metal compounds, etc.).

---

*Bis, R. F., Code R33, Naval Surface Weapons Center, Silver Spring, White Oak, MD, Private Communication, 1984.

PRIMARY BATTERY SYSTEMS

Twenty-two non-lithium primary battery systems were examined in this study. Of this number, six were determined to have little c nce of being developed further or marketed. These systems were:

A   Aluminum-Manganese Dioxide
I   Magnesium-Air
J   Magnesium-Bismuth oxide
N   Magnesium-Sulfur
S   Zinc-Potassium iodate
V   Zinc-Sodium dichromate

Thirteen primary systems are currently available for use as power sources for a variety of U.S. military, commercial; or consumer applications:

C   Cadmium-Mercuric Oxide

No specific safety test results, but case ruptures would occur under severe forced overdischarge and charge conditions; formation of H_2 & O_2. Chemical hazards: Hg/HgO, highly toxic;[2(p. 797)] $Cd/Cd(OH)_2$, highly toxic.[2(p. 456)]

D   Calcium-Calcium Chromate (Thermal)

Nonactivated: no hazards for electrical abuse, incineration: case rupture possibility.

Activated: possibility of thermal runaway and case rupture during short circuit tests.

Discharged: seal rupture during incineration tests, hydrogen flame.

Chemical hazards: cells may contain asbestos, a known carcinogen[2(p. 39i)] calcium chromate, also a carcinogen.[2(p. 504)]

G   Lead-Lead Dioxide (HBF_4)

No specific safety test results, possibility of H_2-air fires or explosions if charged.

Chemical hazard: highly toxic fumes of lead in incineration conditions, known carcinogen[2(p. 765)]; lead dioxide: toxic, poisonous.[2(p. 768)]

H   Lead-Lead Dioxide ($HClO_4$)

No electrical safety test data, possibility of thermal runaway with a resultant fire/explosion. Chemical hazard: highly toxic lead fumes (incineration conditions), known carcinogen[2(p. 765)]; lead dioxide: toxic (poisonous).[2(p. 768)]

K   Magnesium-Lead Chloride

No specific safety test data, clogging of cell could result in a thermal runaway and discharge of hot electrolyte. Hydrogen fire if battery is enclosed.

Chemical hazard: lead chloride - poisonous.[2](p. 766)

L   Magnesium-Manganese Dioxide

Some safety data presented - short circuit, possibility of a hydrogen-air fire or explosion.

Chemical hazard: long term exposure to manganese dioxide could result in Central Nervous System disorders.[2](p. 786)

M   Magnesium-Silver Chloride

No specific safety test data, possibility of a hydrogen-air fire or explosion.

Chemical hazard: little, if any.

O   Zinc-Air

No safety testing reported, cells open to the outside environment.

Chemical hazard: little.

P   Zinc-Manganese Dioxide (Leclanche)

Major safety concerns - pressure rupture of cell container and leakage.

Chemical hazard: long term exposure to manganese dioxide - Central Nervous System disorders.[2](p. 786)

Q   Zinc-Manganese Dioxide (Alkaline)

Major safety concerns - pressure rupture of cell container and leakage.

Chemical hazard: long term exposure to manganese dioxide - could cause Central Nervous System disorders.[2](p. 786)

R   Zinc-Mercuric Oxide

Cell venting under short circuit conditions, violent ruptures under incineration conditions, case bulging and cell ruptures in forced overdischarge testing. Chemical hazards: Hg/HgO, highly toxic.[2](p. 797)

T   Zinc-Silver Chloride

No safety data presented but the possibility for leakage or a case rupture exists.

Chemical hazard: little.

U   Zinc-Silver Oxide

Safety testing reported: incineration and fires as a result of short circuits, possibility for hydrogen-oxygen fires or explosions as a result of water electrolysis (charging or forced overdischarging of cells).

Chemical hazard: silver compounds could cause skin pigmentation (argyria).[2](p. 971)

Three primary systems show promise as prospective power sources for several military applications:

B   Aluminum-Silver Oxide

No safety data reported: System presently being developed for the U.S. Navy ALWT program. Testing may be required.

Chemical hazard: silver compounds could cause skin pigmentation (argyria).[2](p. 971)

E   Calcium-Sulfuryl Chloride

No safety data presented.

Chemical hazard: sulfuryl chloride will form sulfuric and hydrochloric acids by hydrolysis (contact with moist air), under incineration conditions, SO_2Cl_2 will decompose to highly toxic fumes of chlorides and SO_2 (sulfur dioxide - 400 to 500 ppm is immediately dangerous to life).[2](pp. 1002, 1004)

F   Calcium-Thionyl Chloride

Some safety test data using prototype cells was presented - short circuit, forced overdischarge, and incineration tests all resulted in mild venting.

Chemical hazard: Thionyl chloride will decompose to sulfur dioxide and hydrochloric acid in the presence of moisture. Sulfur dioxide - 400 to 500 ppm is immediately dangerous to life. These compounds represent serious toxicity hazards.[2](pp. 1028,1002)

SECONDARY BATTERY SYSTEMS

Nineteen non-lithium secondary battery systems were examined in this study. Of this number, two were determined to have little chance of being developed further or marketed. These systems were:

D   Cadmium-Silver Chloride

Q   Zinc-Lead Dioxide

Six secondary systems are currently available for use as power sources for a variety of military, commercial, or consumer applications:

C   Cadmium-Nickel (III) Oxyhydroxide

Safety test data was presented.
Chemical hazard: Cd compounds, highly toxic.[2(p. 456)]

E   Cadmium-Silver Oxide

Limited safety data available, sealed cells may rupture under extreme abuse conditions.

Chemical hazard: $Cd/Cd(OH)_2$, highly toxic[2(p. 456)] silver compounds could cause skin pigmentation (argyria).[2(p. 971)]

G   Hydrogen-Nickel (III) Oxyhydroxide

Safety data presented indicate that internal pressures could exceed cell container burst strengths when subjected to some tests. Chemical hazard: little, if any.

H   Hydrogen-Silver Oxide

Some safety test data given. Possibility of cell ruptures for cells subjected to incineration conditions. Chemical hazard: silver compounds could cause skin pigmentation (argyria).[2(p. 971)]

M   Lead-Lead Dioxide

Major safety concern relates to hydrogen-air or hydrogen-oxygen fires or explosions as a result of overcharge conditions.

Chemical hazard: highly toxic lead fumes (incineration conditions), known carcinogen[2(p. 765)] lead dioxide, toxic (poisonous).[2(p. 768)]

S   Zinc-Silver Oxide

Safety assessment and safety related details given. Chemical hazard: silver compounds could cause skin pigmentation (argyria).[2(p. 768)]

Eleven secondary battery systems show promise as emerging power sources. Many of these batteries are considered candidates for such applications as load levelling, electric vehicle propulsion, and stand alone power supplies:

A   Aluminum-Air

Not fully developed due to the problem of excessive hydrogen evolution on aluminum. Little safety related data given. Possibility of hydrogen-air fire or explosion in enclosed areas. Chemical hazard: little, if any.

B   Cadmium-Air

No safety data presented for practical batteries. Chemical hazard: Cd/Cadmium compounds, highly toxic.[2](p. 456)

F   Hydrogen ($LaNi_5H_6$)-Air

Little safety related information given relative to practical cells or batteries, reduced hydrogen pressures within cell.

Chemical hazard: not known.

I   Iron-Air

Little data presented for this system. Possibility of a hydrogen-oxygen fire or explosion could exist in cells/batteries with no recombination capabilities.

Chemical hazard: little, if any.

J   Iron (III)-Chromium (II) "Redox"

No safety related studies were detailed. One assessment characterizes the system as "offering the least health and safety problems" with "no hazardous substances". Chemical hazards: see above.

K   Iron-Nickel (III) Oxyhydroxide

Safety details given. Concern relative to the hydrogen evolution in electric vehicle batteries - potential for fires.

Chemical hazard: little, if any.

L   Iron-Silver Oxide

Safety concerns relate to possible hydrogen-air fires or explosions as well as thermal runaway conditions. Chemical hazard: silver compounds could cause skin pigmentation (argyria).[2](p. 971)

N   Sodium-Sulfur

The primary safety concerns relate to the uncontrolled reaction between liquid reactants at elevated temperatures, possible explosions/ruptures.

Chemical hazards: See text.

O   Zinc-Bromine

The major safety related concern is the escape of bromine and bromine complexes to the environment as a result of abusive conditions. Chemical hazards: Bromine, see text.

P Zinc-Chlorine

The major safety related concern is the release of highly toxic chlorine to the environment as a result of abusive conditions.

Chemical hazard: Chlorine. see text.

R Zinc-Nickel (III) Oxyhydroxide

The primary safety concerns involve the possibility of hydrogen-air fires or explosions as a result of exposure to abusive conditions.

Chemical hazards: little, if any.

S Zinc-Silver Oxide

Safety data presented, possibility for hydrogen-oxygen fires or explosions.

Chemical hazard: silver compounds could cause skin pigmentation (argyria).[2(p. 971)]

REFERENCES

1. Johnson, D. M., NAVSEAINST 9310.1A, Dept. of the Navy, Naval Sea Systems
    Command, Washington, DC (1982). Availability: Commanding Officer, Naval
    Publications and Forms Center, 5801 Tabor Ave., Philadelphia, PA., 1911:0.

2. Sax, N. I., Dangerous Properties of Industrial Materials, Fifth Edition,
    (New York: Van Nostrand Reinhold Company, 1979.)

DISTRIBUTION

	Copies		Copies
Office of Naval Research		Air Force Wright Aeronautical	
Attn: G. Neece (Code ONR 413)	1	Labs	
J. Smith (Code ONR 413)	1	Aero Propulsion Laboratory,	
D. Siegel (Code ONR 251)	1	POOC	
800 N. Quincy Street		Attn: D. A. Allen	1
Arlington, VA 22217		W. S. Bishop	1
		R. Marsh	1
Naval Sea Systems Command		Wright Patterson AFB, OH 45433	
Attn: F. Romano (Code 63R3)	1		
E. Anderson (Code 56Z33)	1	NASA Goddard Space Flight	
E. Daugherty (Code 06H3)	10	Center	
J. Pastine (Code 06R)	1	Attn: Library	1
Washington, DC 20362		Greenbelt, MD 20771	
Naval Underwater Systems		NASA Johnson Space Center	
Center		Attn: B. Bragg/EPS	1
Attn: J. Moden (SB332)	1	Houston, TX 77058	
Newport, RI 02850			
		Rockwell International	
Office of Navy Technology		Attn: Dr. S. J. Yosim	1
Attn: Dr. A. J. Faulstich		Atomics International Division	
(MAT 071)	1	8900 DeSoto Avenue	
G. Spalding (MAT 072)	1	Canoga Park, CA 91304	
800 N. Quincy Street			
Arlington, VA 22217		Stanford University	
		Attn: C. J. Wen	1
U.S. Army Electronics Command		Center for Materials Research	
Attn: A. J. Legath		Room 249, McCullough Building	
(DRSEL-TL-P)	1	Stanford, CA 94305	
E. Brooks (DRSEL-TL-PD)	1		
G. DiMasi	1	Globe Union Inc.	
Dr. W. K. Behl	1	Attn: Dr. R. Rizzo	1
Dr. Sol Gilman		5757 N. Green Bay Avenue	
(DELET-PR)	1	Milwaukee, WI 53201	
Fort Monmouth, NJ 07703			

DISTRIBUTION (Cont.)

	Copies		Copies
Hellesens Battery Engineering Inc. Attn: Dr. N. Marincic 1636 Hyde Park Avenue Hyde Park, MA 02136	1	Argonne National Laboratory Attn: Dr. E: C. Gay 9700 South Cass Avenue Argonne, IL 60439	1
Lawrence Berkeley Laboratory Attn: F. McLamore University of California Berkeley, CA 94720	1	Bell Laboratories Attn: Dr. J. J. Auborn 600 Mountain Avenue Murray Hill, NJ 07974	1

TRW Systems
Attn: I. J. Groce
  G. L. Juvinal
  Ed Moon, Room 2251
    Building 01
One Space Park
Redondo Beach, CA 90278
	1
	1
	
	3
		Honeywell, Inc.
		Mat & Process Eng.
		Attn: K. Y. Kim, MN11-1812
		600 Second Street, NE
		Hopkins, MN 55343
			1

PCI Attn: Dr. Thomas Reddy 70 MacQuesten Parkway S Mount Vernon, NY 10550	1	The Aerospace Corporation Attn: H. Bittner P.O. Box 92957 Los Angeles, CA 90009	1
Dr. P. Bro Hyde Park Estates Sante Fe, NM 87501	1	Honeywell Power Sources Center Attn: Dr. D. L. Chua N. Doddapaneni 104 Rock Road Horsham, PA 19044	1 1

Honeywell Corporate Technology Center
Attn: H. V. Venkatasetty
  S. Schafer
10701 Lyndale Avenue, South
Bloomington, MN 55420
	1
	1
		Catalyst Research
		Attn: A. Schneider
		  C. Winchester
		1421 Clarkview Road
		Baltimore, MD 21209
			1
			1

California Institute of Technology
Attn: Library
  B. Carter
  R. Somoano
  H. Frank
  S. Yen
Jet Propulsion Laboratory
4800 Oak Grove Drive
Pasadena, CA 91103
	1
	1
	1
	1
	1
		ESB Research Center
		Attn: Library
		19 W. College Avenue
		Yardney, PA 19067
			1

		EIC Laboratories, Inc. Attn: S. B. Brummer K. M. Abraham 111 Downey Street Norwood, MA 02062	1 1
		Oak Ridge National Laboratory Attn: K. Braunstein Oak Ridge, TN 37830	1

Copies		Copies

Sandia Laboratories
Attn: S. Levy
      (Mail Section 3154-3)   1
P.O. Box 5800
Albuquerque, NM 87715

University of Tennessee
Attn: G. Mamantov   1
Department of Chemistry
Knoxville, TN 37916

Hughes Aircraft Company
Attn: Dr. L. H. Fentnor   1
Aerospace Groups
Missile Systems Group
Tucson Engineering Laboratory
Tucson, AZ 85734

Saft America, Inc.
Attn: Dr. K. Press   1
      N. J. Raman   1
107 Beaver Court
Cockeysville, MD 21030

Lockheed Missiles and Space
  Company, Inc.
Attn: Library   1
Lockheed Palo Alto Research
  Laboratory
3251 Hanover Street
Palo Alto, CA 94304

Duracell International, Inc.
Attn: B. McDonald   1
Battery Division
South Broadway
Tarrytown, NY 10591

Power Conversion, Inc.
495 Boulevard
Elmwood Park, NJ 07407   1

Eagle-Pitcher Industries, Inc.
Attn: R. L. Higgins   1
      J. Dines   1
      L. R. Erisman   1
Electronics Division
P.O. Box 47
Joplin, MO 64802

Foote Mineral Company
Attn: H. R. Grady   1
Exton, PA 19341

Gould, Inc.
Attn: S. S. Nielsen   1
40 Gould Center
Rolling Meadows, IL 60008

Yardney Electric Corporation
Attn: Library   1
82 Mechanic Street
Pawcatuck, CT 02981

Boeing Aerospace Company
Attn: S. Gross   1
      C. Johnson   1
P.O. Box 3999
Seattle, WA 98124

Electrochemica Corporation
Attn: M. Eisenberg   1
2485 Charleston Road
Mt. View, CA 94040

Department of National
  Defense
Attn: Library   1
Defense Research Establishment
  Ottawa
Ottawa, Ontario K1A0Z4

Cordis Corporation
Attn: W. K. Jones   1
P.O. Box 525700
Miami, FL 33152

Eagle-Picher Corporation
Couples Department
Attn: Library   1
Joplin, MO 64801

Duracell International, Inc.
Attn: W. Bowden   1
      A. N. Dey   1
      H. Taylor   1
      Library   1
Laboratory for Physical Science
Burlington, MA 01803

	Copies		Copies
Wilson Greatbatch LTD. Attn: Library R. M. Carey 1000 Wehrle Drive Clarence, NY 14030	1 1	McDonnell Douglas Corporation 1150 17th Street, NW Suite 500 Washington, DC 20036	. 1
Ray-O-Vac Attn: R. F. Udell B. C. Bergum 101 East Washington Avenue Madison, WI 53703	1 1	General Electric Company Attn: Dr. R. W. Race, Manager Advance Programs Marketing Room 2544A-OP#2 100 Plastics Avenue Pittsfield, MA 01201	 1
The Aerospace Corporation Attn: Mr. A. Heller 2350 El Segundo Boulevard P.O. Box 92957 Los Angeles, CA 90009	1	Dr. Robert Murphy Advanced Battery Group 269 Westwood Lancaster, NY 14086	 75
Honeywell, Inc. Power Sources Center Attn: Library 104 Rock Road Horsham, PA 19044	1	GTE Sylvania Attn: Dr. R. McDonald 189 B Street Needham Heights, MA 02194	1
Martin Marietta Aerospace Attn: J. W. Wear P.O. Box 179 Denver, CO 80201	1	Altus Corporation 1610 Crane Court San Jose, CA 95112	1
Spartan Electronics Attn: C. H. Bush 2400 East Ganson Street Jackson, MI 49202	1	Sonatech, Inc. Attn: R. Cyr 700 Francis Botello Road Goleta, CA 93017	1
Union Carbide Battery Products Division Attn: R. A. Powers P.O. Box 6116 Cleveland, OH 44101	1	Sanders Associates Attn: G. Disco 95 Canal Street Nashua, NH 03061	1
Magnavox Department 529 Attn: C. Keuneke 1313 Production Road Fort Wayne, IN 46808	1	GTE Laboratories, Inc. Attn: Library 40 Sylvan Road Waltham, MA 02154	1
		Institute for Defense Analyses R&E Support Division 1801 N. Beauregard Street Alexandria, VA 22314	1

DISTRIBUTION (Cont.)

	Copies		Copies
Battelle Memorial Institute		Internal Distribution:	
Defense Metals & Ceramics	.	E231	9
Information Center		E232	3
505 King Avenue		R30	1
Columbus, OH 43201	1	R33 (Mueller)	2
		R33 (Staff)	20
Defense Technical Information		R33 (Bis)	35
Center			
Cameron Station			
Alexandria, VA 22314	12		